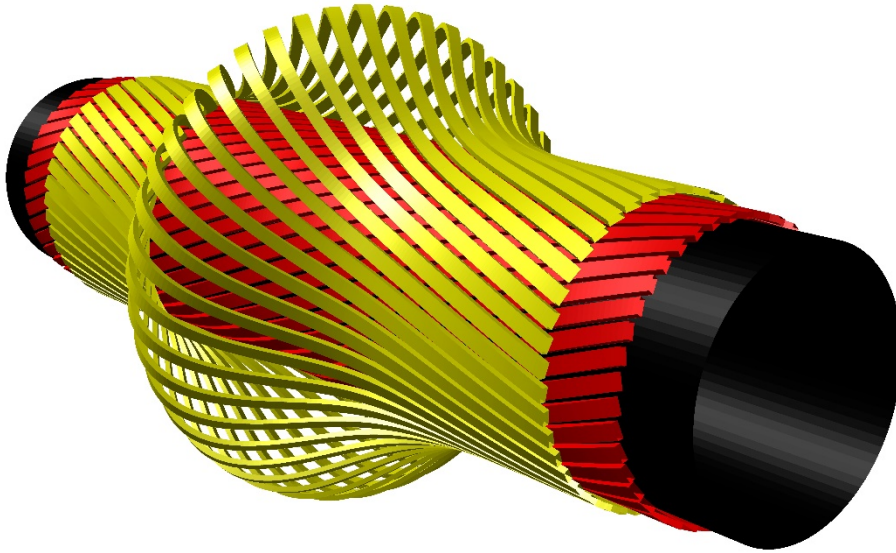




SINTEF



Report

THE TORSION HANDBOOK

Understanding and addressing torsion in the handling of cables, umbilicals and flexible pipes

Authors:

Philippe Mainçon and Vegard Longva

Report No:

OC2022 A-038 - Unrestricted

Clients:

Aker Solutions, Equinor, Hellenic Cables, NKT HV Cables, Petrobras, Ørsted

Report

THE TORSION HANDBOOK

Understanding and addressing torsion in the handling of cables, umbilicals and flexible pipes

KEYWORDS

Torsion, power cables, umbilicals, flexible pipes

VERSION

1.1

DATE

2024-04-18

AUTHORS

Philippe Mainçon and Vegard Longva

CLIENTS

Aker Solutions, Equinor, Hellenic Cables, NKT HV Cables, Petrobras, Ørsted

CLIENT'S REFERENCE

-

PROJECT NO.

302004370

NO. OF PAGES

202

SUMMARY

In September 2019, SINTEF initiated a 3-year Joint Industry Project (JIP). The JIP's objective was to provide the industry with the insights and tools to prevent torsion-related failures. The present document is one of the main deliverables of this project.

The document consists of two parts. Part I aims at providing insight into the mechanisms that lead to the appearance of torsion during handling operations, and in the mechanisms of failure of cross sections subjected to torsion. Part II provides a guideline on how to evaluate the levels of internal torque that may develop in various types of handling operations, on how to evaluate the various torsion-related failure modes of flexible product.

PREPARED BY

Philippe Mainçon

SIGNATURE

Philippe Mainçon (Apr 10, 2024 07:40 GMT+2)

CHECKED BY

Vegard Longva

SIGNATURE

Vegard Longva (Apr 10, 2024 07:59 GMT+2)

APPROVED BY

Naiquan Ye

SIGNATURE

Naiquan Ye (Apr 10, 2024 19:29 GMT+2)

REPORT NO.

OC2022 A-038

ISBN

978-82-7174-458-8

CLASSIFICATION

Unrestricted

CLASSIFICATION THIS PAGE

Unrestricted

The Torsion Handbook © 2024 by SINTEF Ocean AS, Norway, is licensed under CC BY-ND 4.0. To view a copy of this license, visit [creativecommons.org](https://creativecommons.org/licenses/by-nd/4.0/).

Contents

I	Understanding torsion	13
1	Introduction	14
2	State of the art	16
3	Geometry	17
3.1	Route	17
3.2	Coordinates	17
3.3	Curvature	18
3.4	Longitudinal marking	19
3.5	Roll angle	20
3.6	Torsion	20
3.7	Twist	22
3.8	Writhe	23
3.9	Link	25
3.10	Spatial and material roll rates	26
3.11	Mathematical formulation	28
3.11.1	Necessity	28
3.11.2	Relation to knot theory	29
3.11.3	Rotation rate	29
3.11.4	Frenet-Serret families of reference systems	30
3.11.5	Torsion-free families of reference systems	31
3.11.6	Longitudinal marking families of reference system	31
3.11.7	Flowline families of reference system	32
3.11.8	Twist-induced roll	33
3.11.9	Writhe in a helix	34
3.12	Engineering implications	35
3.12.1	Relativity to longitudinal marking	35
3.12.2	Measuring roll rates in the absence of longitudinal marking	36
3.12.3	Measuring torsion	36

4	Cross-section behavior	38
4.1	Internal and external torques and moments	38
4.2	Curvature diagrams	39
4.3	Moment-curvature diagram	40
4.4	Drawing a moment in a curvature diagram	43
4.5	Complex curvature histories	44
4.6	Residual curvatures	45
4.7	Non-uniform curvature	45
4.8	Torsionally unbalanced cross-sections	47
4.9	End-cap effects	48
5	Flip torques	50
5.1	Preliminaries	50
5.2	Transport along a route with change of curvature	52
5.3	Effect of roll rates	53
5.4	Pseudo-external flip torque	54
5.5	Mathematical formulation	55
5.5.1	Equilibrium	55
5.5.2	Integration along the route	56
5.5.3	Interaction between pitch and change of curvature plane	58
5.6	Engineering implications	59
5.6.1	Route optimisation	59
5.6.2	Chutes	60
5.7	Active geometry control in a turntable free span	61
5.7.1	Requirements	61
5.7.2	Monitoring of spatial roll	61
5.7.3	Geometry control	62

6	Storage and routing	65
6.1	Turntables	65
6.2	Spools	66
6.3	Baskets	67
6.4	Chutes and other fixed surfaces	69
6.5	Tensioners and rollers	71
6.6	Hydraulic actuators	73
7	Steady state and transients	75
7.1	Definitions	75
7.2	Occurrence	75
7.3	Mathematical formulation	75
8	Instabilities and irreversibility	78
8.1	Torsion–pressure instability	78
8.2	Mathematical formulation	78
8.3	Curvature–pressure instability	79
8.4	Flip torque–geometry instability	79
8.5	Residual curvature realignment	81
8.6	Helical buckling	82
8.7	Irreversibility	84
9	System behaviour	86
9.1	Introduction	86
9.2	Torsion in factory	86
9.2.1	Unbalanced winding machine	86
9.2.2	Flip torque	87
9.2.3	Bird-nesting	88
9.3	From storage to storage	89
9.3.1	Long-distance conservation of torsion	89
9.3.2	Torque buildup	90

9.3.3	Evolution of a loadout operation	92
9.4	Baskets	97
9.5	J-lay installation	98
9.5.1	Torque build up	98
9.5.2	Touch-down point hocking	99
9.6	Shore pull-in	100
10	Local failure mechanisms	102
10.1	General remarks	102
10.2	Skew-kinking	102
10.3	Birdcaging	103
10.4	Herniation buckling	104
10.5	Inward radial buckling	106
10.6	Lateral buckling of tensile armour	106
10.7	Payload buckling	107
10.8	Unwinding at termination	108
II	Assessing torsion	110
11	Introduction	111
11.1	Intention and disclaimer	111
12	Units	112
12.1	Requirements	112
12.2	Base units	112
12.3	Dimensionless quantities	112
12.4	Derived units	113

13 Cross section properties	114
13.1 Axial and torsional stiffness	114
13.1.1 Definitions	114
13.1.2 Evaluation by numerical analysis	114
13.1.3 Experimental evaluation	115
13.1.4 Stiffnesses at constant torque and axial force	117
13.2 Moment-curvature diagram, friction bending moment	117
13.2.1 Importance and sensitivity	117
13.2.2 Moment-curvature by numerical analysis	118
13.2.3 Moment-curvature by test	119
13.2.4 Evaluation of the friction bending moment	119
14 Overall torque load assessment procedure	121
15 Coiling writhe at steady state	123
16 Flip torque	125
16.1 Introduction	125
16.2 Limitation	125
16.3 Global finite element analysis	125
16.4 Flip torque computation procedure	127
16.5 Flip torque transient close to downstream storage	130
16.6 Steady states	131
16.7 Iteration	133
16.8 Flip torque diagram	133
17 Cranking	135
18 Torsional imbalance	136
18.1 Pull-in operation	136
18.2 J-lay installation on the seafloor	136

19 Residual curvature	138
19.1 Simplified analysis	138
19.2 Advanced analysis	139
20 Local failures	141
20.1 Stresses in the tensile armor	141
20.1.1 Stresses due to bending	141
20.1.2 Stresses due to torque and wall tension	141
20.2 Lateral buckling of tensile armour	142
20.2.1 Notations	142
20.2.2 Moments of inertia	143
20.2.3 Buckling of rectangular wires	143
20.2.4 Buckling of circular wires	144
20.2.5 Torsional-flexural buckling of rectangular wires	144
20.3 Birdcaging	144
20.3.1 Failure of outer supporting layers	145
20.3.2 Birdcaging of tensile armour	145
20.4 Herniation buckling	146
20.5 Inward radial buckling	147
20.6 Carcass collapse of flexible pipes	148
20.7 Tensile yield failure	150
20.8 Skew kinking	150
21 Global failures	152
21.1 Helical buckling	152
21.1.1 Foreword	152
21.1.2 Greenhill's formula	152
21.1.3 Selecting tension for assessment	153
21.1.4 Pitch length	154
21.1.5 Bending stiffness	154
21.1.6 Roller alleys	154
21.1.7 Catenary between two supports	154
21.1.8 Catenary during installation	155

22 Case study	157
22.1 Objective	157
22.2 Cross section	157
22.3 Critical stresses	157
22.4 Global buckling	160
22.5 Route	160
22.6 Steady-state flip torque evaluation	160
22.7 Flip torque in transients	165
22.8 Assessment	165
A J-lay installation on the seafloor	167
B Pull in operation	169
C Flip torque transient close to downstream storage	170
D Flip torque transient close to downstream basket	171
E Stresses in the tensile armour	172
F Herniation buckling	175
G Inward radial buckling	177
H Skew kinking	178
H.1 Assessing M_p	178
H.2 Energy dissipation	178
H.3 Available energy and critical β (pure torsion)	178
I Helical buckling	180
I.1 Stability condition	180
I.2 Hinged boundaries	181
I.3 Infinite domain	182

J	Multilingual glossary	183
K	Literature review of failure modes	184
K.1	Local failure modes	184
K.1.1	Lateral buckling of tensile armor	184
K.1.2	Birdcaging	186
K.1.3	Other local failure modes	186
K.2	Global failure modes	187
K.2.1	Loop formation and kinking	187
L	Example route geometry	189
	References	198

Foreword

Power cables, flexible pipes and umbilicals (but also climbing ropes, sewing threads, gardening hoses etc.) may display torsion-related motion under handling. As an example, while a cable is routed from an onshore turntable to an installation vessel, longitudinal markings can be observed to roll, and torsion starts building up. This progresses until either the cable is damaged (with the tensile armor showing a "bird cage" related behavior), or takes the shape of a helix which is difficult to route and store.

Since 2009, SINTEF has been invited to investigate torsion-related failures that have occurred during production, load-out (to installation vessels), installation, and even during operation. Some of these failures were extremely costly events. SINTEF's role in such investigations is to gather all relevant data from all parties involved in the failure, review and analyze the data and conclude on the mechanism (or the possible mechanisms) of the failure, and, where relevant, to propose solutions to avoid future problems. SINTEF has also provided less comprehensive services for other torsion related events and has studied information from dozens of incidents. Several lessons can be drawn from this experience:

The costs of some of these failures are considerable. Expensive products are damaged, deliveries significantly delayed, installation of vessels remain on stand-by for months, installed flexible products experience downtime and need repairs, and so forth. SINTEF is aware of several events that have each cost of the order of 100 million NOK (10 million Euros).

Failures are unacknowledged. Luckily, the failures we know about have not caused death, injury or pollution. Therefore, they do not have to be reported to the authorities, and the problem remains unmapped and largely unacknowledged. Yet, SINTEF has seen documentation of dozens of events. Further, our understanding of the underlying mechanisms suggests that these incidents can easily happen, so there are probably many incidents we have not yet heard about.

It's complicated. A glossary of all the terms needed to describe torsion-related concepts, just to make it possible to discuss a mishap, a failure or an improved design, takes several pages. The mathematics applied to model the relevant processes includes advanced concepts (rotations in 3D, material vs. spatial derivatives etc.). A variety of torsion-generating mechanisms, including several instability phenomena, have been identified.

In September 2019, SINTEF initiated a 3-year Joint Industry Project (JIP), sponsored by Ørsted, Equinor, Hellenic Cables, NKT HV Cables, Aker Solutions, and Petrobras. The JIP's objective is to provide the industry with the insights and tools to prevent torsion-related failures. The present "Torsion handbook" is one of the main deliverables of this project.

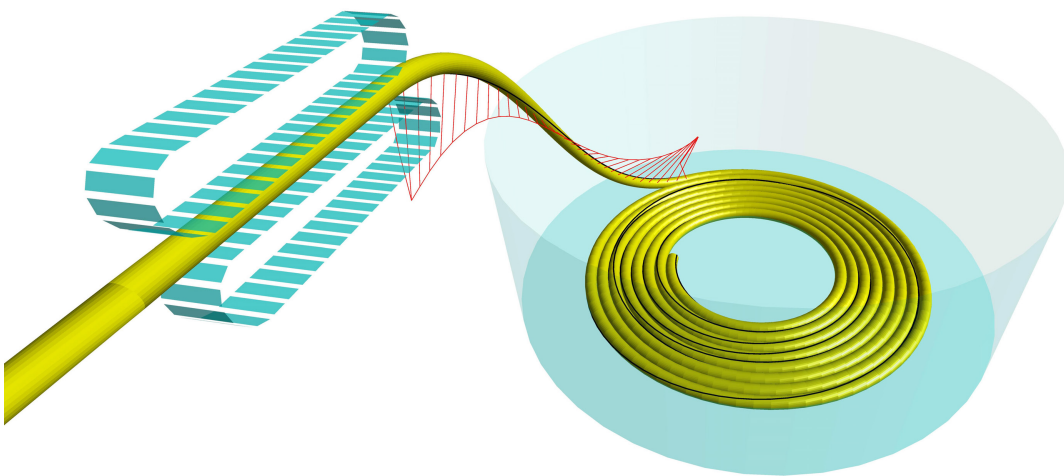
The document consists of two parts. Part I aims at providing insight into the mechanisms that lead to the appearance of torsion during handling operations, and in the mechanisms of failure of cross sections subjected to torsion. Part II provides a guideline on how to evaluate the levels of internal torque that may develop in various types of handling operations, on how to evaluate the various torsion-related failure modes of flexible product.

Nomenclature

$\frac{\partial R}{\partial k}$	Spatial roll rate	deg/m
$\frac{DR}{Dk}$	Material roll rate	deg/m
$\bar{\kappa}$	Curvature vector	m^{-1}
$\bar{\omega}$	Rotation rate vector	m^{-1}
$\bar{\Omega}$	Rotation rate matrix	m^{-1}
\bar{e}	Family of orthonormal reference systems	
\bar{e}^l	Longitudinal marking family of reference systems	
\bar{e}^v	Torsion-free family of reference systems	
\bar{e}^{fs}	Frenet-Serret family of reference systems	
\bar{f}	Distributed external forces	Nm^{-1}
\bar{M}	Internal moments (torque, bending moments)	Nm
\bar{m}	Distributed external moments	N
\bar{R}	Internal forces (axial force, shear forces)	N
τ	Torsion	Nm
τ_{fs}	Frenet-Serret "torsion" of a curve	m^{-1}
ε	Elongation	m/m
k	Payout of flexible product	m
L	Link	deg
M_f	Friction moment	Nm
R	Roll angle	deg
R^*	Twist-induced roll	rad
s	Route coordinate	m
T	Twist	deg
W	Writhe	deg
z	Line coordinate	m

Part I

Understanding torsion



1 Introduction

Part I studies the various mechanisms by which torsion can appear in flexible products while they are being handled, and how this torsion can lead to various forms of failures. Some of the mechanisms are easy to grasp intuitively: if a flexible product is curved, and a transverse load is applied in the correct direction, the flexible product is acting like a crank and will experience an internal torque. Other mechanisms are maybe not immediately intuitive, as for example “flip torques” or geometric instabilities.

Part I aims at providing engineers and operators with an intuitive understanding of these mechanisms. Many concepts are involved, there is no single insight that will unlock comprehension. Hence, understanding the mechanisms of torsion generation does require time and effort. Still, gaining this understanding will make it easier to

- diagnose torsion-related problems,
- describe them with a precise vocabulary,
- make better operational decisions to prevent and mitigate torsion,
- chose modes of operation and route layouts that are less likely to induce torsion,
- apply guidelines for the quantitative assessment of internal torque (Part II) with insight and discernment.

A first step toward understanding torsion is to acquire a good vocabulary: Just like the notion of strain is necessary to study stresses, stiffness and thus equilibrium, the geometrical tools provided in this chapter are necessary to create models of how real-world flexible products behave and thus evaluate the level of internal torque developed under handling. In addition, these geometrical concepts are important in order to be able to report observations on the behavior of a flexible product. Experience has shown that the confusion of various concepts into “there is torsion” in incident reports makes it difficult to diagnose the source of any problem experienced.

Some mathematics are provided in Part I, and for some readers, will provide a deeper understanding. These mathematics are descriptive (just as Isaac Newton’s $F = m a$ describes “how the world goes round”) . However in Part I, no methods are provided for engineering assessment of torsion levels: this is the object of Part II.

Section 2 reviews what is available in the scientific literature about the mechanisms of torsion generation.

Section 3 explores the *geometry* of torsion in flexible products: How to describe (not predict) the shape of a flexible product, and how this shape changes over time. The equivalent in continuum mechanics would be the study of displacements, velocities, and strain – things that can be defined independently of the material. For flexible products, the mathematical vocabulary of 3D curves provides notions like curvature and deflections. But we need to go beyond that to consider “curves with a longitudinal marking” in order to be able to talk of torsion, and how flexible products roll around themselves.

Section 4 looks into *cross-section behavior*: how curvature (and its change over time) affects bending moments, because of internal friction between components, or how “flexible” products turn out to be extremely stiff against some particular patterns of deformations. It also addresses torsionally unbalanced cross-sections.

Section 5 uses the insight from the two previous sections to study how friction between the components of the flexible product can cause large torques to appear.

Section 6 looks into the various forms of storage of flexible product and how they relate to torsion: friction holds the flexible product in place so that it will not roll. Basket continuously introduce writhe, causing the product to be stored with torsion (which does not need to be a problem). The section then discusses friction between the flexible product and rollers, tensioners and chutes, and shows that these often oppose surprisingly little resistance to roll.

Section 7 remarks that many operations tend to stabilize into a state in which the torsion at any given point along the route does not vary much over time. In such operations, the torsion at steady state is the highest that will be induced by internal and external friction.

Section 8 however points out that there is no general guarantee that a steady state will always be achieved. Indeed, there are several forms of instabilities that can cause a rapid build-up of torsion – the equivalent in the realm of torsion and friction, is buckling in columns. The section then comes with a warning: there is no “rewind” or “undo” button in the handling of flexible products. Reverting the actuators of the operation (tensioners, turntables) does not allow to turn back the clock.

Section 9 brings together the insights presented earlier in Part I to discuss several operational cases, in which the overall behavior of the flexible product, affected by several factors, can be quite complex.

Section 10 describes the various types of local failure that may occur under torsion, depending on how the flexible product is made.

2 State of the art

“Curves” in 3 dimensions have have “writhe” [7, 8, 13, 5], a property of high importance when measuring roll angles. This property has been extensively studied in biochemistry, because of its relevance for the behavior of DNA and RNA molecules. It is also of relevance in the study of magnetic fields, and in particular, solar flares.

The resistance to roll in a bent flexible line, due to internal friction is identified as a source of torque in [19]. The study was concerned with an installed riser system (no transport along a route was involved). The relevance of this effect to the appearance of torque in transport was then studied in [31].

Beam theory shows that introducing torque in in a curved beam will introduce bending moments leading to deflections. This, and the unstable response this can induce, have been studied for elastic beams in [27, 4]. A numerical beam model, that accounts for the combination of transport and internal friction described in [31] was presented in [29, 30, 28].

Coilable designs are made a single tensile armor layer, or multiple layers laid in the same direction. Such flexibles are by design strongly torsionally unbalanced. Other designs include two or more tensile armors laid in opposing directions. They are typically designed to be torsionally balanced. Both tests and numerical models [9] have been used to evaluate this coupling.

Flexible products under high torque loads can fail in a variety of ways. Hocking at the touch down point [32, 21, 35] and the related helical buckling

Some failure mechanisms have been studied in contexts unrelated to torsion, but are still relevant: in-layer lateral buckling of armor wires [36, 37].

There is an obvious need to monitor torsion during operations. The use of radio-frequency identification tags embedded in flexible products is patented as a method for measuring roll, and from there assess torsion [56]. The use of optical fibers to measure strain in the tensile armor is patented as a method for assessing torsion [57].

3 Geometry

3.1 Route

During handling (including, production, load-out and installation) the flexible product is often made to follow a given path. The path remains (more or less) unchanged while the flexible product “flows” along the path, much like water following the course of a river. The flexible product is said to be *transported* along a *route*.

Even tough circumstances may require a reversal, every operation has an intended direction of transport (e.g. from onshore storage to vessel). *Downstream* refers to the intended direction of transport, and *upstream* is the opposite direction.

In practice, the route is not completely fixed during an operation: free spans go from slack to tight, the touch down point in a turntable moves from the nave to the wall, and so forth. Still, many explanations in the following will be assuming a *fixed route* for simplicity. Other reasoning will need to explicitly take into account variations of the route over time.

3.2 Coordinates

Coordinates are needed to define points along the flexible product and along the route, using so-called *arc-length coordinates*. These coordinates describe distances “along a path” as opposed to “as the crow flies”. By convention in this document, these *coordinates increase in the downstream direction*. Since flexible products are typically spooled back and forth, this implies that the direction of the line coordinate is changed with the phase of the operation.

Line coordinates z [m]. A line coordinate uniquely defines a material point (“there is a marking on the outer sheath at line coordinate $z = 337\text{m}$ ”). Typically, the tail end is chosen to have line coordinate 0 (the origin of the line coordinate system). Line coordinates increase along the line, and the line coordinate of the head end is the length of the line. In this document, the mathematical symbol for a line coordinate is z with unit [m]. It will be convenient to write z_a , z_b and so forth, to refer to the line coordinates of cross-section **a** and **b** along the line.

Route coordinates s [m]. A route coordinate uniquely defines a point *along the route* (“the tensioner at route coordinate $s = 540\text{m}$ ”). Typically, the place where the flexible product leaves the upstream winding machine/turntable/spool, will be chosen to have route coordinate 0. In this document, the mathematical symbol for a route coordinate is s with unit [m]. It will be convenient to write s_a , s_b and so forth, to refer to the route coordinate of points **a** and **b** along the route.

Payout k [m]. The payout measures progress of the operation: the length of flexible product that has been transported (“we aim for 200m more payout by the end of the shift”). In this document, the mathematical symbol for payout k with unit [m].

If line and route coordinates are oriented in the same direction, then the route coordinate of a material point (defined by its line coordinate) at a given payout can be calculated (Figure 1)

$$s = z + k + s_0 \quad (1)$$

where s_0 is a constant depending on the choice of origins of the line and coordinate system. If for example, at the start of the operation ($k = 0$), the head of the flexible product ($z = L$, where L is the length of the flexible product) is at the point of route coordinate $s = 0$, then the above equation can be written $0 = L + 0 + s_0$, implying that $s_0 = -L$. The above equation is, for that case, $s = z + k - L$.

If line and route coordinates are oriented in opposite directions, with the line coordinates increasing in the upstream direction, then

$$s = -z + k + s_0 \quad (2)$$

In the rest of this document only the case where the line and route coordinates are in the same direction is considered. The other case is handled by switching the sign of z .

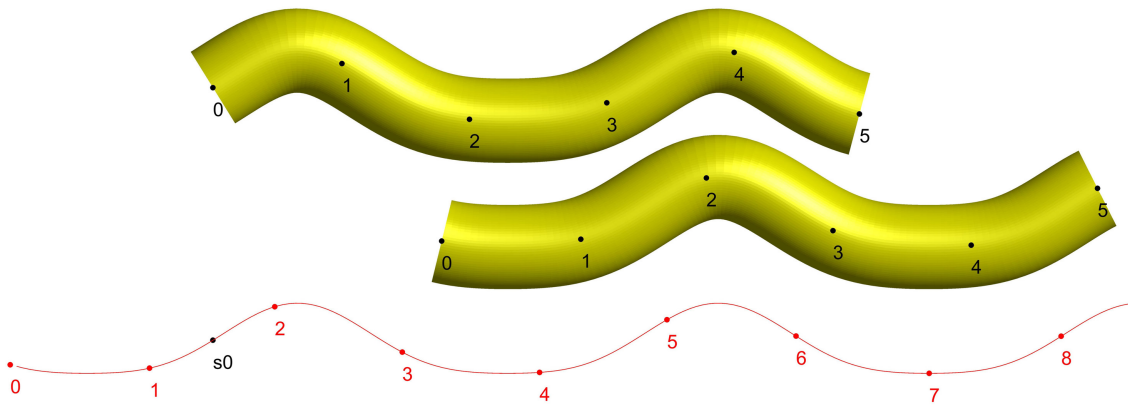


Figure 1: Line coordinates (z , black) and route coordinates (s , red). The top pipe shows the flexible product at $k = 0$, the bottom pipe at $k = 1.8$.

3.3 Curvature

Simply put, the curvature of a route at a given point along the route is the inverse of the bending radius. However, it is useful to describe curvature as a vector $\bar{\kappa}$. The length of the vector is the inverse of the bending radius [m^{-1}], and the vector is orthogonal to the route and points inside the curve (Figure 2).

At a given point along the route, the curvature plane (known in mathematics as the osculating plane) is the plane that contains the vector tangent to the route and the curvature vector (Figure 3).

In places where the route is straight, since the curvature vector has length zero, any plane containing the tangent vector would do, so the curvature plane is undefined. In a segment of the route that is plane (for example, if the segment of the route was all in a given horizontal plane, never changing height), then the curvature plane at any point in this segment, is the plane containing the route.

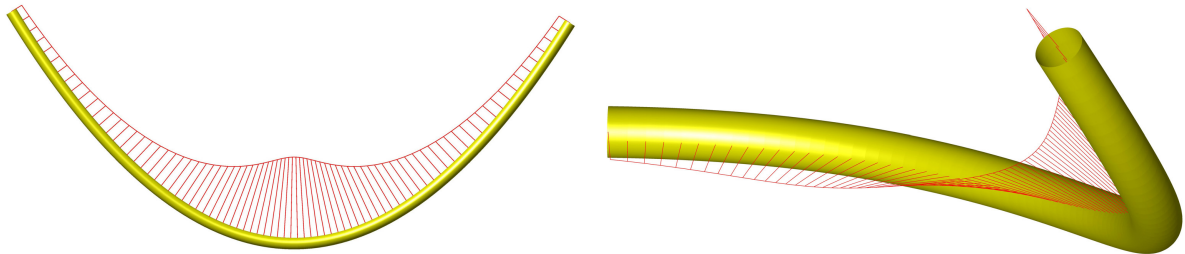


Figure 2: Curvature vectors along a route curved: in a single plane (left), in 3 dimensions (right).

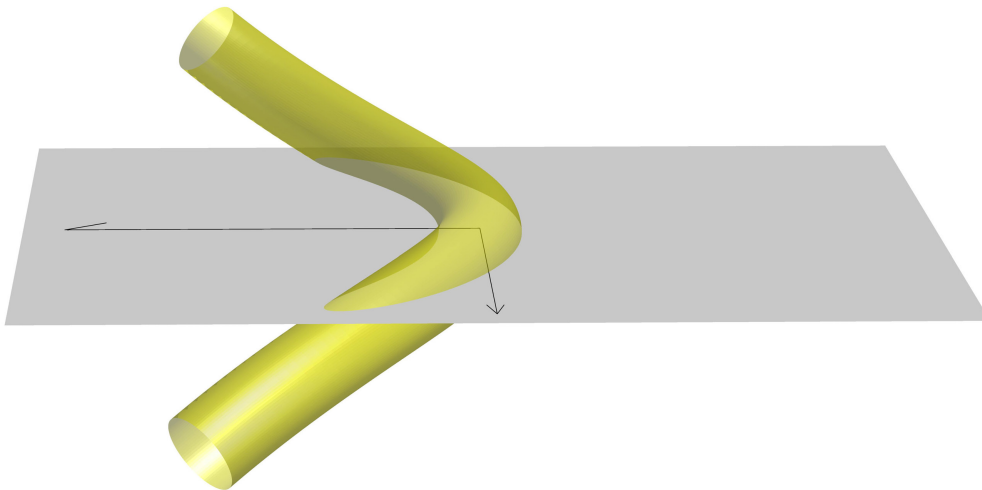


Figure 3: Osculating plane, tangent and curvature vectors.

3.4 Longitudinal marking

Some flexible products carry longitudinal markings along all or part of their lengths (Figure 4). These can be extruded together with the outer sheath, or applied with a marker pen that is fixed on a point along the route while the flexible product runs past it. In the following, longitudinal markings will be discussed as if they were present in all flexible products, although this is not the case. Longitudinal markings are typically not applied to flexible products whose outer layer is made of polypropylene yarn spun around the flexible product. Even when no such marking is present, it is useful to imagine there was one, in order to introduce a variety of important concepts.



Figure 4: Longitudinal marking.

Ideally, if the flexible product was straight and not under tension or internal torque, then the longitudinal marking would be a straight line running along the cylinder. Such a marking is referred to as an *ideal longitudinal marking*. The marking applied to a flexible product may not be ideal, for several possible reasons:

- The flexible product can have been rolling (turning around its own axis) while being transported past the marking system.
- The flexible product can have been loaded in torsion when marked. When relaxed this would transform the marking into a helix.
- Plastic deformations of components of the flexible product, or relative slip between the components change the torsion and elongation at which the flexible product has zero internal torque and axial force.

3.5 Roll angle

At points along a route where the route is horizontal, one can define the roll angle as the angle between the longitudinal marking and the vertical. It can be measured as in Figure 7, except that as the ruler is held, it should be marked with “0” where it reads “90”.

Even if one defines roll as being positive when being clockwise, the sign of roll depends on the direction along which one is looking (Figure 5). This makes it important to agree on which direction along the route is “downstream”, because swapping the direction of the arc-length coordinate system swaps the sign of roll angles. The sign of roll is defined as being positive if it is clockwise *when looking downstream* (Figure 6). A mnemonic is to use the *right* hand with the thumb pointing downstream and the curved index finger pointing in the direction of positive roll.

In this document, the mathematical symbol for a roll angle is \mathbf{R} with unit [deg]. To be more specific, the roll at a point \mathbf{a} can be written $\mathbf{R}(s_{\mathbf{a}})$ “the roll at the arc-length coordinate of point \mathbf{a} along the route”.

3.6 Torsion

Consider a straight piece of flexible product, on which we draw ideal longitudinal marks, and circumferential marks (Figure 8, top). The longitudinal and circumferential marks are originally at right angles to each other. Torsion is the part of the deformation of a flexible product

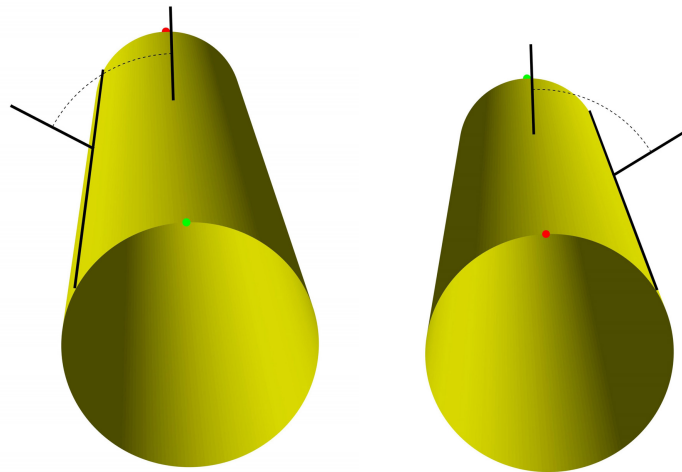


Figure 5: Observing the same roll from two different directions

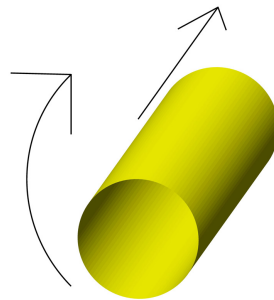


Figure 6: Sign convention for roll. The straight arrow points downstream (increasing route and line coordinates). The curved arrow points in the direction of positive roll.

that changes the angle between longitudinal and circumferential marks (Figure 8, bottom, and Figure 9).

One could hence measure torsion by the change of angle between longitudinal and circumferential marking. However, it turns out to be more convenient to measure it as a change of roll angle ΔR per unit length Δs . In this document, the mathematical symbol for torsion is τ (tau) with unit [$\text{deg} \cdot \text{m}^{-1}$]. For a straight segment

$$\tau = \frac{\Delta R}{\Delta s} \quad (3)$$

Figure 10 shows the same torsional deformation from two different perspective. In contrast to roll, torsion appears the same whether looking downstream or upstream: the sign of torsion is defined independently of the choice of a positive direction along the flexible product. Figure 8 (bottom) shows an example of *positive* torsion, the mirror image of which would be a negative torsion. In positive (respectively, negative) torsion, the roll angle increases (decreases) as one travels along the flexible product in the positive direction (the direction of increasing arc-length coordinate). DNA's double helix, and screws mostly are positive helices. There are



Figure 7: Roll angle measurement.

various nomenclatures for describing the direction of torsion, or the direction in which helical components are laid. Synonyms are shown in Table 1. In the present document, “positive” and “negative” are used, because this facilitates calculations.



	This document	Standards	Rope making	Helix
	Positive	Z-lay	Right lay	Right handed
	Negative	S-lay	Left lay	Left handed

Table 1: Torsion and helix sign nomenclature.

Torsion is also sometimes referred to as a twist angle in the literature. This expression will not be used here, to prevent confusion with *twist* (Section 3.7).

3.7 Twist

The twist between two points \mathbf{a} and \mathbf{b} along a route or flexible product is the part of the difference between the roll angles at these points that is due to torsion. In this document, the mathematical symbol for twist is T with unit [deg]. The twist is the downstream roll minus the upstream roll. So if \mathbf{b} is downstream of \mathbf{a} this can be written, *for a straight flexible product*,

$$T(s_a, s_b) = R(s_b) - R(s_a) \quad \text{with } s_b > s_a \quad (4)$$

Still for a straight flexible product, and if the torsion τ is uniform between both points, then

$$\tau = \frac{T(s_a, s_b)}{s_b - s_a} = \frac{R(s_b) - R(s_a)}{s_b - s_a} \quad (5)$$

If τ is not uniform the relation becomes

$$T(s_a, s_b) = \int_{s_a}^{s_b} \tau(s) ds \quad (6)$$

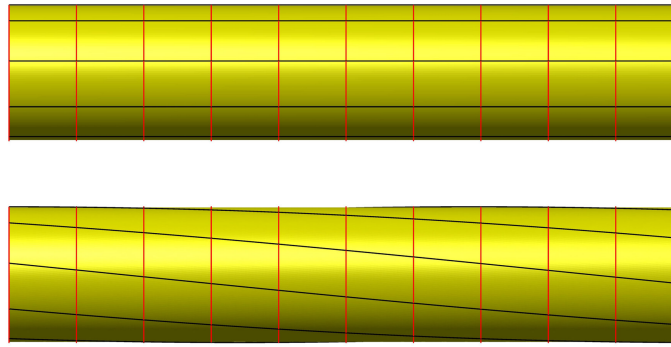


Figure 8: A mesh of longitudinal and circumferential markings. The bottom product has positive torsion.

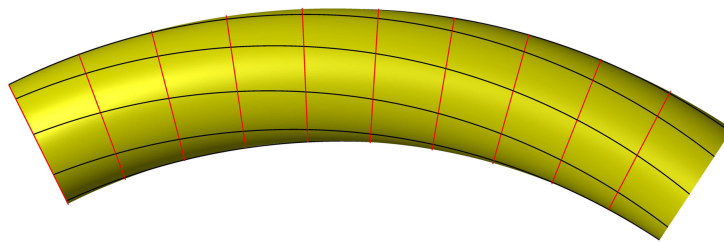


Figure 9: Torsion in a bend.

Swapping the direction of positive arc-length coordinate changes the signs of $\mathbf{R}(s_a)$ and $\mathbf{R}(s_b)$, but it also swaps which point is upstream and which is downstream, so neither twist nor torsion are affected: while a positive roll is only positive for a given direction of arc-length coordinates, the sign of twist is independent of the direction of the coordinates.

Because the line coordinates and route coordinates are arc-length coordinates along the same curve, but with difference in origin (the point of coordinate zero), one can also, if practical use the line coordinates z_a and z_b .

3.8 Writhe

In the above, the relation between torsion, twist and roll angles were given under the important limitation of dealing with a *straight* segment of a flexible product. Ignoring this limitation can lead to wrong estimations of the torsion, because of an interesting effect of 3-dimensional geometry: the writhe.

Figure 11 provides an example of writhe: it shows a segment of flexible product in which each of its 3 thirds are bent. If circumferential markings were shown, as was done in Figure 8, they would everywhere be at a right angle to the longitudinal markings: there is no torsion anywhere along the segment. Still the sequence of bends is such that the black longitudinal marking, which is at 3 o'clock at the lower end of the pipe, is at 6 o'clock at the upper end.

In this document, the mathematical symbol for writhe is \mathbf{W} with unit [deg]. By convention, one will compute the writhe as *the roll at a downstream point minus the roll at an upstream point*,

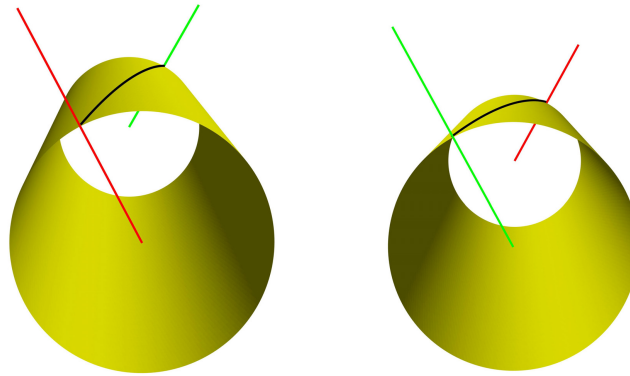


Figure 10: Torsion seen from different viewpoints

in the absence of torsion:

$$W(s_a, s_b) = R(s_b) - R(s_a) \quad \text{with } s_b > s_a \quad (7)$$

In this example, the writhe between both ends of the segment is $+90$ [deg].

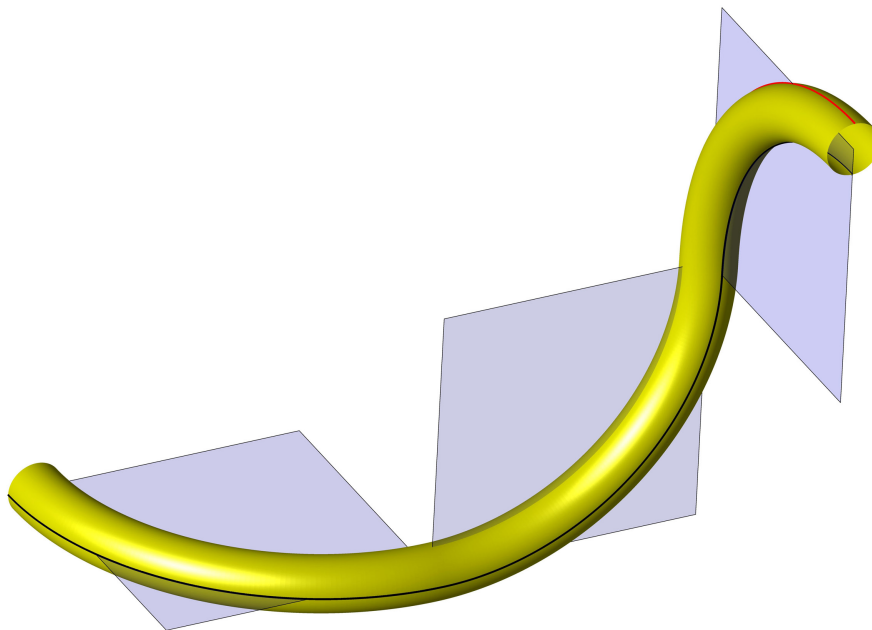


Figure 11: The roll angles at both ends of this flexible product are different because of writhe. The flexible product shown here has no torsion, but is bent successively in three different and orthogonal planes.

Figure 12 shows a more complicated example of a helix. Again it has zero torsion (the longitudinal marking is at a right angle to the (absent) circumferential marking), and yet as can be seen, the roll angle changes from pitch to pitch.

In the helix, the plane of curvature varies continuously while it varies in steps in Figure 11. In both examples above, dividing the difference in roll angle by the length of the pipe segment

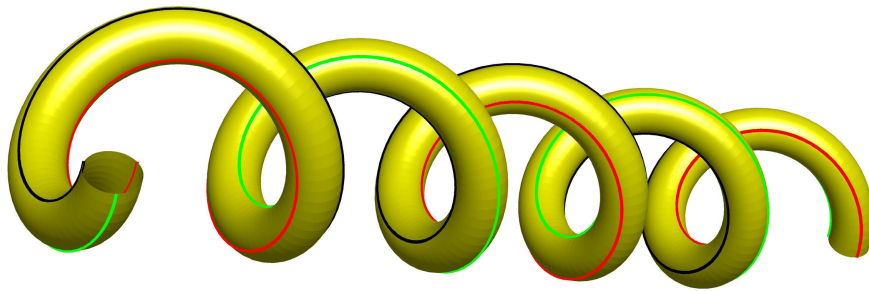


Figure 12: A helix (positive sign) is a more complicated example of writhe (negative sign). The flexible product shown here has no torsion. Three longitudinal markings, 120 [deg] apart.

could lead to the wrong conclusion that the pipe is undergoing twist, while it is only bent. Writhe never occurs in flexible products that deform within a single plane. This is related to the fact rotations around the same axis commute: changing the sequence does not change the final angles. By contrast, general rotations in 3D do not commute, and flexible products that deform in 3D exhibit writhe.

Sections 3.7 and 3.6 discuss twist and torsion, which is twist by unit length. Can one similarly speak of a “writhe per unit length”? The answer is no: the writhe of a segment is a function of the geometry of the whole segment. For example, writhe for a curve in a single plane is zero. The flexible product in Figure 11 is composed of 3 plane segments, yet the writhe is not zero.

In the two examples given above, one can evaluate the writhe analytically (for helices: Section 3.11.9). In more general cases, for example to compute the writhe of a geometry obtained using beam elements, this is not possible. In that case, the writhe must be evaluated numerically (Section 3.11.5).

As an exercise, one might want to consider the effect of coiling a short length of flexible product, starting from a straight line, ending with a single coil. This is relevant when coiling a rope per hand, or feeding a flexible product into a (non-rotating) basket. As Figure 13 suggests, and as experiments with a short length of tape will confirm, creating a coil introduces a 360 [deg] writhe in a flexible product.

3.9 Link

The *link* is simply the difference between the roll at two points along a route. In this document, the mathematical symbol for link is L with unit [deg]. By convention, one will compute the link as the roll at a downstream point minus the roll at an upstream point:

$$L(s_a, s_b) = R(s_b) - R(s_a) \quad (8)$$

where $s_b > s_a$.

In the above, it was discussed that both twist and writhe can contribute to a change of roll angle between two points. Hence *the link is the sum of the twist and the writhe*:

$$L = T + W \quad (9)$$

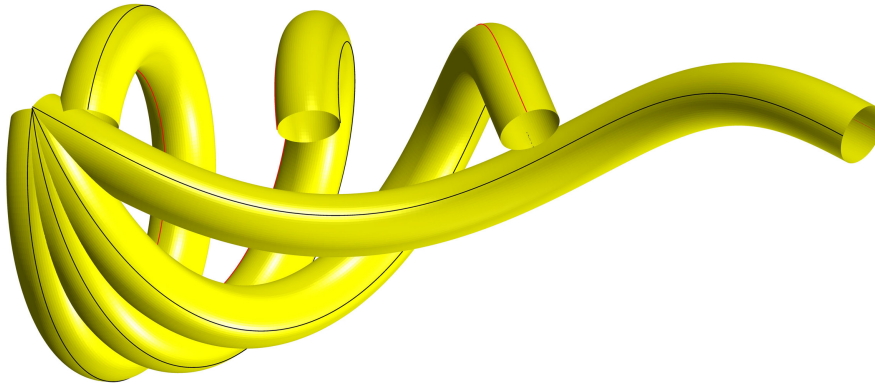


Figure 13: Creating a coil. Several snapshots superimposed. The flexible product is always torsion-free.

This statement is known as Calugareanu's theorem [7, 8].

One way to illustrate Eq. 9 is to consider a ribbon that has been coiled, and to pull one end *without allowing either end to rotate* (as would be the case to a garden hose which coils are born on a hook by the side of the house, or a coilable flexible product in a basket) (Figure14).

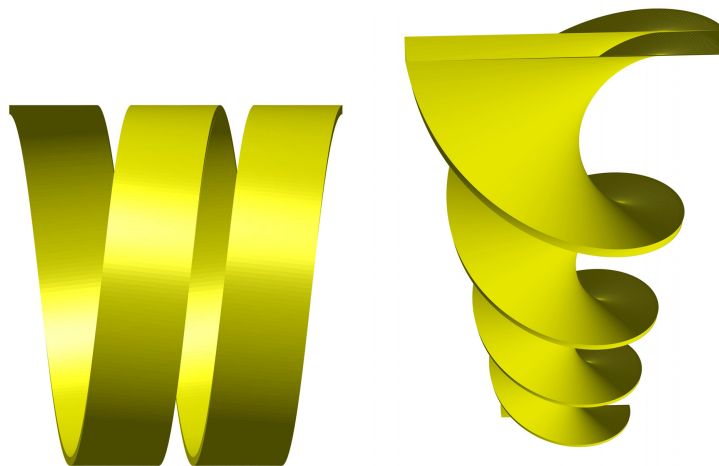


Figure 14: Pulling out a coiled ribbon (writhe) without allowing the ends to rotate results in twist: Link is conserved.

3.10 Spatial and material roll rates

There are two ways to measure the roll rate, that is, the rate of change of the roll angle with time. The first one is to put a bit of sticky tape on a flexible product that is being transported. One then measures the roll angle at the sticky tape, following it as it is transported along the

route. The sticky tape marks a material point on the flexible product, and the roll rate thus measured is called the *material roll rate*.

The second way to measure the roll rate is for the observer to stand still at a given point along the route and measure the roll angle. One could be standing at the touch-down point in a turntable, by a tensioner or a given roller.

If the flexible product has torsion, both methods will yield different results. Consider for example a straight segment of flexible product that has a positive twist. If the segment moves from left to right, without rotating around its axis (zero material roll rate), then

1. A “material” observer (Figure 15, left) following the flexible product will observe no roll: the material roll rate is zero.
2. A “spatial” observer (Figure 15, right) remaining immobile will observe a roll: the spatial roll rate is negative. More specifically, the spatial observer will observe a roll rate equal to minus the torsion, times the speed of the segment towards the right.

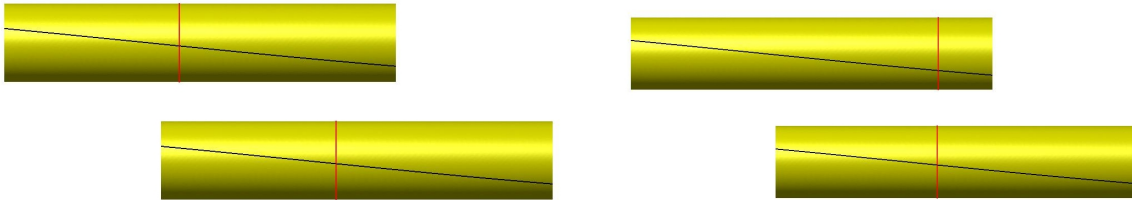


Figure 15: Material (left) and spatial (right) roll rates.

If we repeat the experiment, this time with the segment progressively rolling at the same time as it is translating, then

1. A “material” observer following the flexible product will find a material roll rate identical to the rate at which the segment rolls.
2. A “spatial” observer remaining immobile will find a spatial roll equal to the material roll, minus the torsion times the speed of translation of the segment.

For a straight segment of route, this can be written $\frac{DR}{Dt} = \frac{\partial R}{\partial t} + \tau v$ where DR/Dt is the material roll rate, with unit $[\text{deg} \cdot \text{s}^{-1}]$, $\partial R/\partial t$ is the spatial roll rate (same unit), τ is the torsion and v is the transport velocity. However, this definition will not be used in the following: one can simplify the above expression by using, as unit for time, “the time it takes to pay out 1 [m] of the flexible product”. This unit of time is in effect the payout $k(t)$ (Section 3.2). We then have

$$\frac{DR}{Dk} = \frac{\partial R}{\partial k} + \tau \quad (10)$$

where the material roll rate is defined as DR/Dk , and the spatial roll rate as $\partial R/\partial k$ (Figure 16). The notations D and ∂ have special meanings in mathematics, but this is not important: here DR/Dk and $\partial R/\partial k$ are just notations for material and spatial roll rates. Both have the unit $[\text{deg} \cdot \text{m}^{-1}]$. Equation 10 can be read “the change of roll angle of a material point when the flexible product is transported 1 [m] is equal to the change of roll angle seen by an observer

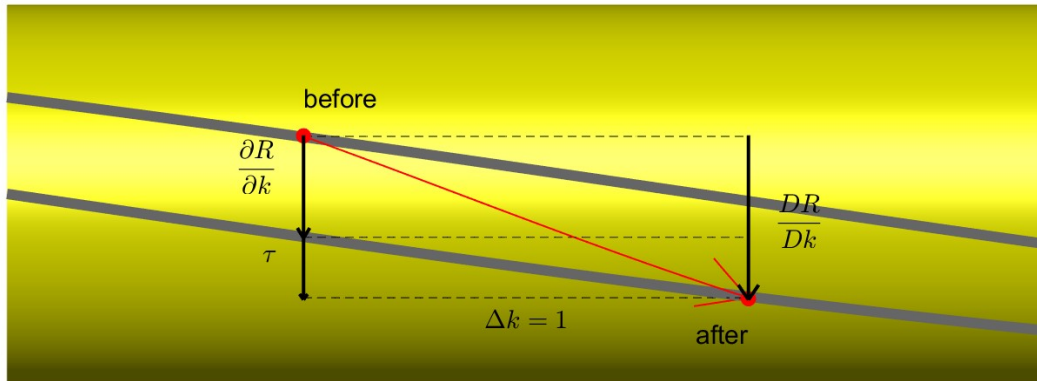


Figure 16: Relation between material roll rate, spatial roll rate and torsion. The longitudinal marking (and a material point, in red) are shown before and after the flexible product is transported by an amount $\Delta k = 1$. Downstream is to the right, so a positive roll is downward, and both roll rates are positive in this example.

standing on the ground, plus the change of roll angle seen by an observer walking 1 [m] along the immobile flexible”.

The sign of material and spatial roll rate is independent of the choice of a positive direction along the flexible product. This is due to the choice of deriving with respect to the payout k – which sign depends on the choice of positive direction.

3.11 Mathematical formulation

3.11.1 Necessity

The present handbook aims at providing a practical and intuitive approach to torsion related problems. This has its limitations, and for some advanced questions, will not be sufficient. The present Section provides a slightly more rigorous mathematical base to the understanding of torsion. It is however fully possible to skip Section 3.11.

The definitions of torsion, twist and writhe provided in Sections 3.6, 3.7 and 3.8 are designed to develop intuition, but lack of rigor, with “twist” being defined as a difference of roll angles in the absence of writhe and “writhe” as a difference of roll angles in the absence of torsion. Further, the definition of roll angle in Section 3.5 breaks down for vertical segments of flexible products.

As a consequence, the above definitions would cause problem when dealing with advanced problem, or when writing software that must handle a range of cases. In the present Section, the above concepts are revisited. Alternative definitions which are rigorous and more widely

appliflexible product are presented. On the other side, these definition require a stronger grasp of the underlying mathematics.

3.11.2 Relation to knot theory

The definition of writhe presented in this section differs from that used in knot theory in several respect. A trivial difference is that here the writhe is measured in degrees, while turns (360 degrees) are used in knot theory.

A deeper difference is that in knot theory, the writhe is defined only for closed curves (loops). This is impractical for engineering purposes, but allows to distinguish “positive” and “negative crossing” in a way the definition below does not. The definition presented below provides values of the writhe “modulo 360 deg”. For example, for a coil added to a straight line, the definition below will lead to a writhe equal (or close) to zero, while the mathematical definition will provide a distinction with a value of +360 deg (or +1 turn) for a negative crossing (coiling one way) and -360 deg (or -1 turn) for a positive crossing (coiling the other way) (cf. Eq. 16 in [61]).

In knot theory, to allow to distinguish the effect of crossings, the writhe is defined as a double integral (the average over all directions in 3D space of the number of crossings in an oriented link diagram). This integral is difficult to assess numerically. In contrast, computations of writhe as defined in this section are fast and stable.

The present definition can be made to provide absolute (as opposed to modulo one turn) values of writhe for open segment, by applying it to a continuous “movie” of curves, starting from a straight segment (defined to have zero writhe) to the actual configuration. The series of values of writhes obtained for each frame of the movie is “unwrapped” (made continuous), providing an absolute value. Computation times are slower of course, and there is the need to define the above-mentioned “movie”.

3.11.3 Rotation rate

The rotation rate of a family of reference systems is not to be confused with the roll rate – although a relation exists.

In the above, the various definitions rely on the existence of a “roll angle”. This concept is problematic, because it makes it difficult to describe cases with vertical or near vertical flexible products. Hence, for the purpose of more general analyses, and in particular for software development, one must define the necessary concepts in another way.

Consider a route \bar{x} , where s is a arc-length coordinate and $\bar{x}(s)$ is a point in a 3-dimensional Euclidean space. To each coordinate s we associate the orthonormal triplet $\bar{e}(s)$ of vectors $\bar{e}_i(s)$ where $i \in \{1, 2, 3\}$, such that $\bar{e}_1(s)$ is tangent to \bar{x} at $\bar{x}(s)$. This leaves many options open on how to orient \bar{e}_2 and \bar{e}_3 . Some of these options are of particular interest and are discussed in Sections 3.11.4, 3.11.5 and 3.11.6.

We define the rotation rate matrix

$$\overline{\overline{\Omega}} \triangleq \lim_{ds \rightarrow 0} \frac{\overline{\mathbf{e}}(s + ds) \cdot \overline{\mathbf{e}}(s)^{-1}}{ds} \quad (11)$$

where the symbol \triangleq represents a definition. We also define the rotation rate vector as

$$\overline{\boldsymbol{\omega}} \triangleq \begin{bmatrix} \Omega_{23} \\ \Omega_{31} \\ \Omega_{12} \end{bmatrix} \quad (12)$$

with coordinates in $\overline{\mathbf{e}}(s)$

$$\omega_i \triangleq \overline{\boldsymbol{\omega}} \cdot \overline{\mathbf{e}}_i \quad (13)$$

and finally the torsion *of the set of reference systems*

$$\tau_{\overline{\mathbf{e}}} \triangleq \omega_1 \quad (14)$$

in $[\text{rad} \cdot \text{m}^{-1}]$.

Since $\overline{\mathbf{e}}_1(s)$ is tangent to $\overline{\boldsymbol{\kappa}}$, the relation between the curvature vector $\overline{\boldsymbol{\kappa}}$ and the rotation rate vector $\overline{\boldsymbol{\omega}}$ can be written as

$$\kappa_2 = \omega_3 \quad (15)$$

$$\kappa_3 = -\omega_2 \quad (16)$$

$$\overline{\boldsymbol{\omega}} = \omega_1 \overline{\mathbf{e}}_1 + \omega_2 \overline{\mathbf{e}}_2 + \omega_3 \overline{\mathbf{e}}_3 \quad (17)$$

$$= \tau_{\overline{\mathbf{e}}} \overline{\mathbf{e}}_1 - \kappa_3 \overline{\mathbf{e}}_2 + \kappa_2 \overline{\mathbf{e}}_3 \quad (18)$$

$$\overline{\boldsymbol{\kappa}} = \overline{\mathbf{e}}_2 \kappa_2 + \overline{\mathbf{e}}_3 \kappa_3 \quad (19)$$

$$= \overline{\mathbf{e}}_2 \omega_3 - \overline{\mathbf{e}}_3 \omega_2 \quad (20)$$

3.11.4 Frenet-Serret families of reference systems

In Frenet-Serret reference systems [59, 18], noted $\overline{\mathbf{e}}^{fs}$, $\overline{\mathbf{e}}_2^{fs}(s)$ point towards the inside (the concave side) of the curvature for all s : $\overline{\mathbf{e}}_2^{fs}$ is within the osculating plane (Figure 17). $\overline{\boldsymbol{\omega}}^{fs}$ is the corresponding rotation rate vector. We then write the Frenet-Serret "torsion" $\tau_{fs} \triangleq \overline{\boldsymbol{\omega}}^{fs} \cdot \overline{\mathbf{e}}_1^{fs}$. It describes the rate of change of the curvature plane in a route, independently of the state of any flexible product that may follow that route. The Frenet-Serret "torsion" is a property of a *route*, and it is important not to confuse it with the torsion τ of a flexible product, as defined in Section 3.6.

One issue with Frenet-Serret coordinates is that for straight segments of route, the plane of curvature, and hence the Frenet-Serret coordinate system and the Frenet-Serret torsion is undefined.

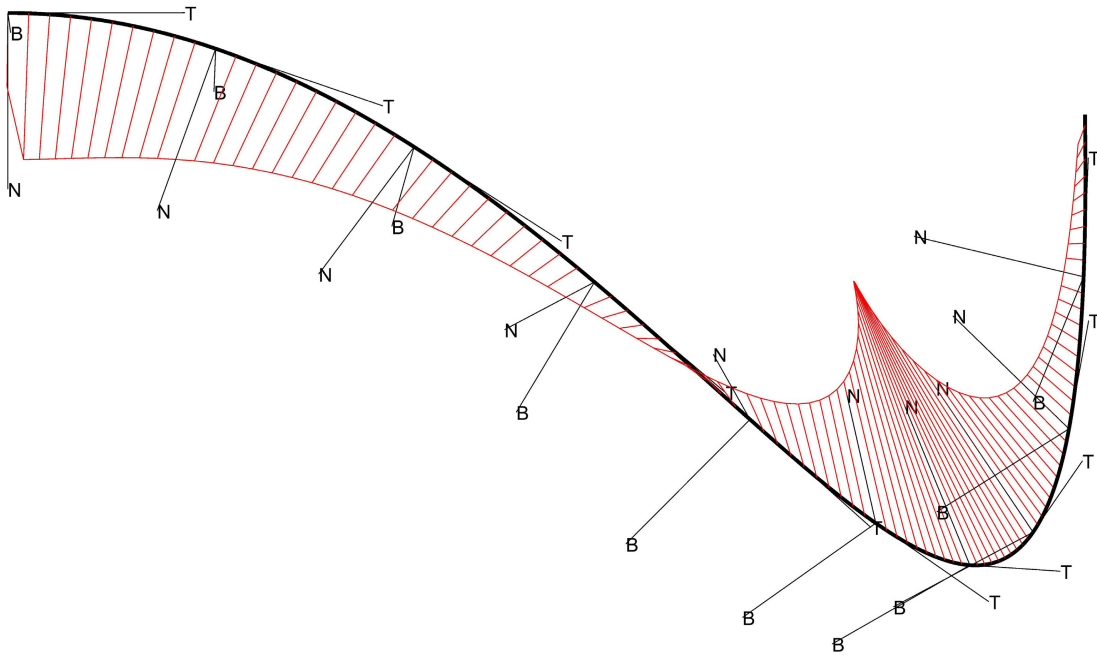


Figure 17: Frenet-Serret reference systems. T, N and B respectively stand for tangential, normal and binormal. N is always aligned with the curvature vector $\bar{\kappa}$.

3.11.5 Torsion-free families of reference systems

We introduce a new family \bar{e}^w or reference systems, with corresponding rotation rate vector $\bar{\omega}^w$. We set the requirement $\tau_w = \bar{\omega}^w \cdot \bar{e}_1^w = 0$ everywhere along the route. This defines a torsion-free family of reference systems (Figure 18). The function which to s associates $r\bar{e}_2^w(s)$ (one could have chosen $r\bar{e}_3^w(s)$) where r is the outer radius of the flexible product, is the trajectory of a material point on a flexible product being transported along the route with zero material roll rate, in other words, an ideal longitudinal marking.

If in a torsion-free marking, $\bar{e}_1^w(s_a)$ and $\bar{e}_1^w(s_b)$ are both orthogonal to a given normal vector \bar{v} (for engineering purposes, the vertical. If non zero, one can take $\bar{v} = \bar{e}_1^w(s_a) \times \bar{e}_1^w(s_b)$) then the writhe can be defined as

$$W(s_a, s_b) = \arctan \frac{\bar{v} \cdot \bar{e}_3^w(s_b)}{\bar{v} \cdot \bar{e}_2^w(s_b)} - \arctan \frac{\bar{v} \cdot \bar{e}_3^w(s_a)}{\bar{v} \cdot \bar{e}_2^w(s_a)} \quad (21)$$

3.11.6 Longitudinal marking families of reference system

We can require $\bar{e}_2^1(s)$ to be oriented everywhere so that the points $r\bar{e}_2^1(s)$ are the longitudinal marking of a given flexible product of radius r . The "longitudinal marking" family of reference systems is noted \bar{e}^1 . By extension, one can refer to the set of coordinate systems as a "marking" (Figure 19).

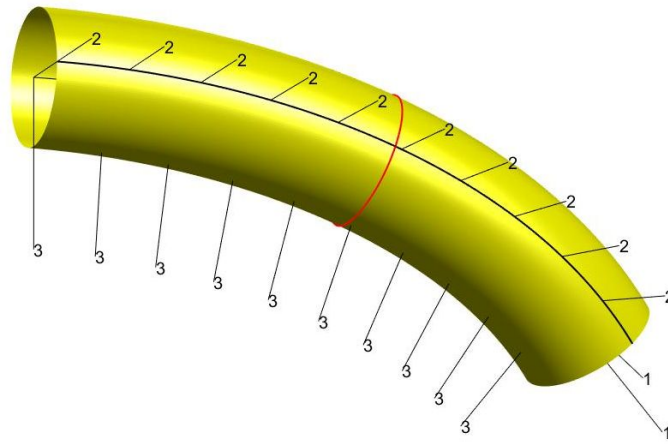


Figure 18: Torsion-free reference systems. Vectors \bar{e}_2^w cross a longitudinal marking that is always at right angle to the circumference.

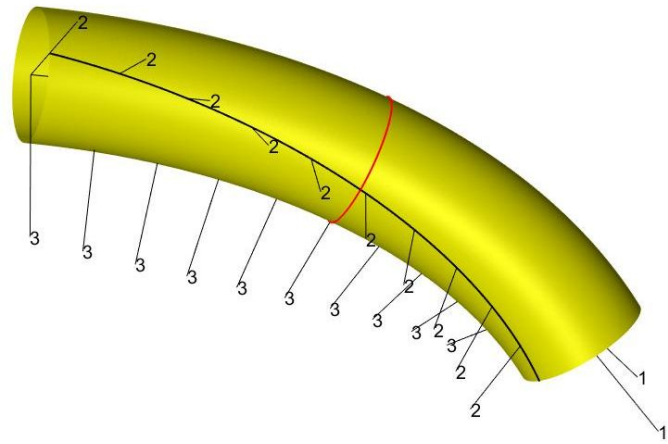


Figure 19: Longitudinal marking reference systems. Vectors \bar{e}_2^l cross a longitudinal marking that is not at right angle to the circumference.

The torsion in $[\text{rad} \cdot \text{m}^{-1}]$ of the flexible product is defined as

$$\tau \triangleq \bar{\omega} \cdot \bar{e}_1^l \quad (22)$$

Where the definition of τ provided in Section 3.6 does not breakdown, it is equivalent to the more general definition provided here.

3.11.7 Flowline families of reference system

If the material roll rate is known, we can introduce a “flowline” family of reference systems. Vectors \bar{e}_2^f are oriented in such a way that if a material point is aligned with $\bar{e}_2^f(s_a)$ at point \mathbf{a} along the route, then it will be aligned with $\bar{e}_2^f(s_b)$ when it reaches point \mathbf{b} . In other words, the intersection of the vectors \bar{e}_2^f with the surface of the flexible product define flowlines.

When expressing the roll angle in flowline reference systems, by definition

$$\frac{DR}{Dk} = 0 \quad (23)$$

so that

$$\frac{\partial R}{\partial k} = -\tau \quad (24)$$

In transient situations, where roll rates at a given position along the route vary over time, the flowlines and hence the family of reference systems change over time.

3.11.8 Twist-induced roll

Introducing a torsion-free set of reference systems, and a longitudinal marking, one can introduce the *twist-induced roll angle* R^* . It is defined as the angle of rotation around \bar{e}_1^w that aligns \bar{e}_2^w (from the torsion free set of reference system) with the longitudinal marking.

This differs from the definition of roll angles relative to the vertical, but has the advantage of not relying on the route being locally in a horizontal plane. The twist-induced roll angle is distinct from the roll angle defined in Section 3.5. Consider a flexible product shaped into a helix, and without torsion. As was discussed in Section 3.5, writhe causes the roll angle to vary along the helix. On the other hand, \bar{e}_2^w (from the torsion free set of reference system) aligns with (or has the same angle to) the longitudinal marking everywhere, so the twist-induced roll is zero everywhere (or at least uniform).

We define

$$\tau \triangleq \frac{\partial R^*}{\partial s} \quad (25)$$

where s is the arc-length coordinate along the flexible product. Where the definition provided in Section 3.6 holds, it is equivalent to the one provided here. The twist is the integral of torsion, so that

$$T(s_a, s_b) = R_b^* - R_a^* \quad (26)$$

Eq. 10 is replaced by

$$\frac{DR^*}{Dk} = \frac{\partial R^*}{\partial k} + \tau \quad (27)$$

which is valid for arbitrary route geometries, including route geometries that change over time.

The advantage of the twist-induced roll rate is that it is well defined for points where the route is not in a horizontal plane. This makes twist-induced roll the definition of choice in the development of computational methods. In fact, it appears naturally when using beam elements.

3.11.9 Writhe in a helix

As discussed in Section 3.8, the writhe is defined between two points along a flexible products. The same applies to twist, but with a significant difference: one can define torsion as the twist per unit length, but as mentioned in Section 3.8, it is not possible to define a “writhe per unit length” which would be a *local* property of the geometry of a flexible product, and which would also be the derivative along the flexible, of the writhe.

In a helix, one can consider a writhe per pitch (since the helix has the same tangent at both ends of a pitch). We consider a helix of pitch p and helix radius a . For a positive helix, $p > 0$, and for a negative one $p < 0$. We introduce

$$b = \frac{p}{2\pi} \quad (28)$$

$$c = \text{sgn}(b) \sqrt{a^2 + b^2} \quad (29)$$

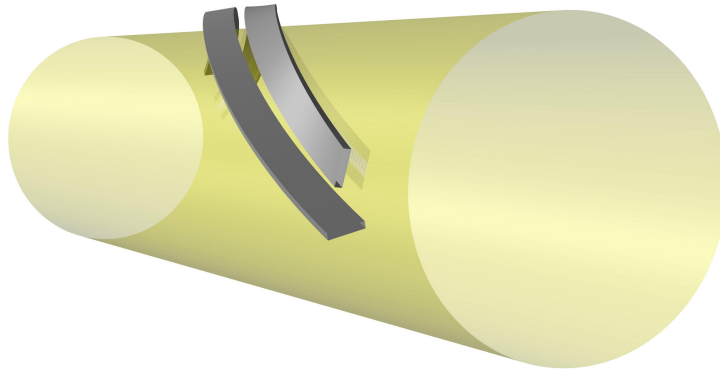


Figure 20: Two tensile armor tendons wound around a flexible product. The left one has zero torsion (and is hence not laid flat), the right one is laid flat (the normal to the wide surface remains parallel with the normal to the cylinder, cf. \bar{e}_2 in Eq. 32).

The helix has equation

$$\bar{x}(\alpha) = \begin{bmatrix} a \cos \alpha \\ a \sin \alpha \\ b\alpha \end{bmatrix} \quad (30)$$

the velocity is

$$\bar{v} = \frac{\partial \bar{x}}{\partial \alpha} = \begin{bmatrix} -a \sin \alpha \\ a \cos \alpha \\ b \end{bmatrix} \quad (31)$$

To help compute the write, we define a family of orthonormal reference systems:

$$\bar{\mathbf{e}}_1 = \frac{\bar{\mathbf{v}}}{c} = \frac{1}{c} \begin{bmatrix} -a \sin \alpha \\ a \cos \alpha \\ b \end{bmatrix} \quad (32)$$

$$\bar{\mathbf{e}}_2 = \begin{bmatrix} -\cos \alpha \\ -\sin \alpha \\ 0 \end{bmatrix} \quad (33)$$

$$\bar{\mathbf{e}}_3 = \bar{\mathbf{e}}_1 \times \bar{\mathbf{e}}_2 = \frac{1}{c} \begin{bmatrix} b \sin \alpha \\ -b \cos \alpha \\ -a \end{bmatrix} \quad (34)$$

Picturing the helix as wound around a cylinder, $\bar{\mathbf{e}}_2$ is normal to the cylinder, pointing inwards. This is the direction of the curvature, so that this is a Frenet-Serret family of reference systems.

The torsion of the family of reference systems (the Frenet-Serret torsion) is

$$\tau = \frac{\partial \bar{\mathbf{e}}_2}{\partial \alpha} \cdot \bar{\mathbf{e}}_3 \quad (35)$$

$$= \frac{1}{c^2} \begin{bmatrix} \sin \alpha \\ -\cos \alpha \\ 0 \end{bmatrix} \cdot \begin{bmatrix} b \sin \alpha \\ -b \cos \alpha \\ -a \end{bmatrix} \quad (36)$$

$$= \frac{b}{c^2} \quad (37)$$

Over a pitch, the length of the helix is $2\pi c$, and we note the writhe as \mathbf{W} . Calugareanu's equation (Eq. 9) can be written

$$2\pi \operatorname{sgn}(b) = 2\pi [c] \frac{b}{c^2} + \mathbf{W} \quad (38)$$

so that

$$\mathbf{W} = 2\pi \operatorname{sgn}(b) \left(1 - \frac{b}{c}\right) \quad (39)$$

The above is valid for any helix, whether this be a flexible product that takes a helical shape, or for components (armor wire, conductor) wound in a helix within the flexible.

In other sciences, the expression would have been $\mathbf{W} = -2\pi b/c$. The difference stems from considering here a straight line to have zero writhe, while in other settings, a circle is considered to have zero writhe.

3.12 Engineering implications

3.12.1 Relativity to longitudinal marking

It is often not practically feasible to have the flexible product free of tension and internal torque when applying a longitudinal marking, so that longitudinal markings may not be ideal

as defined in Section 3.4. As a consequence, we cannot reliably measure *absolute* values of twist, writhe and link, but only their *change* for a given segment, from one time to another.

In contrast, the material roll rate at a given cross-section, does not depend on the position of a dot drawn at that cross-section – it is not affected by the choice of longitudinal marking.

Like twist, writhe and link, the spatial roll rate depends on the longitudinal marking: translating a straight pipe with a wavy longitudinal marking will cause fluctuations of the spatial roll rate.

3.12.2 Measuring roll rates in the absence of longitudinal marking

In the absence of longitudinal marking, it is still possible to mark the flexible product with a dot (an ink mark or a piece of adhesive tape), and to measure the material roll of the mark as the section is transported along a straight segment of the route. Without longitudinal marking, there is no obvious way to measure torsion, and without torsion, it is not possible to use Equation 10 to obtain the spatial roll rate.

Measuring zero material roll (the mark stays on top of the flexible product, for example) does not imply that there is no torsion in the flexible product (see also Section 9.2.1)

3.12.3 Measuring torsion

The Calugareanu theorem (Section 3.9) implies that link (that is, the difference in roll angle between two points along a route) is not the same as twist (which is the accumulated effect (integral) of torsion over the same length). Hence one must be careful when measuring link not to confuse it with twist. Conversely, attempts to force the roll angle to be the same at the top and bottom of a free span in a turntable (or similar) – with the purpose of avoiding torsion – will typically be counterproductive.

A operational case was with the head of a flexible product being latched to the nave of a ship's turntable. Before latching, the head was rotated to zero the link. Because such a span has a writhe that can be significant (90 [deg] is quite common). Forcing the link to be zero will introduce a twist of 90 [deg] (for example, and in absolute value), which over the relative short length of the span, can lead to damaging levels of torsion.

To measure torsion along a general geometry, one needs to know the writhe between the two points. If the flexible follows a “roller highway” that fixes its geometry, one can in principle use a numerically solution (Section 3.11.5) to evaluate the writhe. However, either the roller highway is so tight that one risks to over-stress the flexible (Section 4.7), or the geometry and hence the writhe will vary during the operation. In particular, changes in torque will affect the geometry.

In practice, measuring torsion is done by choosing a segment where the writhe and the flip torque (to be discussed in Section 3.11.5) are both zero. The first choice is a segment which is straight. If this is not practical, then a segment that is within a single plane should be used

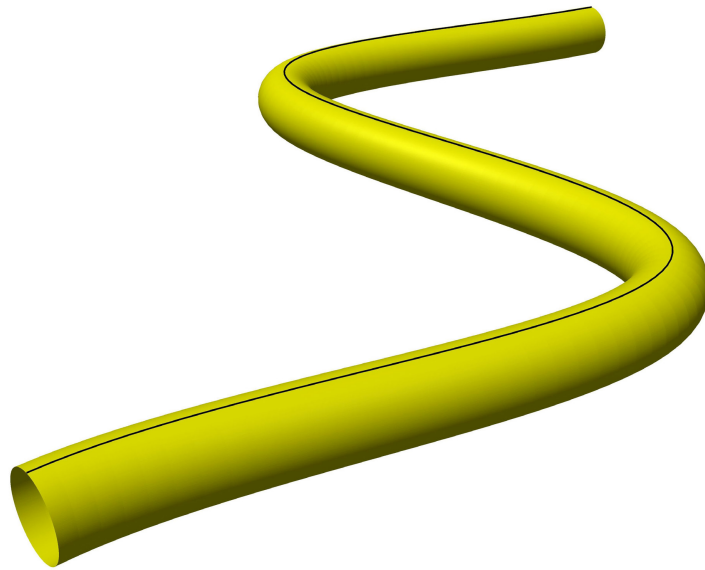


Figure 21: No writhe in segments that are in a single plane.

(Figure 21). Care must be taken that in a route that is nominally in a single plane, torque can cause the flexible product to get out of plane and hence have writhe (cf. Figure 54).

The flexible product must have a longitudinal marking, and the roll angle of the longitudinal marking is measured at both ends of the segments. To evaluate the length L of segment needed to evaluate torsion, one needs to have some idea of the maximum torsion τ that the flexible product can tolerate without failure or without disrupting operations. One must also have some idea of the uncertainty δR with which roll angles are measured. Then the quality q of the torsion measurement is

$$q = \frac{\delta R}{\tau L} \quad (40)$$

If for example $q = 0.05$, (and in the absence of writhe, with an ideal longitudinal marking and assuming uniform torsion) then torsion is evaluated with an uncertainty of 0.05 times the maximum torsion the flexible product can tolerate.

4 Cross-section behavior

4.1 Internal and external torques and moments

The vocabulary of forces in beam theory (which applies to flexible products) is well established and will not be revisited here, except for one point which requires precision: the distinction between *internal* and *external* torques and bending moments.

Considering forces that act in the direction of a beam as an example, it is customary to distinguish between an *axial force*, and *tension* (or compression, or as mathematicians would say, a negative tension). The axial force is applied by an external agent (the pull of a winch – a point force, gravity on a vertical flexible product – a distributed force). If there is a displacement of the point of application of the force, the force produces work, equal to the intensity of the force times the displacement. Scientists would express that by saying that the axial force is the energy conjugate of axial displacement. Tension is an axial force applied by one segment of the beam on the other, it is the axial force acting through the cross-section separating the segments. Tension is the energy conjugate of elongation (axial strain of the flexible product as a whole): think of the energy that would be released if a taut flexible product snapped. Tension is a stress resultant: it can be found by integration of stresses over a cross-section.

Conventional vocabulary is not as precise when it comes to torques: “friction of a flexible product against chutes and rollers applies a *torque* on a flexible product, and the beam carries a *torque*”. In the following, this ambiguity would become problematic, and it is hence necessary to introduce the following definitions:

External torque: The result of one or several external forces acting on the beam. An example is the action of a screwdriver on a screw: there are contact points on the screw head which are off the axis of the screw, and combined, the forces at these contact points exert an external torque on the screw. An example for flexible products is the external torque induced by friction of the surface of a flexible product against chutes, rollers or other coils, thus resisting roll. The energy conjugate of an external torque is roll: think of the effort needed to drive a screw.

Internal torque: The torque induced by one segment of the beam on the next. The energy conjugate of internal torque is torsion: think of the energy stored in a torque bar.

In a bar (or a segment of flexible product), the combination of a positive external torque at the positive end and a negative external torque at the negative end induce a positive internal torque (and a negative internal torque is obtained by swapping the signs of the external torques).

Consider a straight beam, clamped at the left end and free to rotate at the right. Let us say that no external torque is applied at the right end, but external torques are applied at points along the beam (Figure 23, top). In that case, the external torque per unit length is the derivative along the beam of the internal torque, and the internal torque at the right end is zero (Figure 23 a) and b)).

An external torque is positive if it tends to cause a positive roll. Since the sign of roll depends on the choice of a positive direction along the flexible product (Section 3.5), so does the sign of

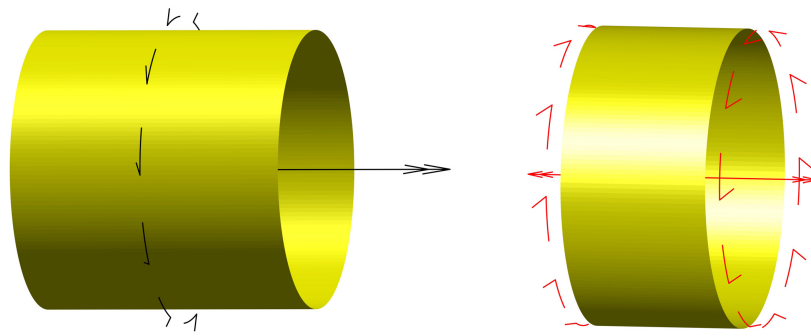


Figure 22: External (left) and internal (right) torque.

external torque. An internal torque is positive if it tends to create a positive torsion. Since the sign of torsion does *not* depend on the choice of a positive direction (Section 3.6), neither does the sign of internal torque. In Figure 23 a) and b), the positive direction was chosen from left to right. Figure 23 c) and d) shows the same physical situation, with the positive direction chosen from right to left. Note that the external torque is still the derivative of the internal torque. For curved beams, the external torque is not the derivative of the internal torque (Sections 5 and 5.5).

For curved beam, the relation between internal and external torque becomes more complicated (cf. the mathematical description in Section 5.5), and indeed, there are several ways to introduce internal torque in a flexible product without applying an external torque (Sections 5 and 6.6).

All the above applies - with the necessary changes, to bending moments as well.

4.2 Curvature diagrams

At a given cross-section, one can introduce two vectors of unit length \bar{e}_2^l and \bar{e}_3^l . They are both in the plane of the cross section, and they are orthogonal to each other. \bar{e}_2^l is chosen to be pointing from the axis of the product towards the longitudinal marking.

The curvature vector $\bar{\kappa}$ has a length equal to the curvature, is in the plane of the cross-section and in the plane of curvature. $\bar{\kappa}$ points inside the curvature (on the concave side of the product).

One can represent the curvature at that cross-section as a point on a graph (Figure 24). κ_2 is the curvature in direction \bar{e}_2^l , while κ_3 is the curvature in direction \bar{e}_3^l . One can write

$$\bar{\kappa} = \bar{e}_2^l \kappa_2 + \bar{e}_3^l \kappa_3 \quad (41)$$

Figure 25 shows the curvature diagram of a cross-section that is originally straight, then curved so that the longitudinal marking is inside the curvature, straightened, and then bent so that the longitudinal marking is outside the curvature. Figure 26 provides another example, with a cross-section that is original curved, and which curvature is then changed in direction (relative to the longitudinal marking) but uniform in intensity.

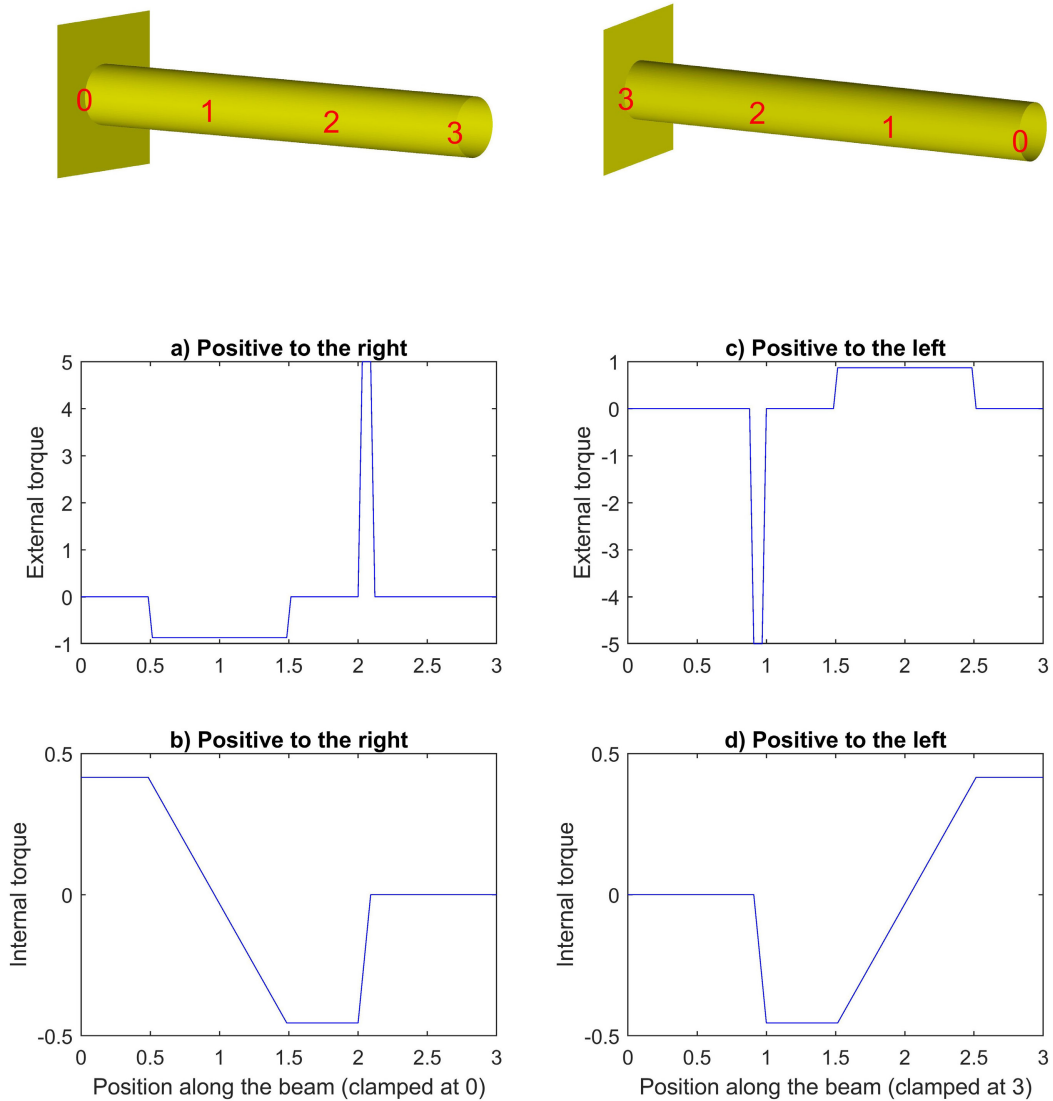


Figure 23: Diagrams of external and internal torque along a cantilever beam, for the two possible choices of positive direction along the beam.

4.3 Moment-curvature diagram

A bending moment is required to change the curvature of a cross-section. Figure 27 shows the relation between curvature and bending moment during loading (increasing curvature starting from a straight configuration) for a typical flexible product. The black curve is typical of what would be measured in a test rig. For low curvature, all components are sticking to each other, and the whole cross-section nearly behaves like a solid, with a high bending stiffness. As components start to slip with respect to each other, the stiffness progressively decreases until most of the length of each components slipping, and the stiffness is the sum of the bending stiffnesses of the components. This is the near-horizontal part of the black curve. As curvature further increases, the stiffness builds up again because of the “curvature-pressure instability” (Section 8.3).

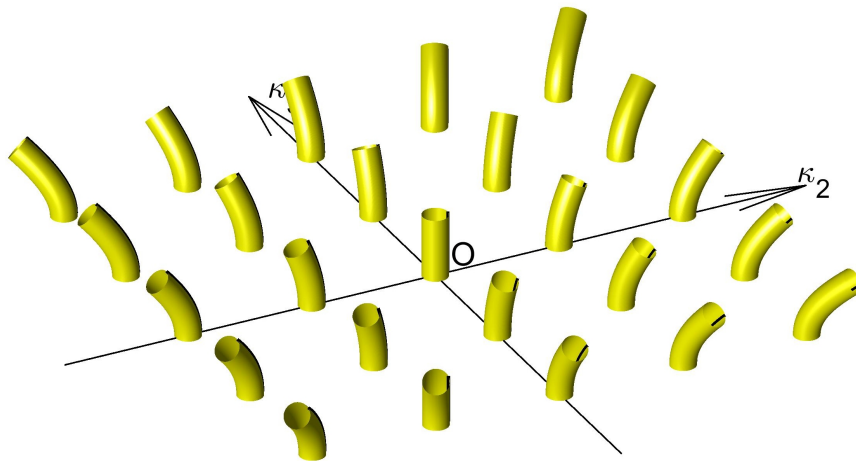


Figure 24: Curved flexible products placed on the corresponding point on a curvature diagram.

In the following, it will be convenient to work with a simplified form of the moment-curvature curve (in red in Figure 27). Two simplifications are introduced. First, there is an abrupt transition between the steep “stick” part of the curve and the slack “slip” part at the slip curvature κ_{slip} . This is because κ_{slip} is typically much smaller than the curvatures applied during operation. For large cross-sections, κ_{slip} is much smaller, compared to the maximum allowed curvature $1/\text{MBR}$ than suggested by Figure 27. Hence, details of this transition are not important. The second simplification is not as innocent however: The secondary increase in stiffness because of bending-pressure instability is ignored.

The bending moment in the slip part of the idealized (red) curve is the sum of two contributions:

Elastic moment: The sum of the bending moments of the individual components making up the cross-section. Assuming that there is no plastic deformation of the components, this moment is zero at zero curvature, and increases linearly with curvature.

Friction bending moment: The moment generated by friction between the components. If the simplification presented in the red curve applies, this moment is independent of the intensity of the curvature. This moment is noted M_f for “friction bending moment”. Figure 27 shows how M_f can be evaluated from test data, by finding the tangent to the slackest point of the moment curvature curve, and finding the point where it cuts the y-axis of the diagram. The friction bending moment plays a key role in some torsion-related problems (Section 5).

The friction bending moment strongly depends on the contact pressure between the components. This contact pressure depends on the production process (for example, shrinkage of extruded sheaths, tension of plies, pre-bending of tensile armor), on the temperature, and the temperature history (because of creep in materials). It also depends on the tension, and torsion (which both change the tension in helical components, and the contact pressure with layers inside and outside of these components). Further, it depends on the curvature, which generates friction, thus tension in the component, affecting contact pressures. As a consequence the friction bending moment is variable during an operation, and hard to calculate.

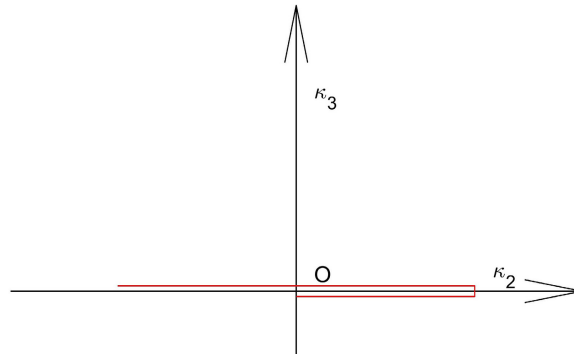


Figure 25: Curvature diagram of a cross-section, that is first straight, then bent with the marking inside the curvature, then bent back in the opposite direction.

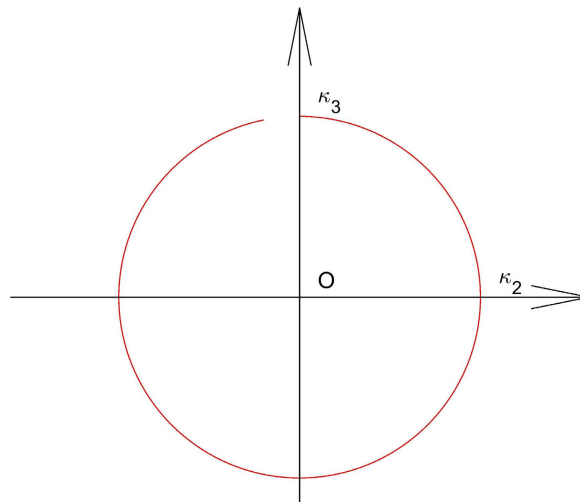


Figure 26: Curvature diagram of a bent cross-section rolling around itself.

Another effect is that some flexible products are built using viscous fluids. These can be used as a form of corrosion protection, or as an electrical insulator in mass-impregnated flexible products. Viscosity implies that friction forces also depend on *rates* of sliding. This effect will *not* be accounted for in the following, unless explicitly mentioned. This amounts to assuming that the friction bending moment does not depend on how fast a given change of curvature occurs.

Some of the components of the flexible product may undergo plastic deformation under bending. This would be the case for example for polymer or lead sheaths, which have large diameters, and are thus subjected to high strains. The above reasoning still holds, but the expression “friction bending moment” must then be understood to stand for a more general “dissipative moment” which is the sum of the moment needed to overcome friction, and the moment needed to drive additional plastic deformation.

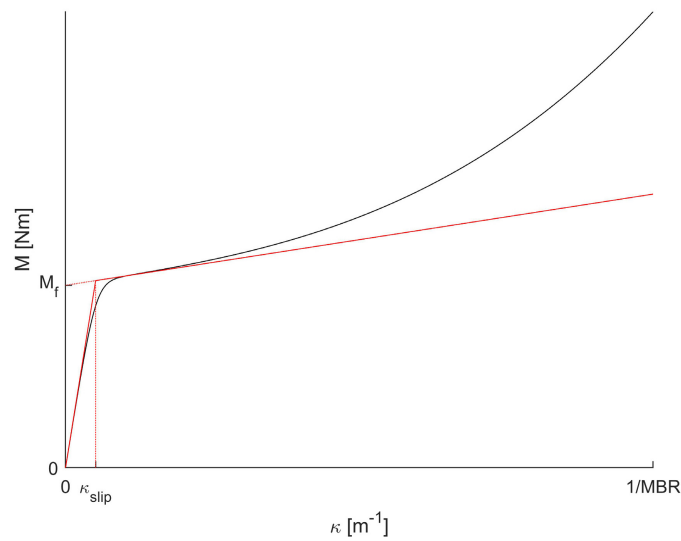


Figure 27: Typical moment curvature diagram of a flexible product. Realistic curve (black) and idealized (red). “MBR” is the minimum bending radius of the flexible product.

4.4 Drawing a moment in a curvature diagram

The arguments in the remainder of Section 4 consider reference systems, but it is not relevant whether this reference system is part of a Frenet-Serret, torsion-free, or longitudinal marking type of family of reference systems. A positive internal bending moment around the \bar{e}_2 axis causes a negative curvature $\kappa_3 < 0$. A positive bending moment around the \bar{e}_3 axis causes a positive curvature $\kappa_2 > 0$ (Figure 28).

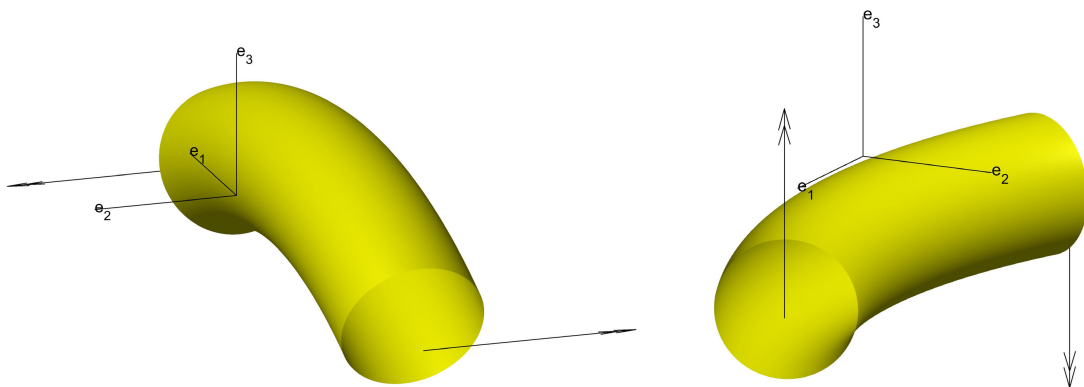


Figure 28: Left: Bending moment $\bar{M} = M_2\bar{e}_2$ in positive \bar{e}_2 direction causes curvature $\bar{\kappa} = -\kappa\bar{e}_3$. Right: Bending moment $\bar{M} = M_3\bar{e}_3$ in positive \bar{e}_3 direction causes curvature $\bar{\kappa} = \kappa\bar{e}_2$.

A point in the curvature diagram, and the associated elastic curvature would look like Figure 29.

In Figure 30, the axes for the curvatures (but not the moments) have been changed, so that the elastic bending moment is shown as an arrow that points in the same direction as the

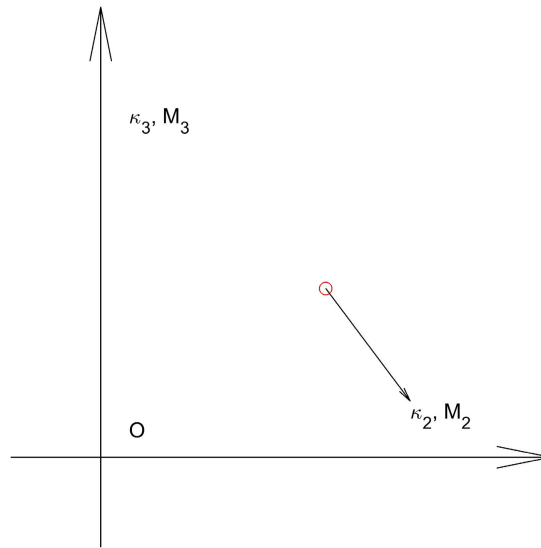


Figure 29: A curvature diagram with the curvature (red circle) and the corresponding moment (arrow).

corresponding curvature. The reader that has studied Section 5.5 will note that $\kappa_2 = \omega_3$ and $-\kappa_3 = \omega_2$.

4.5 Complex curvature histories

As mentioned, the curvatures forced on flexible products during handling are usually considerably higher than the slip curvature κ_{slip} . Hence in practice, it is sufficient to study what happens in the slip domain. Let us consider the two contributions to bending moment described in Section 4.3.

The elastic moment is shown in Figure 31 as red-colored arrows. Several comments are needed. The axes follow the system presented in Figure 30. While this is a curvature diagram, the arrows represent bending moments, so there is a discrepancy in units. The moment arrows are shown with origins at the relevant point along the curvature curve, for readability¹. The red arrows are all on a line going through the origin, and the length of the arrow is proportional to the distance to the zero-curvature origin: the elastic moment is proportional to the curvature.

The friction bending moment is shown in Figure 31 as black-colored arrows. The arrows are tangent to the curvature diagram, and are all of the same length: the moment that needs to be applied to overcome friction in order to change the curvature is always in the direction of the change of curvature, and has intensity equal to M_f , (see Figure 27).

This form of diagram will be exploited in Section 5.

¹The drawback is that this may be misleading: the arrows do not represent forces, their origin do not represent a point in space, and hence there is no question of finding the arm of a force to compute a moment.

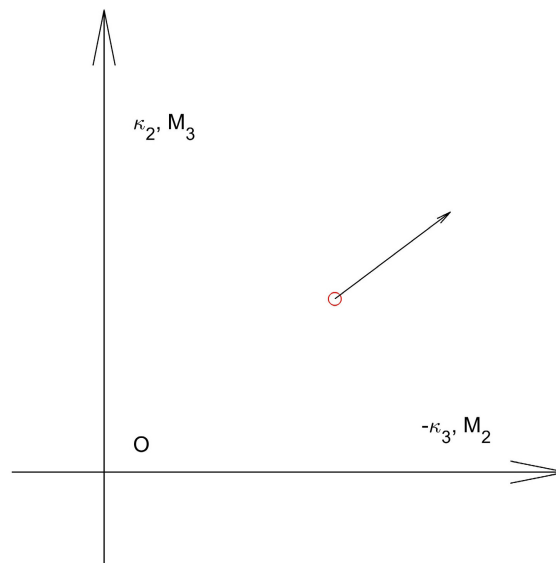


Figure 30: A curvature diagram with the curvature (red circle) and the corresponding moment (arrow). Note the swapping of the moment components on the axes, and the change in sign, compared to Figure 29.

4.6 Residual curvatures

Flexible products can have residual curvature: they can have a curvature in the absence of bending moment. This can come about in several ways. First, as discussed in Section 4.5, internal friction implies that when bent and then released, a flexible product will often almost not spring back. Second, polymer sheaths, lead sheaths, low-alloyed copper or aluminium conductors and so forth can undergo (instantaneous) plastic deformation, or they can creep while coiled in storage. In the context of Section 4.5, a residual curvature means that the curvature history does not start at the origin in a curvature diagram (Figure 31).

Residual curvatures due to creep have a particular effect if for example a polymer sheath, that has crept while coiled, retains its residual curvature during an operation: superimposed to the forces depicted in Figure 31, the polymer sheath will tend to bring back the flexible product to the coiled curvature. This can lead to an instability described in Section 8.5, which has been documented at least for steel pipelines under S-lay or reeling.

4.7 Non-uniform curvature

In Sections 4.2, 4.3, 4.4 and 4.5, it is assumed that the moment at a given cross-section is related to the curvature *at that cross-section*. This is a reasonable approximation when the curvature is uniform (in intensity and orientation) over lengths “significantly” larger than the pitch length of components. What is “significant” will depend on the level of friction (the *lower* it is, the further slip propagates, the worse the approximation). The effect might be most noticeable in flexible products that are designed with low friction between components and low laying angles.

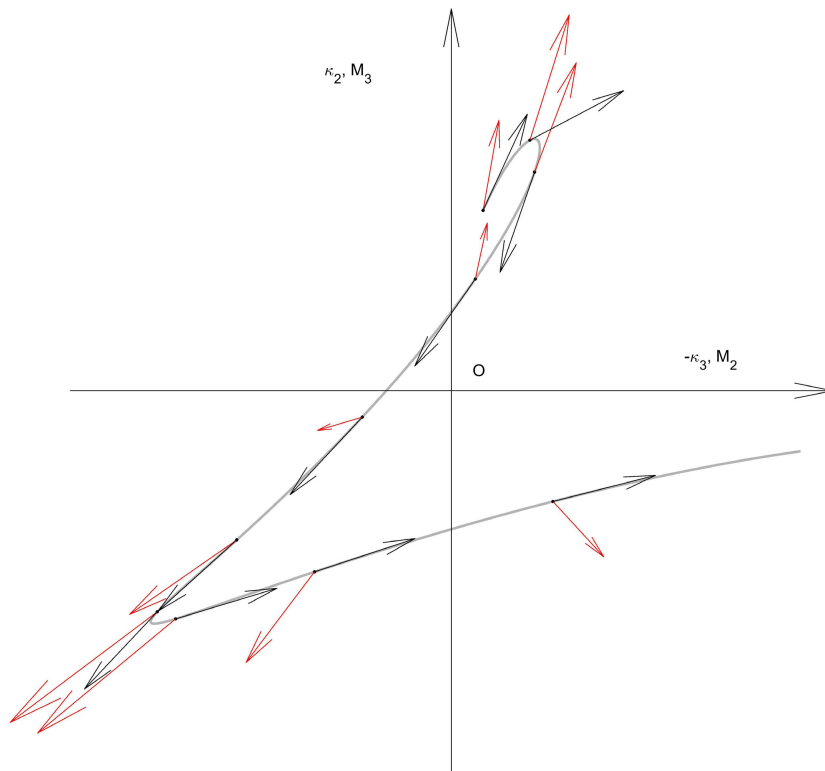


Figure 31: Bending moment in the slip domain.

Consider a flexible product which has an outer and inner tensile armor, wound over each other in opposite directions (a design typical of “dynamic” applications). We assume the flexible product has taken a helical shape (of small amplitude) with the same sign and pitch length as its inner tensile armor (Figure 32). One of the threads (marked in red) of the armor is hence on the outside of the helix over the whole length of the flexible product: the thread is elongated, can not relieve its stress by slipping, and carries large tensile forces. Correspondingly the green thread is heavily compressed: The bending moment in the cross-section is much higher than if the flexible product had been subject to the same curvature within a given plane.

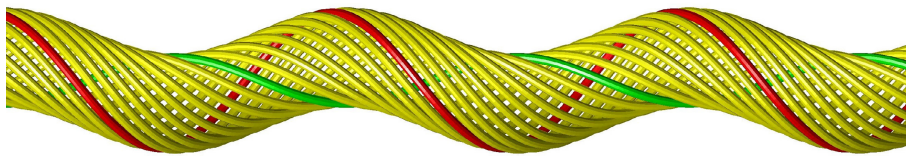


Figure 32: A flexible product following a helix of same pitch length as its tensile armor.

Another example can be borrowed from beam theory: consider a solid beam on which two opposing bending couples are applied: between the couples, the beam has uniform curvature. Outside of the couples the beam is straight. If we replace the beam with a flexible product containing helical components (Figure 33), so that the couples are half a pitch length apart, then the curvature will not be uniform between the couples and will be non-zero close to the

couples and *outside* of them. The difference between beam and flexible product lies in the helical components: the tensile wire or component that is at the top of the product, halfway between the couples would elongate, but avoids that by pulling in length from beyond the couples, leading to some curvature there too.

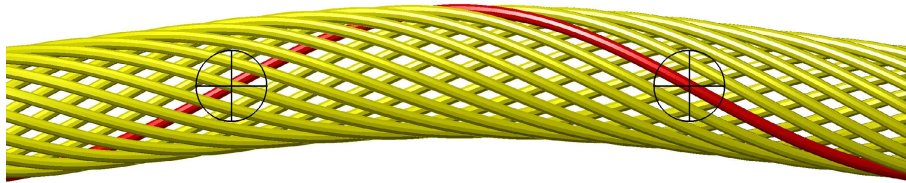


Figure 33: A flexible product subjected to two opposite bending couples (marked), half a pitch length apart.

Non-uniform curvature can be an important effect to consider in several settings:

1. It might affect the internal torque at which helical buckling occurs (See Section 8.6).
2. It must be considered when creating routes: while slow change of curvature plane cause high flip torques, rapid changes of curvature plane can cause high stresses and make the procedure outlined in Section 16 questionable.

Creating software to compute these effects accurately and fast is expected to be a significant challenge, for at least two reasons. First, this requires a good mathematical model of friction at low levels of tension in the components. Second, numerically solving the sliding of components at this level of detail requires high computing power, and will require to deal with convergence problems.

4.8 Torsionally unbalanced cross-sections

A flexible product is torsionally unbalanced if putting it under tension tends to unwind it. A left-laid rope (components are wound as negative helices, Figure 34, top), when forced to elongate, tends to unwind (Figure 34, bottom). A longitudinal marking on the rope becomes a positive helix: the rope has positive torsion.

Flexible products can be designed to be torsionally unbalanced for several reasons, including cheaper production (using only one tensile armor, or even none), and low torsional stiffness in the unwinding direction, which is beneficial for storage in baskets (Section 9.4). On the other hand, torsional unbalance can lead to challenges under pull-in operations (Section 9.6). Torsional balanced products are more suitable when they will carry their own weight under operation – for example for power flexible products between a floating wind turbine and the seafloor, or an umbilical connecting an offshore oil platform to a subsea template.

Torsional unbalance creates an interesting interplay between elongation and torsion on the one hand, and tension and internal torque on the other hand. If the rope is set under a given tension, it will elongate more if allowed to unwind than if the ends are restrained from rolling.

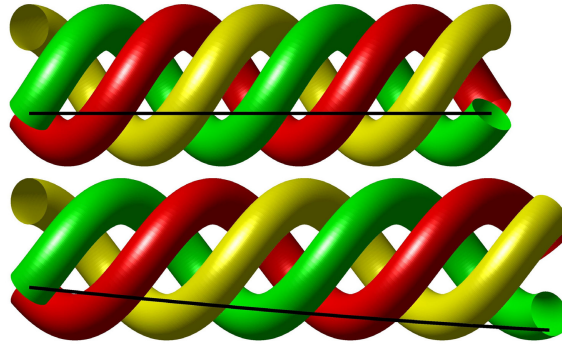


Figure 34: A torsionally unbalanced “rope” (top) unwinding under tension (bottom).

Similarly, if the rope shown in Figure 34 is subjected to a negative (respectively, positive) internal torque, it will have a higher torsion if it is allowed to shorten (respectively, elongate). The torsion in the absence of internal torque depends on the elongation (the higher the tension, the more unwinding occurs). This is why in Section 3.4, ideal longitudinal marking is defined as being straight when the flexible product is “not subjected to any external forces, including in particular tension or internal torques”. Similarly, the elongation in the absence of tension depends on the torsion (an unwound rope is longer than a tightly wound one).

The relation between elongation, torsion, tension and internal torque is generally non-linear in several ways. It takes less internal torque to unwind a flexible product to a given level of the torsion, than it takes to wind the same product the other way (tight direction). Also, internal friction plays a role: one can pre-stretch and pre-twist a flexible product.

Still, it can be useful to work with a linearized form of the relation between elongation ε , torsion τ , wall tension R_1 (see Section 4.9) and internal torque M_1 . This can be written

$$R_1 = K_\varepsilon \varepsilon + K_{\varepsilon\tau} \tau \quad (42)$$

$$M_1 = K_{\varepsilon\tau} \varepsilon + K_\tau \tau \quad (43)$$

It is sometimes convenient to use these equations in matrix form:

$$\begin{bmatrix} R_1 \\ M_1 \end{bmatrix} = \begin{bmatrix} K_\varepsilon & K_{\varepsilon\tau} \\ K_{\varepsilon\tau} & K_\tau \end{bmatrix} \cdot \begin{bmatrix} \varepsilon \\ \tau \end{bmatrix} \quad (44)$$

The coefficient K_ε is the axial stiffness at restrained rotation. K_τ is the torsional stiffness at restrained elongation. $K_{\varepsilon\tau}$ appears twice: it is the internal torque that must be applied to keep torsion to zero, for a unit elongation. It is also the axial force that must be applied to resist elongation, for a unit torsion.

4.9 End-cap effects

Consider a segment of steel pipe, with bore cross section A_i and outer cross section A_e . The pipe has end caps, and each end cap is connected to a wire. The tension in the wires is R_1^e (let

us assume the segment is so short that its weight is negligible). If the internal pressure in the pipe is P_i and the external pressure is P_e , then the tension carried by the wall of the pipe is

$$R_1^w = R_1^e + A_i P_i - A_e P_e \quad (45)$$

In other words, internal pressure forces the end caps apart, and the resulting force is taken up as additional tension in the wall. External pressure forces the end caps together, decreasing the tension in the wall. R_1^w and R_1^e stand respectively for *wall* and *effective* tension [60].

Equation 45 is also valid for flexibles, and (with the exception of flexibles that are constrained and held from deforming) in the absence of end caps. For example, we consider the offshore installing of a cable. In this case, $A_i = 0$. At any point p along the free span, P_e is the hydrostatic pressure, and (neglecting shear force at touch down point) R_1^e is calculated by integrating the submerged weight of the cable from the touch-down point to p .

R_1^e is used in “global” analyses of the laying configuration, including the effect of currents and dynamic response (to waves and vortex-induced vibrations). The effective tension is to be used when assessing the risk for helical buckling, and other “global” buckling (where the flexible as a whole).

R_1^w is the force experienced by the cable. It is to be used when assessing all forms of “local buckling” (with deformations of the cross section and individual components of the flexible). It is also to be used when evaluating torsion due to torsional imbalance (Equation 44).

In principle a similar distinction should be introduced between effective and wall torque. However this would only be relevant when handling an umbilical with tubes under high pressure, arguably not a relevant scenario. In practice effective and wall torque are thus the same.

In the absence of internal pressure, and in shallow water, the distinction between R_1^w and R_1^e is irrelevant. This can be established by comparing $A_e P_e$ at the depth of the sea floor, with the tension R_1^e expected at the touch-down point.

5 Flip torques

5.1 Preliminaries

Consider a straight flexible rod of rectangular cross-section: the rod is stiffer against bending in the plane containing its long faces (the strong axis) than in the plane containing its short faces (the weak axis). If one tries to bend the rod along its strong axis, it will tend to flop (lateral torsional buckling), that is, to roll to present its weak axis to the curvature.

Consider a bent segment of flexible product. We wish to cause it to roll without changing the (vertical) plane within which it is bent (Figure 35). This deformation will cause plastic deformations, and/or slip of helical components, and hence dissipated energy in the form of heat. Hence to achieve this deformation, an external torque (or one external torque at each end, with both torques not necessarily equals) must be applied. Most electrical power cords (with a few exceptions that are almost perfectly elastic) will be convenient to make a small experiment.

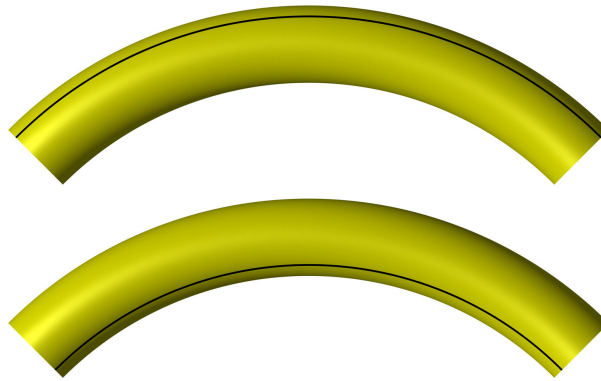


Figure 35: Inducing a curved flexible product to roll requires external torque.

Figure 36 shows another deformation in which the plane of curvature is changed, but the the roll angle is kept constant. A cross-section that is transported along a route with curvature in different planes will experience this kind of deformation. It can be seen that the segments in the lower halves of Figures 35 and 36 are identical, except for a stiff body rotation. Hence getting to the lower half of both figures caused exactly the same plastic deformation and slip, and thus required the same external torque.

The torque that one needs to apply to the segment to thus reshape the flexible product (Figure 36) can be considerable. Consider a segment of flexible of length λ , that has a uniform curvature κ , and friction bending moment M_f (Section 4.3). The required torque, if we disregard the sign, has absolute value (Section 4.5)

$$\Delta M_1 = \lambda \kappa M_f \quad (46)$$

The length times the curvature is the angle α (in radians) of the bend, so that [19]

$$\Delta M_1 = \alpha M_f \quad (47)$$

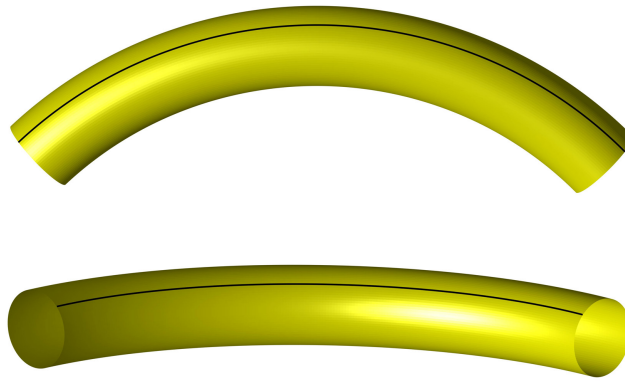


Figure 36: Deformation with zero roll but change of curvature plane.

This is an important result: the torque that must be applied to overcome friction and roll the flexible is independent of whether the curve is short and sharp or long and progressive, it depends only on the angle of the turn (half turn, quarter turn and so forth).

The torque that needs to be applied switches sign as the roll rate switches sign (Figure 37). If the roll rate is zero, no deformation occurs, all components stick (do not slip), and the flexible line behaves as if it was an elastic solid. So with a roll rate of zero, the torque can be anything between $-\alpha M_f$ and αM_f (just like in a contact without slip, the shear contact force can be within a range of values). But, other than that, the torque that needs to be applied is independent of the roll rate: rolling fast and rolling slow in the same direction requires the same torque to be applied.

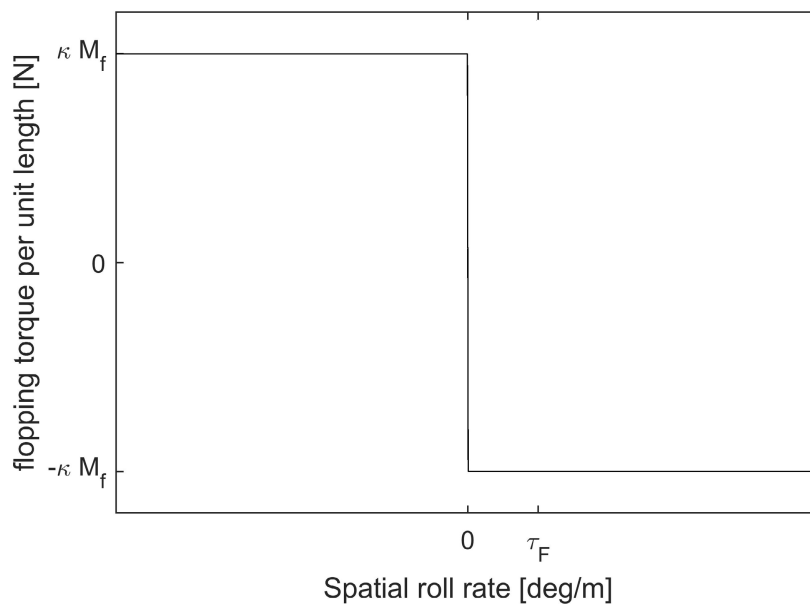


Figure 37: Effect of the spatial roll rate per unit length on the flip torque for a bend.

5.2 Transport along a route with change of curvature

Assuming M_f to be independent of curvature and torsion, let us consider a segment of route with uniform curvature κ . Along the segment, the curvature changes plane, and this change occurs progressively over a length λ . One example would be a segment of positive helix (Figure 38), in which the rate of change of the curvature plane is uniform.

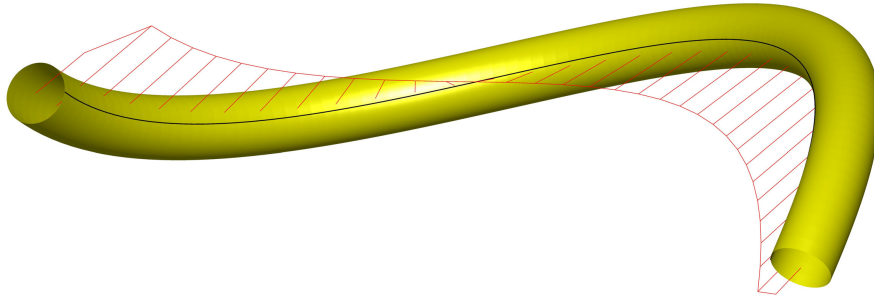


Figure 38: As a cross-section is transported along the route, it experiences curvatures in changing directions (relative to the longitudinal marking) - it needs to be re-bent, and tends to flop.

We now further assume that the flexible product is transported along the route, and that the material roll rate at any point is equal to zero. As a consequence, at any time, all the cross-sections transported over the length λ will experience a change of curvature plane: the rate may differ, but the change of curvature plane is assumed to occur in the same (in Figure 38: positive) direction. The torque that needs to be applied, per meter of length, to overcome this is κM_f , independently of whether the plane of curvature changes fast or slowly along the route. The total torque that must be applied to the segment to overcome friction over the length λ is hence

$$|\Delta M_1| = \lambda \kappa M_f \quad (48)$$

The torque that must be applied to the segment to overcome the friction is equal to the product of the length over which the change of curvature plane occurs, the curvature, and the friction bending moment. *The amount of change of curvature plane does not play a role, only the length over which the change occurs.* This result is important, and is quite counter intuitive.

In practice “the torque that must be applied to the segment” is applied by the neighboring lengths of flexible product: the sum of the torque exerted on the segment by the upstream and downstream lengths must have absolute value $\lambda \kappa M_f$. How much torque is exerted by the upstream and downstream segment depends on many factors, it’s a special case of a *hyperstatic* structure. By the law of action and reaction, the segment applies to its neighbors the opposite torques that the neighbors apply to it. Hence the segment applies to the line as a whole a torque with absolute value $\lambda \kappa M_f$. In many respects (but not all, for mathematical details, see Section 5.5) this is as if “a troll with a pipe wrench” was gripping the segment and applying a torque to it: the “flip torque”.

The sign of the torque can be found intuitively by looking at the direction in which the segment would roll in order to keep the same material point on the inside of the curvature, as transport

progresses. For a positive “helix” (more precisely, for a positive Frenet-Serret torsion, as the rate of change of curvature does not need to be uniform) as shown in Figure 38, the torque is in the positive direction.

The flip torque can be seen as the product of M_f and $\lambda\kappa$. The second term is a characteristic of the geometry of the route: if a route is exactly known (because a flexible is boxed in by rollers), then one can compute the “quality of the route” and compare route designs against each other, independently of the flexible. In practice however, different flexible products will follow slightly different routes, and these differences can impact the “quality” significantly.

Typical routes do not have uniform curvature, or uniform rate of change of the curvature plane. For these cases, Equation 48 must be replaced by a complex expression (Section 5.5).

5.3 Effect of roll rates

Let us consider the above example, but with a modification: while the flexible product is transported (towards the left, defined as the positive direction), the flexible product has a non-zero positive spatial roll rate. We assume torsion to be zero, so that spatial and material roll rates are identical. This is a reasonable approximation, as long as the torsion in the flexible product is small compared to the Frenet-Serret torsion of the segment of route.

For small roll rates, the situation is identical to the one described in Section 5.2: the segment applies a positive flip torque to the rest of the flexible product.

As the spatial roll rate increases (Figure 39), the point eventually arrives where a material point rolls (material roll rate) so as to exactly follow the change of curvature plane of the route. The material roll rate is equal to the Frenet-Serret torsion: the cross-section does not experience relative changes of the direction of the curvature plane, so no moment is generated.

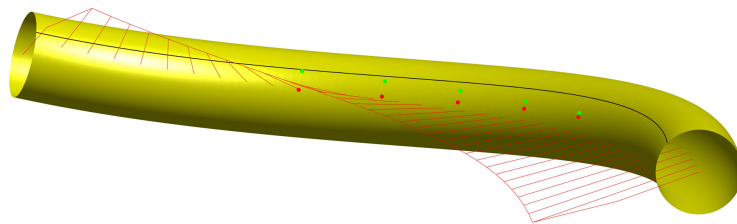


Figure 39: Effect of roll rate. Red: a material point transported with zero material roll rate experiences a change in the direction of curvature. Green: with a non-zero material roll rate, the material point can be made to follow the change in the direction of curvature.

Beyond that point, the flexible is rolling “too much”, and a material point sees the plane of curvature changing orientation in the negative direction, and the flip torque becomes negative. One can make a graph of the flip torque as a function of the spatial roll rate (Figure 40).

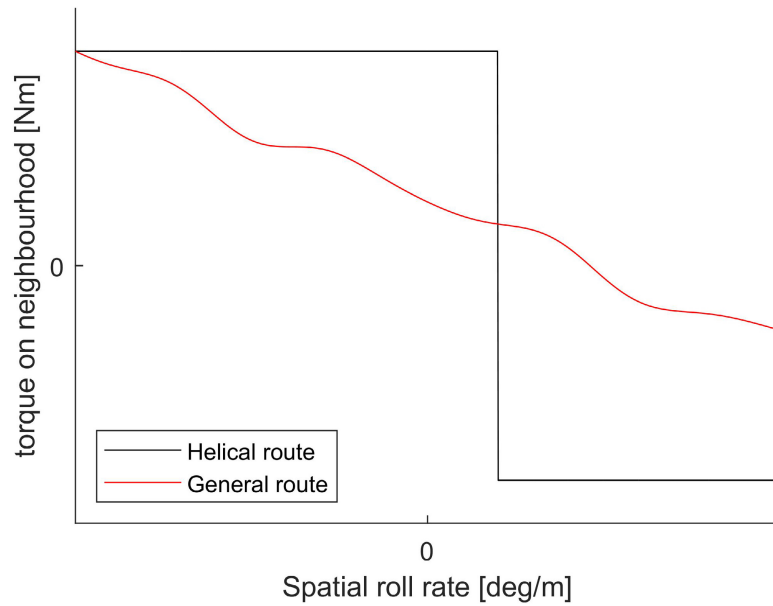


Figure 40: Effect of the spatial roll rate on the flip torque for a helical route (black) and an example of general route (red).

For a negative helix, Figure 40, black curve, remains the same, but the spatial roll rate at which the torque changes sign is negative.

In a more realistic free span, curvature and rate of change of the curvature plane are not uniform, and this results on a more progressive effect of the spatial roll rate on the internal torque. Figure 40, right provides an illustration of how such a relation might look like. If the geometry of the route is more like a positive helix, then the torque at zero spatial roll rate will be positive (as in Figure 40, red curve), otherwise negative.

5.4 Pseudo-external flip torque

The flip torque induced by transport over a segment introduces a difference between the upstream (**a**) and downstream (**b**) internal torque:

$$\Delta M_F = M_a - M_b \quad (49)$$

A positive flip torque cause the torque to decrease as one follows the route from **a** to **b**. Curves with positive Frenet-Serret torsion, including positive helices, and the touch down point area in a basket or turntable where the product is coiled clockwise.

The flip torque is not an external torque: curved beam theory (Section 5.5.1, Eq. 51) shows that a torsional moment can appear in a curved beam in the absence of external torque. One example of this is a wrench: a tool for applying torques on nuts and bolts, which is used by applying a force to the handle to the wrench. Indeed, flip torque are often encountered in free spans where nothing comes into contact with the flexible product.

However, deliberately misrepresenting the flip torque as if it was an external torque can be useful to develop an intuition for which way things go. Equation 63 shows that the change in internal torque along the route is caused by the sum of external torques and flip torque, so a flip torque can be imagined to be an external torque of the same sign (Figure 41). In the figure, the internal torque decreases as one moves into the figure.

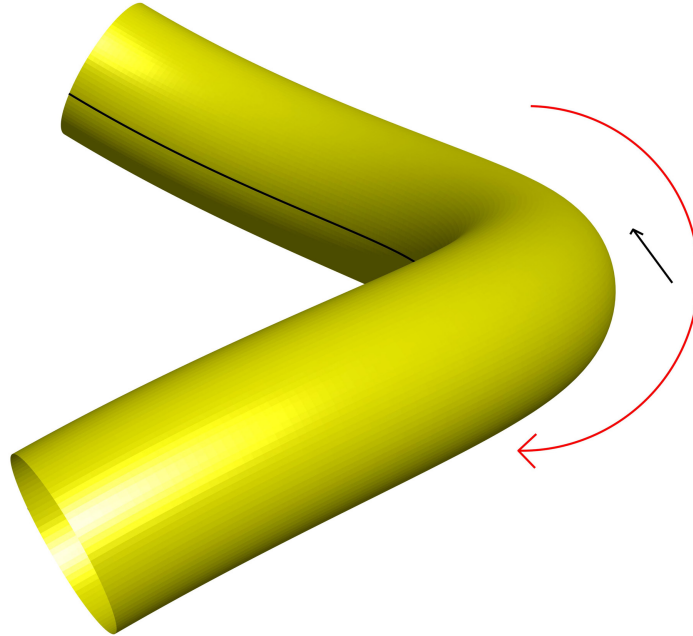


Figure 41: Positive pseudo-external flip torque (red arrow) in a positive helix, with transport (black arrow).

Swapping the direction of transport swaps the direction of the pseudo-external flip torque. If one swaps the coordinate system together with the direction of transport, the pseudo-external torque remains positive. Hence the rule of thumb “[pseudo-] external flip torque is positive in positive helices” and curves with positive Frenet-Serret torsion.

5.5 Mathematical formulation

5.5.1 Equilibrium

Considering an infinitesimal beam segment of length $d\mathbf{z}$ and of tangent unit vector $\bar{\mathbf{t}}$, force equilibrium can be written

$$\frac{\partial \bar{\mathbf{R}}}{\partial z} = -\bar{\mathbf{f}} \quad (50)$$

$$\frac{\partial \bar{\mathbf{M}}}{\partial z} = -\bar{\mathbf{m}} - \bar{\mathbf{t}} \times \bar{\mathbf{R}} \quad (51)$$

where $\bar{\mathbf{R}}$ and $\bar{\mathbf{M}}$ are the forces and moments resultant vectors, $\bar{\mathbf{f}}$ and $\bar{\mathbf{m}}$ are external distributed forces and moments acting on the beam, and \times is the cross product.

In the above, all the terms are vectors, in the sense of objects existing independently of the choice of reference system. Consider a family of orthonormal reference systems $\bar{\mathbf{e}}(\mathbf{z})$ such that any point \mathbf{z} , $\bar{\mathbf{e}}_1 = \bar{\mathbf{t}}$. The evolution of the *components* of the above vectors, in that family of reference systems can be shown to be

$$-\frac{\partial \mathbf{R}_1}{\partial \mathbf{z}} = \mathbf{f}_1 + \omega_2 \mathbf{R}_3 - \omega_3 \mathbf{R}_2 \quad (52)$$

$$-\frac{\partial \mathbf{R}_2}{\partial \mathbf{z}} = \mathbf{f}_2 + \omega_3 \mathbf{R}_1 - \omega_1 \mathbf{R}_3 \quad (53)$$

$$-\frac{\partial \mathbf{R}_3}{\partial \mathbf{z}} = \mathbf{f}_3 + \omega_1 \mathbf{R}_2 - \omega_2 \mathbf{R}_1 \quad (54)$$

$$-\frac{\partial \mathbf{M}_1}{\partial \mathbf{z}} = \mathbf{m}_1 + \omega_2 \mathbf{M}_3 - \omega_3 \mathbf{M}_2 \quad (55)$$

$$-\frac{\partial \mathbf{M}_2}{\partial \mathbf{z}} = \mathbf{m}_2 + \omega_3 \mathbf{M}_1 - \omega_1 \mathbf{M}_3 - \mathbf{R}_3 \quad (56)$$

$$-\frac{\partial \mathbf{M}_3}{\partial \mathbf{z}} = \mathbf{m}_3 + \omega_1 \mathbf{M}_2 - \omega_2 \mathbf{M}_1 + \mathbf{R}_2 \quad (57)$$

where ω_i are the components of the rotation rate vector of the family of reference systems (cf. Section 3.11). This way of rewriting the force equilibrium equations is convenient because, thanks to the choice of reference system, \mathbf{R}_1 is the axial force, \mathbf{R}_2 and \mathbf{R}_3 are shear forces, \mathbf{M}_1 is the internal torque, and \mathbf{M}_2 and \mathbf{M}_3 are internal bending moments.

In Equation 55, \mathbf{m}_1 is an external distributed torque. Such an external torque can be caused by friction against external surfaces when the beam rolls around itself.

If the bending moment components are proportional to the rotation rate components ($\mathbf{M}_2 = \alpha \omega_2$ and $\mathbf{M}_3 = \alpha \omega_3$), then the term $\omega_2 \mathbf{M}_3 - \omega_3 \mathbf{M}_2$ vanishes. Further, in Equation 55, the term is added to \mathbf{m}_1 : $\omega_2 \mathbf{M}_3 - \omega_3 \mathbf{M}_2$ can be seen as an external torque (the flip torque) applied to the beam, that arises when the curvature and the bending moment are misaligned.

This interpretation is imperfect: Substituting $\omega_2 \mathbf{M}_3 - \omega_3 \mathbf{M}_2$ with an external moment of the same value works fine, but setting \mathbf{M}_2 and \mathbf{M}_3 to zeros in Equations 56 and 57 changes these equations.

Because at any time $\partial \mathbf{z} / \partial \mathbf{s} = 1$, all the above equations can also be written with derivatives relative to the route coordinate \mathbf{s} instead of the line coordinate \mathbf{z} .

5.5.2 Integration along the route

We introduce a flowline family of reference systems $\bar{\mathbf{e}}^f$ (Section 64). This is chosen because the $\bar{\mathbf{e}}^f$ reference system follow material roll of the cross-section, making it convenient for the expression of friction-induced moments. Curvatures and moments will now be expressed in this family of reference systems.

In Equation 55, the moments are each the sum of two terms: the elastic moment, and the internal-friction moment.

$$M_i = M_{e i} + M_{p i} \tag{58}$$

$$= EI\omega_i - M_f \frac{\dot{\omega}_i}{\sqrt{\dot{\omega}_2^2 + \dot{\omega}_3^2}} \tag{59}$$

The friction-related part has intensity M_f and is in the direction of the change of curvature. The notation

$$\dot{\omega}_i \triangleq \frac{D\omega_i}{Dk} \tag{60}$$

is used for brevity. As in Section 3.10, D/Dk is a material derivative (the rate of change as payout progresses, at a material point).

The term $\omega_2 M_3 - \omega_3 M_2$ (from Equation 55) can be developed

$$-\frac{\partial M_1}{\partial z} = m_1 + \omega_2 M_3 - \omega_3 M_2 \tag{61}$$

$$= m_1 + \omega_2 EI\omega_3 - \omega_3 EI\omega_2 + M_f \frac{\dot{\omega}_2 \omega_3 - \dot{\omega}_3 \omega_2}{\sqrt{\dot{\omega}_2^2 + \dot{\omega}_3^2}} \tag{62}$$

The expression $\omega_2 M_3 - \omega_3 M_2$ can be recognized as a cross product and a determinant: it is the signed area of a parallelogram which sides are the rotation rate vector $[\omega_2, \omega_3]$ and the friction bending moment vector $[M_2, M_3]$ (Figure 42).

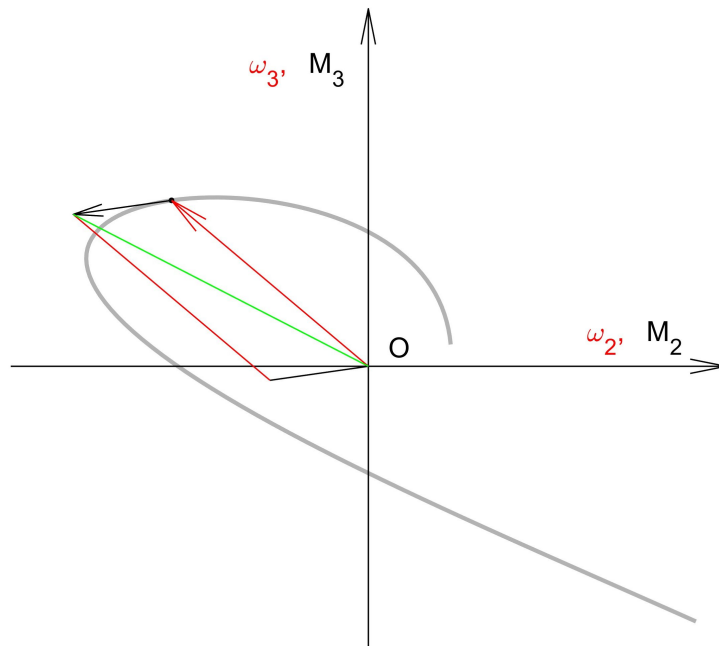


Figure 42: Geometric interpretation of the cross product as the area of a parallelogram. Friction's contribution to moments (black) curvature (red).

Equation 62 can be integrated along a segment of flexible, yielding

$$M_1(a) - M_1(b) = \int_a^b m_1 ds - \int_a^b M_f \frac{\dot{\omega}_2 \omega_3 - \dot{\omega}_3 \omega_2}{\sqrt{\dot{\omega}_2^2 + \dot{\omega}_3^2}} ds \quad (63)$$

The term $\int_a^b m_1 ds$ is the contribution from external torques, including these arising from friction against rollers, chutes, tensioner, other coils, etc. The second term, the “flip torque” is the contribution of internal friction. Figure 43 represents this integral graphically. Note that a slow evolution of the direction of torsion results in many shadowed triangles contributing to the integral.

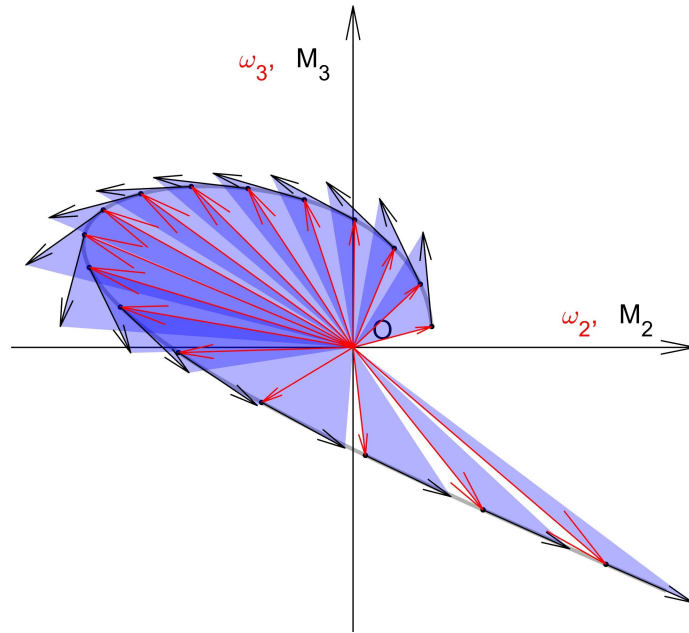


Figure 43: Geometric interpretation of the flip-torque integral. Double shadows count double.

Assuming M_f to be uniform along the route, it can be taken out of the integral, so that the flip torque can be written

$$M_f \int_a^b \frac{\dot{\omega}_2 \omega_3 - \dot{\omega}_3 \omega_2}{\sqrt{\dot{\omega}_2^2 + \dot{\omega}_3^2}} ds \quad (64)$$

The flip torque is the product of M_f (a property of the flexible product) and an integral *which only depends on the geometry of the route*. The simplest way to keep this integral equal to zero is to ensure that $\dot{\omega}_3 \omega_2 - \dot{\omega}_2 \omega_3 = 0$ everywhere along the route. This implies that $[\dot{\omega}_2, \dot{\omega}_3]$ and $[\omega_2, \omega_3]$ are co-linear everywhere: change of curvature can only occur in the direction of curvature, unless the curvature is zero (Section 5.6).

5.5.3 Interaction between pitch and change of curvature plane

Non-uniform curvature (Section 4.7) implies that the moment at a cross-section can not be computed from the curvature (and its history) at that cross-section alone. This is studied in the following.

Let $\bar{\mathbf{e}}^w(z)$ be a torsion-free set of reference systems. The coordinates \mathbf{c}_i of a helical component (e.g. a tensile armor thread) in this reference system are (in the absence of transverse displacement of the component).

$$\mathbf{c}_2 = r \cos \alpha \quad (65)$$

$$\mathbf{c}_3 = r \sin \alpha \quad (66)$$

with

$$\alpha(z) = \frac{2\pi z}{p} + \alpha(0) \quad (67)$$

where z is the coordinate along the flexible product, p and r are the pitch length (positive for positive helical components) and the distance between the component and the flexible product's neutral axes, respectively.

Let us consider a helix-shaped route. It has a curvature of uniform intensity κ and Frenet-Serret torsion τ_f (Section 3.11.4), so that

$$\omega_2 = \cos \beta \quad (68)$$

$$\omega_3 = \sin \beta \quad (69)$$

with

$$\beta = \tau_f z + \beta(0) \quad (70)$$

where ω_i are the coordinates of the rotation vector expressed in the torsion-free family of reference systems.

The elongation of the trajectory of the component at a section z is

$$\epsilon = \kappa (\omega_2 \mathbf{c}_3 - \omega_3 \mathbf{c}_2) \quad (71)$$

$$= \kappa r (\cos \beta \sin \alpha - \sin \beta \cos \alpha) \quad (72)$$

$$= \kappa r \sin (\alpha - \beta) \quad (73)$$

$$= \kappa r \sin \left(\left(\frac{2\pi}{p} - \tau_f \right) z + \alpha(0) - \beta(0) \right) \quad (74)$$

$$= \kappa r \sin (az + \gamma) \quad (75)$$

with $\mathbf{a} \triangleq \frac{2\pi}{p} - \tau_f$ and $\gamma \triangleq \alpha(0) - \beta(0)$. By a change of origin of the reference system, we can set $\gamma = 0$ without loss of generality

$$\epsilon = \kappa r \sin az \quad (76)$$

5.6 Engineering implications

5.6.1 Route optimisation

The results in Section 5.5.2 point to a simple strategy to minimize flip torques: *Keep each curve in a single plane* (Figure 44). This does not mean that the whole route has to be within a

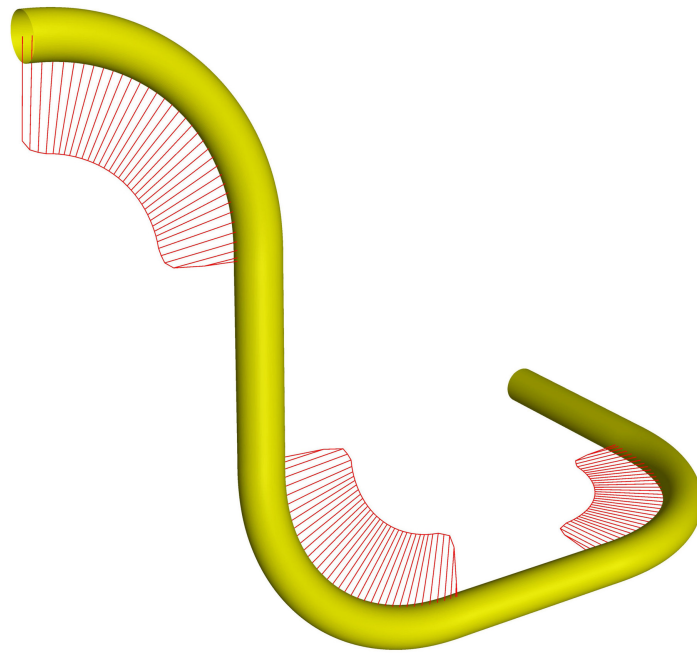


Figure 44: A good route has well-separated areas of curvature, each curve being in a single plane.

single plane, but that when the flexible product comes out of a curve, it needs to be straightened before it is bent in another plane.

The above is usually impractical in free spans of turntables or baskets: the flexible product can not be straightened between the sag bend and the coil - essentially because of the way the turntables tend to be designed. Still, with some skill one can manipulate the free span to ensure a more abrupt change of plane of curvature.

5.6.2 Chutes

Chutes are surfaces positioned at a transition between a section of the route in which the flexible product is well guided, and a free span, and serve to prevent excessive curvature at that transition. They are typically positioned at the bulwark of a vessel or at a quay side.

Some chutes are constructed with hard chines, that is, by welding bent plates together. This can create route geometries with abrupt changes of curvature plane. Figure 45 shows the same geometry seen from three different angles. The crests (in blue, green and red, respectively) show the curvature in the free span, in the part of the flexible product in contact with one side panel, and with a side panel and the bottom panel, respectively.

As can be seen, the plane of curvature changes along the route. In the case illustrated, this results in a negative flip torque.

5.7 Active geometry control in a turntable free span

5.7.1 Requirements

A common torsion problem occurs when flip torque is generated in the free span of a turntable, during the loading out of a flexible product to an installation vessel, or similar operation. A procedure for the mitigation of torsion *during operation* is proposed here. Importantly, at the time of writing, this procedure has not been tested or studied. It is not known under what circumstances the procedure will be able to prevent torsion problems, and it is not known whether it might under some circumstances contribute to cause torsion problems.

The procedure requires that the following conditions are met:

1. The free span in the downstream turntable or basket is the dominating source of flip torque along the route.
2. The flexible product has one (or several) longitudinal markings.
3. The variation over time of the writhe between the upstream end of the route (e.g. on shore carousel) and the downstream end (on board carousel) is small.
4. The spatial roll rate of the flexible product leaving the upstream storage is small. If the upstream storage is a turntable or a spool, this amounts to having only a small torsion in the upstream storage.

The procedure is designed to prevent high torques at steady state, due to flip torque in the downstream storage. To this effect, two measures are to be combined: monitoring of the spatial roll at touch-down-point, and control of the geometry in the free span.

5.7.2 Monitoring of spatial roll

Given that conditions 3 and 4 in Section 5.7.1 are met, then the evolution over time of the twist along the route is approximately equal to that of the spatial roll angle at the entry of the downstream storage. The implication is that, *if the spatial roll angle at the entry of the downstream storage is kept nearly constant from the start of the operation, then the twist, and hence torsion along the route will be small.*

For turntables and spools “the entry of the downstream storage” refers to the touch-down point. However for baskets, this refers to the top of the goose neck (the upper end of the free span into the basket) or alternatively, the touch down point, but correcting the roll angle with one turn per coil. For readability, further description is given assuming a downstream turntable.

The roll angle at the entry of the downstream storage must be measured as the head of the flexible product reaches it, and then monitored regularly. “Regularly” means

- Often enough to avoid confusing one longitudinal marking with another if there are several markings, or to avoid being unsure about whether a whole turn of roll may have taken place since the last measurement.

- Often enough compared to how fast the shape of the free span changes during operation.

The objective is to keep the total change of the roll angle at the entry of the downstream storage to a small value, by reacting early with geometry control when this roll is observed to change.

5.7.3 Geometry control

Flip torque is closely related to the geometry of the route, and in particular, of the free span. In a downstream turntable rotating clockwise, the touch down point area will induce a positive flip torque. With actuators, one can attempt two things to limit or counterbalance the flip torque and hence control the roll angle:

1. Limit the flip torque in the touch down point area. This is achieved by *avoiding* a progressive change of the curvature plane, and promoting an abrupt one (Figure 46). There is however a lack of knowledge on the consequences of doing this: helical components may become overloaded at radii of curvature above the minimum bending radius (MBR), because the components remain on the inside or the outside of the curvature for more than half a pitch length.
2. Use actuators to give the upper free span a negative Frenet-Serret torsion (that is, a shape like a negative helix), this induces a negative flip torque in the upper free span (Figure 47). The flip torques in the lower and upper free span can compensate each other and control the roll rate. Importantly, while this controls the twist upstream in the route, this does not limit the torque between the upper and lower free span. In the above example, a positive internal torque would be present in the free span.

A coilable product entering (for example) a positive downstream *basket* (Figure 49) would have its tensile armor laid in the positive direction. The touch down point area will have a positive Frenet-Serret torsion and a longer length of tensile armour (than would be the case without change of curvature plane) can be outside of the curvature, leading to overloading of the armour.

When using actuators to manipulate the shape of the free span, it is essential to do so by applying small forces continuously while transport is ongoing. High forces can induce cranking torques and thus damage the flexible product (Section 17).

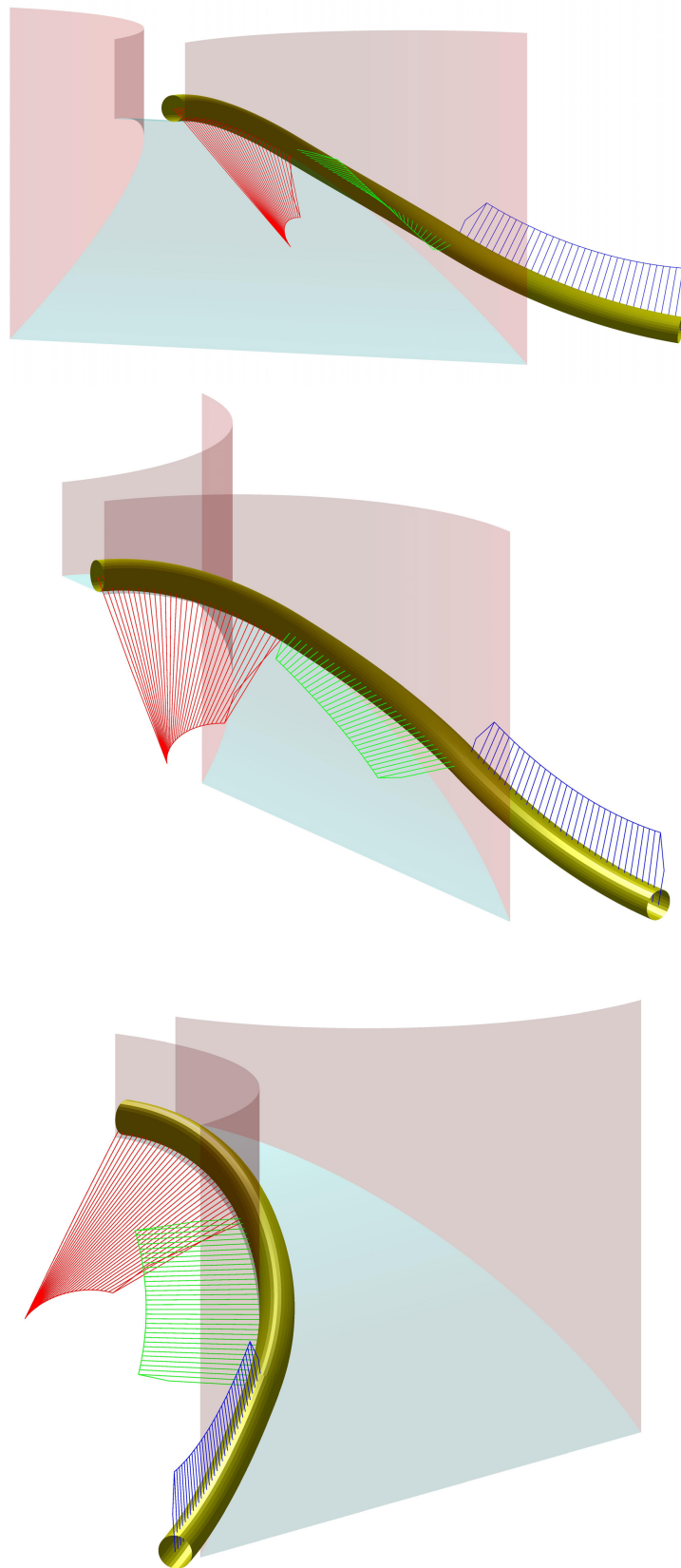


Figure 45: Flexible product in a chute

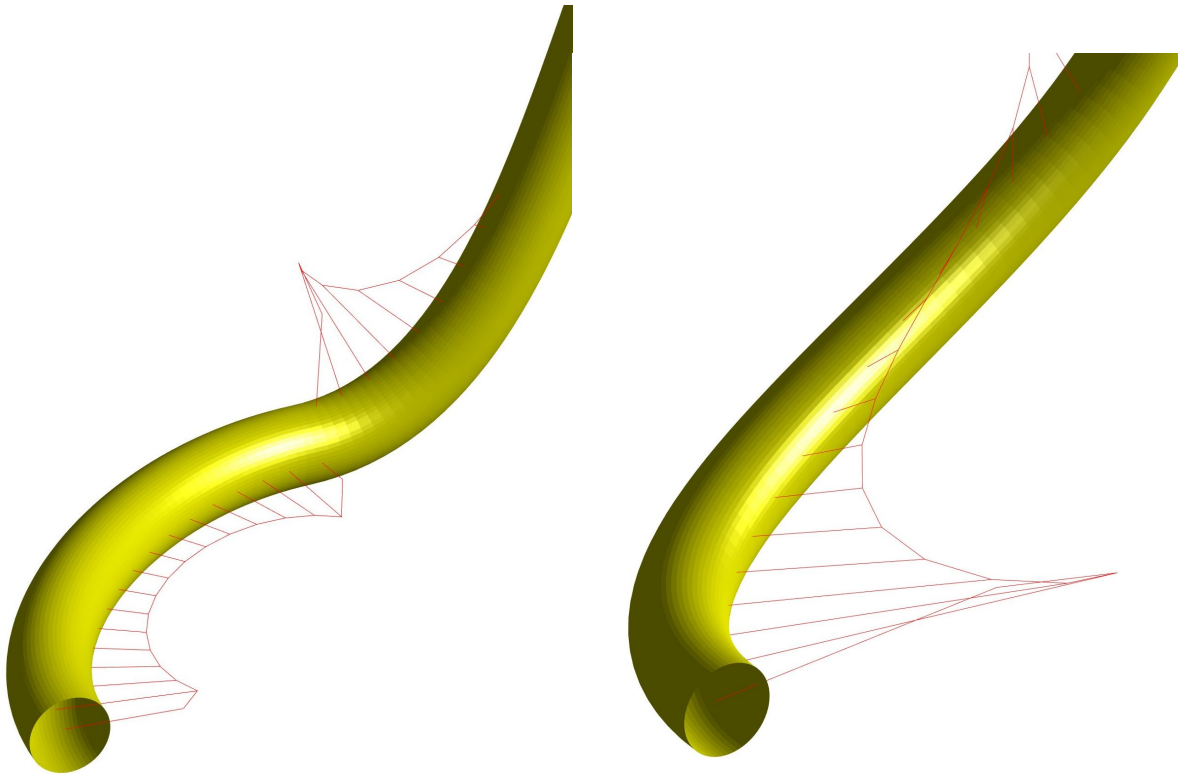


Figure 46: Abrupt and progressive change of curvature plan at touch-down point

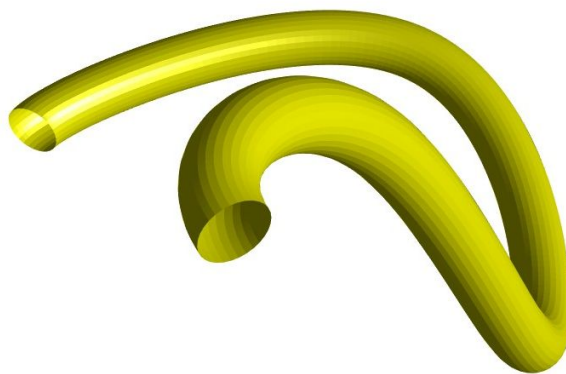


Figure 47: Free span seen from the top deck. The upper part of the free span is manipulated to resemble a positive helix, while the bottom part resembles a negative helix.

6 Storage and routing

6.1 Turntables

A turntable rotates around a vertical axis as the flexible product is fed in or out of it. In an ideal “steady state” (Section 7), in which a flexible is fed into a turntable without any changes to the shape of the free span (which is not completely realistic as the flexible product is fed towards the nave or away from it, and the basket is progressively filled), the writhe in the free span is constant: zero spatial roll rate at the top of the free span entering the basket corresponds to zero spatial roll rate at the touch down point (where the flexible product comes to rest on the flexible product already coiled in the turntable). This is a useful approximation: in practice variations of writhe in the free span of turntables impose limited changes in the roll at the touch-down point. Combined with the changes in the writhe being slow, this does not result in large torsion stored in the turntable. One important exception is discussed in Section 6.6.

We can assume that the flexible stored in the turntable has zero material roll. There are at least two reasons for that. First, one coil of the flexible product is stacked against other coils or the floor, nave or wall of the turntable, and the friction between the components prevents roll. Second, as discussed in Section 5, internal friction prevents a curved flexible product from rolling. More specifically, if the flexible product has an internal torque at the entry of the storage device, the internal torque may win over friction over the first few meters. The roll angle involved will generally be small, so in this section, the discussion will proceed as if absolutely no material roll occurs.

So in the absence of material roll ($DR/Dk = 0$), Equation 10, which states that

$$\frac{DR}{Dk} = \frac{\partial R}{\partial k} + \tau$$

becomes

$$\frac{\partial R}{\partial k} = -\tau \tag{77}$$

This implies that when a flexible product is paid out of a turntable, the torsion in the stored coils is unaffected by the downstream internal torque and torsion, hence the spatial roll rate is the opposite of the stored torsion. When a flexible product is stored into the turntable, the torsion in the upstream product is “frozen” in place by friction in the coils, so the torsion in the coils is equal to the upstream torsion, and the roll rate is the opposite of the torsion.

As an example, a flexible product with an ideal marking is stored in a turntable. It is paid out, but the winch pulling out the flexible product (somehow) also imposes an external torque T , causing a torsion τ in the part paid out (Figure 48). Then, the flexible product is taken back into the turntable, with the winch still maintaining an external torque T . This results in the flexible product being stored with torsion τ . The difference between paying out and taking in is a case of *irreversibility* in operations (Section 8.7).

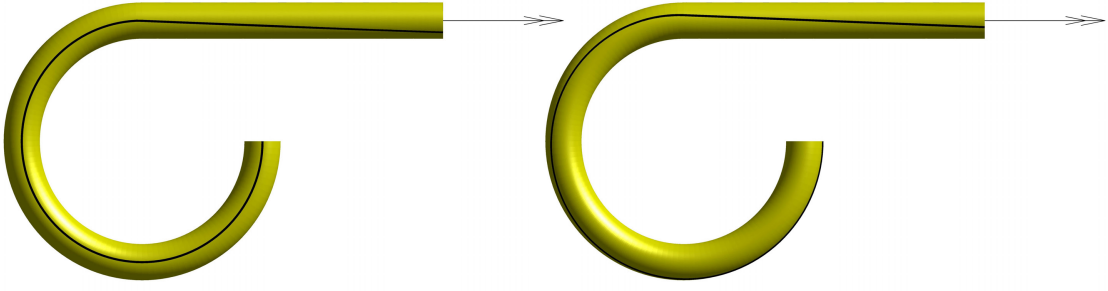


Figure 48: A flexible product is paid out (left) of a turntable while an external torque is applied to its end. When the product is taken in again (right), torsion is stored.

6.2 Spools

In a first approximation, storing a flexible product in a turntable and in a spool is exactly the same, and all the results in Section 6.1. There is one substantial difference however, due to the presence of writhe in the spool. Each layer in the spool has the shape of a helix with pitch $p = \pm 2r$ where r is the external radius of the flexible product. The pitch is positive if the layer is a positive helix. Considering a layer with radius R (the distance to the axis of the spool to the axis of the flexible product), using Equation 39, the writhe per turn (pitch) is (assuming a positive helix)

$$a = R \quad (78)$$

$$b = \frac{r}{\pi} \quad (79)$$

$$c = \sqrt{a^2 + b^2} \quad (80)$$

$$W = 2\pi \operatorname{sgn}(b) \left(1 - \frac{b}{c}\right) \quad (81)$$

$$= 2\pi \operatorname{sgn}(b) \left(1 - \frac{2r}{\sqrt{R^2 + \left(\frac{r}{\pi}\right)^2}}\right) \quad (82)$$

Two extreme cases are worth considering. In the first, the flexible product is stored without torsion on the spool. This is difficult to achieve in practice, but a slow underwater crane lift where the load is allowed to rotate to keep the torque zero in the flexible product would be the least unlikely realization. There is hence no twist in the spool, and the link is equal to the writhe. For each turn in the spool, the link between the head of the flexible product on the spool and the product entering the spool increases by W . Since the head is prevented from rotating by external friction, internal friction, and hitching to the spool, the roll at the touch down changes by $-W$. When spooling out again, the convention in this document is that the direction of increasing coordinates s or z is swapped. So although the direction of roll is swapped, it would still be described as $-W$ for each turn paid out.

The other extreme case is in many cases closer to reality: We assume that the spatial roll at the entrance of the spool is zero. This would occur at steady state (Section 7), assuming there

is zero spatial roll at the point of origin of the flexible product (upstream storage or production machine). In such a situation the link between the head of the flexible product on the spool and the entry to the spool is constantly equal to zero. This implies that the twist is the opposite of the writhe: at any point in the spool, the torsion is

$$\tau = -\frac{W}{2\pi R} \quad (83)$$

negative in layers that are positive helices. When the flexible product is paid out of the spool, "the film plays in reverse" and the spatial roll at the exit of the touch down point remains zero: the flexible product, which had zero torsion before entering storage, has zero torsion after leaving it. More generally, the product has the same torsion before entering and after leaving storage.

Reality will generally be between the two above-mentioned extreme cases.

6.3 Baskets

Baskets can be distinguished according to the direction in which the touch down point turns as flexible product is taken from the basket. Figure 49 shows a *positive* basket. The mirror image of Figure 49 would present a negative basket. The choice of name is related to the geometry being (an irregular) positive helix.

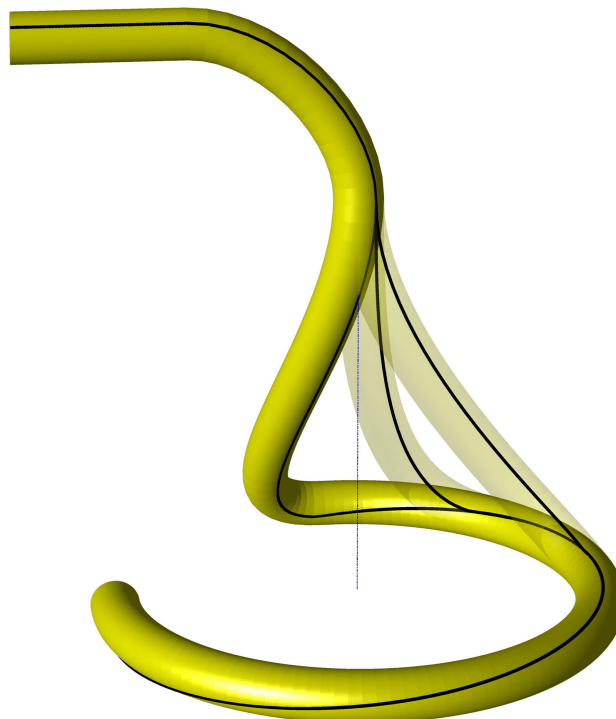


Figure 49: A positive basket (the mirror image is then a negative basket).

In order to understand baskets, let us start with a peculiar *turntable* in which the flexible product is fed vertically (as it would in a basket, and as shown in Figure 49). Imagine that the whole picture of the turntable rotates counterclockwise to compensate for the rotation given to the turntable when feeding flexible product into it. Two things occur:

1. The turntable does not appear to rotate, the touch down point moves counterclockwise when flexible product is fed in: this is now a *basket*.
2. The point in Figure 49 at which the flexible is vertical is now rotating counterclockwise (a negative spatial roll rate): each time a new coil is laid in the basket, the flexible product rotates in the same direction as the touch down point (This is the same as the 360 [deg] roll that occurs when a new coil is created, as shown in Figure 13).

In order to discuss how storing a flexible product in a basket induces torsion, it is necessary to introduce the roll R_{vert} of a cross-section where the flexible product is vertical as it enters the basket (Figure 49). Since the usual definition of roll (relative to the vertical) would fail here, we can define the roll at that point relative to the north. In a positive basket, if the cross-section at the vertical point is not rotating *relative to the touch-down point*, it has a negative roll rate relative to the north. For a positive basket, this can be written (for roll angles in degrees)

$$\frac{\partial R_{\text{tdp}}}{\partial k} = \frac{\partial R_{\text{vert}}}{\partial k} + \frac{360}{\lambda} \quad (84)$$

where λ is the length of a coil.

If the flexible product does not rotate relative to the north, in the vertical part (as would be the case in steady-state operation, Section 7), then for a *positive* basket (Figure 49, a *negative* twist is stored into the basket. In the present case, Equation 77 is

$$\frac{\partial R_{\text{tdp}}}{\partial k} = -\tau \quad (85)$$

Then, using Equation 84, this leads to

$$0 = \tau + \frac{\partial R_{\text{vert}}}{\partial k} + \frac{360}{\lambda} \quad (86)$$

For *negative baskets*, $360/\lambda$ becomes $-360/\lambda$. When the flexible product is *paid out* of the basket, several things happen: The sign of the torsion stored in the basket is unchanged. The movie plays backwards, so roll is physically reversed *but* the positive direction along the product, and hence the convention for roll sign is flipped: the roll rate *value* is unchanged. The same argumentation applies to the writhe term: $360/\lambda$ remains unchanged. To summarize, the equation

$$0 = \tau + \frac{\partial R}{\partial k} + s \frac{360}{\lambda} \quad (87)$$

applies for paying in and out, and with $s = 1$ for positive baskets and $s = -1$ for negative baskets.

6.4 Chutes and other fixed surfaces

A simple but useful engineering model for dry friction is Coulomb's friction model. In its simplest form, consider a body **A** (flexible product) pressing against a body **B** (a chute) with a force orthogonal to the contact surface (a "normal force") F_n . Three source of normal forces are often relevant: weight, tension in a curved product, and wedging and clamping. If the force F_t exerted by **B** on **A** in the direction tangential to the contact surface is small enough

$$F_t < \mu F_n \quad (88)$$

(where μ is the friction coefficient), then no sliding occurs. On the other hand, if **A** does slip relative to **B**, then the friction force has intensity

$$F_t = \mu F_n \quad (89)$$

and direction opposite to the motion of **A** relative to **B**. Friction coefficients vary between 0.02 (walking on wet ice) and 0.9 (rubber on dry rock). Polyethylene against polyethylene or steel has friction coefficients around 0.2. One key feature of this simple model is that the friction force does not depend on how the contact pressure is distributed: the total friction force is related to the total contact force. According to the model, pulling a flexible product over metallic chutes requires the same force: unevennesses of the chute have no effect.

If we look at the direction of the friction force "from above" (from a direction orthogonal to the plane of contact), when slip occurs, the friction force vector has length μF_n (Figure 50). The equation of the "stick circle" is

$$\sqrt{F_{tr}^2 + F_{tt}^2} = \mu F_n \quad (90)$$

where F_{tr} and F_{tt} are respectively the components of the transverse force vector \bar{F}_t in the roll and transport directions.

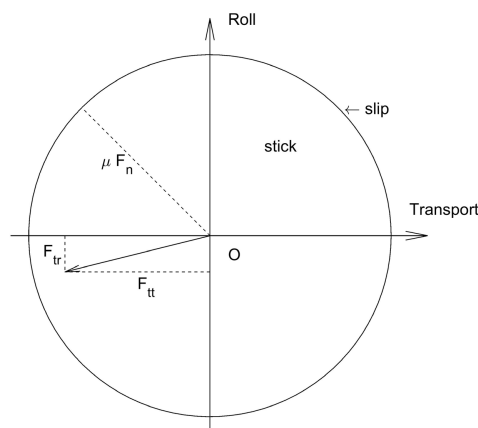


Figure 50: The friction force has a length lower than (when sticking) or equal to (when slipping) μF_n , and direction opposite to the motion.

Consider 1m of flexible product, with outer radius r . The contact force F_n is now a force per unit length. If the flexible product rolls in the positive direction (by sliding against the chute,

not by rolling like a wheel), without any transport, $F_{tt} = 0$, and the chute will exert on the product a friction force

$$F_{tr} = -\mu F_n \quad (91)$$

in the direction orthogonal to the direction of rotation. This amounts to an external moment per unit length

$$m_x = rF_{tr} \quad (92)$$

$$= -r\mu F_n \quad (93)$$

on the product.

The situation changes significantly if the product is being transported: As the product is transported, it has a material roll rate DR/Dk (positive, for example). For every meter the flexible product is transported downstream, the surface of the product also slides in the direction orthogonal to transport, by an amount rDR/Dk . The component of the friction force in the direction orthogonal to the direction of transport has value (Figure 51)

$$F_{tr} = -\mu F_n \frac{r \frac{DR}{Dk}}{\sqrt{\left(\frac{\partial R}{\partial k}\right)^2 + \left(r \frac{DR}{Dk}\right)^2}} \quad (94)$$

$$= -\mu F_n \frac{r \frac{DR}{Dk}}{\sqrt{1 + \left(r \frac{DR}{Dk}\right)^2}} \quad (95)$$

where $\partial k/\partial k$ is the rate of displacement in the transport direction. Since we use the convention to measure "time" by the length k of product transported, this rate of transport is equal to 1.

Hence in the presence of transport, the moment (per unit length) applied by the chute on the flexible product is

$$m_x = rF_{tr} \quad (96)$$

$$= -r\mu F_n \frac{r \frac{DR}{Dk}}{\sqrt{1 + \left(r \frac{DR}{Dk}\right)^2}} \quad (97)$$

$$\approx -r\mu F_n r \frac{DR}{Dk} \quad (98)$$

the last simplification being good for small roll rates.

The term DR/Dk in Equation 98 is important: *the moment m_x is proportional to the roll rate*. In the absence of transport, even for a completely straight flexible product, friction against chutes would be so high that the product, in practice, does not roll, no matter how large the internal torques are in the product. Here, under transport, small roll rates result in small external torques from friction: under transport, with slip occurring anyway in the axial direction, friction does not prevent roll, it only limits the roll rate.

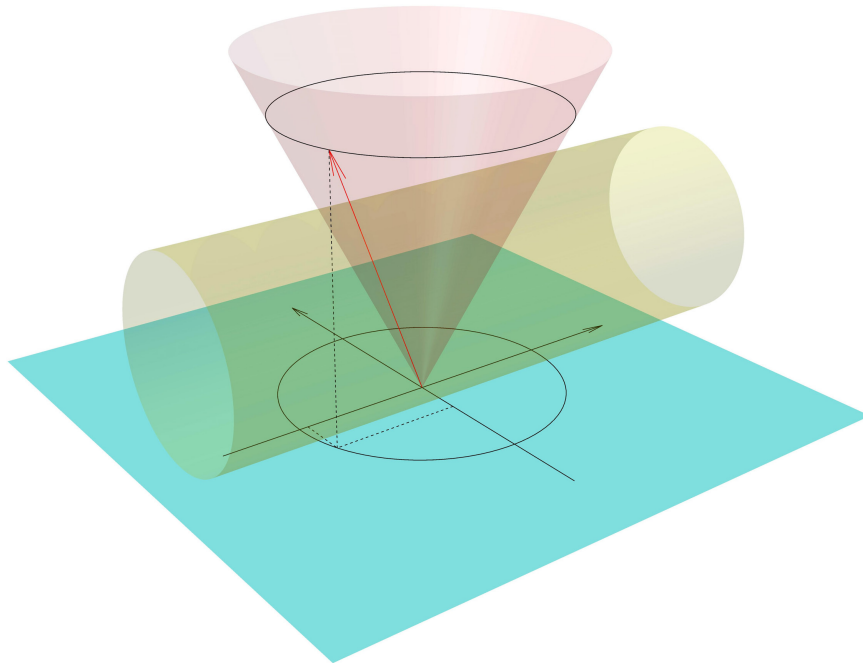


Figure 51: A flexible product is transported downstream (to the right) and rolls in the positive direction. The red arrow shows the force exerted by the chute on the flexible product. It is on the “stick cone” (Equation 90): the component that resists roll is small, yet there is roll.

6.5 Tensioners and rollers

Usually, tensioners are operated with clamping forces (and hence contact pressures σ_{nn}) high enough to prevent slip. In principle, this would imply that the material roll rate at a tensioner is zero. If for example, the upstream torsion entering the tensioner is zero, this would imply that the spatial roll rate upstream of the tensioner is zero. Experience, however, shows that this is not the case: torsion downstream of a tensioner has been documented to propagate upstream (against the direction of transport) during operation.

In tensioners, the mechanism is thought to be as follows (Figure 52): the track plates have some slack, allowing them to move sideways, or the track plates carry pads with some compliance, and the outer sheath (or ply of yarn) also deforms under load. This allows a material point of the flexible product to roll as it passes through the tensioner. The material roll rate is directly related to the tracking angle α^2 :

$$\frac{DR}{Dk} = \frac{\alpha}{r} \quad (99)$$

where r is the outer radius of the flexible product. For tires operating well within the stick domain, the tracking angle is modeled as being proportional to the transverse force on the wheel. In our context, the tracking angle is modeled as being proportional to the external torque that the tensioner exerts on the flexible product. No experimental confirmation of this

²The term of “slip angle” common in tire engineering is avoided here, to avoid confusion with actual slipping between surfaces.

model is available. There is no known procedure available to compute the proportionality factor between the above-mentioned external torque and the tracking angle.

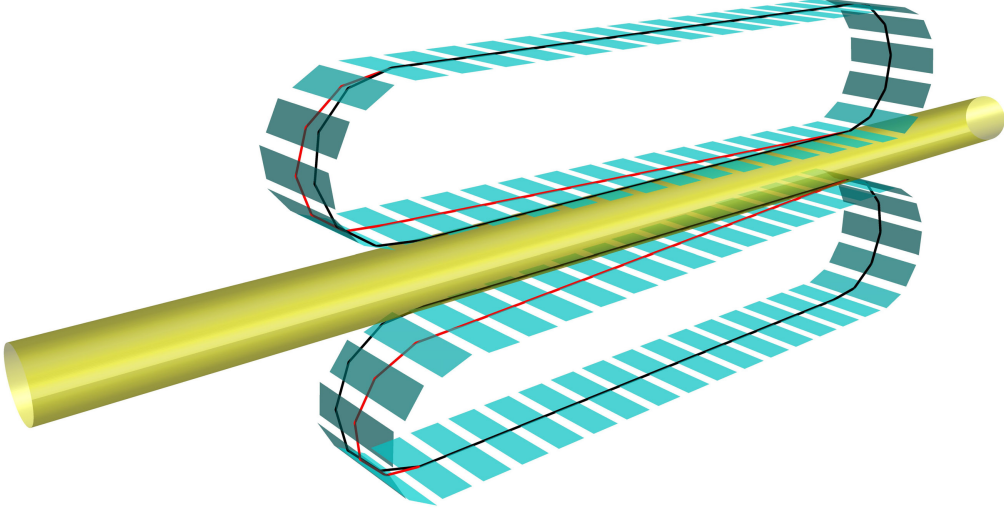


Figure 52: Flexible product passing a tensioner towards the left in the picture, with positive spatial roll. This causes the pads in contact with the product to shift: original center-line in black, shifted center-line in red. The angle between the original and shifted centerlines is the tracking angle α .

A similar thing happens in support rollers (and in automobile tires, where the phenomena is well studied). Here the compliance does not come from pads shifting, but from tiny deformations in the roller and the surface of the flexible product (and in the tire).

Another effect comes into play, that is present even if the tracking angle remains equal to zero, so that the material roll is zero (Equation 99).

The tracking angle is related to the *material* roll. Material and spatial roll are related by Equation 99 (cf. Section 3.10). The implication is that, if there is torsion, even for a zero roll angle, the spatial roll rate will be non-zero. More specifically, it is the torsion *entering* the tensioner that is relevant (Section 6.2).

To produce an equation that models tensioners and rollers in the absence of slip, we note M_1^- and M_1^+ the internal torque in the product respectively upstream and downstream of the tensioner (or roller). The external torque applied by the tensioner on the product is

$$\Delta M_1 = M_1^- - M_1^+ \quad (100)$$

The resulting track angle is

$$\alpha = \frac{c}{r} (M_1^+ - M_1^-) \quad (101)$$

where c measures the compliance of the tensioner and r is the outer radius of the product. Replacing this in Equation 99 gives

$$\frac{DR}{Dk} = \frac{c}{r^2} (M_1^+ - M_1^-) \quad (102)$$

The torsion of the product frozen in the tensioner is equal to the upstream torsion

$$\tau = \frac{M_1^-}{K_{rr}} \quad (103)$$

where K_{rr} is the torsional stiffness. Replacing Equations 102 and 103 into the relation between spatial and material roll (Equation 10) and rearranging leads to the “tensioner roll equation”

$$\frac{\partial R}{\partial k} = \frac{c}{r^2} M_1^+ - \left(\frac{c}{cr^2} + \frac{1}{K_{rr}} \right) M_1^- \quad (104)$$

An *ideal tensioner* has no compliance ($c = 0$) in which case

$$\frac{\partial R}{\partial k} = -\frac{1}{K_{rr}} M_1^- \quad (105)$$

downstream internal torque does not cause any roll. When compliance is considered, upstream internal torque cause more roll than the same downstream internal torque, but importantly, downstream internal torque does cause roll: tensioners (and rollers) do not prevent the propagation of roll against the direction of transport.

6.6 Hydraulic actuators

A crank is a tool that transforms a force (applied by hand, or a piston) into an internal torque. The internal torque is equal to the force (in [N]) times the arm (in [m]). Hydraulic tools used to guide large-diameter flexible products during operations, in particular to stack them into turntables can thus generate significant internal “cranking” torques. Even though these forces may only be present for a short duration, they come in addition to flip torques induced by the route geometry, and the combination of both can cause a failure. The mathematics of how a force can induce a internal torque in a curved beam are discussed in Section 5.5, where the actuator force appears as \bar{f} in Equation 50.

The objective in using hydraulic tools is not actualy to apply *forces* to the flexible product, but to control its *position*. There is a parallel with external friction resistance to roll (Section 6.4): In the present case, internal friction between the components of the flexible product, makes the product very stiff, opposing with large forces attempts to deform it. But if the deformation is applied progressively while the flexible product is being transported, the product is more compliant: Changes of curvature induced by routing already cause the components to slip relative to each other. The hydraulic tool then only needs moderate forces to adjust the pattern of slipping of the components. From a practical point of view, good use of hydraulic actuators reminds of the way a potter “throws” (works) a ball of clay on a potter’s wheel: the fingers press gently and continuously on the material while the wheel spins.

When handling products with long component pitch lengths in small spaces (the free spans of on-board turntables can be short), one must account for non-uniform curvature (Section 4.7). The changes of curvature planes induced by the hydraulic actuator can occur over lengths comparable to the pitch lengths of the components. This can make the flexible product much stiffer, leading to large actuator forces and hence internal torques.

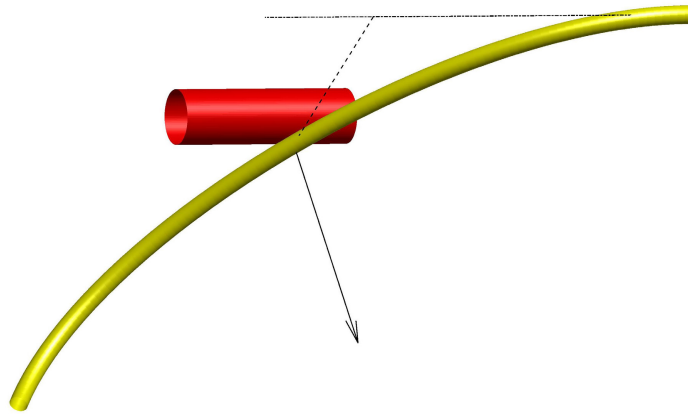


Figure 53: An actuator (red) exerts a sideways force which induces an internal torque at the upper end of the flexible product.

7 Steady state and transients

7.1 Definitions

A transport operation is said to be in a steady state if:

1. The geometry of the route does not change over time.
2. The tension and the internal torque at any given point along the route do not change over time.

A transport operation is defined to be in a transient state if it is approaching a steady state over time.

7.2 Occurrence

Even if the route and the tension are constant (they do not change over time), there is no guarantee that a steady state for the internal torque will be reached. Sections 8.2, 8.6 and 8.4 discuss mechanisms that would prevent a smooth evolution towards a steady state.

A real transport operation will typically not have an *exactly* constant route. For example the route has to change when feeding a flexible product into a turntable: from empty to full turntable, from laying near the nave to near the wall. Variations in tension occur, due to the difficulty to coordinate tensioners, spools and turntables.

While there is no general guarantee that a near constant route and tension will move towards a near-steady state situation in which the internal torque changes little over time at any given point along the route, successful operations do approach such a steady state.

The results from Section 7.3 imply that, *under the restrictions stated there*,

1. Operations with constant route geometry on flexible products with balanced cross-sections will approach a steady state.
2. *If starting from configuration with no internal torque*, the steady state is the situation with the highest internal torques.

7.3 Mathematical formulation

We lack general results on the existence of steady states, and the same goes for transients. But with a set of assumptions, relevant results can be obtained. We assume

- a route of constant geometry,
- M_f unchanged over time at any point along the route,

- the graph relating the flip torque to the spatial roll rate, at any point along the route, (Figure 40) is linear,
- the cross-section is torsionally balanced,
- the torsional stiffness K_{RR} is a constant.

Under the above assumptions, using Equation 55, the differential equation defining the evolution of roll at a flip location is of the form

$$-\frac{\partial}{\partial s} \left(K_{RR} \frac{\partial R(s, k)}{\partial s} \right) = a(s) - b(s) \frac{\partial R(s, k)}{\partial k} \quad (106)$$

where $a(s)$ is the flip torque at zero roll rate at point s along the route, and $-b(s)$ the influence of the spatial roll rate on the flip torque, and $b(s) \geq 0$ for any geometry. The above is a linear differential equation, of the first order (with only first derivatives) with respect to the payout k . This can be rewritten

$$-K_{RR} \frac{\partial^2}{\partial s^2} R(s, k) + b(s) \frac{\partial}{\partial k} R(s, k) = a(s) \quad (107)$$

$$-\frac{K_{RR}}{b(s)} \frac{\partial^2}{\partial s^2} R(s, k) + \frac{\partial}{\partial k} R(s, k) = \frac{a(s)}{b(s)} \quad (108)$$

$$\frac{\partial}{\partial k} R(s, k) = \alpha(s) + \gamma(s) \frac{\partial^2}{\partial s^2} R(s, k) \quad (109)$$

The roll at tensioners follows Equation 104

$$\begin{aligned} \frac{\partial}{\partial k} R(s, k) &= \frac{c}{r^2} M_1^+ - \left(\frac{c}{r^2} + \frac{1}{K_{rr}} \right) M_1^- \\ \frac{\partial}{\partial k} R(s, k) &= \frac{c}{r^2} K_{RR} \frac{\partial}{\partial s} R(s, k) \Big|_+ - \left(\frac{c}{r^2} + \frac{1}{K_{rr}} \right) K_{RR} \frac{\partial}{\partial s} R(s, k) \Big|_- \end{aligned} \quad (110)$$

$$\frac{\partial}{\partial k} R(s, k) = \beta(s) \frac{\partial}{\partial s} R(s, k) + \gamma(s) \frac{\partial^2}{\partial s^2} R(s, k) \quad (111)$$

where $\gamma(s)$ can be described using Dirac's distribution.

The roll at chutes follows Equation 98

$$\begin{aligned} m_x &= -r\mu F_n r \frac{D}{Dk} R(s, k) \\ -K_{RR} \frac{\partial^2}{\partial s^2} R(s, k) &= -r\mu F_n r \left(\frac{\partial}{\partial k} R(s, k) + K_{RR} \frac{\partial}{\partial s} R(s, k) \right) \end{aligned} \quad (112)$$

$$\frac{\partial}{\partial k} R(s, k) = \beta(s) \frac{\partial}{\partial s} R(s, k) + \gamma(s) \frac{\partial^2}{\partial s^2} R(s, k) \quad (113)$$

Storage follows Equation 77

$$\frac{\partial}{\partial k} R(s, k) = -\tau \quad \text{upstream storage (stored torsion)} \quad (114)$$

$$\frac{\partial}{\partial k} R(s, k) = -K_{RR} \frac{\partial}{\partial s} R(s, k) \Big|_- \quad \text{downstream storage} \quad (115)$$

$$\frac{\partial}{\partial k} R(s, k) = \alpha(s) + \beta(s) \frac{\partial}{\partial s} R(s, k) \quad (116)$$

Combining these equations together to obtain a differential equation for the whole system yields an equation of the form

$$\frac{\partial}{\partial k} \mathbf{R}(s, k) = \alpha(s) + \beta(s) \frac{\partial}{\partial s} \mathbf{R}(s, k) + \gamma(s) \frac{\partial^2}{\partial s^2} \mathbf{R}(s, k) \quad (117)$$

where $\gamma(s) > 0$ everywhere.

Deliberately using notations from linear algebra, we note $\bar{\mathbf{R}}(k)$ the function $s \rightarrow \mathbf{R}(s, k)$, and $\bar{\Gamma} \cdot \bar{\mathbf{R}}(k)$ the transformation of that function by the differential operator appearing on the right hand side of Equation 117. Equation 117 is of the form

$$\frac{\partial}{\partial k} \bar{\mathbf{R}}(k) = \bar{\mathbf{v}} + \bar{\Gamma} \cdot \bar{\mathbf{R}}(k) \quad (118)$$

which has solutions of the form

$$\bar{\mathbf{R}}(k) = \bar{\mathbf{R}}_0 \exp(\bar{\Gamma}k) - \bar{\Gamma}^{-1} \cdot \bar{\mathbf{v}} \quad (119)$$

8 Instabilities and irreversibility

8.1 Torsion-pressure instability

In the present document, and in particular in Section 5, it was a convenient simplification to assume the friction bending moment M_f to be a constant for any given cross-section. However, this is not always realistic. For example, a positive internal torque will press positive-helix component inwards, negative-helix component outwards increasing the contact pressure between these layers and hence the friction forces.

The dependency of M_f on the internal torque makes the following feedback loop possible, depending on circumstances:

1. Increased internal torque,
2. Increased contact pressure between some layer,
3. Increased friction bending moment,
4. Increased flip torque,
5. and so on.

Typically, the flip torque is balanced by internal torsion upstream of the 3D curve in which the flip torque is generated. However, because the flip torque is distributed along the span, part of the span do experience internal torque, making the instability a possibility.

A simple mathematical model for torsion-pressure instability is shown

8.2 Mathematical formulation

Consider again Equation 63, but we now assume that M_f is a function of the internal torque M_1 .

$$-\frac{\partial M_1}{\partial z} = m_1 + M_f(M_1) \frac{\dot{\omega}_3^1 \omega_2^1 - \dot{\omega}_2^1 \omega_3^1}{\sqrt{\dot{\omega}_2^{12} + \dot{\omega}_3^{12}}} \quad (120)$$

As a simple example, let us assume than $m_1 = 0$ (no applied external torque) and that $\gamma \triangleq \frac{\dot{\omega}_3^1 \omega_2^1 - \dot{\omega}_2^1 \omega_3^1}{\sqrt{\dot{\omega}_2^{12} + \dot{\omega}_3^{12}}}$ is uniform along the route (as would be the case in a helix). Further, we assume that $M_f = \mathbf{a}M_1 + \mathbf{b}$, where \mathbf{a} and \mathbf{b} are constants. This is a reasonable approximation over a limited range of values of M_1 . In this range, M_f must remain positive.

Then Equation 120 can be written

$$-\frac{\partial M_1}{\partial z} = \mathbf{a}\gamma M_1 + \mathbf{b}\gamma \quad (121)$$

This differential equation has solutions of the form

$$M_1(s) = M_1^0 \exp(-\alpha\gamma s) - \frac{b}{a} \quad (122)$$

from which we can compute the friction bending moment

$$M_f(s) = aM_1^0 \exp(-\alpha\gamma s) \quad (123)$$

In other words, if M_f depends on M_1 , then M_1 , instead of varying linearly along a helix, can vary exponentially, leading to finite but very high internal torques, a situation dubbed a "torsion-pressure instability". Qualitatively, the same remains true for more complex route geometries, including for routes with separate bends, as internal torque is transmitted between bends.

8.3 Curvature-pressure instability

In fatigue analysis of marine risers that are bending dynamically under wave loads, it is often convenient to assume the contact pressure between components to be almost constant as the riser bends: the contact pressure is mostly dictated by the tension in the components (and other components further out). The tension in the components is mostly related to the tension in the flexible product, and the contribution from bending, while important for fatigue because it varies over time, is moderate. In such a context, it makes sense to assume M_f to be a constant.

In handling operations, tension in the flexible product is often low, so that the friction associated to bending can contribute significantly to the tension in the component and then again to the contact pressure. The result is that as the curvature at a given point along the flexible product is increased, the following feedback loop comes into effect:

1. Bending causes components to slip, inducing friction forces,
2. Friction forces increase tension in the components,
3. Increased tension leads to increased contact pressures,
4. and so on, with increasing friction forces.

8.4 Flip torque-geometry instability

In the flip effect (Section 5) the geometry of a route has a major influence on the internal torques that will develop. On the other hand, if one considers the force equilibrium in a free span, the internal torque in the flexible product influences the geometry. In some cases, the influence on the geometry is such that it will exacerbate the flip effect, typically with geometries of free span that tend towards helices (Figure 54).

This effect is quite different from helical buckling (Section 8.6): helical buckling is not driven by friction or other energy dissipation, and does not require transport. One can induce helical

buckling in a thin rod by subjecting it to a internal torque and low tension. By contrast, flip torque-geometry instability can start with an initial internal torque too low to cause helical buckling internal torque, but it requires both transport and friction.

As an example, consider a sag-bend – a long portion of flexible product hanging free between rollers or chutes. The sag-bend is originally within a vertical plane (Figure 54, left). Then, for some unspecified reason, a positive internal torque appears in the sag bend. This can be caused, by a geometry, somewhere downstream, inducing flip torque. This positive internal torque alters the geometry of the free span (Figure 54, right). The new geometry has positive Frenet-Serret torsion (it is like a positive helix). Transport of the flexible product along this geometry generates a positive flip torque.

What happens next depends on how stiffly the downstream (respectively upstream) flexible product will resist a roll at the downstream (upstream) end of the free span. Let us consider two limit cases. In the following “increase” and “decrease” must be understood as “change to a more positive value” (respectively: negative). For example, torque “increases” from $-5 \text{ kN} \cdot \text{m}$ to $-2 \text{ kN} \cdot \text{m}$.

1. The downstream end of the free span does not resist roll. In other word, the internal torque downstream does not change as the flip torque in the span increases. The increase of the flip torque thus causes a increase in the upstream internal torque.
2. The upstream end of the free span does not resist roll. In other word, the internal torque upstream does not change as the flip torque increases. The increase of the flip torque thus causes a *decrease* downstream internal torque.

The flip torque is actualy distributed, so in case 1. we get an increase of the internal torque (mostly in the upstream half of the free span). This increases the internal torque that originally made an out-of-plane geometry appear. While there are stabilising factors, in particular gravity, these could be overwhelmed, causing an instability. In case 2., on the contrary, the internal torque is decreased (mostly in the downstream half of the free span), stabilizing the situation.

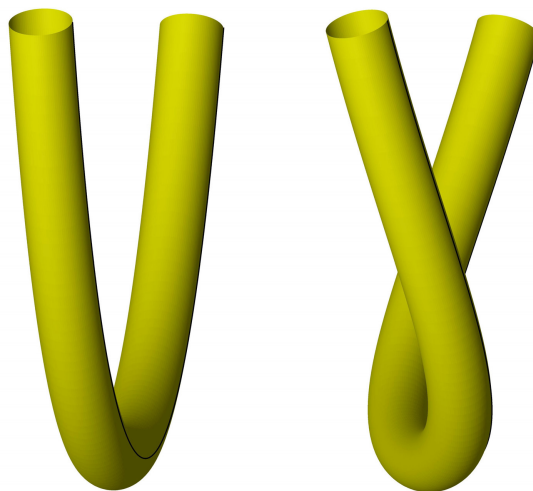


Figure 54: A sag-bend, foreshortened by perspective, looking downstream. Left: in the absence of internal torque, right: with positive internal torque.

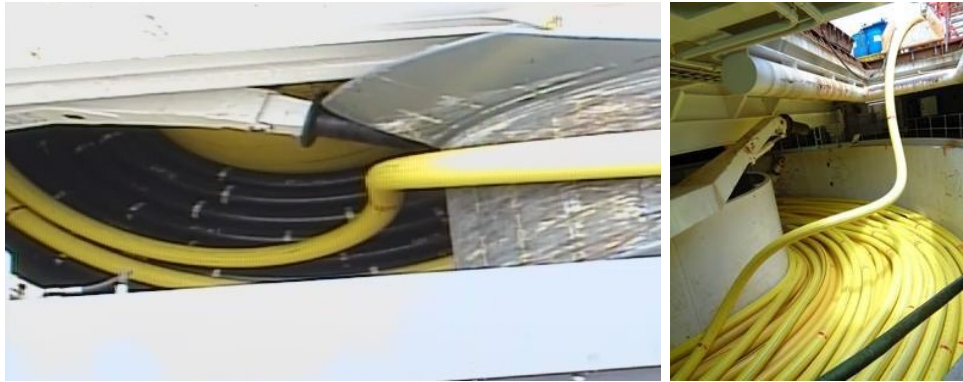


Figure 55: The positive flip torque in the free span is increased as the span deforms under a positive internal torque (left). The situation can evolve into helical buckling (right) (anonymous source, by permission).

To summarize, the feedback loop, supposing that there is a bent free span, and that there is transport, is as follows:

1. Internal torque in the span causes the span to deform out of plane (Figure 54),
2. This results in a curvature that changes of curvature plane,
3. This produces a flip torque,
4. If the downstream flexible product is compliant, the flip torque increases the internal torque in the span,
5. and so on.

8.5 Residual curvature realignment

Section 4.6 mentions the special case of sheaths that have crept while the flexible product was in storage, inducing a residual curvature. Simply put, if a flexible product with such a residual curvature “to the right”, passes at a point along the route that takes a turn “too the left”, rolling the product 180 [deg] (either in the positive or negative direction), will release stresses in the sheath. This type of instability has been documented in the installation of steel pipelines [14, 15, 55], but not, to the authors knowledge, in flexible products.

This effect is distinct from flip (Section 5). The roll in residual curvature is self limiting: for a purely elastic product (no plasticity or friction), the roll to realign the curvature is at most 180 [deg]. In contrast, flip require friction (or plastic deformation), and roll is not limited by the flip mechanism itself, only by (typically) the fact that spatial roll is zero (or related to stored torsion) at the upstream turntable.

The idea of feedback loop is adequate for self-amplifying phenomena. If the curvature is already at a 90 [deg] angle to the bending moment, this just generates a torque, that will decrease as bending and moment align. But starting with curvature and moment in the same plane, yet both in opposite directions, the feedback loop is:

1. The curvature is slightly out of plane with the moment,
2. This produces a torque,
3. The torque drives the curvature further out of plane,
4. and so on.

8.6 Helical buckling

Helical buckling is not typically a mechanism of internal torque generation. This is however treated in the present Section I for two reasons. First, this Section is close to Section 8.4, to emphasize that helical buckling and flop-torque-geometry instability are two distinct mechanisms, that occur under quite distinct circumstances. At the same time, helical buckling changes the geometry of the flexible product, and so does indeed influence internal torque generation.

As discussed in Section 3, the link between two ends of a segment of flexible product is the sum of the twist and the writhe. Consider a straight segment that has a link (Equation 56,top). Since it is straight, there is no writhe, and the link is equal to the twist: the segment is under torsion.

A segment under torsion, like a loaded spring, stores elastic energy ("careful when releasing"). If the link is completely transformed into writhe (if the straight flexible product takes the shape of a helix), then the torsion in the segment is zero, and the torsional elastic energy has been released (Equation 56,bottom). But whether this transformation happens depends on how much energy is absorbed to create the new shape: the segment has now some bending energy (some spring-back if the boundary condition are released). But mostly, the energy has been dissipated as heat produced by sliding of components to accommodate the new geometry. Another "energy cost" is that, since the straight line is the shortest path between two points, the helix is not: to create the helix, it was necessary to pull in neighboring flexible product.

All in all, whether buckling occurs depends on whether the torsional energy that could be released is larger than all the work that has to be spent (bending, friction, pulling in).

The feedback loop is:

1. A small curvature, combined with torque, gives rise to moments,
2. The moments drive the curvature,
3. and so on until the helix reaches a stable form.

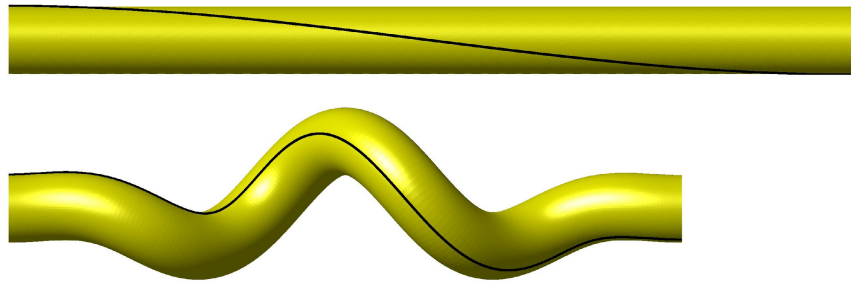


Figure 56: Flexible product under torsion (top), and after helical buckling (bottom).



Figure 57: Examples of helical buckling (left: courtesy of TenneT, right: anonymous source, by permission)

In a typical scenario, the internal torque along a route increases over time (see Section 7), and some slacker free span will suddenly take a helical shape. Alternatively, the internal torque may be at a constant level, but the tension in a free span decreases, triggering helical buckling. Buckling can also occur during a pause in transport if tension is released.

While the helical geometry may not necessarily cause damage to the flexible product, it is awkward to handle and store. In general reverting the operation will not undo the buckling (Section 8.7). In particular, pulling on a helix or a loop thus created is likely to create a hockle, [62], in which the bending is concentrated very locally, causing potentially severe damage to the cross-section.

The pitch length of the helix *at the initiation* of buckling is roughly

$$P = 2\pi\sqrt{\frac{EI}{R_1}} \quad (124)$$

where EI is the bending stiffness and R_1 the tension (Figure 58).

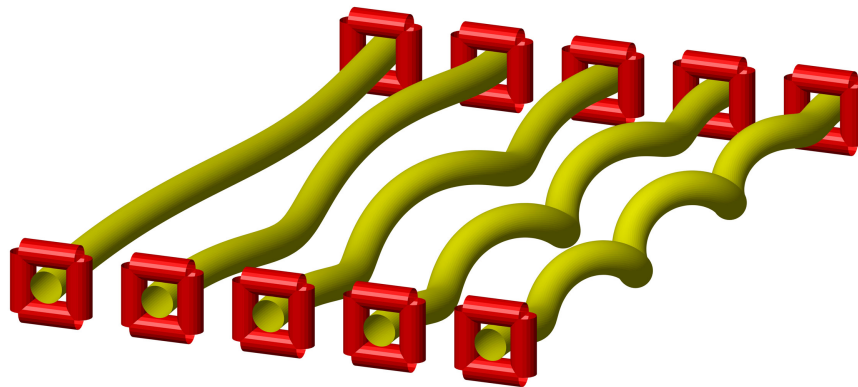


Figure 58: Buckling shapes: increasing tension (from left to right) result in lower pitch length P

8.7 Irreversibility

When a transport operation leads to an unwanted state with for example a build up of internal torque, one option that comes under consideration is to backtrack to a safe situation, and from there, to make a second attempt.

In practice, this may or may not work. As an example, consider a heavy cube on a smooth slope. As the cube is left undisturbed, friction is sufficient to prevent the cube from sliding down the slope. Let us assume that we can only apply forces towards the left or the right (following altitude contours), but not up or down (Figure 59). We apply a force to move the cube 1m to the right, then another force to move 1m to the left. However, as the cube slips right and left, it will also slip downwards (Section 6.4). As a consequence, without applying vertical forces, we can never bring the cube back to its original height. The 2nd law of thermodynamics (“entropy can not decrease”) translates in practical mechanical engineering as follows: in the presence of friction, viscosity flow or plastic deformations (anything that creates heat), reverting what can be controlled will often not revert the parameters that can not be directly controlled.

The handling of flexible products offers many examples of this: actuators (winches, tensioners, turntables etc.) give control over some aspects of the movement of the flexible product (movements along the route, some aspects of the shape of free spans) but not over others (roll, the details of the shape of free spans, the sliding of internal components). The reverting the controllable aspects will generally not revert the uncontrollable ones, and this may be significant.

One example of irreversibility is helical buckling (Section 8.6) followed by hocking: in a straight product under internal torque and tension, reducing tension can give rise to helical buckling. If the span is long compared to the diameter, the instability can give rise to small curvatures and no slip occurs. In more realistic cases, this buckling is accompanied by slip of the components

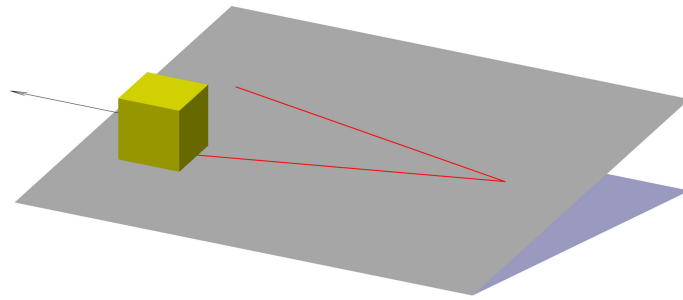


Figure 59: A cube on a slope can not be brought back to its original state by forces across the slope.

and hence energy dissipation into heat. Increase the tension back above the value at which the instability occurred can cause a hockle to occur [62]. Even if the helix was so little pronounced that a damaging hockle does not appear, the flexible product will not be straight. The particular issue of hockling at the touch-down point during installation on the seafloor is considered in Section 9.5.2.

Another example of irreversibility was discussed in Section 6.2: spooling and unspooling behave differently.

9 System behaviour

9.1 Introduction

The object of Part 9 is to present relevant cases that show the interplay between the effects discussed so far in preceding sections. This interplay is sometimes complex and can give rise to surprising behaviour of the operation as a whole. The emphasis here is on providing an insight in these interplay, and so the discussions presented here are qualitative: no hand calculations or numerical simulations are provided.

The behaviors described in this Section all come from reports received in confidence from the industry. They are presented in anonymized form. The cases were reported with various degrees of documentations. For some of them, the mechanism was established with a high degree of confidence. In other cases, the mechanism described here may be only one of several possible causes of the reported event, given the available data.

9.2 Torsion in factory

9.2.1 Unbalanced winding machine

A winding machine has the potential to apply considerable external torque to the flexible product that it builds. The winding machine can apply external torque through tension in the components, and through radial forces applied to wrap components around the product. This raises the question of how to ensure that the flexible product coming out of a winding machine does not carry a significant internal torque (Figure 60).

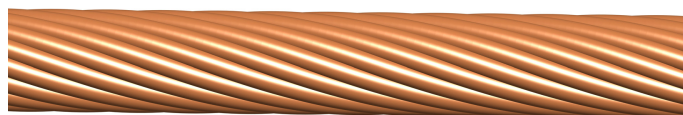


Figure 60: Example of component for which there is no obvious way of defining “zero torsion”.

At the beginning of the production of the flexible product, the head end is typically attached to a steel flexible product through a swivel with which it is pulled through the extrusion machinery: there is at this stage little or no resistance against roll from the product downstream of the production machinery, and hence little torsion. One can easily measure the material roll rate by setting a tag (for example a patch of adhesive tape) on the product (Section 3.12.2), and in the absence of torsion, material and spatial roll rates are identical. This provides an opportunity to tune the winding machines by zeroing the roll rate.

The situation changes later in production, when the head of the flexible product is stored in a downstream turntable or spool, adding resistance against roll (Sections 6.2 and 6.1), so that torsion can no longer be relied upon to be zero. Without ideal longitudinal marking, there is

no obvious way to measure torsion, and without torsion, it is not possible to use Equation 10 to obtain the spatial roll rate.

A longitudinal marking extruded on the polymer sheath does not provide additional information: A straight longitudinal marker is the same as having a series of point markers and observing zero material roll on all of them (Figure 61). With reference to Section 3.4, this is not necessarily an *ideal* longitudinal marking, and absence of material roll does not imply the absence of internal torque. A parallel might be helpful: consider a piece of metal that is under tension. A strain gauge is glued to the metal under tension, and calibrated. Reading zero strain does not imply zero stress.

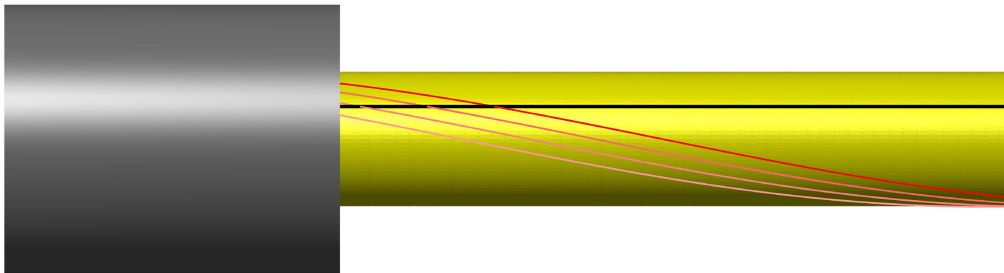


Figure 61: Unbalanced winding machine (in grey) and longitudinal markings. The marking in black is what would be applied by e.g. extrusion. The markings in red are ideal longitudinal markings following a positive helix because of the positive internal torque. The multiple red markings show the motion of a single ideal longitudinal marking. Downstream to the right.

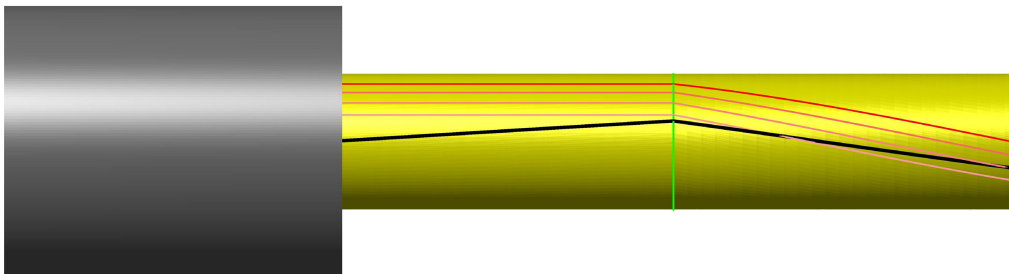


Figure 62: Same as Figure 9.2.1, but the winding machine does not apply an external torque, while the route geometry applies a negative flip torque (cross-section marked in green).

A situation in which a flexible product is stored (spool or turntable) out of the production machine, with internal torque, yet with a straight (non-ideal) longitudinal marking is referred to as “built-in torsion”.

9.2.2 Flip torque

A related behavior can occur with the following (idealized) situation: the winding machine leaves the flexible product free to roll and does thus not apply any torque to it. The flexible

product then passes through a route which geometry induces a flip torque (Section 5) which will be assumed to be negative, before being stored in a turntable.

At steady state (Section 7), the flip torque must be balanced by external torques applied upstream or downstream. During transport, external torques from friction against chutes (Section 6.4), tensioners and rollers (Section 6.5) are generally small, and in this case, it is conservative to neglect them. As a result, the flip torque is counterbalanced by the downstream turntable: the downstream segment carries a positive internal torque (Figure 62).

Hence at the winding machine, there is no external torque, but the flexible product is rolling in the negative direction. A longitudinal marking extruded there will be seen to follow a negative helix around the flexible product, even though the flexible product carries no internal torque. Downstream of the flip geometry, the positive internal torque induces a negative torsion. Whether the longitudinal marking then will follow a negative or positive helix depends on the torsional stiffness of the product, and on the effect of roll rate on the flip torque (Section 5.3).

The scenarios presented in Section 9.2.1 and the present Section are limit cases: more realistically, winding machines *and* route geometry will both introduce internal torques in the product. The two scenarios show that it is difficult to guarantee that a longitudinal marking is an *ideal* longitudinal marking (Section 3.4). In other words, a flexible product with a straight longitudinal marking can have a internal torque. The situation complicates further if the flexible product is torsionally unbalanced (Section 4.8). Scenarios with torsional unbalance are discussed in Sections 9.5.2 and 9.6.

9.2.3 Bird-nesting

The scenarios discussed in Sections 9.2.1 and 9.2.2 result in similar situations at the downstream turntable (or spool): the flexible product carries a positive internal torque (due to negative external torques applied upstream), and material-rolls steadily in the negative direction.

In mild cases, the internal torque is stored in the turntable in the form of a negative torsion (being measured with an ideal longitudinal marking) (Section 6.2). In more severe case, “bird nesting” can occur. Typically, the tension drops downstream of the last tensioner before the turntable, below the tension at which helical buckling can occur (Section 8.6).

Helical buckling can be “self-limiting”: the formation of a positive helix relaxes internal torque, and only a limited length of helix appears. However in the present scenario, the upstream setup induces a continued spatial roll, so that the helix formation does not stop: the helix is continually generated downstream of the last tensioner and is stored in the turntable. The product stored in the turntable has an aspect suggestive of a bird’s nest (Figure 63). Flexible products of smaller diameters are typically undamaged, yet unserviceable if no solution is found to remove the link in the flexible product.

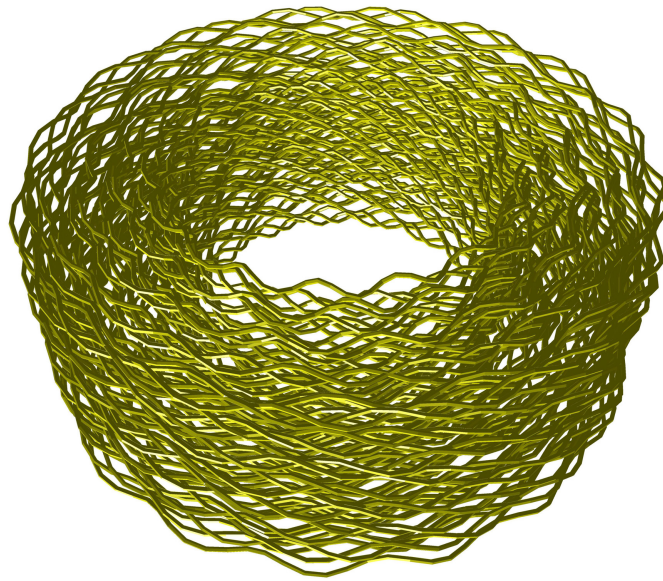


Figure 63: Bird's nest: a flexible product having undergone continuous helical buckling.

9.3 From storage to storage

9.3.1 Long-distance conservation of torsion

In the following “storage” will stand for turntables, spools and the seafloor – locations in which friction prevents the flexible product from rolling over long distances. The special case of baskets will be addressed in Section 9.4. Transfer of flexible products between storages are made in a variety of settings, including:

- In factory, when a product is shuttled between two turntables, to perform several passes through winding, extruding or other machines.
- In load-out operation, where the flexible product is transferred from a turntable storing the completed product, to a turntable on board and installation vessel.
- During installation, where the product is transferred from an on-board turntable to the seafloor.
- In a detailing operation, where the flexible product is transferred to spools and segmented for road transport.

Generally, the distance between storages is small compared to the length of flexible product being transported. This makes it reasonable, barring instabilities, to assume the operation will approach a steady state (Section 7). Further assuming *ideal longitudinal marking* (Section 3.4), internal torque and tension both not changing over time implies that torsion will be constant over time at any given point. Hence the twist between any two points along the route will be constant. Since for a fixed route the writhe between any two points along the route does not change with time, the link between two points does not change with time. This implies that *at steady state with an ideal longitudinal marking, the spatial roll rate is uniform along the*

route. In practice, the value of that roll rate depends on the upstream boundary condition. In particular, if a flexible product is stored without twist in the upstream storage, then at steady state the roll-rate will be zero along the whole route.

The material roll rate $\partial R/\partial k$ at the upstream storage has to be zero, so Equation 77

$$\frac{\partial R}{\partial k} = -\tau$$

applies here, where τ is the torsion of the flexible product *in storage*. Let us assume that τ is uniform along the flexible product in the storage. $\partial R/\partial k$ at the downstream storage is the same as at the upstream one, and hence *at steady state the torsion τ of the flexible product stored in the downstream storage is the same as in the upstream storage*.

Hence over long lengths of flexible products, and as a first approximation, the torsion in the installed product is equal to the built-in torsion (Section 9.2).

The above reasoning is not applicable for the head and tail section of the flexible product: while the head of the flexible product is traveling along a route, it is relatively free to roll (Sections 6.4 and 6.5). In the absence of flip torque, for example, this implies that the internal torque in the segment behind the head can be released (and the same applies to the tail).

9.3.2 Torque buildup

An important class of problems occurs when a flip torque (Section 5) is present along a route between two storages (as defined in Section 9.3.1). To simplify the discussion, it is assumed that the upstream storage stores product with zero torsion, the flip torque is applied in a positive direction, at one single point on the route, and the route does not vary over time. The conclusions will still largely hold when relaxing these assumptions. The setup is schematized in Figure 64.

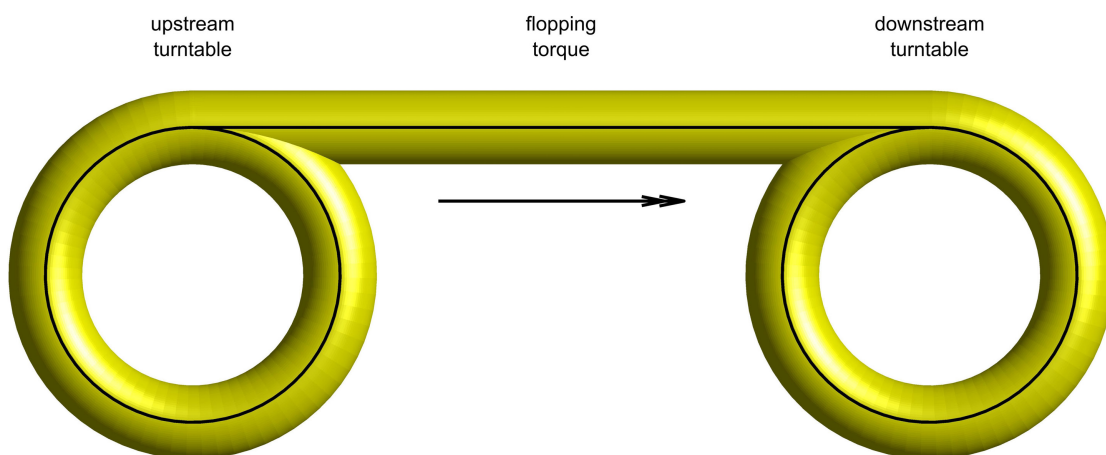


Figure 64: Upstream and downstream storages and flip torque.

To further simplify reasonings, let us imagine that the head of the product has reached the downstream storage, and that somehow it does so with zero torsion everywhere along the

route. Then again somehow, the flip torque is “switched on”, and the operation continues. The flip torque causes a positive roll at the point of application, spreading upstream and downstream as the operation progresses. The spread is slowed down but not stopped, by rollers and tensioners (Section 6.5), curves (Section 5.3) and chutes (Section 6.4).

At the upstream storage, since no torsion is stored in it, the spatial roll rate is zero (Section 6.2), so that a positive twist builds up between the upstream storage and the point with flip torque. At the downstream storage, the downstream twist gets stored (Section 6.2).

If the operation reaches a steady state (Section 7), then the spatial roll rate everywhere becomes zero. Downstream, since the twist between the head of the flexible product and the point of flip torque is distributed over that whole length, the torsion approaches zero. At zero spatial roll rates, the external torques from rollers, tensioners, curves and chutes becomes zero: the flip torque is balanced by external torque at due to friction at the upstream storage. As a consequence, the internal torque in the flexible product, upstream of the flip torque point, is equal to the flip torque (Figure 65).

One should be careful to assume that the steady state provides a safe upper bound for the torques that can be produced during installation: It is suspected that instabilities like torsion-pressure instability (Section 8.2) and flop-torque-geometry instability (Section 8.4), as well as cracking with hydraulic tools (Section 6.6) can cause significant increases in torques.

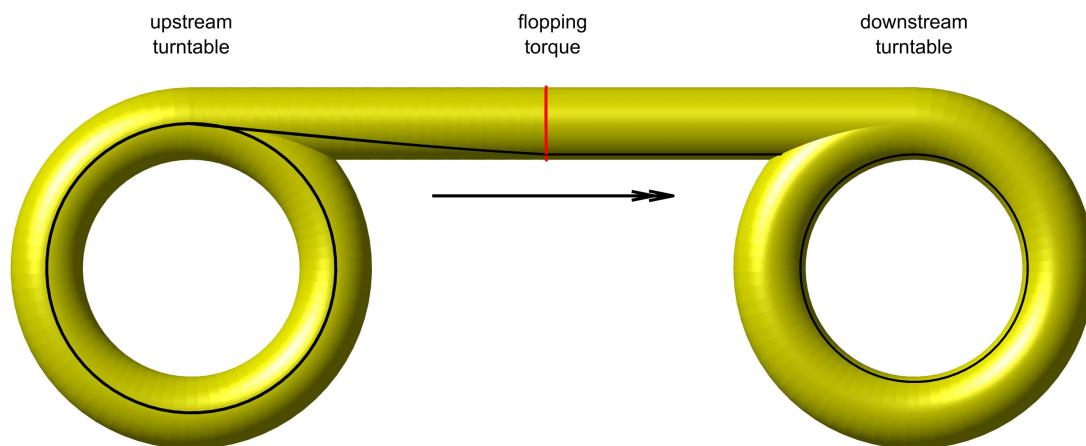


Figure 65: Steady state configuration.

If the flip torque is high enough, the internal torque can be high enough to cause helical buckling (Section 8.6), or local damage to the cross-section (Section 10), somewhere between the upstream storage and the flip torque point.

Multiple incidents are thought to share the mechanism described above. In a load-out operation, the free span above the onboard turntable generated a flip torque. The intensity of the flip torque varied with the geometry of the free span, and waves of roll were documented to propagate upstream, across several tensioners. The internal torque ultimately caused damage to the cross-section, rendering the product unfit for use, causing severe financial loss. Similarly, in various operations, multiple documentations of helical buckling near the upstream storage have been seen.

9.3.3 Evolution of a loadout operation

A loadout operation between two turntables is considered. Tens of kilometers of flexible product are to be out-loaded, to an installation vessel. The length of the route is a few hundred meters. It is assumed that near the downstream turntable, the route geometry imposes a positive pseudo external flip torque (Section 5.4).

At the start of the operation, the flexible product is stored in the upstream turntable with zero internal torque (Figure 66). The longitudinal marking is ideal, so there is zero torsion.

The head of the flexible product is winched along the route (Figure 67). The head of the flexible product has not yet reached the flip area, and so there is neither torque nor torsion in the flexible product.

The head of the flexible product has just reached the flip area (Figure 68). Because there is no flexible product downstream of the flip area, the downstream torque is zero. Because roll has just started, no torsion build-up has yet occurred upstream, and the upstream torque must thus be zero. To respect force equilibrium, the flip torque must hence be zero. This in turn implies that the roll rate (in the absence of torsion: material as well as spatial) is equal to the value for which the flip torque becomes zero (Figure 40, red curve), which is roughly “the” Frenet-Serret torsion of the flip geometry (typically, this Frenet-Serret torsion is not uniform over the span).

The head of the flexible product has just reached the floor of the turntable (Figure 69), and it is either latched to the turntable, or enough flexible product has been stored that friction prevents material roll at the touch down point. Under the same argument as above, the upstream torque is still zero. Because the distance between the flip area and the downstream turntable is very short, the spatial roll rates at both points are equal, and hence the spatial roll rate in the flip area is positive equal to the opposite of the downstream torsion. By stating that spatial and material roll rates in the flip area are nearly the same (assuming that the torsion is small compared to the Frenet-Serret torsion), this allows to determine the roll rate from the “effect of roll rate on flip torque” diagram.

The level of downstream torsion thus generated depends on the torsional stiffness of the product. Two limit cases are of interest: If the torsional stiffness is high, torsion will be small, and the torque will be the opposite of the flip torque at near-zero material roll rate. If it is low, the downstream torsion will be the opposite of the Frenet-Serret torsion. Either way, in this phase, the consequences of flip are felt downstream, and torque-induced failures would be observed in the vicinity of the touch down point in the downstream carousel.

As the operation progresses, the positive spatial roll at the flip area leads to the build up of positive torsion upstream. This has several effects: the spatial roll rate at the flip area is reduced, increasing the flip torque. Reducing the spatial roll rate also reduces (in absolute value) the downstream torsion. This progresses until steady state is reached (Figure 70) in which the upstream torsion is constant, causing the downstream torsion and torque to be zero, so that the upstream torque is equal to the flip torque. The flip torque is a value corresponding to zero spatial roll rate (near zero material roll rate).

At this point of the operation, the maximum value of the upstream torque is reached, and failure can be experienced anywhere between the upstream turntable and the flip area.

The tail of the flexible product has just left the upstream turntable, and is thus no longer restrained to a material roll equal to zero (Figure 71). The upstream torque is just relaxed by roll of the flexible product along the route. Relatively rapidly, the upstream torque gets close to zero. From the point of view of torque equilibrium at the flip area, the situation is very similar to that just after the head of the flexible product reached the downstream turntable: this is another phase of the operation where failure at the touch down point can occur.

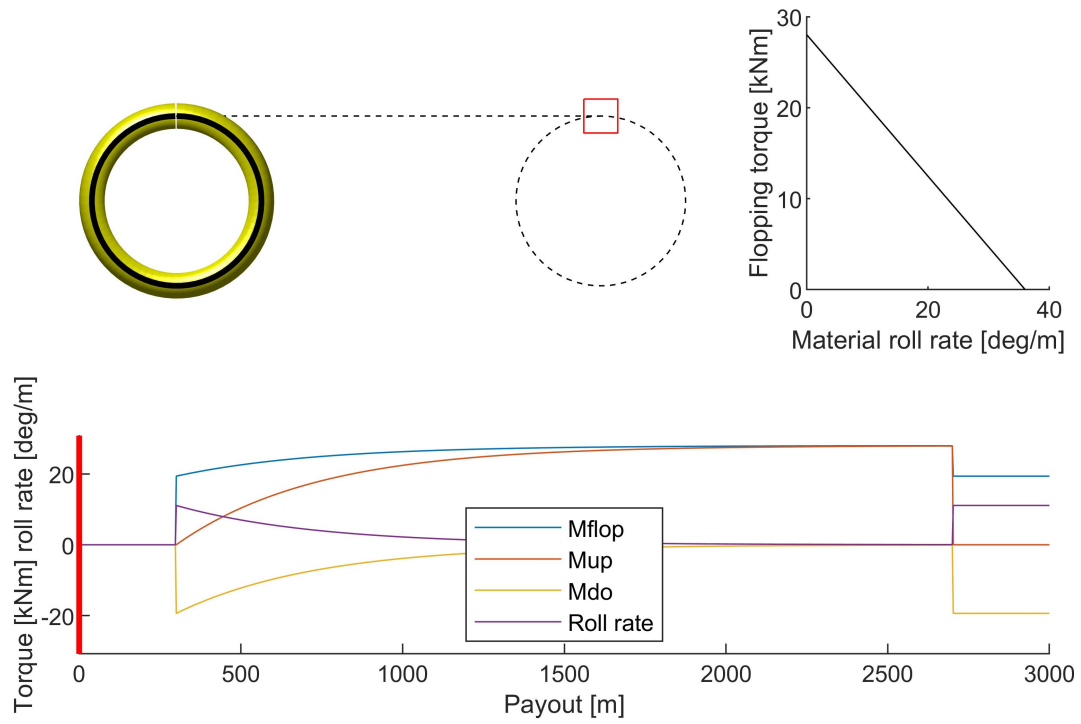


Figure 66: Flexible product stored in the upstream turntable.

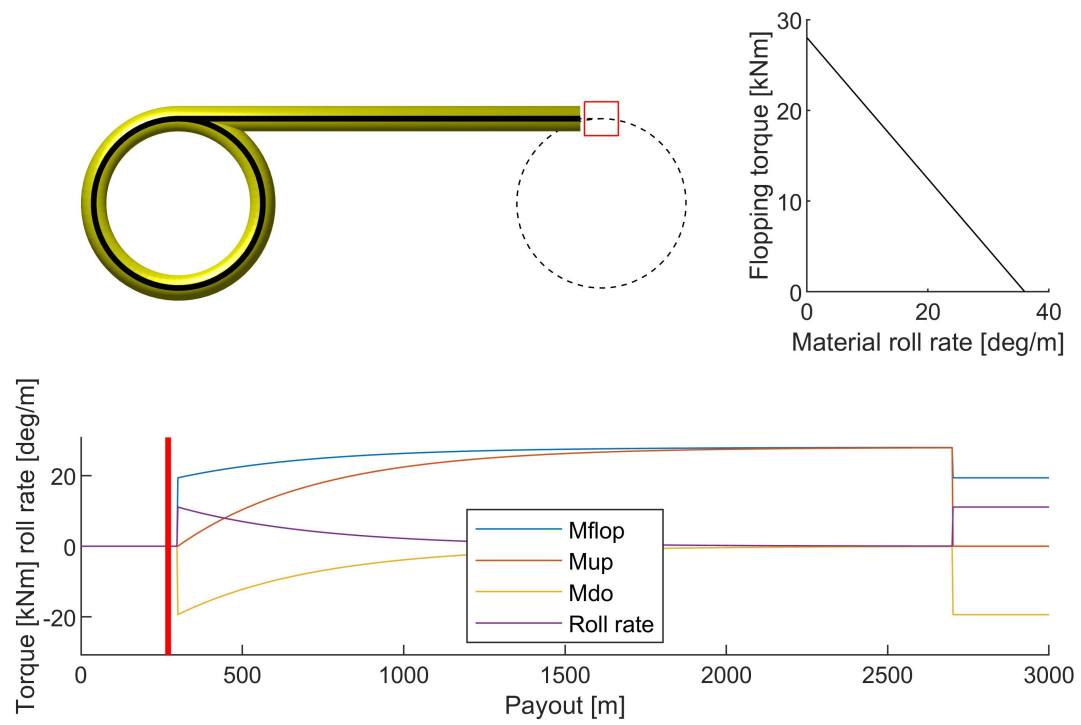


Figure 67: Flexible product winched along the reach approaches the flip area.

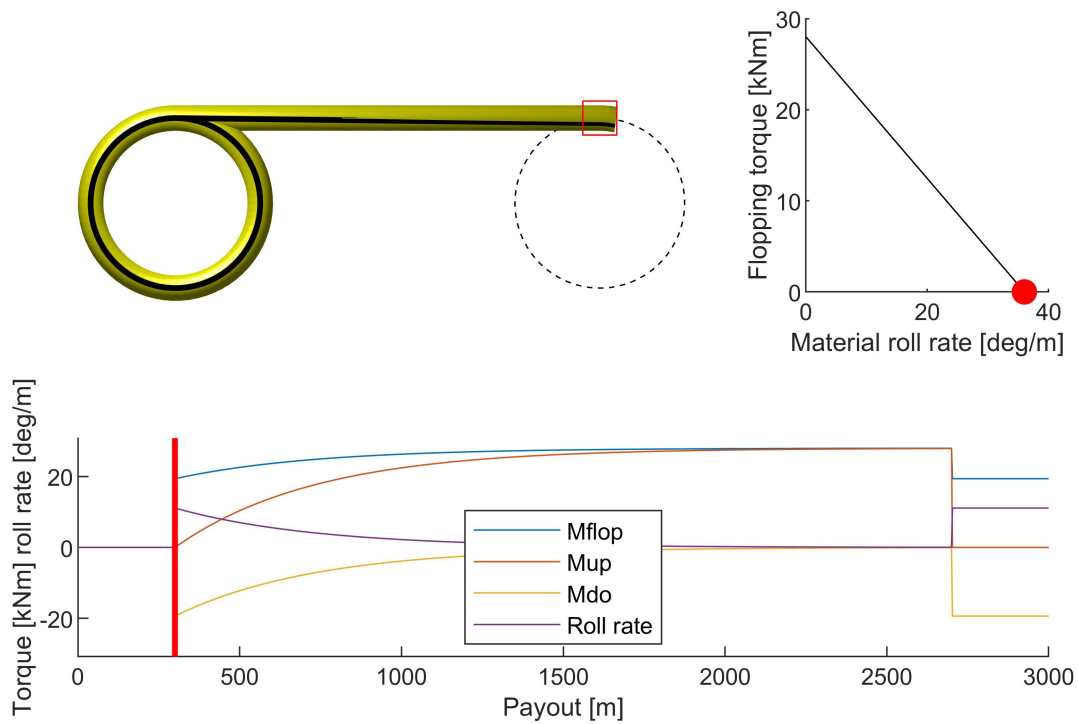


Figure 68: Flexible product enters the flip area and experiences high roll rate.

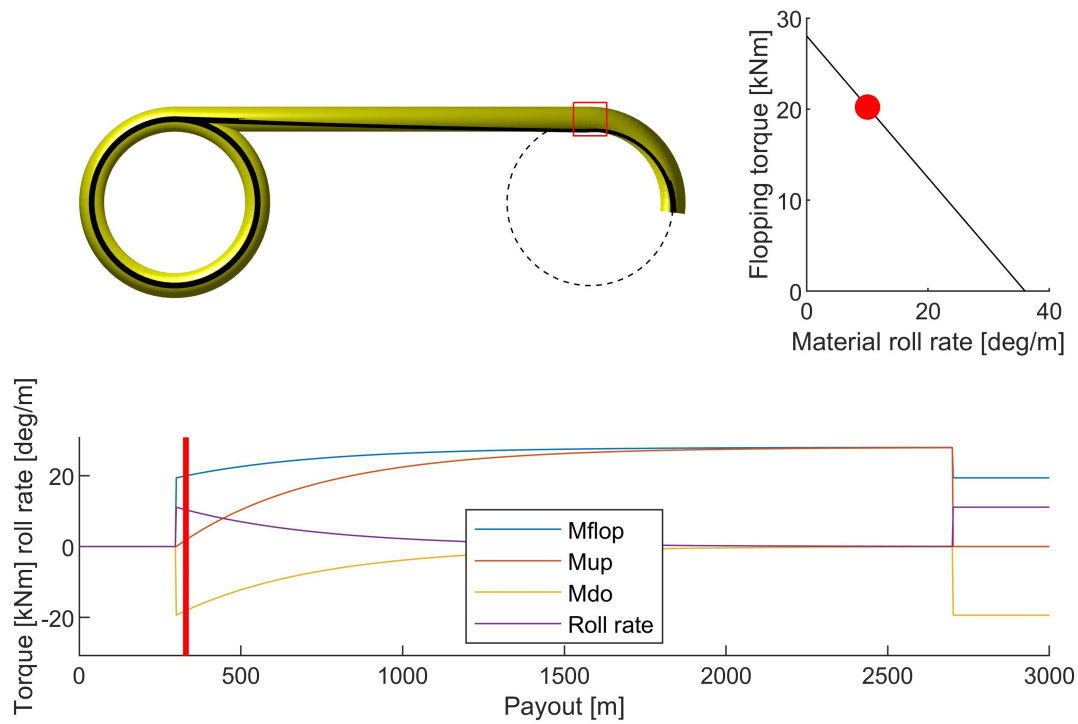


Figure 69: Flexible product latched to the turntable, high torsion or torque downstream of the flip area.

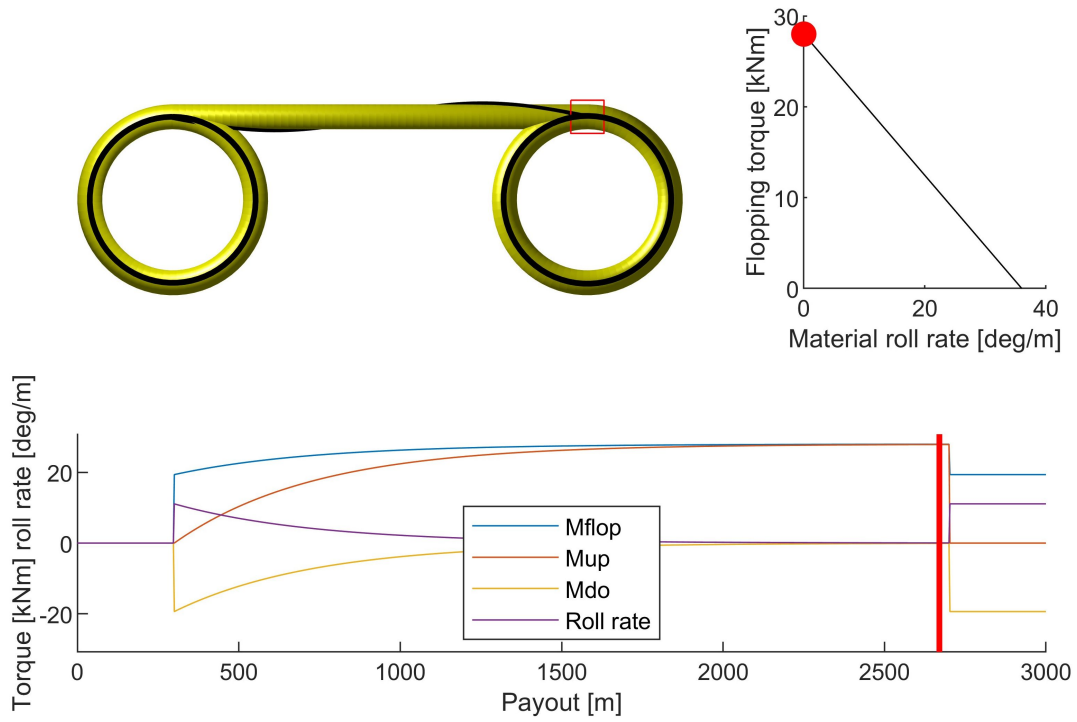


Figure 70: Steady state, with flip torque taken up upstream.

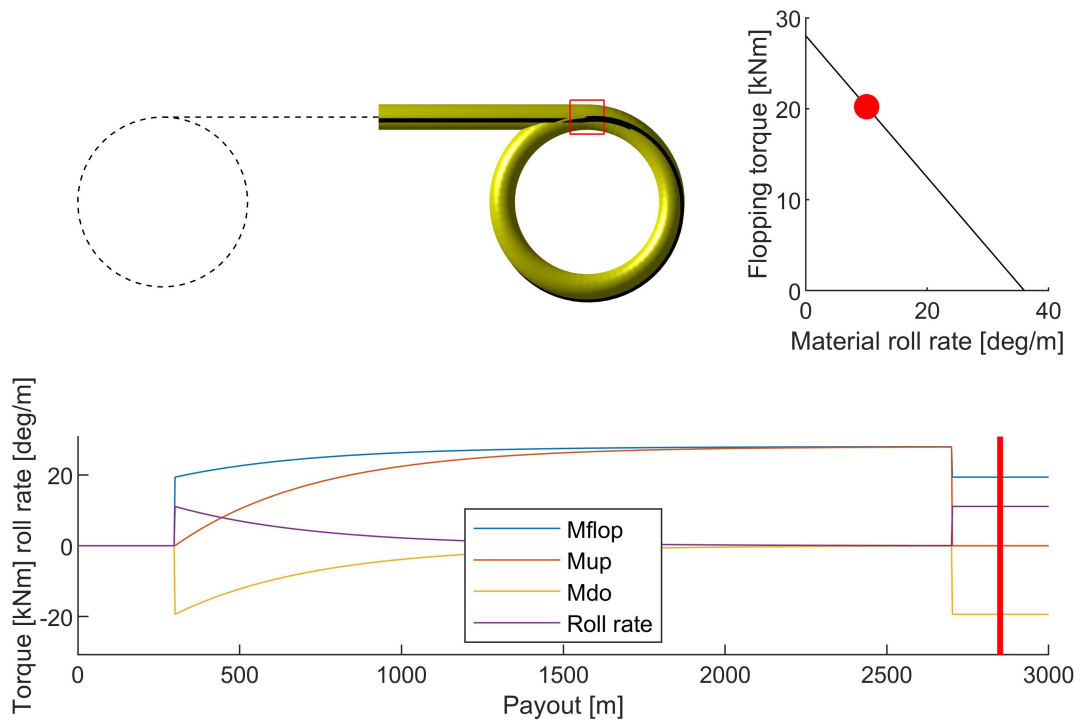


Figure 71: New transient as the cable tail leaves the upstream turntable.

9.4 Baskets

Unlike turntables, baskets do not rotate around a vertical axis, and as a consequence, storing a flexible product in a basket induces torsion in the stored product (Section 6.3)

Let us consider a positive basket (Figure 49) in which a flexible product is stored as it is produced, coming from a winding machine that induces zero spatial roll rate, or from a spool or turntable. Equation 86 states

$$0 = \tau + \frac{\partial R}{\partial k} + \frac{360}{\lambda}$$

where λ is the length of a coil and τ the torsion stored in the coils.

At steady state with the above mentioned absence of spatial roll at the winding machine, $\partial R/\partial k = 0$ near the basket, hence $\tau = -360/\lambda$ (here steady state is a simplification, assuming all coils to have the same length). This means that there is a negative internal torque stored in the basket. In order to ensure equilibrium, this implies that there is a negative internal torque in the flexible product between the winding machine and the basket (assuming that there is no flip torque, Section 5). In the period before steady state, this negative internal torque will propagate upstream from the basket, slowed down but not stopped by tensioners, rollers (Section 6.5) and chutes (Section 6.4).

The torsion $\tau = -360/\lambda$ is usually quite large, and hence baskets are used with either flexible products of small diameters, or flexible products in which by construction have a low torsional stiffness. Low torsional stiffness in one direction is achieved by winding all layers in the same direction. In the present case, a basket with positive top feed, inducing negative torsion, this would require components laid as positive helices (Z-laid).

When the flexible product is taken out of storage, "the movie is played backwards" but the sign convention for roll is flipped, so the spatial roll has the same *value* as when paying in. In mathematical terms. The sign of the stored torsion is unchanged, because it is independent of the choice of positive direction along the route.

$$\frac{\partial R}{\partial k} = - \left(\tau + \frac{360}{\lambda} \right) \quad (125)$$

$$= - \left(-\frac{360}{\lambda} + \frac{360}{\lambda} \right) \quad (126)$$

$$= 0 \quad (127)$$

As can be seen in Figure 72, with the two spatial roll rates being identical, this is in a way as if the storage in the basket had not happened - and this is also true before steady state. However, as mentioned above, while being loaded, the basket imposes an external negative internal torque, resulting in a negative internal torque upstream. While being unloaded, under the above assumptions and at steady state, the basket imposes $\partial R/\partial k = 0$. Whether there will be a internal torque downstream of the turntable depends on the rest of the route.

Industrial experience leads to favoring top-feeding into baskets from points placed high above the basket. A possible explanation is as follows: in a positive basket, the free span is a positive

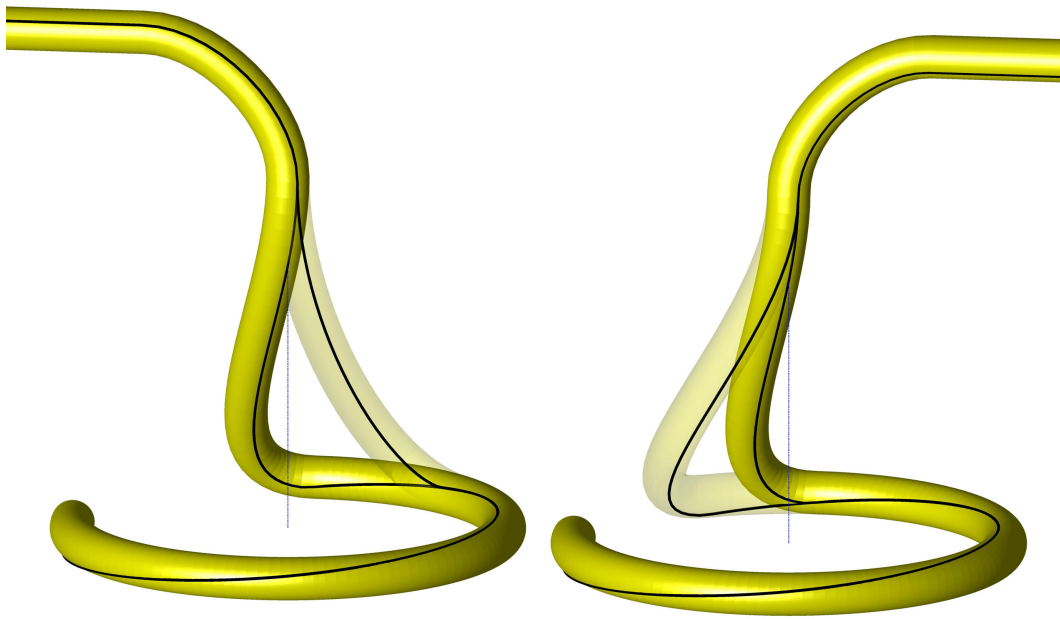


Figure 72: Flexible product entering (left) and leaving (right) a positive basket, with zero spatial roll at the top.

spiral, and feeding the flexible product through the free span induces a positive flip torque. This external torque partly balances the negative internal torque in coils, thus decreasing the internal torque upstream of the basket. When paying out from the basket, the flip torque is still positive (with the sign convention flipped). The internal torque tends to release the torsion stored in the coils, and is balanced by friction in the basket. An obvious challenge is to choose the height of the free span adjust the length over which the curvature changes plane, in order to approximately cancel out the internal torque stored in the coils.

9.5 J-lay installation

9.5.1 Torque build up

During the installation of a flexible product from a vessel to the seafloor, the same situation as described in Section 9.3.2 can occur: The seafloor takes the place of the downstream storage, freezing material roll through friction. “Spatial roll” then needs to be understood relative to the vessel, or to the touch-down point, not relative to a point on the seafloor.

The geometry of the route on board the vessel is often a source of flip torque. Another potential source that needs to be excluded is strong cross currents, which may cause the free span between the touch down point and the installation vessel not to be restricted within a vertical plane.

In one case, an offshore laying operation had to be interrupted when helical buckling appeared between the on-board storage and a part of the on-board route generating flip torque. It was

not possible to pass the buckled geometry through tensioners and thence overboard, so the product ultimately had to be cut and abandoned on the seafloor.

9.5.2 Touch-down point hocking

In the free span between the installation vessel and the touch down point, the tension will vary, increasing from the seafloor towards the vessel. If the flexible product is torsionally unbalanced (Section 4.8), then torsion τ and elongation ϵ both influence internal torque M_1 and axial force R_1 (Equation 6). The axial force R_1 appearing in this equation is the tension in the flexible product, not the *effective* tension [60].

To simplify reasoning, it is assumed that the free span to the touch down point is in a vertical plane, so that no flip torques are developed there. Also, the unbalanced cross-section has a behavior dominated by a tensile armor laid as a positive helix (Z-laid). This implies that if elongated, it tends to unwind and acquire a negative torsion. Alternatively, if elongated but prevented from rolling, it acquires a positive internal torque.

If the depth and the top tension have been held constant long enough, steady state is approached (Section 7): The internal torque in the free span will approach zero (Section 6.2), hence there is a negative torsion, varying in intensity with depth (Figure 73 b).

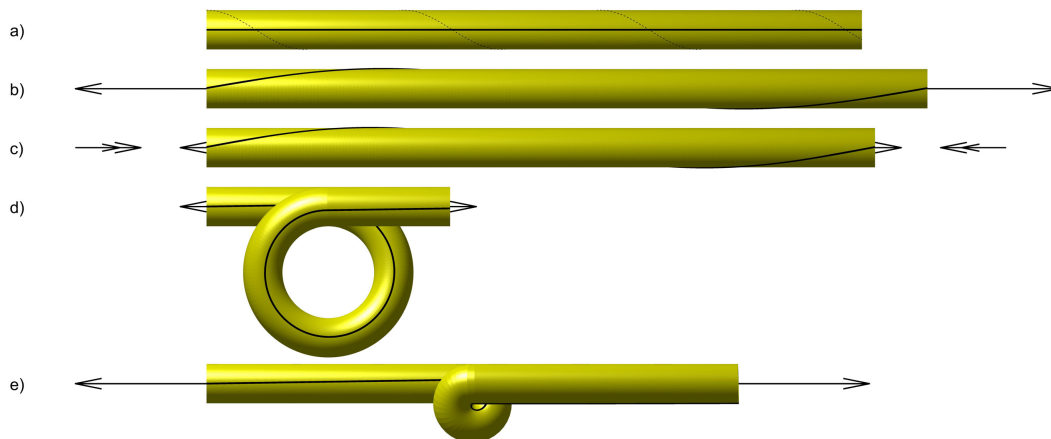


Figure 73: a) Unloaded product, with tensile armor in positive direction (stippled helix). b) Under high tension and at steady state, negative torsion and no internal torque. c) As tension is relaxed under constant link, negative internal torque. d) With decreasing tension, internal torque is relaxed by helical buckling. e) Reapplying tension may lead to a damaging hockle.

In the next step, the top tension is rapidly decreased by paying out a length of flexible product without the laying vessel moving forward by the same length, or by holding the top of the flexible product and letting the vessel surge aft. This decreases the tension along the catenary. Because the decrease is rapid, the link (Section 3.9) in the free span does not change and the torsion remains unchanged³ (Figure 73 c).

³Actually the torsion can redistribute along the free span, but the link, which is the integral of the torsion, does not change. This does not affect the present reasoning.



Figure 74: Helical buckling, liable to cause a hockle if tensioned (anonymous source, by permission)

With the elongation decreasing while torsion remains unchanged, a negative internal torque appears along the free span. Tension is lowest at the touch-down point. The combination of internal torque, and low tension can be unfavorable enough to cause helical buckling (Section 8.6) near the touch down point (Figure 73 d).

Reapplying a higher top tension may either resolve the helical buckling, or lead to a localized hockle with the potential for serious damage to the cross-section (Figure 73 e).

9.6 Shore pull-in

At the start of a shore pull-in operation, the flexible product is stored on board an installation vessel anchored or beached as close to the high tide line as possible. The head of the flexible product is then hitched to a steel flexible product and winched to the shore terminal. The product paid out can either be carried by an alley of rollers temporarily set up on the beach, or supported by a series of floaters. In this section, only the scenario of an alley of rollers is discussed.

The winch force needs to be large enough to drive the deformation of the flexible product as it passes the rollers. The longer the pull in, the higher the force becomes. If the cross-section is torsionally unbalanced, the flexible product will tend to unwind. In Figure 75, it is assumed that the flexible product has a single tensile armor laid as a positive helix (Z-laid). The head of the flexible product is usually free to roll (it is hitched to the winch flexible product via a swivel), and the rollers only slow down roll during the pullout (Section 6.5). Towards the end of the pullout, the flexible product is elongated, has torsion, but a low internal torque (Figure 75 middle).

Once the flexible product head has reached the shore terminal, the winch load is slowly released. Spring back, from relaxing tension in the flexible product is small. So although the head is free to roll, friction against the rollers, as well as internal friction, will almost completely

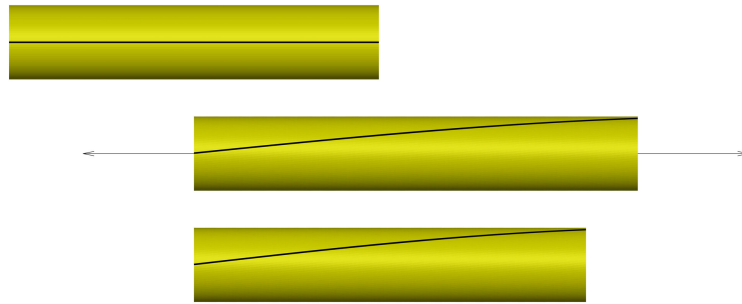


Figure 75: Flexible product at rest (top) at steady state during pull-in (middle) and after relaxing tension (bottom).

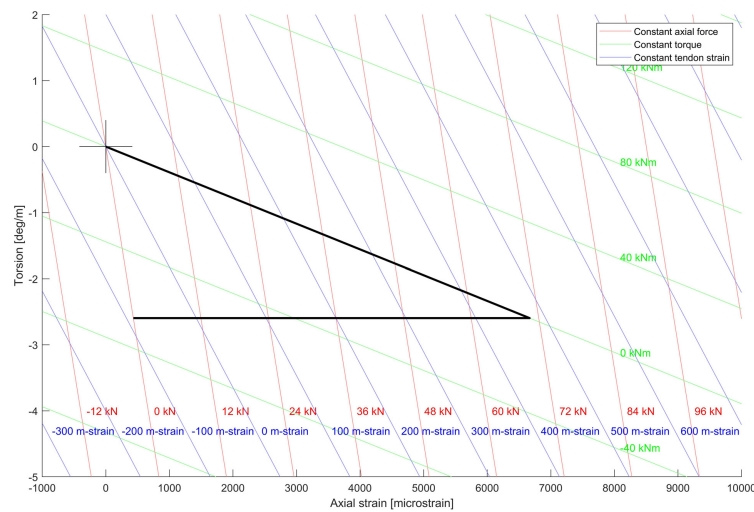


Figure 76: Phases of a pull-in operation and effect of armor wire strain.

prevent the roll of the flexible product so that torsion is unchanged. This results in a internal torque (Figure 75 bottom).

Figure 76 shows series of lines of constant value of tension and torque in the flexible product, and strain in the tensile armor, as a function of elongation and torsion. The bold line shows the idealized history of elongation and torsion of a cross-section: it first follows a line of constant (zero) torque, and then a line of constant torsion to the point of zero tension. As can be seen, this leads to compressive strains in the tensile armor. This may result in a local failure of the tensile armor (Section 10). Helical buckling (hocking) is expected to be prevented by the high amount of work needed to pull in “slack” needed for the helical geometry.

10 Local failure mechanisms

10.1 General remarks

Section 10 discusses the various mechanisms by which flexible products can fail when subjected to torque. More specifically, failures with large local plastic deformations are described. Helical buckling is handled in Section 8.6 because of its apparent similarity with mechanisms of torque generation.

While torque generation is related to only a few properties of the flexible product (for example the friction bending moment M_f), failure mechanisms are more dependent on details of the construction of the flexible product. Skew-kinking (Section 10.2) is only relevant for flexible pipes, while herniation buckling (Section 10.4) is strongly influenced by the presence or absence of multiple tensile layers around the product.

Design codes do not, generally, address the issue of determining the torque that a flexible product can safely be exposed too. Attempts to use extent codes to do so may thus lead to unconservative results. Further, the failures modes are not always recognized as torque related, making it more difficult to improve future operations.

In the following, figures depict the aftermath of failure under a *positive* internal torque. The corresponding figures for negative internal torque are obtained by mirroring. This mirroring will also change the sign of the helices in the component. For example, a product with a single tensile armor will fail differently if torque increases, or decreases tension in the armor.

10.2 Skew-kinking

Skew-kinking is a mechanism that has been observed in flexible pipes, and that is related to kinking. Kinking can occur when e.g. a pipe is bent: it first ovalizes. Then as bending is increased, the ovalization becomes more pronounced and localizes, leading to local high plastic deformations. Ultimately, this results in a kink, that is a flattened cross-section of the pipe, with the wall of the pipe (nearly) self-contacting along a line orthogonal to the axis of the pipe (red line in Figure 77, left).

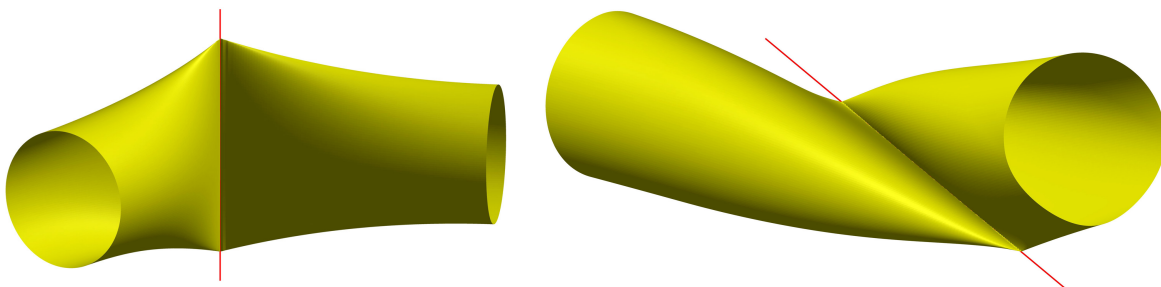


Figure 77: Kinked pipe (left), and skew-kinked pipe under positive internal torque (right).

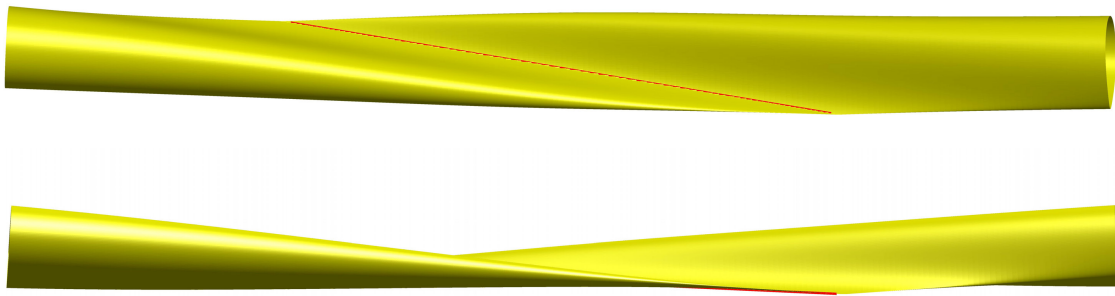


Figure 78: Skew-kinking can easily be confused with crushing.

When torque is present in addition to bending moment, the kink-line is no longer orthogonal to the axis of the pipe, and the kink can occur at curvatures that would otherwise have been acceptable (Figure 77, right).

Where the torque is high, the kink axis can be almost tangent to the pipe, and this gives rise to a geometry that can be misinterpreted as resulting from crushing (Figure 78). High external pressures or high tensioner contact forces can contribute to this failure mode.

The mechanism is not known to have occurred in cables or umbilicals: clearly the “payload” (e.g. insulators and conductors) resists compression and thus limits ovalization.

10.3 Birdcaging

Birdcaging is a failure of the tensile armor of a flexible product, in which the tendons, near a given cross-section of the flexible product, displace outwards radially, creating the name-giving “birdcage” shape. The birdcage is limited in extent along the flexible product because of the resistance of outer layers (for example an outer PE sheath or PP twine).

Birdcaging is due to compression of the tensile armor(s), around the circumference of the flexible product. Compression of a tensile armor can have several causes:

- Compression (negative “wall” tension) of the whole cross-section.
- Torque in the product. A tensile armor laid as a positive (respectively negative) helix will experience compression under a negative (respectively positive) internal torque. This is the so called “slack” direction, in which torsion decreases the contact pressure between the tensile armor and the underlying layers or components.

For products with two tensile armors laid in opposite directions, the two load scenarios above are expected to cause different patterns of failure, providing more forensic information on the mechanism of failure:

- Compression would cause both tensile armors to buckle (Figure 79).

- A positive (respectively negative) torque would cause the outer armor to buckle if it is a negative (respectively positive) helix. This is a torque in the “slack” direction, meaning it decreases the contact pressure between the two tensile armors. The inner tensile armor would be in tension, pressing against underlying layers and would not buckle (Figure 80).
- A torque that sets the outer armor in tension and the inner in compression (in the “tight” direction) will not cause birdcaging, but possibly herniation-buckling (Section 10.4).

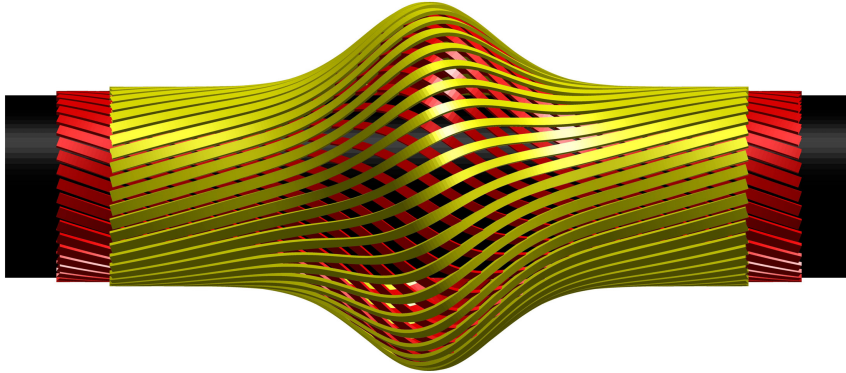


Figure 79: Birdcaging due to compression: the inner tensile armor buckles.

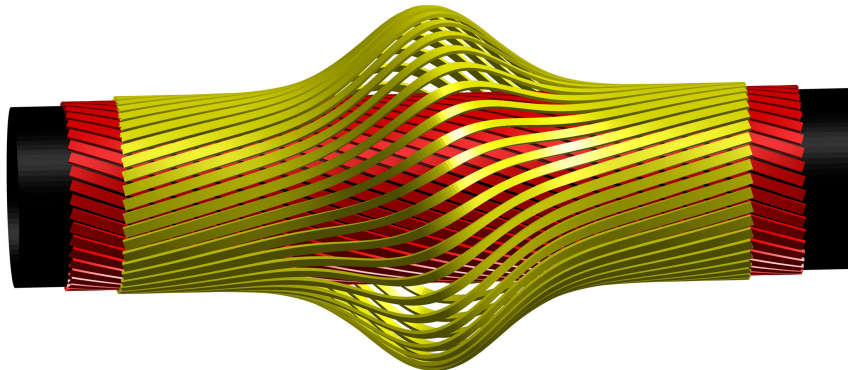


Figure 80: Birdcaging under positive internal torque: the inner tensile armor does not buckle.

10.4 Herniation buckling

Herniation buckling can occur when a flexible product with two tensile armor laid in opposite directions has been subjected to an excessive torque in the “tight” direction: the torque has put the outer tensile armor in tension, and the inner armor in compression. A known variation is a flexible product with a tensile armor surrounded by a layer of yarn (typically polypropylene) laid in the opposite direction to the armour’s.

The number of tensile tendons in tensile armor layers is normally chosen so that there is some slack between the tendons and they do not press against each other in the hoop direction. Hence it is possible to create a larger gap between two neighboring tendons, by pressing together all the other gaps.



Figure 81: Probable birdcaging (Courtesy of TenneT)

If the compressive forces in the inner tensile layer is high enough, it can buckle outwards through the gap in the outer tensile armor, causing large local plastic deformation (Figure 82). The name hernia is borrowed from medicine.

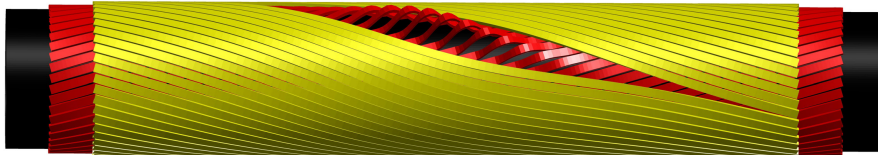


Figure 82: Herniation buckling under positive internal torque.

Friction could be expected to prevent transverse motions of the tendons of the outer armor to pack, thus making it improbable to have one major gap: if torsion causes the internal tensile armor to expand, and the external tensile armor to contract in the radial direction, there will be high contact forces between the layers. According to the Coulomb friction model (Section 6.4), any slip will be resisted by contact forces tangent to the surface of contact. Yet, experience shows that herniation buckling can occur as soon as, assuming there is a gap in the outer tensile layer, the compression in the inner tensile layer are enough to cause local deformation: somehow friction is “effectively zero”.

It is believed that when the flexible product is being transported, bending and unbending cause the tendons to slip in their longitudinal direction. As discussed in Section 6.4, slip in the longitudinal direction makes it possible to have slip in the transverse direction driven by very small transverse forces. This opens for an instability with the following feedback loop:

1. At some position over the surface of the flexible product, the inner tensile armor is raised.
2. The combination of slope on the inner tensile armor, and tension in the outer tensile armor result in a “downhill” transverse force.
3. With bending and unbending effectively “canceling” friction, this results in transverse displacement of tendons of the outer tensile armor, away from the bulge of the inner tensile armor.
4. This results in fewer tendons of the outer tensile armor (or a gap in the outer armor), and thus less forces preventing the inner tensile armor from bulging.
5. and so on.

10.5 Inward radial buckling

Inward radial buckling is a situation in which a tensile armor (in compression) works its way inward in a flexible product (Figure 83). For it to occur, the layer under the tensile armor must be soft and the layer above stiff. This has been observed to occur with an inner tensile armor within an outer tensile armor (stiff) laying on a layer with filers (soft) as found in three-phase power cables or umbilicals.

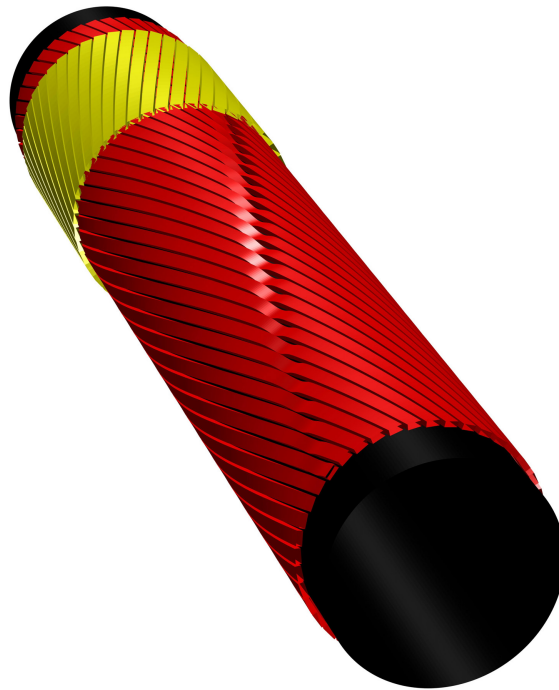


Figure 83: Inward radial buckling under positive internal torque

10.6 Lateral buckling of tensile armour

Lateral buckling is another form of buckling of a tensile armor in compression. Again, compression of a tensile armor can be due to wall compression, and to torque (or any combination

of both). In this failure mode, instead of buckling in the radial direction (as in birdcaging or herniation buckling, Sections 10.3 and 10.4), the tendons of the armor buckle within the layer, displacing in the hoop direction as illustrated in Figure 84. The dramatic consequence of this failure for round armour wires is shown in Figure 86.

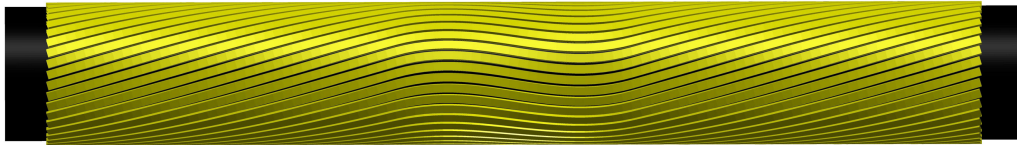


Figure 84: Lateral buckling under positive internal torque.

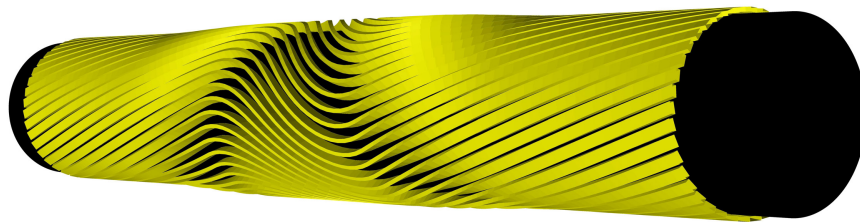


Figure 85: Torsional-flexural lateral buckling under positive internal torque.

Where the tendons are not circular in cross-section, a variant of this failure mode exists, in which the tendons undergo torsional-flexural buckling: they flip by a quarter turn to present their “weak axis” to the curvature introduced by buckling as shown in Figure 85. This is known as torsional-flexural lateral buckling.

10.7 Payload buckling

Payload buckling is an in-layer buckling of “payload components” (phases in an electrical cable, tubes or wires on an umbilical). It has been observed both in flexible products with single tensile armor and two tensile armors wound in opposite direction. The mechanism of failure in the later case is not well understood.

For a single tensile armor, wound in the direction opposite to that of the payload, then a torsion that puts the tensile armor in tension (Figure 87, top) puts the payload in compression causing buckling. This is not a typical construction of a coilable product: payload and tensile armor are wound in the same direction, but a similar mechanism applies: if the lay angle of the payload is lower than that of the tensile armor (Figure 87, middle), then torsion in the tight direction will compress the payload in the axial direction. If the lay angle of the payload is higher than that of the payload (Figure 87, bottom), then torsion in the slack direction compress the payload in the axial direction.

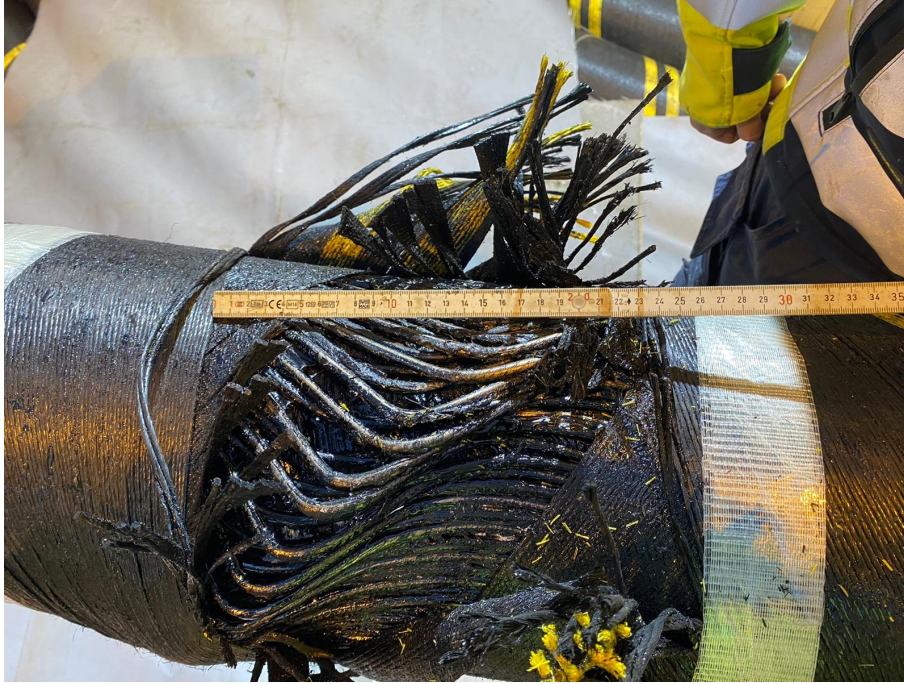


Figure 86: Example of lateral buckling of tensile armour (Courtesy of TenneT)

10.8 Unwinding at termination

Pulling heads - the termination to a flexible product allowing to tow it through a route may be based on different principles. One of them is to attach each wire in the tensile armor to the pulling head. In a torsionally unbalanced cross section, this can result in the unwinding of the tensile armor in the vicinity of the pulling head (Figure 88).

When this happens, the tensile armor must slide over the underlying layers. As a consequence, friction limits the distance from the pulling head over which unwinding occurs. If the flexible product is subjected to curvature changes while under tension, the tensile armor slips in the tendons axial direction, facilitating slip in the transverse direction and thus unwinding.

A flexible product always unwinds under tension, but generally does so as a whole - with each cross section rolling as a whole, without relative slip of the components. Thus other components contribute to the torsional stiffness. When slip occurs near the pulling head, the tensile armor is free to unwind, and indeed has been documented to align with the flexible product.

As the tensile armor unwinds, its lay angle approaches zero: for the same length along a tendon, more length along the flexible product is covered, and the pulling head rolls and moves forward relative to layers under the tensile armor (in black in Figure 88, seen through gaps in the tensile armor).

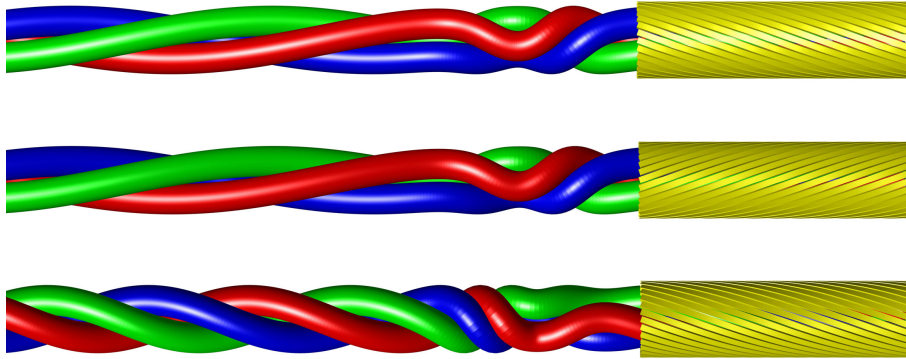


Figure 87: Buckling of the phases in an electrical cable

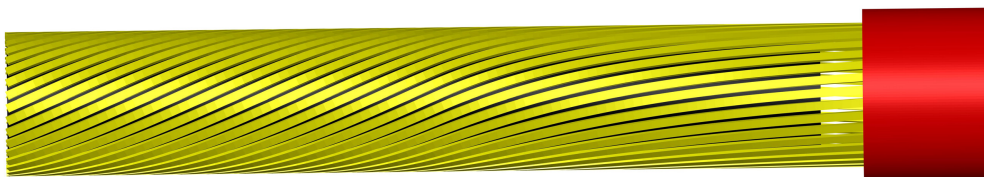


Figure 88: Unwinding of an unbalanced flexible product near the pulling head (red)

Part II

Assessing torsion

11 Introduction

11.1 Intention and disclaimer

Part II of the present document provides a guidance for the assessment of the level of torques that are likely to develop during the handling of flexible products, as well as for the assessment of the level of torque that the product can tolerate without incident or damage.

Many of the criteria proposed in this document have not been validated experimentally yet. Also, no partial safety factors have been introduced, as would be necessary to provide satisfactory reliability in the presence of uncertainties. Finally, not all known failure mechanisms are satisfactorily understood and covered in this guidance.

This document is not prescriptive or normative: Users remain free to create and market innovative products, solutions, tests or analysis procedures not foreseen in the guideline. Neither is the application of the present guideline absolving its users from their respective responsibilities towards ensuring successful operations.

Neither the SINTEF Ocean nor its affiliates, nor the members of the Torsion JIP consortium, accept responsibility for any consequence arising from the use of the present guideline.

12 Units

12.1 Requirements

All calculations described in this guideline should be carried out using a “consistent unit system”, to be chosen for that purpose, as described in the remainder of Section 12. This is in order to prevent mistakes arising from the use of quantities with inconsistent units.

Where inputs to the assessment are available in other units than those in the chosen consistent unit system, they should first be converted to the consistent unit. Where the results of analyses need to be reported in other units, the output of the procedures presented in this document should be converted after completion of the respective procedures.

12.2 Base units

Units for time, length and mass can be freely chosen. One possible choice is the SI base units second **s**, the meter **m**, and the kilogram **kg**. Other choices are acceptable.

Units for the other basic quantities defined in e.g. the SI unit system (electric current, temperature, amount of substance and luminous intensity) will not appear in calculations, although some properties may be tabulated as a function of temperature. There is no need to select base units for these quantities.

12.3 Dimensionless quantities

Angles should be expressed in **rad** (radians). Other measures of angle should be used with care: firstly, most numerical programming languages use radians in their trigonometric function. Secondly, some results presented in the following are only valid for radians. In particular, moments (whether bending moments or torque) are energy conjugate of angle in gradients, and the symmetry of the stiffness matrix in Eq. 44 will consequently be lost if an other angular measure is used.

All strains should be calculated as the length after deformation divided by length before deformation, minus one. The use of non-linear strain measures is acceptable, the only requirement being that linearisation for small deformations and rotations is equal to the above definition. This is the case for strain measures like Euler-Lagrange or Almansi-Euler strains. The use of microstrains is not recommended, again because it is not the energy conjugate of stress in a consistent system of units.

12.4 Derived units

The unit for any other quantity is derived from the base units and measures described in Sections 12.2 and 12.3.

For example, assuming the SI base units are chosen, then

- The unit for a force must be $\text{kg} \cdot \text{m} \cdot \text{s}^{-2}$, which is the Newton **N** (the kilogram force is not the correct unit for force with this choice of base units).
- The unit for torsion must be $\text{rad} \cdot \text{m}^{-1}$.
- The unit for weight per length is $\text{N} \cdot \text{m}^{-1}$ (not to be confused with mass per length).

13 Cross section properties

13.1 Axial and torsional stiffness

13.1.1 Definitions

Equation 44 provides the relation between elongation and torsion and the corresponding tension and torque:

$$\begin{bmatrix} R_1 \\ M_1 \end{bmatrix} = \begin{bmatrix} K_\varepsilon & K_{\varepsilon\tau} \\ K_{\tau\varepsilon} & K_\tau \end{bmatrix} \cdot \begin{bmatrix} \varepsilon \\ \tau \end{bmatrix} \quad (128)$$

where ε and τ are respectively the elongation and torsion of the product and R_1 and M_1 are respectively the axial force and torque. The matrix entries are:

Axial stiffness K_ε is the change of the tension divided by the change of elongation of the cable, when neither end of the cable is free to rotate.

Torsional stiffness K_τ is the change of torque divided by the change of torsion of the cable, when neither end of the cable is free to translate.

Axial-torsional cross stiffness $K_{\varepsilon\tau}$ is the change of tension divided by the change of torsion of the cable, when neither end of the cable is free to translate.

Torsional-axial cross stiffness $K_{\tau\varepsilon}$ is the change of torque divided by the change of elongation of the cable, when neither end of the cable is free to rotate.

Unless significant energy dissipation occurs in torsion and in elongation, and provided angles are measured in radians, then $K_{\varepsilon\tau} = K_{\tau\varepsilon}$ are equal. Procedures in the following are based on the assumption that $K_{\varepsilon\tau} = K_{\tau\varepsilon}$.

Torsional stiffness and axial-torsional cross stiffness can change significantly with the sign of the torque, due to the loss or gain of contact between components. This is true both for coilable products and torsionally balanced products. The procedures in the following must be repeated to provide values of stiffness the stiffness coefficients for both signs of torsion.

13.1.2 Evaluation by numerical analysis

The evaluation can be carried out with a numerical analysis software that models a segment of the flexible product (which may be short), and satisfying the following requirements:

1. It represents the geometry of the various components.
2. At the cross section at each end of the model, each component is free to rotate in all directions.
3. At the cross section at each end of the model, each component is free to translate in the radial direction of the flexible product. If the component is itself a sub-component of a larger component (for example a copper wire within one of three conductors within a cable), then the sub-component must be free to translate in the larger component's radial direction, instead of the product's radial direction.

4. At the cross section at each end of the model, each component is constrained to translate in the axial direction and in the hoop direction together with the cross section of the flexible product.
5. The elasticity of the materials involved is correctly represented.
6. Components can gain and loose contact with respect to each other.

2D formulations considering only a cross section are acceptable if they are formulated to carry out an analysis equivalent to what is mentioned above.

The following load cases are to be applied:

1. An elongation ΔL is applied to the model, which is of length L , to produce tensions up to the product's rated tension. The end cross sections are **not** allowed to roll. The axial strain is computed as $\Delta\varepsilon = \Delta L/L$. The tension ΔR_1 in the flexible product and the torque ΔM_1 are logged. The axial stiffness and the torsional-axial cross stiffness are computed as

$$K_\varepsilon = \frac{\Delta R_1}{\Delta\varepsilon} \quad (129)$$

$$K_{\tau\varepsilon} = \frac{\Delta M_1}{\Delta\varepsilon} \quad (130)$$

2. A twist ΔT is applied to the model, to produce internal torques up to the product's rated torque, or a torsion up to the product's rated torsion. The end cross sections are **not** allowed to translate. The torsion is computed as $\Delta\tau = \Delta T/L$. The tension ΔR_1 in the flexible product and the torque ΔM_1 are logged. The torsional stiffness and the axial-torsional cross stiffness are computed as

$$K_\tau = \frac{\Delta M_1}{\Delta\tau} \quad (131)$$

$$K_{\varepsilon\tau} = \frac{\Delta R_1}{\Delta\tau} \quad (132)$$

3. Verify that

$$K_{\tau\varepsilon} \approx K_{\varepsilon\tau} \quad (133)$$

13.1.3 Experimental evaluation

A straight sample of flexible product must be terminated by end-fittings so that all components are prevented from moving relative to each other, at each end of the sample.

The length L of the sample between the terminations should preferably be longer than 10 times the outer diameter of the sample, and no shorter than 5 times the outer diameter of the sample, in order to limit the uncertainty related to compliance in the end-fittings.

The test rig should be able to apply tension the highest tension that the flexible product will encounter during the operation. For each direction of torque, the test rig should be able to

apply a torsion or torque up to 100% of the flexible product's rated torsion or torque for that direction. The tests can also be carried out at lower loads provided that they explore all the relevant contact conditions and that there are no material non-linearities that would invalidate a linear extrapolation of response at higher loads,

The test rig must allow to measure elongation, tension, torsion and torque in the specimen.

The load cases and the procedure for determination of the stiffness coefficients are identical to what is described in Section 13.1.2.

An alternative procedure is the following:

1. An axial force is applied through the end fittings, to produce a tension ΔR_1 up to the product's rated tension. The end fittings are **allowed** to roll freely (no external moments, either from actuators or friction are applied by the rig to the end fittings). $\Delta \varepsilon = \Delta L/L$ and $\Delta \tau = \Delta T/L$ are measured as before. We then compute

$$a = \frac{\Delta \varepsilon}{\Delta R_1} \quad (134)$$

$$b = \frac{\Delta \tau}{\Delta R_1} \quad (135)$$

2. External torques are applied to the end fittings, to produce an internal torque ΔM_1 up to the product's rated torque, or a torsion $\Delta \tau$ up to the product's rated torsion. The end fittings are **allowed** to translate freely (no axial forces, either from actuators or friction are applied by the rig to the end fittings). $\Delta \varepsilon = \Delta L/L$ and $\Delta \tau = \Delta T/L$ are measured as before. We then compute

$$c = \frac{\Delta \varepsilon}{\Delta M_1} \quad (136)$$

$$d = \frac{\Delta \tau}{\Delta M_1} \quad (137)$$

3. Verify that

$$b \approx c \quad (138)$$

4. Compute

$$K_\varepsilon = \frac{d}{ad - bc} \quad (139)$$

$$K_{\tau\varepsilon} = -\frac{b}{ad - bc} \quad (140)$$

$$K_\tau = \frac{a}{ad - bc} \quad (141)$$

$$K_{\varepsilon\tau} = -\frac{c}{ad - bc} \quad (142)$$

13.1.4 Stiffnesses at constant torque and axial force

K_ε is the axial stiffness at constant torsion. The axial stiffness at constant torque K_ε^* is relevant in situations where an unbalanced cross section can unwind freely as the flexible product elongates. It is computed as

$$K_\varepsilon^* = K_\varepsilon - \frac{K_{\varepsilon\tau}K_{\tau\varepsilon}}{K_\tau} \quad (143)$$

$$= K_\varepsilon - \frac{K_{\varepsilon\tau}^2}{K_\tau} \quad (144)$$

K_τ is the torsional stiffness at constant elongation. The torsional stiffness at constant tension K_τ^* is relevant in situations where an unbalanced cross section can elongate (or shorten) freely as the flexible product undergoes torsion. It is computed as

$$K_\tau^* = K_\tau - \frac{K_{\tau\varepsilon}K_{\varepsilon\tau}}{K_\varepsilon} \quad (145)$$

$$= K_\tau - \frac{K_{\varepsilon\tau}^2}{K_\varepsilon} \quad (146)$$

$K_{\tau\varepsilon} = K_{\varepsilon\tau}$ is the “cross stiffness” term: it gives the increase in tension due to an increase in torsion at constant axial strain, and the increase in torque due to an increase in axial strain at constant torsion. $K_{\tau\varepsilon}^* = K_{\varepsilon\tau}^*$ gives the increase in tension due to an increase in torsion at constant torque, and the increase in torque due to an increase in axial strain at constant tension

$$K_{\varepsilon\tau}^* = K_{\varepsilon\tau} - \frac{K_\varepsilon K_\tau}{K_{\varepsilon\tau}} \quad (147)$$

Where the inverse is needed, it is convenient in numerical procedures to use

$$K_{\varepsilon\tau}^{*-1} = \frac{1}{K_{\varepsilon\tau}^*} = \frac{K_{\varepsilon\tau}}{K_{\varepsilon\tau}^2 - K_\varepsilon K_\tau} \quad (148)$$

to prevent division by zero when $K_{\varepsilon\tau} = 0$ for balanced cross sections.

13.2 Moment-curvature diagram, friction bending moment

13.2.1 Importance and sensitivity

In the assessment of torque generation, the moment-curvature curve is important for two reasons. First, it is needed in order to carry out a global static analysis, to obtain the geometry of the flexible product, in particular in free spans. Second, the moment-curvature relation is used in order to assess the friction bending moment M_f , which in turn is needed in the assessment of flip torque.

The moment curvature curve of the flexible product depends on the material properties of each cross-section component, the friction properties of the tensile armour and neighbouring layers, and interlayer radial contact pressures. These properties are affected, in particular, by temperature.

Assuming dry friction, the friction forces depend on the contact forces between the components. These are affected by temperature: in particular, temperature causes polymer sheaths to contract, pressing their contents together. Tension also causes helical components to move or press in the radial direction. Torsion, affecting tension in individual components, also causes changes in the contact pressures and hence in the friction forces.

Viscous fluids (including tar or asphalt-like compounds) are used in some flexible products for corrosion protection, partially or completely filling the space between components. The viscous property of the fluid affects M_f in terms of both the temperature and deformation rates.

When evaluating M_f for the purpose of torque assessment it is crucial to obtain an upper bound value. This will typically be achieved by assuming lower bound temperatures, maximum expected tension in the operation, and both negative and positive torque with magnitude as close as possible to the maximum expected torque in the operation.

13.2.2 Moment-curvature by numerical analysis

The analysis can be carried out with a numerical analysis software satisfying the following requirements:

1. It represents the geometry of the various components
2. At the cross section at each end of the model, each component is free to rotate in all directions, and free to translate in the radial direction of flexible product. If the component is itself a sub-component of a larger component (for example a copper wire within one of three conductors within a cable), then the sub-component must be free to translate in the larger component's radial direction, instead of the product's radial direction.
3. At the cross section at each end of the model, each component is free to translate in the axial direction, but constrained to translate in the hoop direction of the flexible product, together with the cross section.
4. The elasticity of the materials involved is correctly represented
5. Components can gain and lose contact with respect to each other.
6. The software must be able to model friction forces between components, correctly accounting for contact pressures between the components.
7. The model is 4 times or more the longest pitch length of any component.

The following load case is to be applied: one end of the specimen is constrained to neither translate nor rotate. The specimen should be modelled without gravity load. An external bending moment is applied to the other end. The external bending moment is increased in

steps until the minimum bending radius is reached. This should be repeated for various values of torque applied to the cross section.

Curvature at the middle of the model (to minimize effect from either end of the truncated model) is extracted at each step, and plotted against the applied bending moment (cf. Figure 89).

2D formulations assume constant curvature in the longitudinal direction. Such formulations are acceptable if they allow to carry out an analysis equivalent to what is mentioned above.

13.2.3 **Moment-curvature by test**

The specimen must be either terminated as described in Section 13.1.3, or simply cut at both ends, with components free to translate in and out of the cross sections.

The length of the specimen between terminations (or between point of application of couples) must be at least equal to twice the longest pitch length of any helical component.

The test rig must allow to apply a load on the specimen equivalent to that described in Section 13.2.2.

The curvature of the specimen must be evaluated at the middle of the specimen. Care must be taken when doing this, because the curvature will generally not be uniform along the specimen due to end effects. The curvature is continuously monitored and plotted against the applied bending moment.

The effect of gravity must be corrected for when a horizontal rig is used. Further, the specimen is likely to have an initial curvature in its moment-free state. These effects are simply corrected for by setting the zero-reference for the curvature measurements equal to the curvature prior to application of the external bending moment.

Where possible, the test should be repeated with various values and direction of torque applied to the specimen.

A test rig for bending may not allow to apply tension up to the level encountered in some operations (J-lay, beach pull in). In that case, the data obtained from the test at low tension must be completed by values computed by numerical analysis for high tension

13.2.4 **Evaluation of the friction bending moment**

Once a moment-curvature graph has been obtained from the specimen, the graph can be used to estimate the friction bending moment M_f , as shown in Figure 89. Where any doubt arises concerning the selection of a tangent to the curve in the "full slip" area, a conservative choice is made by selecting the highest value of M_f .

An alternative method is shown in Figure 90.

Where moment curvature curves have been established under various conditions of torque and/or temperature, one value of M_f is evaluated for each condition.

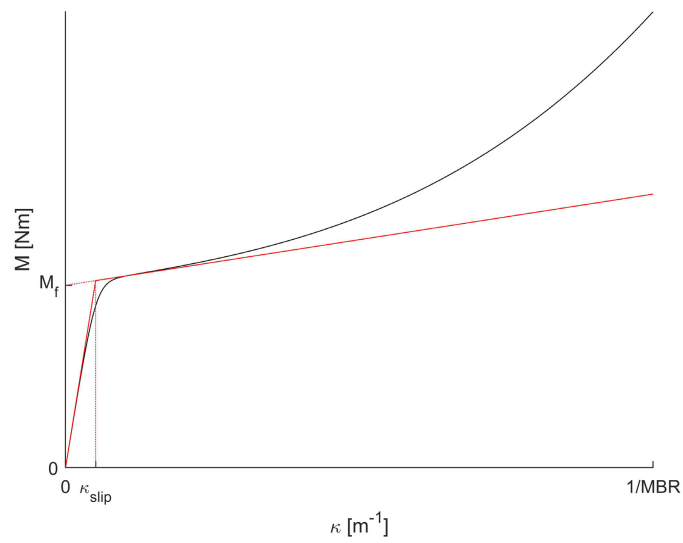


Figure 89: Typical moment curvature diagram of a flexible product. Realistic curve (black) and idealized (red). MBR is the minimum bending radius of the flexible product.

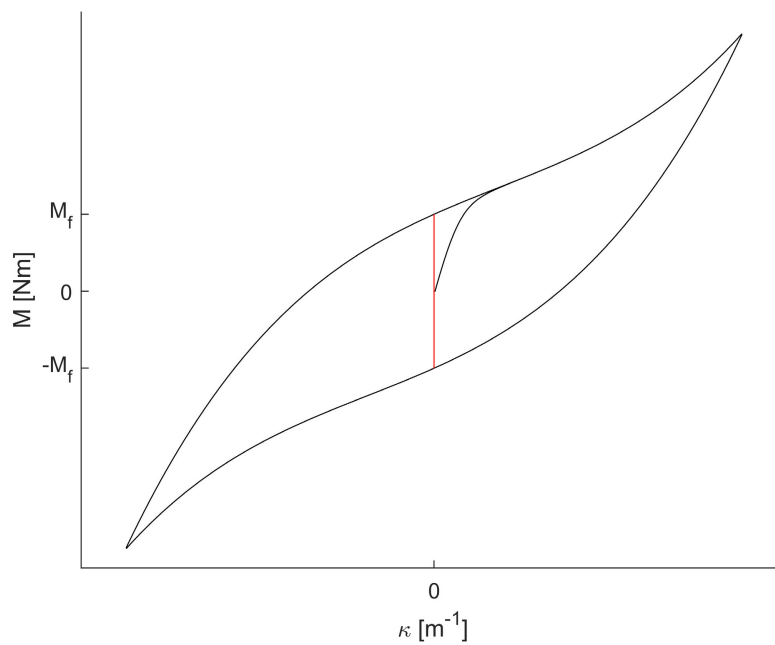


Figure 90: Alternative method: the specimen is bent back and forth. This difference between moments for loading and reversed loading, at zero curvature, is equal to $2M_f$.

14 Overall torque load assessment procedure

The handling of a flexible product, from production to installation is, for analysis purposes, separated into *phases*. For each route the product is following, up to three phases are relevant: the early transient, steady state, and the late transient. The phases of handling can include:

1. Start of the winding process, before the cable head reaches the downstream turntable.
2. Steady state of winding process.
3. End of winding process, after the cable tail leaves the winding machines.
4. Start of the extrusion process, before the cable head reaches a new downstream turntable.
5. Steady state of extrusion process.
6. End of extrusion process, after the cable tail leaves the extrusion machines.
7. Start of loadout operation, before the cable head reaches the installation vessel.
8. Steady state of loadout operation.
9. End of loadout operation, after the cable tail leave onshore storage.
10. Start of installation operation, while the head of the cable is routed out of the vessel.
11. Pull in while cable head is pulled over the beach.
12. Steady state of installation operation.
13. End of installation operation, as tail of the cable leaves the vessel.

For each phase a variety of *mechanisms* may generate torques:

1. Coiling writhe (Section 15).
2. Flip torque (Section 16).
3. Cranking (Section 17).
4. Torsional imbalance (Section 18).
5. Residual curvature (Section 19).

In principle each mechanism must be assessed for each phase, leading to a substantial analysis matrix. However some combinations can quickly be dismissed as irrelevant: for example, if a product follows a straight line between two spools at low tension, then coiling writhe, flip torque, cranking and torsional imbalance can be judged irrelevant for the corresponding transients and steady state.

For each phase and mechanism, a diagram of the torque along the route is obtained. Each diagram is split into a positive part and a negative part (Figure 91, top).

For each phase, the positive parts for all mechanisms are added into one diagram of total positive torque for the phase, and the same for the negative part (Figure 91, bottom). In Figure 91, the sums of the positive (respectively negative) parts is drawn in black. The highest positive torque is extracted from the diagram of sums of positive torque for the phase (marked with a small circle). The same is done for the negative parts.

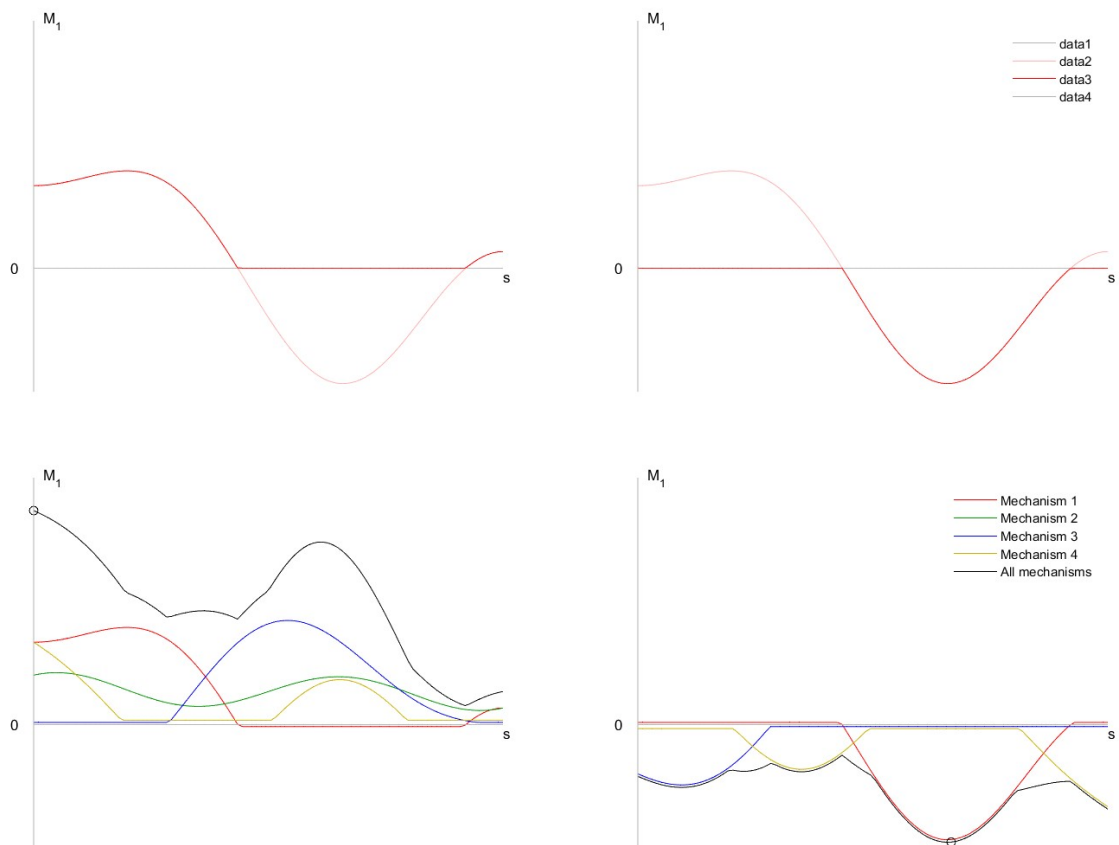


Figure 91: For a phase, addition of the positive (left) and negative (right) parts of the torque induced by various mechanisms. Small offsets between the curves were introduced for readability. No such offsets are to be introduced in an actual assessment.

Once all the phases have been analyzed, the overall highest positive torque for all phases is identified, and the same is done for the overall highest negative torque. These two values are then to be compared to the torque capacity (Sections 20 and 21).

15 Coiling writhe at steady state

Coiling refers here to the storage of a flexible product in a basket or ship hold which can not rotate (as opposed to a spool or a turntable). Typically, each coil is within a horizontal plane.

Figure 92 shows a positive basket (the mirror image would be a negative basket).

When coiling a flexible product into a positive basket, at steady state, torsion and torque

$$\tau = -\frac{1}{r} \quad (149)$$

$$M_1 = -\frac{K_\tau^*}{r} \quad (150)$$

are caused by change of writhe. r is taken as the smallest radius of curvature in the coil. For a negative basket, the signs are changed

$$\tau = \frac{1}{r} \quad (151)$$

$$M_1 = \frac{K_\tau^*}{r} \quad (152)$$

Only the coiling writhe from a downstream basket is considered as a source of torque for the route: Coiling writhe from an upstream basket is considered not to induce torques. Coiling writhe from a downstream basket is ignored in the early transient phase, and considered to be uniform over the route during the steady-state and late transient phases.

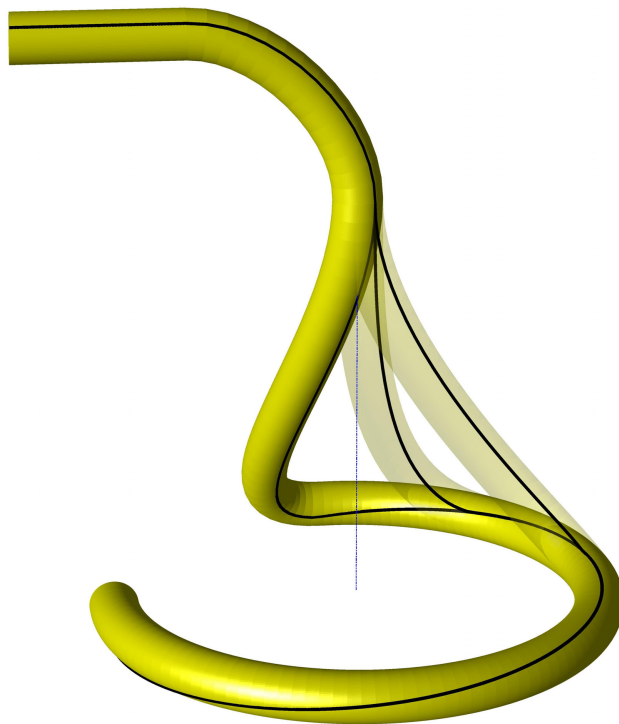


Figure 92: A positive basket (the mirror image is then a negative basket).

16 Flip torque

16.1 Introduction

The assessment of flip torque is done in two phases (Sections 16.3 and 16.4), with the possibility for iterations (Section 16.7). The first phase is a global static analysis using a linear elastic beam element model, in order to obtain an approximation of the geometry of the cable along the route, in particular, in free spans (Section 16.3). Once the geometry of the route has been computed, this is used to compute the flip torque (Section 16.4). Where flip torque geometry instability is a potential concern, the approach must be iterated (Section 16.7).

The choice of segments to analyze depends on the context, as discussed in Section 7.

16.2 Limitation

The procedure presented in this chapter has an important limitation in its domain of validity: it assumes that the material roll rate is uniform along the segment of route that is analysed. This is only valid if, at the relevant levels of torque, the torsion in the flexible product is small compared to the Frenet-Serret torsion of the segments of the route that generate flip torque.

Flexible products with two or more tensile armour layers will as a rule of thumb have so high torsional stiffness that the above assumption is verified. On the other hand, "coilable" flexible products, and other flexible products designed with a low torsional stiffness (with a single tensile armour or none at all) will generally not verify the above assumption, and the flip torque assessment procedure is not valid.

A procedure that does not assume that torsion is small would require the solution of what is called a boundary value problem, and so in practice, a finite element solution of the torsion along the route. Combined with the need for a finite element solution to determine the geometry of the route by a separate finite element analysis (Section 16.3), and for the need to iterate (Section 16.7), this points to the future of flip torque evaluation by a single, specialised, finite element analysis tool.

16.3 Global finite element analysis

The objective of the global finite element analysis is to compute an approximate geometry for the flexible product along the route. The flexible product is modeled using Euler-Bernoulli beam elements (as opposed to Timoshenko beam elements that account for shear deformations), with a linear elastic bending stiffness. The transport of the flexible product along the route is not modeled. The bending stiffness is to be taken equal to the product's bending stiffness at full slip. This is determined as the smallest slope in the moment-curvature diagram (Figure 93).

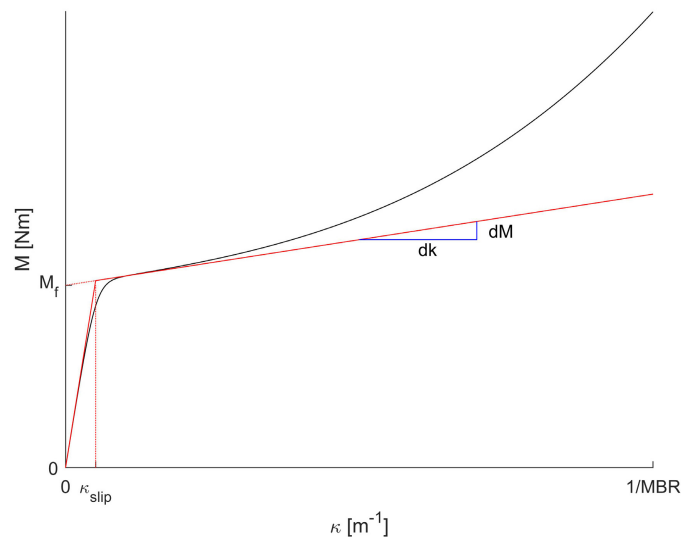


Figure 93: For the FE analysis, the bending moment is taken as $dM/d\kappa$ as illustrated

A convergence study should be carried out to verify that the mesh is sufficiently dense: halving the length of the beam elements should not influence the results significantly. In addition, the mesh must be sufficiently dense in order to provide nodal positions at closely spaced intervals, for the procedure in Section 16.7. As a rule of thumb, the angle between the tangents to the flexible product, at both ends of an element, should be under 2 degrees (a quarter turn should thus be meshed with 23 elements or more). Also, all the beam elements in the model should be meshed with the same length to reduce numerical noise in the finite difference scheme applied to compute the torque (it is possible to eliminate that requirement, but this would require a more advanced procedure than what is described in Section 16.7).

Surfaces that are in contact with the flexible product, including turntables, seafloor, chutes, roller highways, tensioners and so forth must be modeled with correct geometry. The friction properties (dry friction against chutes, rolling of supporting rollers, the grip and tracking of tensioners) can be modeled in any ad-hoc fashion, as long as that the length of flexible product found to be in each free span (the slack in the span) is realistic for the operation. Regarding external friction, the flexible product must be moved a short distance in the longitudinal direction in order to fully activate friction forces in the intended direction.

The finite element analysis must consider a set of load cases that encompass what will be experienced in the operation. This includes free spans with torsion in the slack and tight direction, and for turntables or baskets: full and empty, laying by the outer wall and by the nave.

Stringent convergence criteria must be used, to ensure that the positions (coordinates) of the nodes are determined with high precision. It is recommended to apply load-based or energy-based convergence norms. Displacement-based norms are to be avoided if most of the product is supported by rollers, chutes or other rigid geometries.

Once the analysis of a load case is completed, the positions (coordinates) of the nodes of the model are exported. Care must be taken to export the numbers with full precision (15

significant digits). The high precision of nodal coordinates is needed because this data will be subjected to multiple differentiation, a process which strongly amplifies any noise in the data. “High precision” here means that the solution *to the model, with all its assumptions and simplification* is obtained with high precision, while the effect of these assumptions and simplification on the solution is acknowledged.

16.4 Flip torque computation procedure

The result of the flip torque analysis is, for each material roll rate, a diagram of the internal torque along the route. The procedure described here is a slight simplification of what is implemented in the code `Jordan.py`. However, the essential steps are identical.

The procedure starts with an array x_{ij} where $i \in \{1, 2, 3\}$ is the index for three coordinates in space and $j \in \{1, 2, \dots, n\}$ is the node number from the finite element analysis. n is the number of nodes in the FE model.

In the following, an index notation like $x_{i\cdot}$ stands for “the i -th coordinate of all nodes”. So while x is a matrix, $x_{i\cdot}$ is a vector with n components. Similarly, the vector $x_{\cdot j}$ contains the 3 coordinates of node j . The notation $\mathbf{a} \cdot \mathbf{b}$ represents the multiplication of two matrices, or of two vectors (the usual dot product) or the multiplication of a matrix by a vector.

In the following, we will introduce a family of reference systems with a torsion equal to the material roll rate: Each node j along the route has 3 orthogonal and unit length vectors. The 3 vectors are numbered $k \in \{1, 2, 3\}$. The i th coordinate of vector k at point j along the route is denoted e_{ij}^k . The collection of 3 coordinates of vector k at point j is denoted $\mathbf{e}_{\cdot j}^k$.

A finite difference scheme will be used several times in the following. If z_j is some quantity known for each node j , then \mathbf{z} is the collection of these quantities for all nodes. Its finite difference $\mathbf{d}(\mathbf{z})_j$ (the value at point j of the finite difference $\mathbf{d}(\mathbf{z})$ of \mathbf{z}) is computed as

$$\mathbf{d}(\mathbf{z})_j = \frac{3(z_{j-4} - z_{j+4}) - 32(z_{j-3} - z_{j+3}) + 168(z_{j-2} - z_{j+2}) - 672(z_{j-1} - z_{j+1})}{840} \quad (153)$$

Because z_{j-4} and z_{j+4} appear in the scheme, $\mathbf{d}(\mathbf{z})_j$ can only be computed for nodes $j \in \{5, 6, \dots, n-4\}$. In the procedure below, finite differences will be applied repeatedly to compute 3rd order derivatives. Hence some results will only be available for nodes $j \in \{13, 14, \dots, n-13, n-12\}$. This must be accounted for during the finite element analysis by having 12 elements outside of the area of interest.

1. Establish an arc-length coordinate for each node

1.1. Set

$$s_1 = 0 \quad (154)$$

1.2. For $j \in \{1, 2, \dots, n-1\}$ compute

$$s_{j+1} = s_j + \sqrt{(x_{1j+1} - x_{1j})^2 + (x_{2j+1} - x_{2j})^2 + (x_{3j+1} - x_{3j})^2} \quad (155)$$

1.3. For $j \in \{5, 6, \dots, n-4\}$, compute

$$ds_j = d(s)_j \quad (156)$$

2. Establish a family of local reference systems along the flexible product, with one reference system at every node of the finite element model. The torsion of the family of reference system is equal to the material roll rate (the choice of values for the material roll rate is discussed in Section 16.5).

2.1. For $j \in \{5, 6, \dots, n-4\}$, compute the coordinates $i \in \{1, 2, 3\}$ of the tangent vector at node j as

$$t_{ij} = d(x_{i:})_j \quad (157)$$

Normalize the tangent vectors $t_{:j}$

$$e_{:j}^1 = \frac{t_{:j}}{|t_{:j}|} \quad (158)$$

2.2. At point $j = 5$, chose a unit vector $e_{:5}^2$ orthogonal to $e_{:5}^1$. Unless $e_{:5}^1$ is vertical,

$$e_{:5}^2 = [-e_{25}^1 \quad e_{15}^1 \quad 0] / |[-e_{25}^1 \quad e_{15}^1 \quad 0]| \quad (159)$$

is an adequate choice in the horizontal plane.

2.3. Compute

$$e_{:5}^3 = e_{:5}^1 \times e_{:5}^2 \quad (160)$$

2.4. For $j \in \{5, 6, \dots, n-5\}$

2.4.1. Compute the rotation vector

$$v_{:j} = e_{:j}^1 \times e_{:j+1}^1 - (x_{:j+1} - x_{:j}) \frac{DR}{DK} \quad (161)$$

where DR/Dk is the material roll rate defined in Section 3.10 and k is the payout defined in Section 3.2. DR/Dk is assumed constant along the route, which is a simplifying assumption.

2.4.2. Compute the rotation rate matrix

$$K_{::} = \begin{bmatrix} 0 & -v_3 & v_2 \\ v_3 & 0 & -v_1 \\ -v_2 & v_1 & 0 \end{bmatrix} \quad (162)$$

2.4.3. Compute the rotation matrix

$$N_{::} = \begin{bmatrix} 1 & 0 & 0 \\ 0 & 1 & 0 \\ 0 & 0 & 1 \end{bmatrix} + K_{::} \frac{\sin |v_{:j}|}{|v_{:j}|} + K_{::} \cdot K_{::} \frac{1 - \cos |v_{:j}|}{|v_{:j}|^2} \quad (163)$$

The functions $\sin |v| / |v|$ and $(1 - \cos |v|) / |v|$ are both fractions where numerator and denominator tend to zero as $|v|$ becomes small or zero. This will occur for straight locations along the route and zero material roll rate. Small $|v|$ will thus cause run-time errors depending the programming language. A typical presentation is the appearance of "NaN"-valued results. To avoid this, for small $|v|$, the functions can be replaced with 1 and 1/2 respectively.

2.4.4. Compute

$$\mathbf{e}_{j+1}^2 = \mathbf{N}_{::} \cdot \mathbf{e}_j^2 \quad (164)$$

$$\mathbf{e}_{j+1}^3 = \mathbf{N}_{::} \cdot \mathbf{e}_j^3 \quad (165)$$

3. At each node j , compute curvature κ_j and express it in the local reference system.

3.1. For $j \in \{9, 10, \dots, n-8\}$

3.1.1. Compute

$$\kappa_{ij} = \frac{d(\mathbf{e}_{i:}^1)_j}{ds_j} \quad (166)$$

3.1.2. Compute

$$\kappa_{2j}^{\text{loc}} = \kappa_j \cdot \mathbf{e}_j^2 \quad (167)$$

$$\kappa_{3j}^{\text{loc}} = \kappa_j \cdot \mathbf{e}_j^3 \quad (168)$$

4. At each node, compute the bending moment in the cross section by Eq. 170, and use Eq. 172 to compute the flip torque per unit length.

4.1. For $i \in \{2, 3\}$

4.1.1. For $j \in \{13, 14, \dots, n-12\}$ compute

$$\mathbf{h}_{ij} = d(\kappa_{i:}^{\text{loc}})_j \quad (169)$$

4.2. For $i \in \{2, 3\}$

4.2.1. For $j \in \{13, 14, \dots, n-12\}$ compute

$$M_{ij} = -M_f \frac{\mathbf{h}_{ij}}{|\mathbf{h}_{:j}|} \quad (170)$$

This step fails if $|\mathbf{h}_{:j}|$ is zero, or extremely small. This will occur in parts of the route that remain in uniform curvature (in direction and intensity), including straight part of the route. The simplest way to handle this is only to handle the parts of the route with change of curvature plane (which is where flip torque is produced). Another way is to chose a value $d\mathbf{h}$ which is large compared to values of $|\mathbf{h}_{:j}|$ obtained in segments of the route where the curvature is uniform in intensity and direction, but small compared to values of $|\mathbf{h}_{:j}|$ obtained elsewhere along the route, and compute

$$M_{ij} = -M_f \frac{\mathbf{h}_{ij}}{\max(d\mathbf{h}, |\mathbf{h}_{:j}|)} \quad (171)$$

4.3. For $j \in \{13, 14, \dots, n-12\}$ compute

$$dM_{1j} = (M_{2j} \kappa_{3j}^{\text{loc}} - M_{3j} \kappa_{2j}^{\text{loc}}) ds_j \quad (172)$$

5. Integrate along the route to obtain the distribution of the internal torque M_1 .

5.1. Set

$$M_{113} = dM_{113} \quad (173)$$

5.2. For $j \in \{14, 15, \dots, n - 12\}$ compute

$$M_{1j} = M_{1j-1} + dM_{1j} \quad (174)$$

5.3. For $j \in \{n - 11, n - 10, \dots, n\}$ compute

$$M_{1j} = M_{1n-12} \quad (175)$$

The above procedure yields a torque curve M_1 : that is zero upstream $M_{11} = 0$. In reality however, the distributions of internal torque obtained in this way are defined *to an integration constant*, meaning that the whole distribution can be uniformly shifted up or down. The choice of that shift depends on the boundary conditions at both end. The procedures for specific situations, presented in Sections 16.5 and 16.6 take care of this issue.

Important results that should be extracted from M_1 : once the proper integration constant has been added to account for the boundary conditions, are M_{1n} (the total flip torque generated by the flip area), $\max(M_1)$ and $\min(M_1)$ the maximum and minimum torque found in M_1 .

16.5 Flip torque transient close to downstream storage

We consider a situation where a route has a flip torque-inducing geometry, that is a short distance of a downstream storage (turntable or spool), compared to the length of the rest of the route upstream.

The present procedure is generally not relevant if the downstream "storage" is the seabed: the distances within the installation vessel are typically small compared to the free span, so a steady state situation (Section 16.6) will be reached without the downstream torque build-up considered in the following.

At the start of an operation, a transient will occur when the head of the flexible product reaches the downstream storage. At the end of the operation, a new transient will occur when the tail of the flexible product leaves the upstream storage. The aim of the assessment is to evaluate the downstream internal torque at these stages.

In the transient, the upstream torque is small (conservatively, it is set to zero), and thus the flip torque must be balanced by the downstream internal torque. This is reflected in the assessment procedure below.

The red curve in Figure 94 shows an example of a torque-torsion diagram. Importantly, this diagram must be established assuming zero tension, hence the slopes in the diagram are noted K_τ^* , and not K_τ . In the example, positive torsion corresponds to the tight direction, and negative torsion to the slack direction of the flexible product.

The black curve in Figure 94 is the flip-torque diagram, obtained as specified in Section 16.8. This black curve is rotated 180 degrees around the origin to obtain the green curve⁴. In other

⁴This is because 1) a positive roll causes a negative torsion further upstream, and 2) a positive flip torque causes a negative flip torque further upstream.

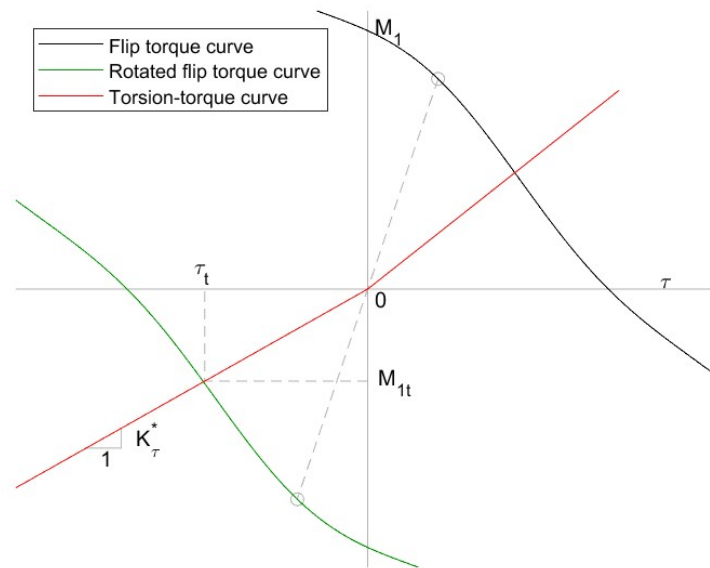


Figure 94: Assessment of torque transient for a turntable of spool

words, if the black curve is obtained by plotting M_{1f} against τ , the green curve is obtained by plotting $-M_{1f}$ against $-\tau$. The black curve is an example of flip torque diagram for a flip area with positive Frenet-Serret torsion.

The assessed transient downstream torsion τ_t and the transient downstream torque M_{1t} are found at the intersection of the (green) rotated flip torque curve and the (red) torsion-torque curve (Appendix C). The torque diagram (to be entered in Figure 91) is zero upstream of the flip torque inducing geometry, and torque M_{1t} in, and downstream of, the flip torque inducing geometry.

16.6 Steady states

In an operation where the flexible product comes from an upstream “storage” that determines the upstream material roll rate, and goes to a downstream storage that absorbs torsion, the operation will generally approach a steady state in which the flip torque produced at various flip areas is taken up by upstream internal torque. At steady state, the material roll rate in flip areas will approach zero.

Flip areas along the route are numbered with $\alpha \in \{1, 2, \dots, n_\alpha\}$, counting from upstream to downstream. At each flip area along the route, the flip torque is evaluated by following the procedure described in Section 16.4, for $DR/Dk = 0$, and M_{1n}^α , $\max(M_{1i}^\alpha)$ and $\min(M_{1i}^\alpha)$ are documented (see Section 16.4 for the convention on the use of the semicolon as a subscript).

If it is possible to cover the whole length of the route with one FEM analysis, and carry out the procedure described in Section 16.4 for the whole length, then there is no need to carry out the following procedure.

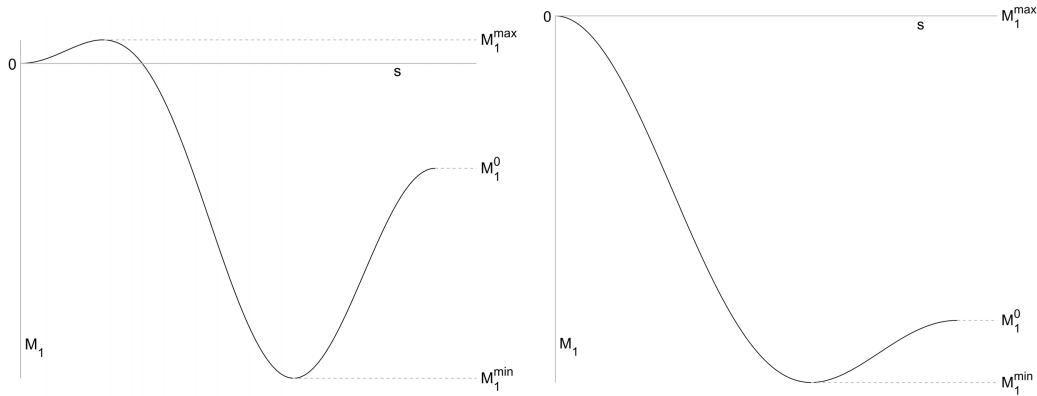


Figure 95: Two torque distributions obtained using the procedure in Section 16.4

The highest torque along the route is assessed as follows:

1. Set

$$M_1 = 0 \quad (176)$$

$$M_1^{\max} = 0 \quad (177)$$

$$M_1^{\min} = 0 \quad (178)$$

2. For $\alpha \in \{1, 2, \dots, n_\alpha\}$

- 2.1. Compute

$$M_1^{\max} = \max(\max(M_{1:\cdot}^\alpha) + M_1, M_1^{\max}) \quad (179)$$

$$M_1^{\min} = \min(\min(M_{1:\cdot}^\alpha) + M_1, M_1^{\min}) \quad (180)$$

where $\max(\mathbf{A})$ is the highest element in vector \mathbf{A} , and $\max(\mathbf{a}, \mathbf{b})$ is the largest of \mathbf{a} and \mathbf{b} .

- 2.2. Compute

$$M_1 = M_1 + M_{1:n}^\alpha \quad (181)$$

3. Compute

$$M_1^{\max} = M_1^{\max} - M_1 \quad (182)$$

$$M_1^{\min} = M_1^{\min} - M_1 \quad (183)$$

Step 3 ensures that the values of M_1^{\max} and M_1^{\min} are for $M_1 = 0$ at the downstream end.

The values of M_1^{\max} and M_1^{\min} obtained after step 3 are then kept for comparison with the flexible product's torque capacity.

Figure 95 shows two torque distribution obtained using the procedure in Section 16.4. Figure 96 shows the values M_1^{\min} and M_1^{\max} as computed using the above procedure.

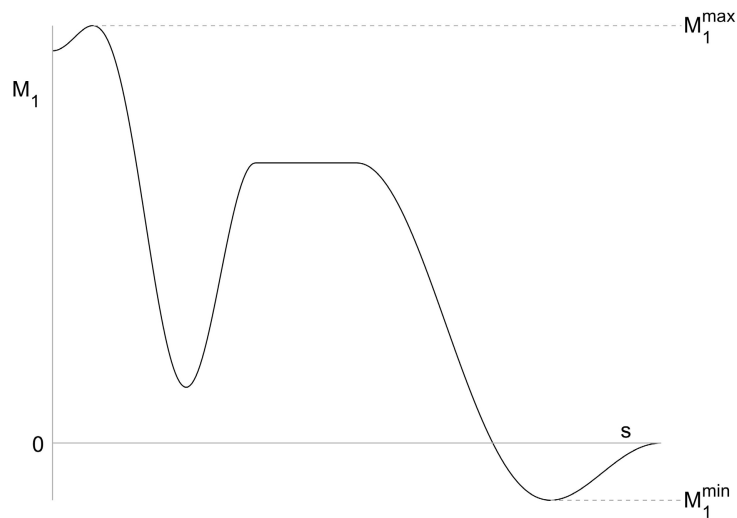


Figure 96: Torque distribution along the whole route, with M_1^{\min} and M_1^{\max} obtained using the steady-state assessment procedure.

16.7 Iteration

Internal torque affects the geometry of free spans, and this is not captured in the finite element analysis described in Section 16.3. If there is any suspicion that this may be significant, the analyses in Sections 16.3 and 16.4 should be repeated as follows:

The flip torque per unit length dM_1/ds , evaluated in Section 16.4, is applied as a distributed external torque along the flexible product, when repeating the FE analysis. When doing so, the choice of boundary conditions for roll degrees of freedom becomes critical. This choice depends on the phase of the operation that is being analyzed (Sections 16.5 and 16.6).

The finite element analysis is repeated and the new geometry thus obtained is used to update the flip torque analysis (Section 16.4). The sequence of finite element analysis and flip torque analysis is iterated until the geometry of the route is stable from one iteration to the next. If the iteration cannot be made to converge towards a stable route, then the operation must be deemed liable to flip torque geometric instability (Section 8.4).

16.8 Flip torque diagram

The flip torque diagram for a segment of route is obtained by carrying out the analysis described in Section 16.4, for a range of values of the material roll rate DR/Dk . At least the material roll rates between 0 and the value at which the flip torque becomes zero must be covered. If, in further analyses, material roll rates are encountered that fall outside the covered range, then the range of material rates in the flip torque diagram must be extended by further applying the procedure in Section 16.4.

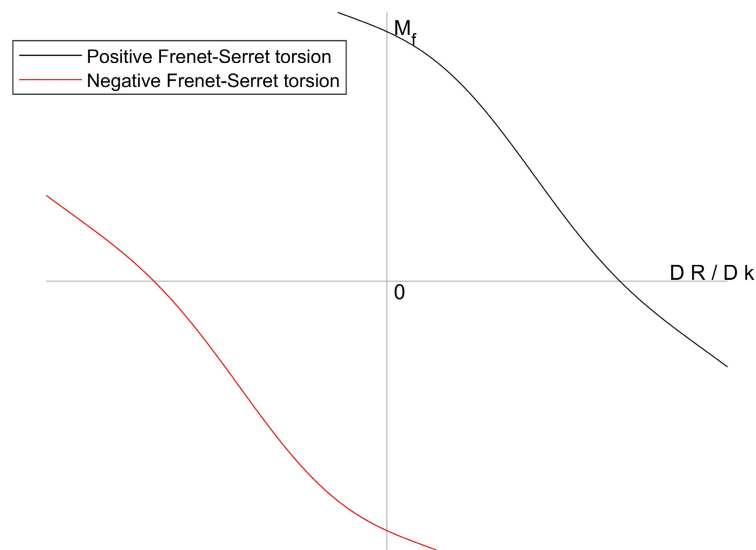


Figure 97: Relation between the sign of Frenet-Serret torsion and the position of the flip torque diagram

It is often convenient to make the approximation that the diagram provides the relation between the *spatial* roll rate and the flip torque. This approximation is reasonable if the torsion in the flexible product within the length of the route covered by the diagram is small (in absolute value) compared to the Frenet-Serret torsion of the route. If this is not verified, and torsion is large, then the flip torque diagram might become a questionable tool, because the torsion, and hence the material roll rate might change significantly along the length of the route covered by the diagram. If this is the case, then more advanced analysis methods will have to be devised. Coilable flexible product are designed to be very compliant in the slack direction, and they can, under the right circumstances have very high torsion.

Figure 97 shows examples of flip torque diagrams for a segment of the route dominated by positive (and negative) Frenet-Serret torsion. This is provided as a check against sign mistakes when setting up such a diagram.

17 Cranking

Cranking assessment accounts for actuators that can force displacements of the flexible product in a direction orthogonal to the route.

Examples of actuators that must be included in the cranking assessment are

- Roller boxes that can be displaced transverse to the route.
- Manipulators to stack the flexible product in a turntable. This can be direct handling by personnel in the turntable, or a hydraulic guiding arm.

Examples of actuators that must not be included in the cranking assessments are

- roller and chutes: these apply forces in the direction radial to the flexible product but do not give *displacement* in that direction.
- Tensioners, winches working along the route, spools and turntables: these introduce displacements, but in the route's longitudinal direction.

The assessment is made using a FE analysis of the relevant part of the route with an elasto-plastic bending model. An elasto-plastic model for the bending response must be used, as otherwise actuator forces will induce no torque. Further, without an elasto-plastic bending model one will lose the roll resistance associated with change of curvature plane. Transport is *not* represented. The model must also represent roll-resisting friction of the flexible product against rollers, chutes etc. Friction coefficients (including in tensioners, where the increase of friction by clamping forces must be accounted for) are set to conservatively high values along the route. Because transport is not modelled, tracking (Section 6.5) is *not* to be accounted for in this procedure.

For a given actuator force, a diagram of the force along the route is produced. Where several actuators can induce torque on the same segment of the route, the analysis must consider simultaneous actuator forces. The analysis produces a torque diagram along the route for each actuator load case.

The above torque diagram is combined with the torques diagrams from other sources, using the procedure outlined in Section 14. If the total torque thus assessed is acceptable, then the actuator loads are acceptable. Otherwise, the procedure must be repeated with reduced actuator loads.

The forces thus obtained are then used as an upper limit to allowable actuator forces for this operation, and are used also for actuator forces while the flexible product is transported.

18 Torsional imbalance

18.1 Pull-in operation

Pull-in operation with unbalanced product may induce torsion by unwinding the product while transported under tension, then relaxing the tension, without transport (Section 9.6).

For a pull-in operation, or during the transport of a flexible product over long distances and using significant tension, the maximum tension $R_{1 \max}(s)$ that may occur at coordinate s along the route must be evaluated. The simplest assessment would be to add the rated strength of winch and each tensioner, at all the points upstream of the point of application of the force. A more advanced assessment could account for the reduction of tension due to friction (external and internal) – but no guidance is offered for this here.

$R_{1 \min}(s)$ should be zero for all route coordinates s unless special precautions are taken to ensure a minimum tension, or unless it is known that compression can occur.

For all route coordinates, the “unwinding torsion” $\tau_u(s)$ is the torsion under $R_{1 \max}(s)$, and is computed according to Appendix B

$$\tau_u(s) = \frac{R_{1 \max}(s)}{K_{\varepsilon\tau}^*} \quad (184)$$

with

$$K_{\varepsilon\tau}^* = \frac{K_{\varepsilon\tau}^2 - K_\varepsilon K_\tau}{K_{\varepsilon\tau}} \quad (185)$$

At $R_{1 \min}(s)$, the same torsion will induce a “tension-relaxation” torque

$$M_1(s) = \frac{K_{\varepsilon\tau}}{K_\varepsilon} (R_{1 \min}(s) - R_{1 \max}(s)) \quad (186)$$

This computation is carried out at many points s along the route, resulting in a “tension-relaxation” torque diagram.

18.2 J-lay installation on the seafloor

The procedure described in the following is the only procedure in the present guideline that is relevant to the assessment of torque in the catenary between an installation vessel and the sea floor (Section 9.5). This must not be confused with the assessment of torque on board the installation vessel, where a variety of sources (e.g. flip torque, cranking) are to be assessed. The present procedure differs from other ones in that instead of producing a diagram of the torque along the free span, only the torque at the touch down point is to be assessed. This is because torque will be approximately uniform along the catenary, and the tension lowest at the touch-down point, so failures, if any, would occur there.

The assessment procedure is based on a catenary solution, which does not account for bending stiffness, sea currents and dynamic response. For any given water depth, the assessment procedure requires the conservative choice of both a minimum tension (slack) and maximum tension (tight) configuration. The choice of these configurations should strive to account, conservatively, for the wave response of the vessel. Both configurations are described based on the bending radius at touch-down point, r_{\min} and r_{\max} respectively. In the following, where the symbol "m" appears, computations are to be repeated replacing "m" with "min" and then "max".

For the purpose of choosing r_{\min} and r_{\max} it is useful to note that the effective tension (cf. Section 4.9) at the hang-off point, is

$$R_{1m}^e = \omega (z + r_m) \quad (187)$$

where z is the height of the hang-off point over the seabed and where ω is the submerged weight per unit length (in $[\text{N} \cdot \text{m}^{-1}]$) of the flexible product. Also, the horizontal distance between hang-off point and touch-down point is

$$\Delta x_m = r_m \cosh \left(1 + \frac{z}{r_m} \right) \quad (188)$$

where $\cosh x = \frac{e^x + e^{-x}}{2}$ is the hyperbolic cosine function. Finally, the length of the free span is

$$L_m = \sqrt{z^2 + 2zr_m} \quad (189)$$

The torque-free twist in the free span is (Appendix A):

$$T_{u\ m} = K_{\varepsilon\tau}^{*-1} g \left[\frac{m}{2} \left(L_m (r_m + z) + r_m^2 \log \left(1 + \frac{L_m + z}{r_m} \right) \right) - z \rho_w L_m A_e \right] \quad (190)$$

where g is the acceleration of gravity, m the mass of the flexible product per unit length, ρ_w is the density of seawater and A_e the outer cross section of the cable.

When the span rapidly goes from a tight to a slack configuration (without forward movement of the installation vessel), the twist in the flexible product laid on the seafloor is conservatively assessed using the assumption that the torsion at touch down point is equal to the torque-free torsion:

$$T_l = K_{\varepsilon\tau}^{*-1} \frac{gm}{2z} \left(\frac{1}{3} L_{\max}^3 - \frac{1}{3} L_{\min}^3 \right) - K_{\varepsilon\tau}^{*-1} z \left(\frac{gm}{2} + \rho_w g A_e \right) (L_{\max} - L_{\min}) \quad (191)$$

The torque at the touch down point in the slack configuration is evaluated as

$$M_l = K_{\tau}^{*-1} (T_{u\ \max} - T_{u\ \min} - T_l) \quad (192)$$

with

$$K_{\tau}^* = K_{\tau} - K_{\varepsilon\tau} K_{\varepsilon}^{-1} K_{\varepsilon\tau} \quad (193)$$

19 Residual curvature

Residual curvature can occur if a flexible product is stored, and either plastic deformation, or creep in sheaths (typically polymer or lead) occurs so that these sheaths have a curved shape in the absence of load on the sheath (including loads coming from other components in the flexible product). When the flexible product is transported, the residual curvature of the sheath may not align with the curvature of the route. This may induce roll, and torsion.

The residual curvature must be provided as an input, to assess how it may result in torsion. A conservative approach is to model the beam elements with a moment-free curvature equal to the curvature in the upstream storage. Less conservative values can be obtained by detailed analysis, but no guidance is provided here.

A simplified method to assess this is to model the flexible product using Euler-Bernoulli beam finite elements, that models the whole route, from storage to storage. The ends of the route must be at the points where the flexible product gets in contact with other coils (or the seabed). The bending-curvature relation of the flexible product must be represented by the beam elements. If the relation is not available or cannot be accommodated by the software, then a linear bending-curvature relation can be used, with the bending stiffness corresponding to the absence of slip (resulting in a upper bound for the stiffness). The torsional stiffness K_{τ^*} is the stiffness assuming free axial deformation, and torsion in both tight and slack torsional direction must be accounted for.

External friction is set to zero in the transverse direction: friction is assumed *not* to impede roll.

19.1 Simplified analysis

The global static finite element analysis is based on a standard linear-elastic bending model

$$M_2 = EI\omega_2 \quad (194)$$

$$M_3 = EI\omega_3 \quad (195)$$

where EI is the bending stiffness and ω_2 and ω_3 are the curvature components.

Two sets of boundary conditions are to be considered:

1. The flexible product is restrained from rolling at the upstream end and free to roll at the downstream end. The roll angle at the upstream end is chosen to align the residual curvature with the curvature in the upstream storage.
2. The flexible product is free to roll at the upstream end and restrained from rolling at the downstream end. The roll at the upstream end is chosen to align the residual curvature with the curvature in the downstream storage.

For particularly short routes, two additional sets of boundary conditions need to be considered. Starting from load case 1 above, the roll at the downstream end is set to align the residual curvature in the downstream storage by

1. applying a positive 180 degree roll to the downstream end,
2. applying a negative 180 degree roll to the downstream end.

The internal torque along the route are retrieved for all load cases studied and further evaluated as described in Section 14

19.2 Advanced analysis

If the simplified analysis method proves to be overly conservative, a more accurate global static finite element analysis may be performed if the software tool includes a linear-elastic bending model that accounts for residual curvature:

$$M_2 = EI [\omega_2 - \omega_2^0 \lambda_2(k)] \quad (196)$$

$$M_3 = EI [\omega_3 - \omega_3^0 \lambda_3(k)] \quad (197)$$

where ω_2^0 and ω_3^0 are the residual curvature components which are assigned scale factors $\lambda_2(k)$ and $\lambda_3(k)$ as a function of payout k . The other quantities are defined in Section 19.1. The scale factors are typically kept at zero until the gravity load has been applied and the contact forces from the supporting rollers, chutes and the storage geometries have converged. Thereafter, the load scale factors are increased to 1.0.

The whole route is modelled from the upstream storage to the downstream storage including all contact geometries that are required to support the flexible product along the route. The model should extend a quarter coil into both the downstream and upstream storage so that one can set appropriate boundary conditions. The translation degrees of freedom at both ends are kept fixed, except in the axial direction at one end where an appropriate tension load is applied. The rotation degrees of freedom at both ends are kept fixed, except for the roll rotation at the downstream end which is kept free. A shorter part of the route may be modelled provided that it is possible to set realistic boundary conditions for the reduced model.

The torsional stiffness for both the tight and slack directions shall be considered. If the analysis shows that the flexible product will roll such that only the torsional stiffness for the slack direction is relevant, the tight direction torsional stiffness can be disregarded: this will result in smaller torque values.

The residual curvature components ω_2^0 and ω_3^0 are selected based on the expected residual curvature at the upstream storage. The beam element should be oriented to get one of the element coordinate axes aligned with the upstream storage axis. Then, one of the residual curvature components can be assigned zero value, and the other one can be set equal to the expected residual curvature at the upstream storage. In the most conservative case, one may assume that the residual curvature will be equal to the curvature of the innermost coil at the upstream storage.

The scale factors for the residual curvature components $\lambda_2(k)$ and $\lambda_3(k)$ may be assigned uniform values along the whole route. If the software tools allows the user to easily apply scale factors for each beam element, it will be possible to simulate that the residual curvature

spreads with the transport velocity from the upstream storage to the downstream storage similar to what happens in the transient phase at start-up of the operation. This effect is only relevant to simulate if it is likely that it will lead to different equilibrium configuration compared to the configuration that results when $\lambda_2(\mathbf{k})$ and $\lambda_3(\mathbf{k})$ are uniform along the route. The flexible product will in most cases be kept in place along the route by numerous supports in the vertical and lateral directions. In these cases, the final equilibrium configuration and the resulting torque are not expected to differ with respect to how the load scale factors $\lambda_2(\mathbf{k})$ and $\lambda_3(\mathbf{k})$ are applied along the route. If the final equilibrium configuration shows that the flexible product is not coiled nicely at the downstream storage, the model should be extended at the downstream end until the beam elements are coiled as intended at the downstream storage.

The main advantage of applying the bending model in Eqs. 196 and 197 is that the torque induced along the route from the residual curvature is accounted for. At a point along the route, the induced internal torque per unit length due to residual curvature will be equal to

$$\frac{\partial M_1}{\partial z} = EI [\omega_2 \omega_3^0 \lambda_3(\mathbf{k}) - \omega_3 \omega_2^0 \lambda_2(\mathbf{k})] \quad (198)$$

which follows by inserting Eqs. 196 and 197 into Eq. 55 assuming $\mathbf{m}_1 = 0$.

The internal torque along the route are retrieved for all load cases studied and further evaluated as described in Section 14

20 Local failures

20.1 Stresses in the tensile armor

20.1.1 Stresses due to bending

The contribution from friction between the layers, to the stresses in the tensile armour is difficult to compute for two reasons:

1. Curvature may change direction (Frenet-Serret torsion, Section 3.11.4) over distances that are not large compared to the pitch length of the tensile armor. This invalidates the assumption of uniform curvature (in intensity and direction) used in extent in theories of bending induces stresses [49, 50, 48].
2. The contact pressure and hence the friction between armor layers and surrounding layers is influenced by tension, torque, internal constraints induced by fabrication (shrinkage of polymer sheaths, creep, tightness of laying various layers), temperature, and curvature-pressure instability (Section 8.3).

Assuming the flexible product is designed so that the maximum axial stress σ_{11} in the tensile armours due to bending reach yield stress at minimum bending radius then a rough approximation for the sum of the friction-induced stresses and the component bending stresses is

$$\sigma_{11}^b = \pm \kappa \text{ MBR SMYS} \quad (199)$$

where $\kappa = |\bar{\kappa}|$ is the norm of the curvature vector (Section 3.3), MBR is the minimum bending radius of the flexible product and SMYS is the specified minimum yield strength of the tensile armor wires.

For simplicity, the bending stresses are considered uniform over the cross section of any given armor wire. The stresses are considered tensile on the outside of the curvature and compressive on the inside of the curvature.

20.1.2 Stresses due to torque and wall tension

Global analysis provides estimated *effective* tension R_1^e and torque M_1 . In situations where the flexible product is submerged, Eq. 45 is to be used to compute the *wall* tension R_1^w (Section 4.9): outside of water (and in the absence of pressurization of internal components), this simplifies to $R_1^w = R_1^e$.

While some cases can be treated analytically, generally, given R_1^w and M_1 , stresses in the tensile armor must be computed using dedicated finite element software capable of handle axisymmetric loading conditions (such as Caflex, Helica and UFLEX). In such analyses it is important that geometry, lay angles and materials are adequately represented. The software must allow for components losing and gaining contact with each other. In terms of boundary

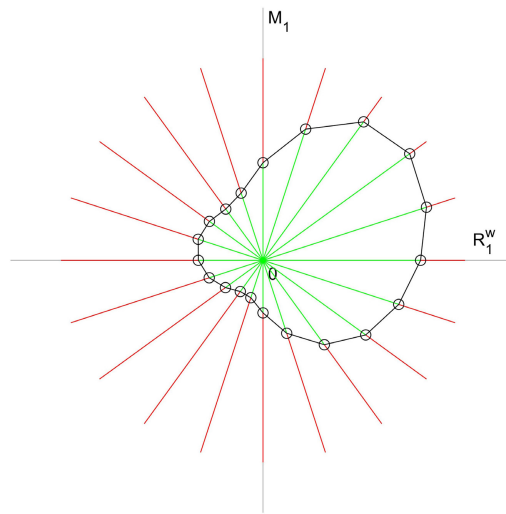


Figure 98: Assessment of the envelope of allowable force resultants. Each radial line corresponds to a value of r . The envelope joins the points where the stress reaches a critical value (at any point in the cross section, and for any local failure mechanisms).

conditions, the software must, in effect, consider a slice of the flexible product, which the cross sections at both ends remaining plane, and normal to the axis of the flexible product. One plane is fixed. The other plane can translate along the axis and rotate around it. All components must move with the plane, except that they can have radial displacements.

A procedure for the determination of combinations of R_1^w and M_1 is to model the cross section using a software as mentioned. A variety of ratios $r = R_1^w/M_1$ is selected. For each ratio r , progressively increase M_1 while keeping $R_1^w = r M_1$, until critical stress is reached in one of the component. In a graph (Figure 98), plot the values of R_1^w and M_1 for which critical stress was reached. The procedure is repeated with negative values of M_1 , and then all the above is repeated for each value of r so that "rays" are sent in all directions around the origin.

20.2 Lateral buckling of tensile armour

20.2.1 Notations

The wire's lay angle, cross section area, shear and Young's moduli are denoted α , A , G , and E . For rectangular wires, the width and thickness are w and t . For circular wires the diameter is d . The mean radius of the layer is R , and the number of wires in the layer is n . Where relevant, subscripts i and o refer to the inner and tensile armour layer, respectively.

σ_{1c} is the critical axial stress in the wire. For buckling failures, $\sigma_{1c} < 0$, and one must ensure that $\sigma_{1c} < \sigma_1$ to prevent failure.

20.2.2 Moments of inertia

For a rectangular wire, the wire's moments of inertia for torsion J , bending around the weak axis I_2 and around the strong axis I_3 are computed as:

$$J = wt^3 \left[\frac{1}{3} - \frac{64}{\pi^5} \frac{t}{w} \right] \quad (200)$$

$$I_2 = \frac{1}{12} wt^3 \quad (201)$$

$$I_3 = \frac{1}{12} tw^3 \quad (202)$$

For a circular wire, the moments of inertia are

$$J = \frac{\pi D^4}{32} \quad (203)$$

$$I_2 = I_3 = \frac{\pi D^4}{64} \quad (204)$$

20.2.3 Buckling of rectangular wires

This buckling mode is illustrated in Figure 84 and has been extensively studied for flexible pipes subjected to axial compression in previous research efforts, see Section K.1.1. Equation 205 has been validated against tests and shown to be in very good agreement for double-armoured flexible pipes subjected to axial compression.

The critical stress in a wire is [26]

$$\sigma_{1c} = -\frac{\sin^2 \alpha}{wtR^2} [EI_3(1 + \cos^2 \alpha) + 4EI_2 \cos^2 \alpha - GJ \cos 2\alpha] \quad (205)$$

It is interesting to note that the buckling stress in Equation 205 corresponds to a lateral sinusoidal buckling mode where the buckling length is equal to the wire length along a half pitch:

$$l = \frac{\pi R}{\sin |\alpha|} \quad (206)$$

A smaller buckling length than in Equation 206 may occur if the armour wires are very closely packed so that neighbouring wires restrict lateral displacement. A smaller buckling length implies increased capacity. However, this beneficial effect cannot be accounted for in a simple manner and therefore the capacity shall be calculated by Equation 205.

20.2.4 Buckling of circular wires

The critical buckling stress for a circular wire may be calculated as follows [25]

$$\sigma_{1c} = -\frac{ED^2 \sin^2 2\alpha}{16R^2} \left[1 + \frac{2G \cos^2 \alpha}{E \sin^2 2\alpha + 2G} \right] \quad (207)$$

The critical buckling stress for a circular wire is 7.5% larger than the one for a rectangular wire as given in Equation 205 with J , I_2 and I_3 based on Eqs. 203 and 204. The larger buckling stress does not necessarily imply larger capacity because the steel area fill factor is normally smaller for armour layers with circular wires.

20.2.5 Torsional-flexural buckling of rectangular wires

This failure mode is shown in Figure 85 and may occur for armour layers subjected to outward radial motion where a significant gap is formed at the inside of the armour layer. In that case, the gap may allow the wires to rotate about their own axis. The final deformed state consists of combined lateral deflection and axial rotation of the wire.

The failure mode is however not likely to occur because the wire compressive axial force will stabilize the axial rotation [26]. The stabilizing effect is significant because the compressive axial force is always large whenever buckling is relevant. Further, the stabilizing effect will be present also if a large gap occurs at the inside interface of the outer armour layer. The axial rotation is therefore unlikely to be initiated even if a significant gap is formed. However, if large lateral deflections occur due to e.g. the buckling mode in Section 20.2.3, the wires may start to rotate due to lateral contact between neighbouring wires. This will only occur when the wire state is close to the lateral stability limit or in the post-buckling state.

Based on the above arguments, the lateral buckling mode in Section 20.2.3 will occur prior to the torsional-flexural failure buckling collapse mode. Hence, the failure mode is not relevant to consider in design. The capacity shall instead be computed by Equation 205.

20.3 Birdcaging

Birdcaging refers to the radial failure mode illustrated in Figure 80. This failure mode may occur in two different ways:

1. Failure of outer supporting layer(s)
2. Birdcaging of tensile armour

The first mode is addressed in Section 20.3.1 and represents tensile failure of the supporting layers due to radial expansion of the tensile armour. The second mode is addressed in Section 20.3.2 and may occur if the supporting layers do not have sufficient radial stiffness to prevent the tensile armour from buckling radially.

20.3.1 Failure of outer supporting layers

High-strength tape wound around the tensile armour may be applied to increase the birdcaging capacity. Failure of the high-strength tape layer is normally not acceptable. Hence, the failure criterion may be taken as the ultimate tensile capacity of the tape when subjected to radial expansion of the underlying tensile armour layer. For products with an external sheath, this failure criterion yields the following critical wire stress in the tensile armour layer:

$$\sigma_{1c} = -\frac{R^2 \cos \alpha}{nA \sin^2 \alpha} \left[\frac{\sigma_{ut} n_t A_t \sin^2 \alpha_t}{R_t^2 \cos \alpha_t} + 2\pi E_s \epsilon_{ut} \frac{t_s}{R_s} \right] \quad (208)$$

where the layer mean radius R , the wire area A , the number of wires n and the lay angle α refer to the considered tensile armour layer. The tape's ultimate strength is denoted σ_{ut} , the number of tape plies is n_t , the tape's layer radius is R_t , and the tape's lay angle is α_t . The second term in the square brackets accounts for the radial load-carrying contribution from the external sheath at onset of failure. Here, E_s denotes Young's modulus, ϵ_{ut} is the ultimate strain of the high-strength tape, t_s is the sheath thickness and R_s is the sheath layer radius.

For products based on outer yarn layers, the same failure criterion leads to

$$\sigma_{1c} = -\frac{R^2 \cos \alpha}{nA \sin^2 \alpha} \frac{\sigma_{ut} n_t A_t \sin^2 \alpha_t}{R_t^2 \cos \alpha_t} \quad (209)$$

where the load-carrying capacity of the yarn layers are neglected as they "always" are designed to have the same lay angle as the underlying tensile armour [66]. The contribution to the load-carrying capacity from yarn layers would in any case be insignificant.

Note that the beneficial effect of external over-pressure is conservatively neglected in Eq. 208.

20.3.2 Birdcaging of tensile armour

The birdcaging problem may be studied by using curved beam theory for the tensile armour and by considering the supporting layers as an elastic foundation. The elastic radial buckling stress can then be derived by assuming a sinusoidal buckling mode.

The plastic sheaths outside the tensile armour restrain it from lifting. This is accounted for by computing the radial stiffness of each restraining layer number j

$$c_j = 2\pi E_j t_j \frac{\cos \alpha}{nR} \quad (210)$$

Each wound layer (antibuckling tape, yarn) contributes with the following radial stiffness

$$c_j = n_j E_j A_j \frac{\sin^4 \alpha_j \cos \alpha}{\cos \alpha_j R^2 n} \quad (211)$$

Importantly, in the two expressions above, the mean radius R and the number of wires n refer to the underlying armour wire layer (which is being checked for buckling), not to the restraining

sheath or tape layer. The subscript j refers to the restraining layer, where n_j is the number of yarns or the number of tape plies, E_j is the Young's modulus, A_j is the cross-section area of the tape or a single yarn thread, and the lay angle is denoted α_j . The stiffness contributions from all restraining layers are added together

$$c = \sum_j c_j \quad (212)$$

The wire initial curvature components are given by

$$\kappa_1 = \frac{\cos \alpha \sin \alpha}{R} \quad (213)$$

$$\kappa_2 = \frac{\sin^2 \alpha}{R} \quad (214)$$

The buckling shape is sinusoidal and is defined in terms of the following parameters

$$a_1 = \kappa_2^2 - 2\kappa_1^2 - 4\frac{I_3}{I_2}\kappa_1^2 \quad (215)$$

$$a_2 = \frac{c}{EI_2} + 2\frac{GJ}{EI_2}\kappa_1^2\kappa_2^2 + \kappa_1^4 - \kappa_1^2\kappa_2^2 \quad (216)$$

$$a_3 = \kappa_2^2 - \kappa_1^2 \quad (217)$$

which yields the number of sinusoidal half-waves per length m representing the number of sinusoidal half-waves per length

$$m^2 = \frac{a_3}{\pi^2} - \frac{a_3}{\pi^2} \sqrt{1 - \frac{a_1}{a_3} + \frac{a_2}{a_3^2}} \quad (218)$$

With this, the elastic buckling stress is calculated as [54]

$$\sigma_{1c} = -\frac{\pi^2 EI_2}{A} \left[\frac{m^4 - \frac{a_1}{\pi^2} m^2 + \frac{a_2}{\pi^4}}{m^2 - \frac{a_3}{\pi^2}} \right] \quad (219)$$

20.4 Herniation buckling

See Section 10.4 for a description of the mechanism and Appendix F for the theory behind this assesment. The failure mode involves an "inner" armor layer herniating outwards through either a layer of yarn or through another layer of tensile armor. This later layer, wether yarn or actual tensile armor, is in teh following refered to as the "outer tensile armor". The lay

angles of the inner and outer armor, α_i and α_o , must be of opposite signs. σ_{yi} is the specified minimum yield strength of the material of the inner layer.

In the following, w_i and w_o are the widths of the threads in the inner and outer tensile armors, n_i and n_o the numbers of threads and R_i and R_o the middle radii. The width of the largest possible gap in the outer layer (in the direction orthogonal to the threads of the outer layer), is

$$G = c (2\pi R_o \cos \alpha_o - n_o w_o) \quad (220)$$

where $c = 1.2$ if the outer layer is a tensile layer and $c = 2$ if it is a yarn layer. For yarn layers, it is important to take w_o as a minimum value when the yarns are pressed together. We compute

$$L = \frac{G}{2 \sin (|\alpha_i - \alpha_o|)} \quad (221)$$

$$\beta = \frac{L \sin \alpha_i}{R_i} \quad (222)$$

$$B = \frac{L \cos^2 \alpha_i + R_i \sin \beta \sin \alpha_i}{R_i (\cos \beta - 1)} \quad (223)$$

We compute the vectors

$$\bar{\Delta} = [L \cos \alpha_i, R_i (\cos \beta - 1), R_i \sin \beta] \quad (224)$$

$$\bar{D}_1 = [0, 1, 0] \quad (225)$$

$$\bar{D}_2 = [\cos \alpha_i, 0, \sin \alpha_i] \quad (226)$$

and

$$C = \frac{|(\bar{D}_2 - B\bar{D}_1) \times \bar{\Delta}|}{|\bar{\Delta}| |\bar{\Delta}|} \quad (227)$$

where \times is the cross product.

The plastic-hinge moment of a rectangular wire of the inner layer is calculated as

$$M_p = \frac{1}{4} w_i t_i^2 \sigma_{yi} \quad (228)$$

and for circular wires as

$$M_p = \frac{1}{6} t_i^3 \sigma_{yi} \quad (229)$$

The critical stress is

$$\sigma_{1c} = -\frac{2M_p C}{A} \quad (230)$$

20.5 Inward radial buckling

See Section 10.5 for description of this failure mode and Appendix G for the theory behind this assessment. For a rectangular wire cross section

$$\sigma_{1c} = -\frac{\pi}{4} \sigma_y \quad (231)$$

and for a circular one

$$\sigma_{1c} = -\frac{2}{3}\sigma_{yi} \quad (232)$$

20.6 Carcass collapse of flexible pipes

Excessive torsion that results in high inward radial contact pressure may cause collapse of the carcass. An approach for calculating the critical radial pressure is presented in the following, which mainly is based on the procedure proposed in the Handbook on Design and Operation of Flexible Pipes [17].

As a first step, calculate the equivalent ring bending stiffness per unit length of the flexible pipe

$$EI_{eq} = \sum_j^{N_p} n_j K_j \frac{E_j I_{2,j}}{L_{p,j}} \quad (233)$$

where the summation index j is taken over the pressure spiral layer and the carcass layer, provided that there is no gap between them. The quantity n_j is the number of helices in layer j and E_j is the Young's modulus. The factor K_j is close to 1.0 for massive cross-sections and depends generally on the lay angle and the smallest moment of inertia $I_{2,j}$ about the cross-section's principal axes. The quantity $L_{p,j}$ is the pitch length defined as

$$L_{p,j} = \frac{2\pi R_j}{\tan \alpha_j} \quad (234)$$

where R_j is the mean layer radius and α_j is the helix lay angle of the considered layer.

The sum in Eq. 233 implies that the utilization of the pressure spiral is so low that it will contribute fully with supporting stiffness to the carcass. Further, if there is a gap, the stiffness contribution is lost and consequently only the carcass contribution shall be included in the sum. The carcass collapse capacity will then be significantly reduced. For the case of excessive torsion where the innermost tensile armour transmits high radial contact pressures onto the pressure spiral, it is very likely that there is contact between the pressure spiral and the carcass, and then the sum in Eq. 233 should include both layers.

For installation scenarios and during the product operation phase, one should carefully assess whether or not the pressure spiral will provide supporting stiffness to the carcass. The failure scenario will often be water ingress in the annulus due to a damaged external sheath. This may introduce a gap between the carcass and the pressure spiral, and further the external hydrostatic pressure will be carried by the carcass and the internal plastic sheath. Due to ovality and manufacturing imperfections, it is in practice very difficult to determine the true gap values representing loss of radial contact pressure and loss of supporting stiffness. As an example, Chen et. al. [10] found that the stiffness contribution from the pressure spiral for a 6 inch pipe shall be set to zero if the gap is larger than 2.5 mm. Further recommendations on the limiting gap values are not provided in this document.

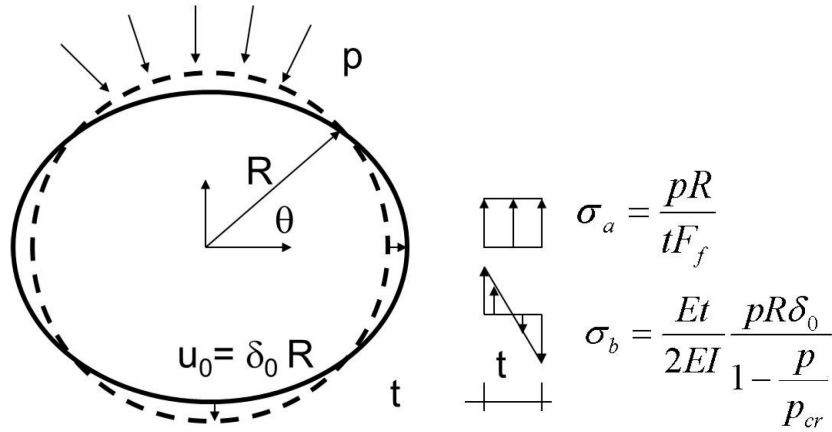


Figure 99: Ovalization parameter δ_0 and circumferential stress components [17]

Next, the elastic buckling pressure of the carcass is calculated as

$$p_e = \frac{3EI_{eq}}{R_c^3} \quad (235)$$

where R_c is the carcass mean radius.

Ovality of the cross-section will reduce the capacity significantly. According to API 17B [1], the maximum initial ovalization around the cross-section may be estimated as (see Figure 99)

$$\delta_0 = \frac{D_{max} - D_{min}}{D_{max} + D_{min}} \geq 0.002 \quad (236)$$

In a handling operation, the initial ovalization parameter suggested by API 17B in Eq. 236 may be too small if the flexible pipe is subjected to high external radial contact forces and/or large bending. In such cases, one should consider to perform a detailed FE analysis or performing tests to verify the δ_0 -parameter.

A further reduction of the capacity is caused by residual stresses. This may be accounted for by assuming full plastification during manufacture and thereafter elastic unloading to zero moment. This corresponds to the following residual stress in the outer fiber of the carcass cross-section

$$\sigma_r = \sigma_u \frac{W_p}{W_e} - \sigma_u \quad (237)$$

where W_p is the cross-section plastic section modulus, W_e is the cross-section elastic section modulus and σ_u is the ultimate compressive stress of the carcass. This results in the following effective compressive yield stress

$$\sigma_{fe} = \sigma_f - \sigma_r \quad (238)$$

Thereafter, the critical collapse pressure of the carcass p_c is calculated by solving the following second order equation

$$p_c^2 - \left[\frac{\sigma_{fe} F_f t}{R_c} + p_e \left(1 + \frac{Et^2 F_f R \delta_0}{2EI_{eq}} \right) \right] p_c + \frac{p_e \sigma_{fe} F_f t}{R_c} = 0 \quad (239)$$

where the carcass fill factor carcass is defined as,

$$F_f = \frac{nA}{L_p t} \quad (240)$$

in which n is the number of helices (normally 1 or 2) with cross-section area A , Eq. 234 defines L_p and t is the thickness of the carcass corrugated plate profile. The carcass fill factor is typically $F_f \approx 0.55$.

Carcass collapse is then avoided by ensuring

$$p < p_c \quad (241)$$

where p is the pressure acting on the carcass outside. The pressure p due to excessive torsion must be computed by an axi-symmetric loading software as described in Sec. 20.1.2. An expression for p can be derived if there is only one tensile armour layer, however, flexible pipes "always" have either two or four tensile armour layers.

20.7 Tensile yield failure

Tensile yielding is in principle relevant for all product types. When double-armoured products are subjected to torque, one of the tensile armour layers will be subjected to compressive stresses. In that case, one of the compressive local failure modes described under Section 20 is more likely to occur, at least for high tensile strength materials. Tensile yield failure is most relevant for single-armoured products provided that the supporting layers/components have sufficient strength to withstand the radial pressure load from the tensile armour.

Tensile yielding is prevented by ensuring

$$\sigma_1 < \sigma_{1c} \quad (242)$$

$$\sigma_{1c} = \sigma_y \quad (243)$$

where σ_y is the yield strength of the wire.

20.8 Skew kinking

This failure mode is relevant only for flexible pipes which can flatten and create a hinge, as sketched in Figure 100.

In the absence of external pressure, the critical torque at which skew-kinking would occur is roughly

$$T_c \approx 2W_m R \quad (244)$$

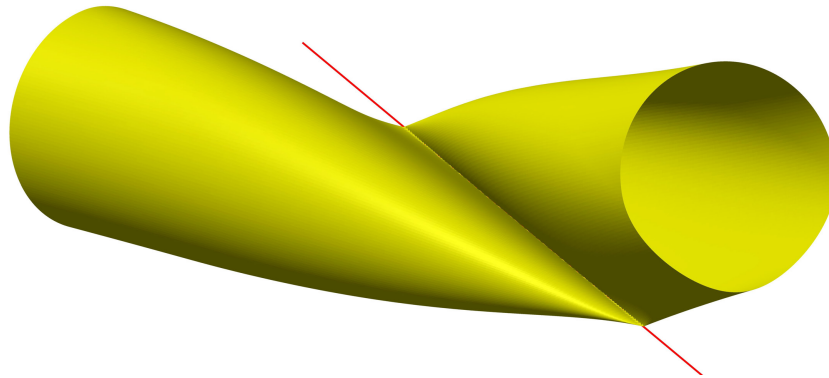


Figure 100: Skew kinking

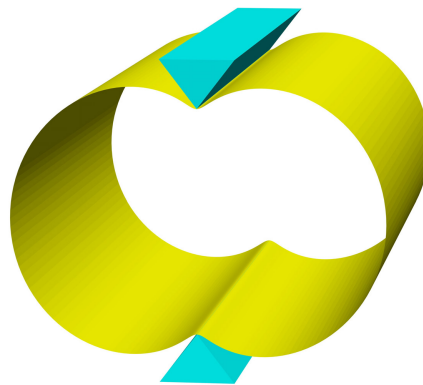


Figure 101: Flexible pipe crushing test

where R is the mean radius of the innermost metallic component (carcass or pressure armor), and W_m is the work needed to squash a pipe segment of unit length (Figure 101), to the point where the inner component comes in contact with itself. This value is obtained experimentally by taking a length of pipe and applying compressive loads along opposite longitudinal lines along the pipe.

See Appendix H for theory.

21 Global failures

21.1 Helical buckling

21.1.1 Foreword

If helical buckling is initiated, the pitch length P of the helical buckling mode depends chiefly on the value of the torque and the tension. However, the post-buckling evolution of the shape of the flexible product after buckling is also influenced by the stiffnesses related to these forces, that is, how the tension and torsion at the boundaries of the buckling area evolve, as the buckling progresses. Self-contacting loops requires lengths of flexible product to be pulled in. Hence a tension at the boundaries, that does not increase as the buckling segment pulls in length will promote the formation of self contacting loops. Similarly, a torsion that only decreases slowly as buckling progresses will cause a large writhe to be concentrated in the buckling area, resulting in a large helix diameter. In a handling operation, where the flexible product is being transported along a route, correctly modelling of these boundary conditions, and thus the post buckling behavior will generally be challenging. Furthermore, whether a self contacting loop, will, subjected to increasing tension, open up or result in a localization of deformations (a hockle) depends on the torque, on stiffnesses, and on the dissipation of energy by friction and plastic deformation. Hence the strategy offered here for handling helical buckling is to ensure that helical buckling is not initiated.

However this strategy is not unproblematic so caution will have to be exerted: consider the buckling of columns in compression (Euler's buckling criteria). If a column is bent before being subjected to compression, it will collapse at lower loads than predicted by Euler's theory. The same applies to helical buckling: The theory behind Eq. 245 considers a *straight* rod for which a bifurcation (singular stiffness matrix) will occur under certain loads. In contrast, in the handling of flexible products, helical buckling is most likely to occur in free spans, which can be far from straight. An attempt is made to account for this in Eq. 245, which is Greenhill's equation, modified to account for a final state (a self-contacting loop) with lower energy than the energy of the system at bifurcation.

21.1.2 Greenhill's formula

To prevent helical buckling of a flexible product in a span between two supports separated by a distance L , one must ensure that everywhere between the supports

$$m_1^2 - \beta 2r_1 < \left(\frac{\alpha 2\pi}{l} \right)^2 \quad (245)$$

with

$$m_1 \triangleq \frac{M_1}{EI}, \quad r_1 \triangleq \frac{R_1}{EI} \quad (246)$$

where R_1 is the effective tension in the flexible and M_1 is the torque. The formula is adapted from [20] (see also [2]), with the introduction of a factor α on the length L and a factor β on the tension r_1 . Where the supports prevent transverse displacement in both directions, $\alpha = 1$. Where the supports allow some transverse displacement in one direction (typically: either horizontal or vertical), $\alpha = 0.5$. Where the supports allows some transverse displacement in two directions, including because the support does no prevent the flexible to lift, the supports are ineffective for helical buckling prevention. One must then use $\alpha = 0$, or re-categorize the free span by ignoring such ineffective supports. The factor $\beta = 1$ must always be used, except if the flexible cable is absolutely straight (high tension and no sag), in which case $\beta = 2$ is allowable.

In particular, for large spans $L \rightarrow +\infty$, this simplifies to

$$m_1^2 < 4r_1 \quad (247)$$

This can be used as a requirement for the minimum tension to be maintained at the touch-down point during installation on the sea floor: the distance to the next support (the vessel) is very large. The minimum tension must be evaluated by including the influence of sea current and wave loads.

The following Sections provide further guidance on the use of Eq. 245.

An alternative capacity assessment approach based on Greenhill's equation is available in work by Gay Neto and Martins [33].

21.1.3 Selecting tension for assessment

At any point along the route, the most negative value of R_1 that may possibly occur at a given location is to be used. For typical handling routes, $R_1 = 0$ is generally an adequate value because the flexible product can sag between supports, thus avoiding compression. In that case Eq. 245 shows that the maximum allowable length L between supports is

$$L < \frac{\alpha 2\pi}{|m_1|} \quad (248)$$

Special cases may arise for the selection of the value of R_1 , including:

1. If at a given point along a span, tension is guaranteed to be maintained above R_1 at all times, then the value R_1 can be used.
2. If at any point along the route, compressive forces may occur, then the most negative value of R_1 must be used in Eq. 245. Such a situation can arise for example if two tensioners are used with an inadequate control system, and are close to each other or are separated by close-spaced roller boxes that prevent lateral displacements in all directions.

21.1.4 Pitch length

If buckling occurs, the pitch length P of the helix that is formed depends on the torque needed to trigger buckling (Figure 58)

$$P = \frac{4\pi}{|m_1|} \quad (249)$$

This applies both for short spans and long spans.

For long spans only:

$$P = \frac{2\pi}{\sqrt{r_1}} \quad (250)$$

21.1.5 Bending stiffness

In the above, the bending stiffness EI is to be taken equal to the sum of the bending stiffnesses of the individual components. Where components are themselves divided into sub-components (as the conductor of an electric phase, itself made of metal strands wound together), the sum of the bending stiffnesses of the sub-components are to be taken. Where plastic deformations are expected to occur in some components during handling, the tangential stiffness under plastic deformation of these components is to be used.

21.1.6 Roller alleys

If along a straight segment of the route, rollers are regularly spaced with a distance L between them, and the rollers do not prevent the flexible product from lifting, then the flexible may buckle with a pitch length $P = L/\alpha$ with $\alpha = 0.5$ if

$$m_1 \geq \frac{\alpha 2\pi}{L} \quad (251)$$

$$r_1 \leq \left(\frac{\alpha\pi}{L}\right)^2 \quad (252)$$

See Appendix I for theory.

21.1.7 Catenary between two supports

If two supports *at the same height* are separated by a distance L , and the maximum deflection between the supports is d (Figure 102), then compute

$$z/x = \frac{2d}{L} \quad (253)$$

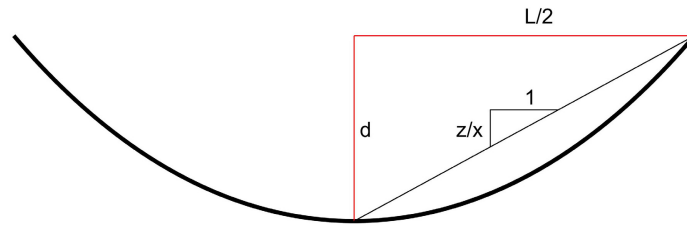


Figure 102: Geometry of a free span (catenary)

Read the corresponding value of r/x (the ratio of curvature radius at the bottom of the catenary to width) from Figure 103 (The plotted curve has equation $z/x = r/x \left(\cosh \left(\frac{1}{r/x} \right) - 1 \right)$) and compute r (the radius of curvature at the middle of the span, not to be confused with $r_1 = R_1/EI$)

$$r = r/x \cdot \frac{L}{2} \quad (254)$$

The lowest tension, to be used for helical buckling assessment is then

$$R_1 = gmr \quad (255)$$

where m is the mass per unit length of the flexible product and $g = 9.81 \text{ m} \cdot \text{s}^{-2}$ is the acceleration of gravity. Figure 103 is established assuming that the shape of the flexible in the span is not significantly affected by the stiffness of the flexible product (a catenary solution). For short spans the results will be unconservative: for spans with L smaller than 40 diameters, use a finite element analysis instead.

21.1.8 Catenary during installation

As a screening analysis, one can use a catenary solution to assess the tension at the touch down point when laying a flexible product on the seabed. If x and z are respectively the horizontal and vertical distance from the installation vessel's chute to the touchdown point (Figure 104), then Figure 103 can be used to evaluate r/x . The tension at the touch down point is then

$$R_1 = w_s r \quad (256)$$

$$= w_s (r/x) x \quad (257)$$

where w_s is the submerged weight of the flexible product.

Such an analysis can easily over estimate R_1 and thus be unconservative: current, and wave induced motions of the installation vessel, as well as the uncertainty over the length of cable paid out will all affect R_1 .

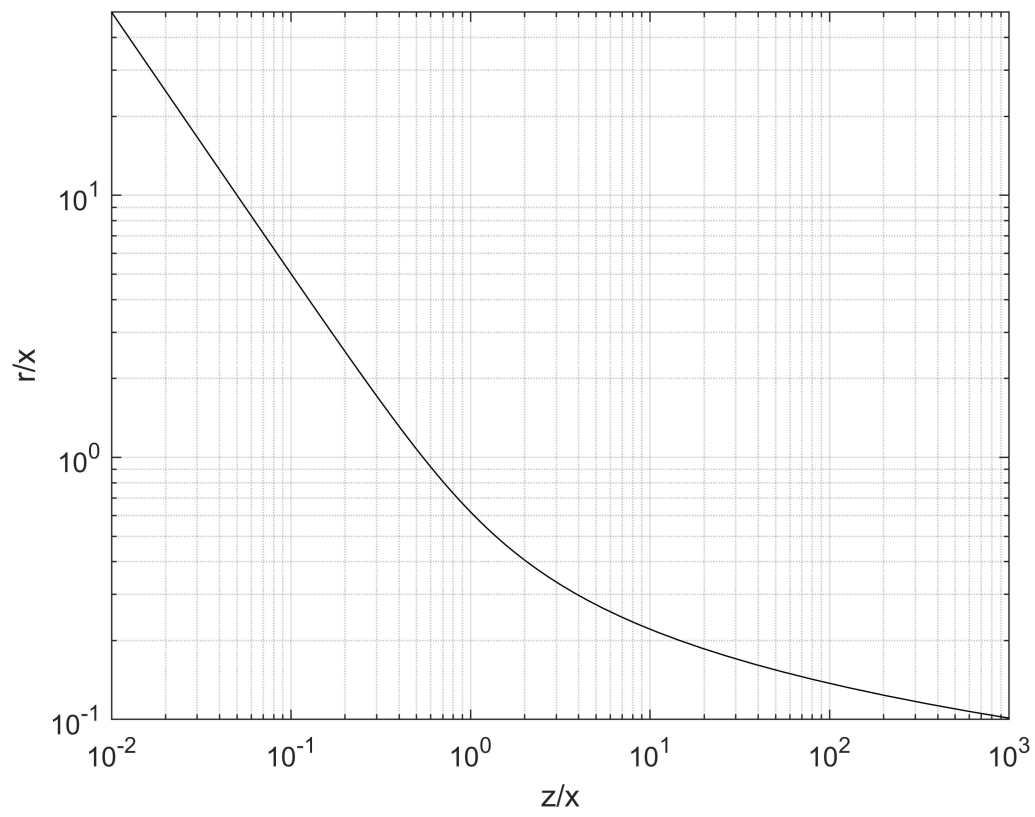


Figure 103: Relation between deflection and curvature radius in a catenary.

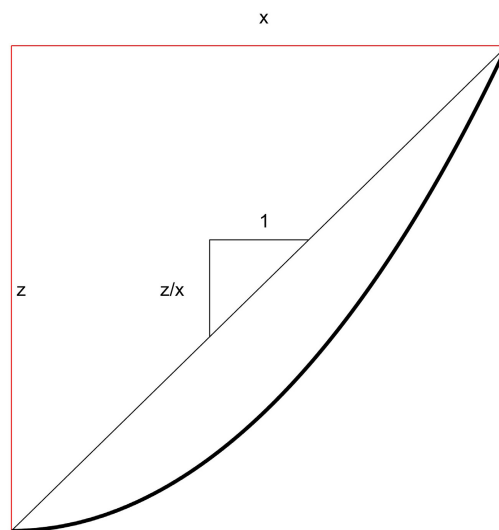


Figure 104: Geometry of a free span (catenary)

22 Case study

22.1 Objective

This section provides a worked example of torsion assessment. While this section does not provide an example for every procedure outlined in this guideline, it should give a better idea of the typical sequence of actions to be taken in an assessment, and of the inputs required.

This section covers phases 7, 8 and 9 of a cable's lifetime, as discussed in Section 14: these are the initial and final transient, as well as the steady state in a load-out operation. This section addresses the mechanisms "coiling writhe" and "flip torque". For the sake of brevity, only a single route geometry is considered. In reality, multiple geometries need to be considered, in particular to account for the various possible positions of the touch-down points in the storages at both ends of the route.

22.2 Cross section

We consider a cable with 149.2mm outer diameter (Figure 105, Table 2). The cable has two tensile armours wound in opposite directions. An anti-buckling tape is wound around the outer armour, and a layer of PP yarns is wound outermost. Key results from a finite element analysis of the cross section are presented in Table 3.

22.3 Critical stresses

All relevant buckling mechanisms are evaluated. When no unit is specified after a value (for intermediate results), base SI units are used:

Lateral buckling of the inner armour

Assuming $E = 2.1e5\text{MPa}$ and $\nu = 0.3$, calculations yield $G = 0.81e11$ and $\sigma_{1c} = -11.3\text{MPa}$.

		Inner armour	Outer armour	Tape	Yarn
Section	[mm]	∅5	∅5		∅4
Pitch length	[mm]	-2800	2800	84	60
Mean radius	[mm]	81	88	90.3	92.5
Number		92	92		140
Material		steel	steel	UHMWPE	PP
E	[GPa]	211	211		
ν	[.]	0.3	0.3		

Table 2: Outer layers of example cable

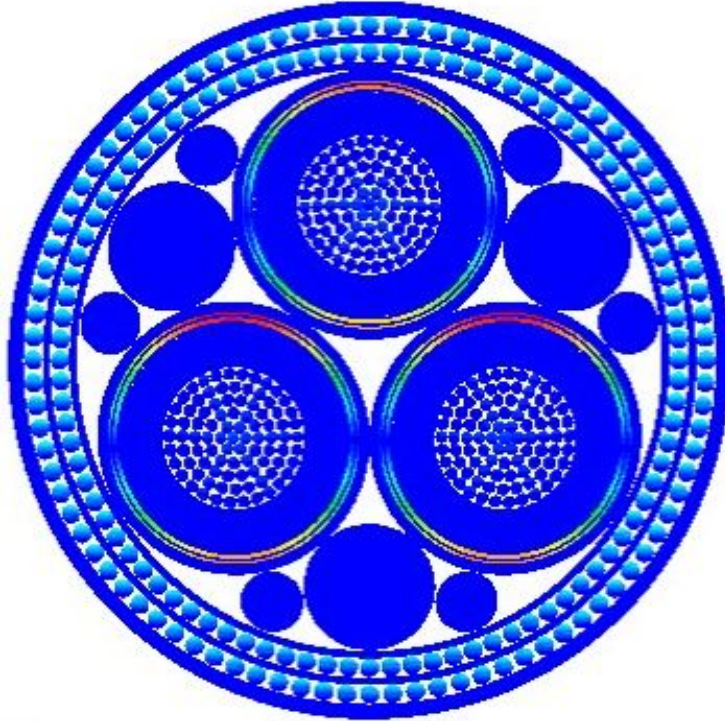


Figure 105: Cross section of example cable

	+ torsion (tight)	- torsion (slack)	
M_f	0.96		[kN · m]
$K_{\varepsilon\tau}^*$	241.12	239.93	[kN · m ² · rad ⁻¹]
K_τ^*	266.50		[kN · m ² · rad ⁻¹]
EI (slip)	35.54		[kN · m ²]
$\partial\sigma_1/\partial M_1$ (inner)	-14.35	-14.19	[MPa · kN ⁻¹ · m ⁻¹]
$\partial\sigma_1/\partial M_1$ (outer)	12.63	12.09	[MPa · kN ⁻¹ · m ⁻¹]

Table 3: Results from FE analysis of the cross section: bending moment of friction, torsional stiffness at constant tension, bending stiffness at full slip, stress from torque

Herniation buckling of the inner armour through the outer armour

Calculations yield $G = 0.0989$, $L = 0.1351$ (the outer layer is well packed), $\beta = -0.298$, $B = -37.74$, $\Delta = \begin{bmatrix} 0.133 & -0.00358 & -0.0238 \end{bmatrix}$, $D_1 = \begin{bmatrix} 0 & 1 & 0 \end{bmatrix}$, $D_2 = \begin{bmatrix} 0.984 & 0 & -0.179 \end{bmatrix}$, $C = 279.0$ and $\sigma_{1c} = -355.8\text{MPa}$.

The outer armour layer is well packed, leaving only a short gap, so that this is not a critical failure mode.

Lateral buckling of the outer armour

Calculations yield $\sigma_{1c} = -11.1\text{MPa}$.

Herniation buckling of the outer armour through yarn

Yarn can compress in the radial direction, permitting the formation of a larger gap than what its nominal diameter would indicate. Here the gap width is computed assuming a yarn diameter of 3.5mm.

Calculations yield $G = 0.0219$, $L = 0.0197$ (the outer layer is well packed), $\beta = 0.0434$, $B = -238.$, $\Delta = \begin{bmatrix} 0.0193 & -8.27 & -0.00382 \end{bmatrix}$, $D_1 = \begin{bmatrix} 0 & 1 & 0 \end{bmatrix}$, $D_2 = \begin{bmatrix} 0.981 & 0 & 0.194 \end{bmatrix}$, $C = 12087.$ and $\sigma_{1c} = -15389\text{MPa}$.

The failure mode thus seems very unlikely. The actual gap width should be tested, using forces to create a gap. Also, the assessment methods ignores the antibuckling tape. We have no experience of the effect of such a tape on herniation buckling, but it could be quite beneficial.

Birdcaging of the outer armour

Calculations yield $\alpha = 1.96e-5$, $G = 0.8077e11$, $c_1 = 1.83e7$, $c_2 = 4.59e6$, $c = 1.88e7$, $\kappa_1 = 2.16$, $\kappa_2 = 0.426$, $\alpha_1 = -27.8$, $\alpha_2 = 2.918$, $\alpha_3 = -4.48$, $m = 13.14$. $\sigma_{1c} = -1127\text{MPa}$. This is a high value, thanks in particular to the antibuckling tape.

Summary

The critical failure mode is lateral buckling, for both tensile armours. The inner tensile armour (wound in the negative direction) has a critical stress $\sigma_{1c} = -11.3\text{MPa}$, which corresponds to a critical torque

$$M_{1c} = \sigma_{1c} \cdot \partial\sigma_1/\partial M_1 = -11.3 \cdot -14.35 = 162 \text{ [kNm]} \quad (258)$$

The outer tensile armour (wound in the positive direction) has a critical stress $\sigma_{1c} = -11.1\text{MPa}$, which corresponds to a critical torque

$$M_{1c} = \sigma_{1c} \cdot \partial\sigma_1/\partial M_1 = -11.1 \cdot -12.09 = -134 \text{ [kNm]} \quad (259)$$

In other words, the cable is safe from *local buckling* if the torque remains within the interval

$$-134 \text{ [kNm]} < M_1 < 162 \text{ [kNm]} \quad (260)$$

22.4 Global buckling

Assuming that the product will never experience compressive forces, we assume $R_1 = 0$, Greenhill's criteria simplifies to

$$|M_1| < \frac{\alpha 2\pi EI}{L} \quad (261)$$

We assume that the supports only prevent displacement in the vertical direction, so $\alpha = 0.5$. The bending stiffness is conservatively taken as the stiffness under full slip, $EI = 35.54 \text{ [kN}\cdot\text{m}^2]$. If for example, supports are placed 5m apart, then this results in

$$|M_1| < 22.33 \text{ [kNm]} \quad (262)$$

This suggests that global buckling would become a concern before local buckling.

22.5 Route

The cable is to be transported from a negative on-shore turntable, in which it is stored torsion free, to a positive turntable on board an installation vessel. The coordinates of points along the route are detailed in Appendix L, and the geometry of the route is shown in Figure 106. The shore is on the left, the vessel on the right. The reference systems are of the torsion-free family. The red crest show the intensity and direction of curvature. The radius of the cable is not to scale. The route is deliberately shortened for this example, making it easier to provide visualisations of the route as a whole that also show what is going on at critical sections along the route.

22.6 Steady-state flip torque evaluation

The code Jordan for flip torque assessment is used. The inputs are:

1. The geometry of the whole route (cf. Appendix L).
2. A material roll rate of 0 [deg/m] .
3. The friction bending moment $M_f = 0.96 \text{ [kN}\cdot\text{m]}$.

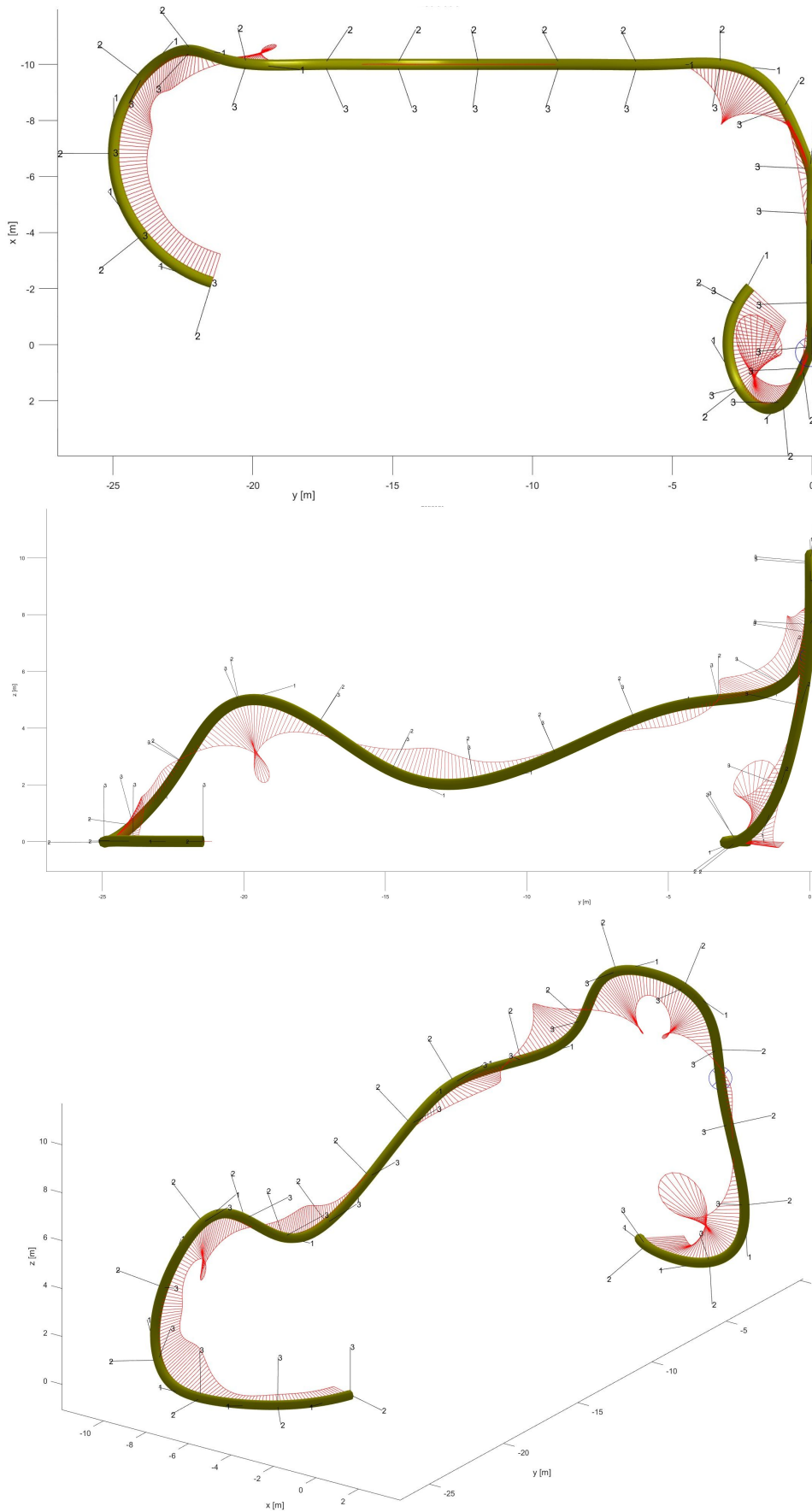


Figure 106: Example loadout route: plan, elevation and isometric view

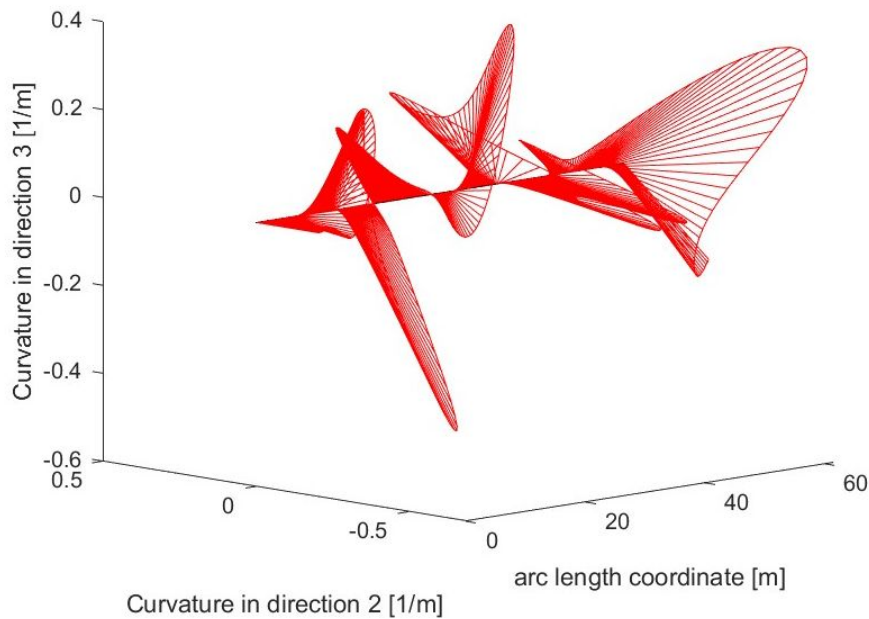


Figure 107: Route curvature

The analysis produces the following outputs.

Figure 107 show the intensity of the curvature along the route, as well as its direction within a torsion-free family of reference systems.

Figure 108 shows the evolution over time of the curvature experienced by a cross section (which is directly relevant for the computation of click torque). This is computed for the material roll rate of 0 [deg/m] specified as input to the analysis.

Figure 109 shows the effect of the material roll rate on the accumulated flip torque along the whole route. This output is not relevant because a non-zero uniform material roll rate is not likely to occur along the whole route. This type of output is relevant when studying single free spans.

Figure 110 shows the distribution along the route of the internal torque (top) and flip torque (bottom).

Figure 111 shows the writhe angle along the route. This result only serves to show that a torsion-free longitudinal marking will change roll angle along the route.

To conclude, at steady state, internal friction induces negative torque along the route. The torque is strongest far upstream along the route. This suggests that in addition to local buckling, a flip torque–geometry instability could develop in the free span of the upstream turntable. Treating this requires iterations as described in Section 16.7.

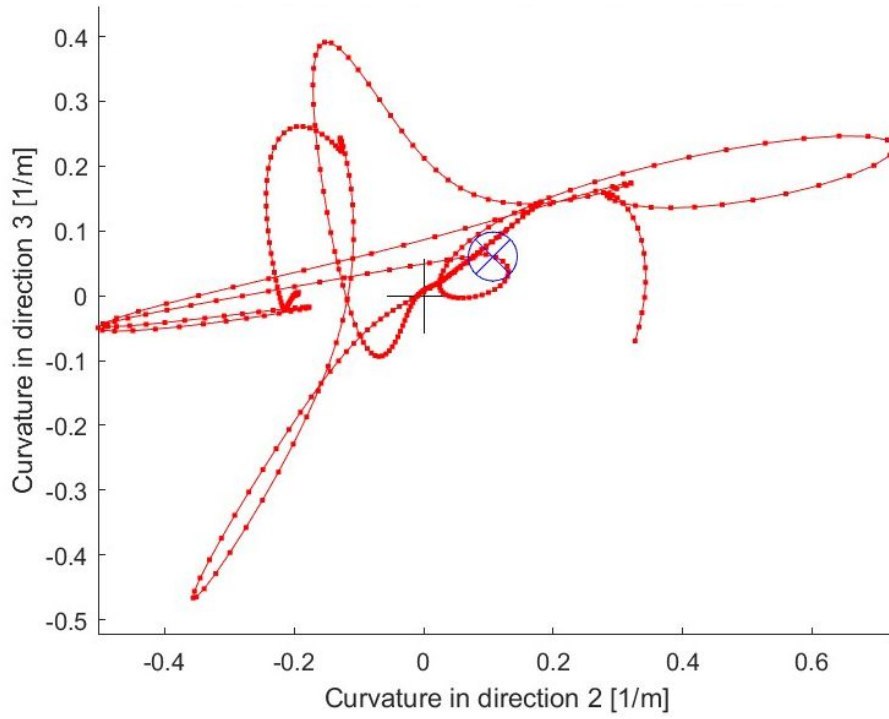


Figure 108: Curvature experienced by a cross section

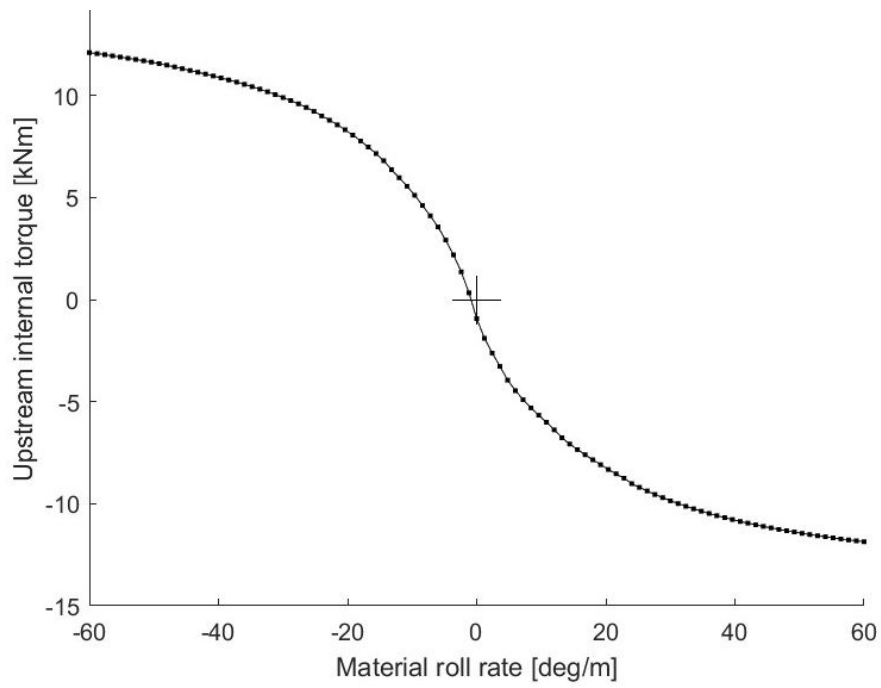


Figure 109: Effect of the material roll rate on flip torque

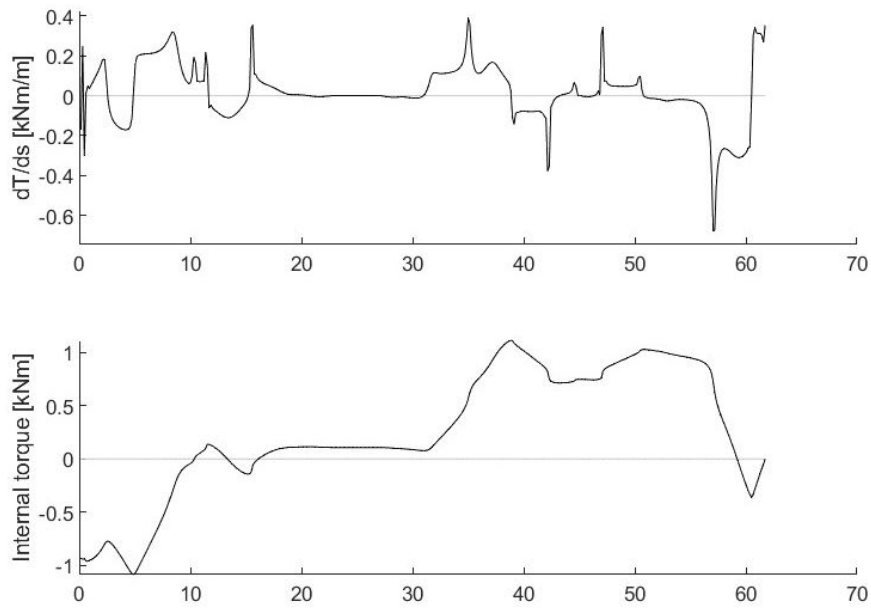


Figure 110: Flip torque distribution at zero material roll rate

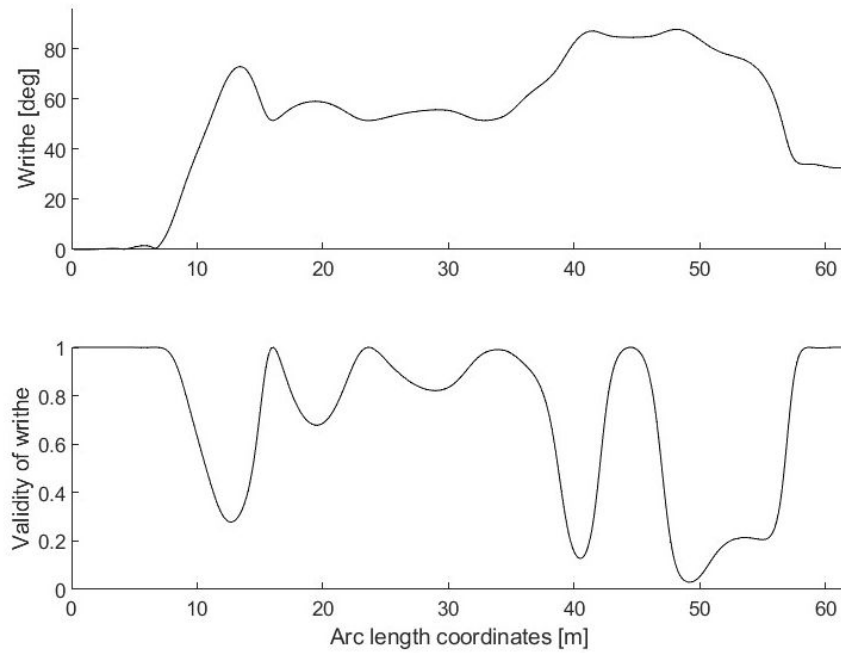


Figure 111: Writhe along the route

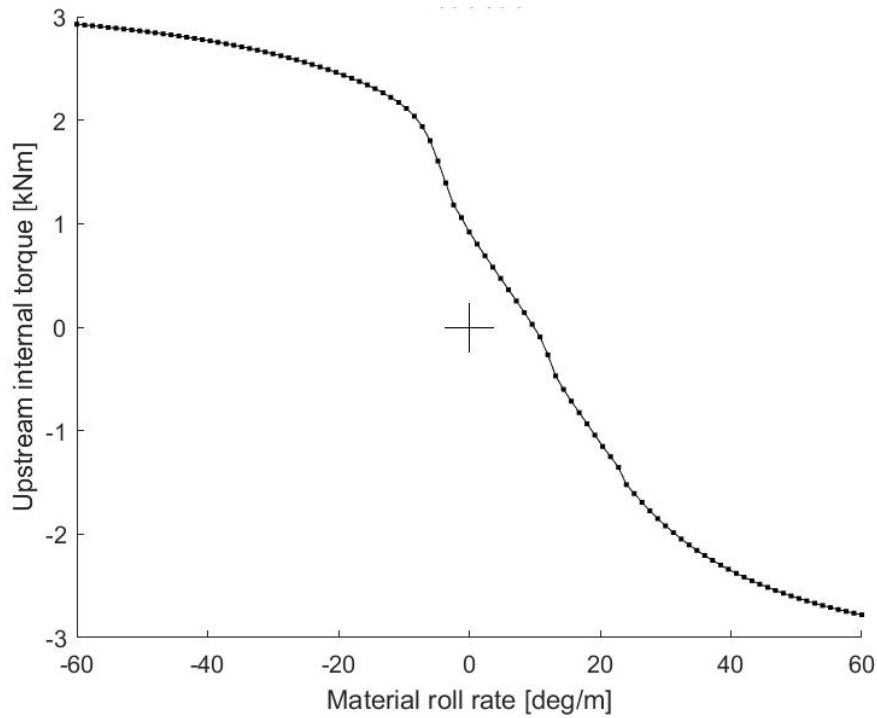


Figure 112: Effect of roll rate on flip torque

22.7 Flip torque in transients

The analysis presented in Section 22.6 is repeated with the change that the first 319 points of the route are cut out: the analysis only considers the free span in the onboard turntable. Figure 112 shows that the flip torque in the free span is zero for a material roll rate of -9.6 [deg/m].

The roll rate and hence the local torsion are found as described in Section 22.6, and the result is shown in Figure 113.

At the start of the operation, upstream torsion and torque are low, and the flip torque is taken up by downstream internal torque. Downstream, friction in the turntable causes material roll rate to be zero. High stiffness implies that the flip torque causes a small torsion downstream, so the spatial roll rate is small: 0.38 [deg/m]. For the flip torque to be taken up upstream (steady state), upstream torsion must be about 0.24 [deg/m]. So steady state will be approached when roughly an amount of cable equal to the length of the route has been paid out after the cable head is secured in the downstream turntable.

22.8 Assessment

The torques found in Figure 110 are well within the safe range for local buckling (Eq. 260) and global buckling (Eq. 262). The same is true of the torques expected in a transient (-1 [kNm], Figure 113) just downstream of the on-board turntable free span).

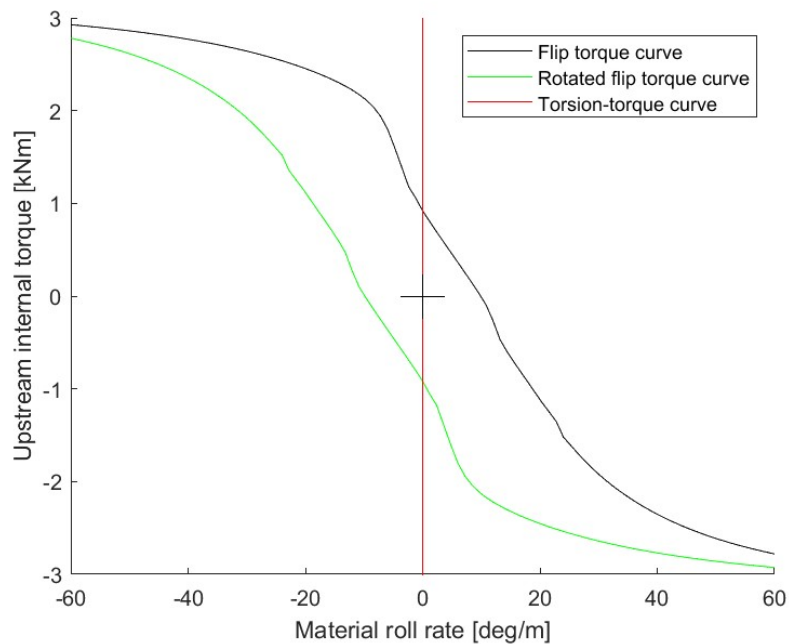


Figure 113: Transient assessment

This suggest that the operation would be safe with a good margin. One should however keep in mind the limitations of our ability to date to prove before hand that an operation will be safe. Several moments should be pointed out:

- M_f was estimated as a single value, using finite element computation. Assessment of M_f at low torque and tension is difficult, because it depends on details of the fabrication process and material behaviour which are difficult to capture. Further, in reality, M_f is a function of torque (and tension) opening the possibility for curvature-pressure instability (Section 8.3).
- Figures 110 and 113 are established *for a given route geometry*. This geometry changes during the operation as the turntable is filled, but also because the torques that appear change the shape of the free spans. Ultimately, this includes the flip torque-geometry instability (Section 8.4).

A J-lay installation on the seafloor

We call x the horizontal distance from the touch-down point, ζ the vertical distance from the touch down point, $z > 0$ the depth of the touch-down point, r the bending radius at the touch-down point, ρ_w the density of sea water, g the acceleration of gravity, m the mass per unit length of the flexible, and A_e the outer area of the product. The torque-free twist in a free span is assessed as follows.

Assuming the product follows a catenary shape

$$\zeta = r \left(\cosh \frac{x}{r} - 1 \right) \quad (263)$$

The arc-length from touch-down point is

$$\xi = \sqrt{\zeta^2 + 2\zeta r} \quad (264)$$

and we note that

$$\sqrt{r^2 + \xi^2} = \sqrt{r^2 + \zeta^2 + 2\zeta r} \quad (265)$$

$$= \zeta + r \quad (266)$$

and

$$r = \frac{\xi^2 - \zeta^2}{2\zeta} \quad (267)$$

The submerged weight of the product is

$$\omega = g (m - A_e \rho_w) \quad (268)$$

The effective tension at a point at arc-length ξ from the touch-down point, or at a height ζ above it is

$$R_1^e = \omega \sqrt{r^2 + \xi^2} \quad (269)$$

$$= \omega (\zeta + r) \quad (270)$$

The wall tension at the same point is (see Equation 45)

$$R_1^w = R_1^e - P_e A_e \quad (271)$$

$$= g (m - A_e \rho_w) (\zeta + r) - \rho_w g (z - \zeta) A_e \quad (272)$$

$$= gm (\zeta + r) - \rho_w gz A_e \quad (273)$$

$$= gm \sqrt{r^2 + \xi^2} - \rho_w gz A_e \quad (274)$$

Torque-free torsion is (see Section B)

$$\tau_u = \frac{R_1^w}{K_{\varepsilon\tau}^*} \quad (275)$$

with

$$\frac{1}{K_{\varepsilon\tau}^*} = \frac{K_{\varepsilon\tau}}{K_{\varepsilon\tau}^2 - K_{\varepsilon}K_{\tau}} \quad (276)$$

hence

$$\tau_u = \frac{1}{K_{\varepsilon\tau}^*} \left(gm\sqrt{r^2 + \xi^2} - \rho_w gz A_e \right) \quad (277)$$

The torque-free twist over the free span is thus

$$T_u = \int_0^L \tau_u d\xi \quad (278)$$

$$= \frac{1}{K_{\varepsilon\tau}^*} \left(gm \int_0^L \sqrt{r^2 + \xi^2} d\xi - L\rho_w gz A_e \right) \quad (279)$$

$$= \frac{gm}{2K_{\varepsilon\tau}^*} \left[\xi\sqrt{r^2 + \xi^2} + r^2 \log \left(\xi + \sqrt{r^2 + \xi^2} \right) \right]_{\xi=0}^{\xi=L} - K_{\varepsilon\tau}^{*-1} L\rho_w gz A_e \quad (280)$$

$$= \frac{gm}{2K_{\varepsilon\tau}^*} \left[\xi(r + \zeta) + r^2 \log(\xi + r + \zeta) \right]_{\xi=0}^{\xi=L} - K_{\varepsilon\tau}^{*-1} L\rho_w gz A_e \quad (281)$$

$$= \frac{gm}{2K_{\varepsilon\tau}^*} \left(L(r + z) + r^2 \log \left(1 + \frac{L+z}{r} \right) \right) - K_{\varepsilon\tau}^{*-1} L\rho_w gz A_e \quad (282)$$

$$T_u = \frac{g}{K_{\varepsilon\tau}^*} \left[\frac{m}{2} \left(L(r + z) + r^2 \log \left(1 + \frac{L+z}{r} \right) \right) - z\rho_w LA_e \right] \quad (283)$$

The following is an assessment of the twist laid on the seabed when suddenly going from a tight ($L = L_{\min}$) to a slack ($L = L_{\max}$) configuration. It is done assuming that the torsion laid on the seabed is equal to the torque-free torsion. This is conservative, because in reality, torque will increase in the free span during release, limiting the laid torsion.

$$\tau = \frac{R_{1td}^w}{K_{\varepsilon\tau}^*} \quad (284)$$

$$= \frac{1}{K_{\varepsilon\tau}^*} (gmr - \rho_w gz A_e) \quad (285)$$

$$= \frac{1}{K_{\varepsilon\tau}^*} \left(gm \frac{L^2 - z^2}{2z} - \rho_w gz A_e \right) \quad (286)$$

$$T_l = \int_{L_{\min}}^{L_{\max}} \tau dL \quad (287)$$

$$= \frac{gm}{2zK_{\varepsilon\tau}^*} \int_{L_{\min}}^{L_{\max}} L^2 - z^2 dL - \frac{L_{\max} - L_{\min}}{K_{\varepsilon\tau}^*} \rho_w gz A_e \quad (288)$$

$$= \frac{gm}{2zK_{\varepsilon\tau}^*} \left(\frac{1}{3}L_{\max}^3 - \frac{1}{3}L_{\min}^3 - z^2L_{\max} + z^2L_{\min} \right) - \frac{L_{\max} - L_{\min}}{K_{\varepsilon\tau}^*} \rho_w gz A_e \quad (289)$$

$$= \frac{gm}{2zK_{\varepsilon\tau}^*} \left(\frac{1}{3}L_{\max}^3 - \frac{1}{3}L_{\min}^3 \right) - z \left(\frac{gm}{2} + \rho_w g A_e \right) \frac{L_{\max} - L_{\min}}{K_{\varepsilon\tau}^*} \quad (290)$$

B Pull in operation

A linear coupled elongation-torsion system, can be described with

$$\begin{bmatrix} K_\varepsilon & K_{\varepsilon\tau} \\ K_{\varepsilon\tau} & K_\tau \end{bmatrix} \cdot \begin{bmatrix} \varepsilon \\ \tau \end{bmatrix} = \begin{bmatrix} R_1 \\ M_1 \end{bmatrix} \quad (291)$$

If $M_1 = 0$ and $R_1 \neq 0$ then

$$\varepsilon = \frac{R_1}{K_\varepsilon} - \frac{K_{\varepsilon\tau}}{K_\varepsilon} \tau \quad (292)$$

and

$$\varepsilon = -\frac{K_\tau}{K_{\varepsilon\tau}} \tau \quad (293)$$

so that

$$K_{\varepsilon\tau} \frac{R_1}{K_\varepsilon} - \frac{K_{\varepsilon\tau} K_{\varepsilon\tau}}{K_\varepsilon} \tau + K_\tau \tau = 0 \quad (294)$$

$$\frac{K_{\varepsilon\tau}}{K_\varepsilon} R_1 + \left(K_\tau - \frac{K_{\varepsilon\tau} K_{\varepsilon\tau}}{K_\varepsilon} \right) \tau = 0 \quad (295)$$

$$\frac{\frac{K_{\varepsilon\tau}}{K_\varepsilon}}{\frac{K_{\varepsilon\tau} K_{\varepsilon\tau}}{K_\varepsilon} - K_\tau} R_1 = \tau \quad (296)$$

$$\frac{K_{\tau\varepsilon}}{K_{\varepsilon\tau}^2 - K_\tau K_\varepsilon} R_1 = \tau \quad (297)$$

and so one introduces

$$\frac{1}{K_{\varepsilon\tau}^*} = \frac{K_{\tau\varepsilon}}{K_{\varepsilon\tau}^2 - K_\tau K_\varepsilon} \quad (298)$$

At zero torque, a force $R_{1\max}$ will thus induce a torsion

$$\tau_u = \frac{R_{1\max}}{K_{\varepsilon\tau}^*} \quad (299)$$

If, maintaining this torsion, the axial force is set to $R_{1\min}$, and the change in axial strain is

$$\Delta\varepsilon = \frac{R_{1\min} - R_{1\max}}{K_\varepsilon} \quad (300)$$

inducing a change in torque

$$M_1 = K_{\varepsilon\tau} \Delta\varepsilon \quad (301)$$

$$= K_{\varepsilon\tau} \frac{R_{1\min} - R_{1\max}}{K_\varepsilon} \quad (302)$$

C Flip torque transient close to downstream storage

Assuming a short distance between the flip area and the downstream storage (compared to the longer distance between upstream storage and flip area). The subscript **f** and **d** refer to the flip area and the downstream storage. The transient in the route as a whole is a steady state in the **fd** part of the route.

The rate of change of twist **T** in the part of the route between the flip area and the downstream storage is

$$\frac{\partial T}{\partial k} = \frac{\partial R_d}{\partial k} - \frac{\partial R_f}{\partial k} \quad (303)$$

$$\frac{\partial T}{\partial k} = \frac{DR_d}{Dk} - \frac{DR_f}{Dk} - \tau_d + \tau_u \quad (304)$$

$$\frac{DR_f}{Dk} = -\tau_d \quad (305)$$

where τ_u is the "upstream" torsion of the flexible product entering the flip area. $\partial T/\partial k$ is zero assuming local steady state between the flip area and the downstream storage. DR_d/Dk is zero because of friction in the downstream storage. τ_u is zero because torsion has not had the time to build up so soon after the onset of flip.

Torque equilibrium is (M_{1f} standing for the flip torque)

$$M_{1f} \left(\frac{DR_f}{Dk} \right) = \cancel{M_1(\tau_u)} - M_1(\tau_d) \quad (306)$$

$$-M_{1f}(-\tau_d) = M_1(\tau_d) \quad (307)$$

which justifies Figure 94. $M_1(\tau_u)$ is zero early after the onset of flip.

D Flip torque transient close to downstream basket

We can write

$$\frac{\partial T}{\partial k} = \frac{\partial R_d}{\partial k} - \frac{\partial R_f}{\partial k} - b \frac{2\pi}{2\pi r} \quad (308)$$

$$\frac{\partial \mathcal{V}}{\partial k} = \frac{\cancel{DR_d}}{\cancel{Dk}} - \frac{DR_f}{Dk} - \tau_d + \cancel{\mathcal{V}_f} - \frac{b}{r} \quad (309)$$

$$\frac{DR_f}{Dk} = -\tau_d - \frac{b}{r} \quad (310)$$

where $b = +1$ for a positive basket and $b = -1$ for a negative basket.

Torque equilibrium is (M_{1f} standing for the flip torque)

$$M_{1f} \left(\frac{DR_f}{Dk} \right) = \cancel{M_1(\tau_u)} - M_1(\tau_d) \quad (311)$$

$$-M_{1f} \left(-\tau_d - \frac{b}{r} \right) = M_1(\tau_d) \quad (312)$$

E Stresses in the tensile armour

Single armor, tight direction

$$\sigma_{ij} = \lambda \delta_{ij} \varepsilon_{kk} + 2\mu \varepsilon_{ij} \quad (313)$$

$$\varepsilon_{ij} = \frac{1}{2\mu} \sigma_{ij} - \frac{\lambda}{2\mu(3\lambda + 2\mu)} \delta_{ij} \sigma_{kk} \quad (314)$$

$$E = \frac{1}{2} \varepsilon_{ij} \sigma_{ij} \quad (315)$$

$$= \frac{1}{4\mu} \sigma_{ij} \sigma_{ij} - \frac{\lambda}{4\mu(3\lambda + 2\mu)} \sigma_{kk} \sigma_{kk} \quad (316)$$

$$= \frac{1}{4\mu} (\sigma_{ij} \sigma_{ij} - \xi \sigma_{kk} \sigma_{kk}) \quad (317)$$

with

$$\xi = \frac{\lambda}{3\lambda + 2\mu} \quad (318)$$

$$= \frac{\lambda}{3K} \quad (319)$$

$$= \frac{\nu}{1 + \nu} \quad (320)$$

$$\approx 0.2308 \quad (321)$$

For a lay angle α and mean radius r , the tensile armor takes loads

$$M_1^t = xr \sin \alpha \quad (322)$$

$$R_1^t = x \cos \alpha \quad (323)$$

where x is the total tensile force in the direction of laying, carried by the layer. The remaining load to be taken up is thus

$$M_1^r = M_1 - xr \sin \alpha \quad (324)$$

$$R_1^r = R_1^w - x \cos \alpha \quad (325)$$

If we assume this load is taken up by a sheath of same radius r , then it induces stresses in the sheath

$$\sigma_{12} = \frac{1}{A} \left(\frac{M_1}{r} - x \sin \alpha \right) \quad (326)$$

$$\sigma_{11} = \frac{1}{A} (R_1^w - x \cos \alpha) \quad (327)$$

so that the elastic energy in the sheath is proportional to

$$E \propto \left(\frac{M_1}{r} - x \sin \alpha \right)^2 + (1 - \xi) (R_1^w - x \cos \alpha)^2 \quad (328)$$

$$= x^2 (\sin^2 \alpha + (1 - \xi) \cos^2 \alpha) - 2x \left(\frac{M_1}{r} \sin \alpha + (1 - \xi) R_1^w \cos \alpha \right) + \dots \quad (329)$$

$$= x^2 (1 - \xi \cos^2 \alpha) - 2x \left(\frac{M_1}{r} \sin \alpha + (1 - \xi) R_1^w \cos \alpha \right) + \dots \quad (330)$$

so that the energy in the sheath is minimum for

$$x = \frac{r^{-1} M_1 \sin \alpha + (1 - \xi) R_1^w \cos \alpha}{1 - \xi \cos^2 \alpha} \quad (331)$$

Here we minimize the energy in the sheath instead of the energy for the whole system. This is an approximation that is valid if most of the elastic energy is stored in the sheath, that is if the sheath is more compliant than the tensile armor. The advantage of this approximation is that it is not necessary to establish the stiffness of the rest of the components in the cross section.

The tension force in each tendon of the tensile armor is

$$R_t = \frac{x}{n_t} \quad (332)$$

where n_t is the tension in each tendon. Correspondingly, the axial stress in the tendons is

$$\sigma_{ax} = \frac{x}{a_t n_t} \quad (333)$$

where a_t is the cross section area of each tendon.

Double armor, contact between armors This case includes the situations where the inner armor is tight against, or lifts from, the inside of the flexible product.

In this case, the inner armor gets in compression, and contacts the outer armor, which is in tension. As simple analysis can be obtained by considering the stiffness to be dominated by the contributions from both armors.

The inner and outer layer have mean radius, lay angle, tendon cross section and number of tendons r_i , α_i , a_i , n_i and r_o , α_o , a_o , n_o . If the axial stress in each layer is σ_i and σ_o respectively, then the axial force and moment for the flexible product are

$$M_1 = A \sigma_i + B \sigma_o \quad (334)$$

$$R_1 = C \sigma_i + D \sigma_o \quad (335)$$

with

$$A = r_i n_i a_i \sin \alpha_i \quad (336)$$

$$B = r_o n_o a_o \sin \alpha_o \quad (337)$$

$$C = n_i a_i \cos \alpha_i \quad (338)$$

$$D = n_o a_o \cos \alpha_o \quad (339)$$

We compute

$$\Delta = AD - BC \quad (340)$$

and get

$$\sigma_i = \frac{D}{\Delta} M_1 - \frac{B}{\Delta} R_1 \quad (341)$$

$$\sigma_o = -\frac{C}{\Delta} M_1 + \frac{A}{\Delta} R_1 \quad (342)$$

F Herniation buckling

The failure mode involves an armor layer herniating outwards through either a layer of yarn or through another layer of tensile armor. The two layers involved will be referred to as the inner and outer layers, respectively.

The width of the largest possible gap in the outer layer (in the direction orthogonal to the threads of the outer layer), is

$$G = c (2\pi R_o \cos \alpha_o - n_o w_o) \quad (343)$$

where R_o is the mean radius of the outer layer, n_o is the number of threads in the outer layer, w_o is the width of each thread in the outer layer and α_o the lay angle in the outer layer. $c = 1.2$ if the outer layer is a tensile layer and $c = 2$ if it is a yarn layer.

The half length of thread of the inner layer, exposed under the gap is

$$L = \frac{G}{2 \sin (|\alpha_i - \alpha_o|)} \quad (344)$$

where α_i and α_o are the lay angle of the inner and outer layers. If the layers are laid in opposite directions, then α_i and α_o must be of opposite signs. This length corresponds to an angle around the helix

$$\beta = \frac{L \sin \alpha_i}{R_i} \quad (345)$$

We consider a reference system centered on the axis of the flexible, with \bar{e}_1 parallel to this axis, and \bar{e}_2 pointing towards the middle of the gap. The point on the inner thread at the middle of the gap has coordinates

$$\bar{P}_1 = [0, R_i, 0] \quad (346)$$

A point on the same thread at the border of the gap has coordinates

$$\bar{P}_2 = [L \cos \alpha_i, R_i \cos \beta, R_i \sin \beta] \quad (347)$$

We define

$$\bar{\Delta} = \bar{P}_2 - \bar{P}_1 \quad (348)$$

$$= [L \cos \alpha_i, R_i (\cos \beta - 1), R_i \sin \beta] \quad (349)$$

As the thread herniates, these points move in the directions

$$\bar{D}_1 = [0, 1, 0] \quad (350)$$

$$\bar{D}_2 = [\cos \alpha_i, 0, \sin \alpha_i] \quad (351)$$

by amounts d_1 and d_2 respectively. After displacement, the distance between the points is

$$d^2 = \sum_i (\Delta^i + D_2^i d_2 - D_1^i d_1)^2 \quad (352)$$

$$\approx \sum_i (\Delta^{i2} + 2\Delta^i (D_2^i d_2 - D_1^i d_1)) \quad (353)$$

So for the displacements to preserve the distance to the first order, we thus require

$$\bar{\Delta} \cdot \bar{D}_1 d_1 = \bar{\Delta} \cdot \bar{D}_2 d_2 \quad (354)$$

$$R_i (\cos \beta - 1) d_1 = (L \cos^2 \alpha_i + R_i \sin \beta \sin \alpha_i) d_2 \quad (355)$$

$$d_1 = B d_2 \quad (356)$$

with

$$B = \frac{L \cos^2 \alpha_i + R_i \sin \beta \sin \alpha_i}{R_i (\cos \beta - 1)} \quad (357)$$

The new vector between the points is

$$\bar{\Delta}^* = \bar{\Delta} + \bar{D}_2 d_2 - \bar{D}_1 d_1 \quad (358)$$

$$= \bar{\Delta} + (\bar{D}_2 - B \bar{D}_1) d_2 \quad (359)$$

The angle between these vectors is, to the first order

$$\gamma = \frac{|\bar{\Delta}^* \times \bar{\Delta}|}{|\bar{\Delta}^*| |\bar{\Delta}|} \quad (360)$$

$$\approx C d_2 \quad (361)$$

with

$$C = \frac{|(\bar{D}_2 - B \bar{D}_1) \times \bar{\Delta}|}{|\bar{\Delta}| |\bar{\Delta}|} \quad (362)$$

C is the angle of bending at the joint near the edge of the gap, per unit of sliding at the edge of the gap.

If the threads of the inner layer have rectangular cross section, the plastic-hinge moment of a thread is calculated as

$$M_p = \frac{1}{4} w_i t_i^2 \sigma_{yi} \quad (363)$$

where σ_{yi} is the specified minimum yield strength of the inner layer, and t_i the thickness of the inner layer. If the threads are circular,

$$M_p = \frac{1}{6} t_i^3 \sigma_{yi} \quad (364)$$

The energy dissipated by the hinges is $M_p 4C d_2$ while the work on the part of the thread in the gap is $2F d_2$ where F is the axial force in the thread. Hence instability arises when

$$F_i > 2M_p C \quad (365)$$

For a flexible product subjected to torsion only (no axial compression or bending), and with forces borne exclusively by the inner and outer layer:

$$F_o n_o \cos \alpha_o + F_i n_i \cos \alpha_i = 0 \quad (366)$$

so that

$$F_o = -\frac{F_i n_i \cos \alpha_i}{n_o \cos \alpha_o} \quad (367)$$

The torque born by the two layers together is

$$T = R_o F_o n_o \sin \alpha_o + R_i F_i n_i \sin \alpha_i \quad (368)$$

G Inward radial buckling

The work needed to displace a 90° hinge (which implies bending thread reached by the hinge and straightening thread left by the hinge) by a distance δ is

$$W = \pi M_p \frac{\delta}{\mathbf{t}} = -\delta \mathbf{a} \sigma_1 \quad (369)$$

where \mathbf{t} is used as a characteristic of the longitudinal extent of the plastic hinge. In reality, the longitudinal extent will depend on the wire cross section and the work hardening of the material.

This leads to

$$\sigma_{1c} = -\pi \frac{M_p}{\mathbf{t} \mathbf{a}} \quad (370)$$

For a rectangular cross section this gives

$$\sigma_{1c} = -\frac{\pi}{4} \sigma_y \quad (371)$$

and for a circular one

$$\sigma_{1c} = -\frac{2}{3} \sigma_{yi} \quad (372)$$

The details of the constant in front of σ_y depend on the (arbitrary) choice of the distance (here taken as \mathbf{t}) over which plastic work is equal to πM_p , hence the actual uncertainties are quite large, and testing or FEM analysis would be required. For circular threads, lateral buckling would always occur first.

H Skew kinking

H.1 Assessing M_p

Let M_p be the plastic moment, per unit length, of a longitudinal plastic joint in the pipe wall. The work needed to squash a unit length of the pipe (with four plastic joints) is

$$W_m = 4 \frac{\pi}{2} M_p = 2\pi M_p \quad (373)$$

which allows to assess M_p based on a squash test.

H.2 Energy dissipation

We assume that under skew kinking, each originally circular cross section will develop four hinges. Two will be the skew hinges, and two will be longitudinal hinges. The hinges will have deformed with the following angles

1. Two skew hinges with angles $\alpha_1 = \frac{\pi}{2} + \gamma$ and $\alpha_2 = \frac{\pi}{2} - \gamma$ (Figure 114), where γ is the angle of relative rotation of the segments on both sides of the skew hinge. Each hinge is of length L , and at an angle β with the axis of the pipe.
2. Two longitudinal hinges with angles α_3 and α_4 with $\alpha_3 + \alpha_4 = \pi$. Each hinge is of length $L |\cos \beta|$.

The hinge length L is related to the pipe diameter (conservatively) by

$$L |\sin \beta| = \pi R \quad (374)$$

Neglecting membrane energy and the energy stored in elastic deformation, assuming M_p is not affected by β , and noting c and s for $\cos \beta$ and $\sin \beta$, the energy absorbed in the hinges is

$$W_r = M_p L (\alpha_1 + \alpha_2 + \alpha_3 |c| + \alpha_4 |c|) \quad (375)$$

$$= M_p L \pi (1 + |c|) \quad (376)$$

$$= M_p \pi^2 R \frac{1 + |c|}{|s|} \quad (377)$$

H.3 Available energy and critical β (pure torsion)

Assuming that this deformation is driven by torque T , the work is

$$W_d = T \gamma \cos \beta \quad (378)$$

For $B = 0$, the critical value of β is that which maximizes W_d/W_r , or equivalently, maximizes

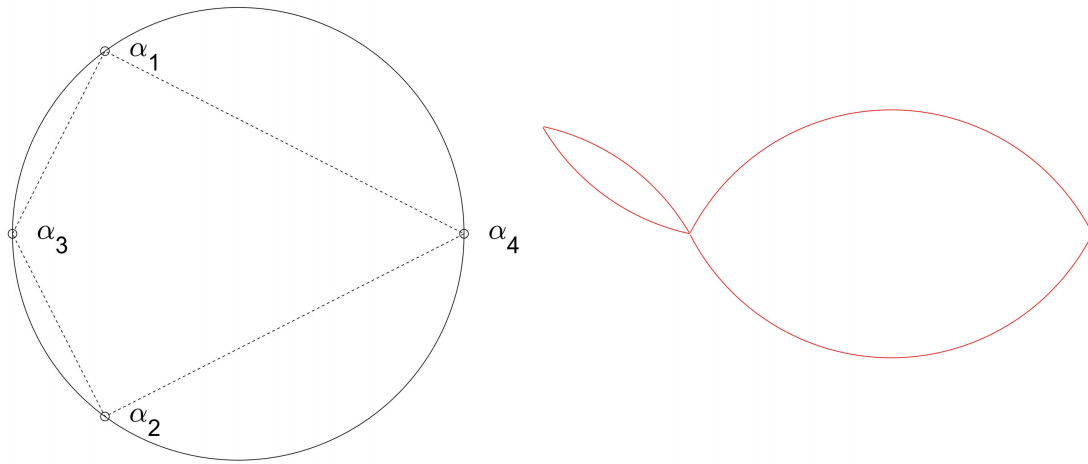


Figure 114: Skew-kinking hinges

$$f(\beta) \triangleq \frac{|s|c}{1+|c|} \quad (379)$$

For $\beta \in [0, \pi/2]$, $s = |s|$ and $c = |c|$. Over that interval:

$$\frac{\partial f}{\partial \beta} = 0 = \frac{(c^2 - s^2)(1+c) + s^2c}{(1+c)^2} \quad (380)$$

$$0 = (2c^2 - 1)(1+c) + (1-c^2)c \quad (381)$$

$$0 = c^3 + 2c^2 - 1 \quad (382)$$

$$0 = (c+1) \left(c - \frac{-1+\sqrt{5}}{2} \right) \left(c - \frac{-1-\sqrt{5}}{2} \right) \quad (383)$$

$$c = \frac{\sqrt{5}-1}{2} \quad (384)$$

$$\beta = \arccos c \approx 52^\circ \quad (385)$$

For this critical angle, and choosing $\gamma = \pi/2$ (a large value leads to lower critical load)

$$T_c = \frac{\pi^2 M_p R}{\gamma} \frac{1+c}{\sqrt{1-c^2} c} \quad (386)$$

$$= W_m R \frac{1+c}{\sqrt{1-c^2} c} \quad (387)$$

$$\approx W_m R 3.843... \quad (388)$$

$$> 2W_m R \quad (389)$$

I Helical buckling

I.1 Stability condition

See [20, 2].

The equilibrium of a straight beam (following axis \bar{e}_1) under constant tension can be written

$$\frac{\partial \bar{M}}{\partial s} + \frac{\partial \bar{x}}{\partial s} \times \bar{R} = \bar{0} \quad (391)$$

$$\bar{M} + \bar{x} \times \bar{R} = \bar{0} \quad (392)$$

$$EI\kappa\bar{f}_3 + M_1\bar{f}_1 + \bar{x} \times \bar{R} = \bar{0} \quad (393)$$

where \bar{f}_i form an orthonormal base where \bar{f}_1 is tangent and \bar{f}_3 points inside the curvature. This leads to

$$EI \frac{\partial^2 x_2}{\partial s^2} + M_1 \frac{\partial x_3}{\partial s} - x_2 R_1 = 0 \quad (394)$$

$$EI \frac{\partial^2 x_3}{\partial s^2} - M_1 \frac{\partial x_2}{\partial s} - x_3 R_1 = 0 \quad (395)$$

which, by introducing $x = x_2 + ix_3$ can be written

$$EI \frac{\partial^2 x}{\partial s^2} - iM_1 \frac{\partial x}{\partial s} - xR_1 = 0 \quad (396)$$

We are looking for solutions of the form $x = X \exp ibs$ where b is an angular wave number. Replacing in the above and dividing by $\exp ibs$ leads to

$$(EIb^2 - M_1 b + R_1) X = 0 \quad (397)$$

which has non-trivial solutions iff

$$EIb^2 - M_1 b + R_1 = 0 \quad (398)$$

which is achieved for

$$b_{1,2} = \frac{M_1 \pm \sqrt{M_1^2 - 4R_1 EI}}{2EI} \quad (399)$$

allowing general solutions of the form

$$x = X^1 \exp ib_1 s + X^2 \exp ib_2 s \quad (400)$$

1.2 Hinged boundaries

If the boundary conditions are hinged at $s = 0$ and $s = L$ then

$$X^1 + X^2 = 0 \quad (401)$$

$$X^1 \exp ib_1 L + X^2 \exp ib_2 L = 0 \quad (402)$$

This system of equation has non-zero roots iff

$$\exp ib_1 L = \exp ib_2 L \quad (403)$$

$$b_1 - b_2 = n \frac{2\pi}{L} \quad (404)$$

$$\frac{\sqrt{M_1^2 - 4R_1 EI}}{EI} = n \frac{2\pi}{L} \quad (405)$$

$$\left(\frac{M_1}{M_1^0}\right)^2 - \frac{R_1}{R_1^0} = n^2 \quad (406)$$

with

$$M_1^0 = \frac{2\pi EI}{L} \quad (407)$$

$$R_1^0 = \frac{\pi^2 EI}{L^2} \quad (408)$$

We arbitrarily chose $b_1 \geq b_2$. For $n = 0$ it is not possible to satisfy the boundary conditions. The lowest critical loads are for $n = 1$.

The buckling shape is thus of the form

$$x = \frac{X}{2i} (\exp ib_1 s + \exp ib_2 s) \quad (409)$$

$$= X \exp\left(i \frac{b_1 + b_2}{2} s\right) \sin\left(\frac{b_1 - b_2}{2} s\right) \quad (410)$$

$$= X \exp\left(i \frac{M_1}{2EI} s\right) \sin\left(n \frac{2\pi}{L} s\right) \quad (411)$$

Hence, for a given torque M_1 , the pitch length of helical buckling is

$$L_p = \frac{4\pi EI}{M_1} \quad (412)$$

and the critical tension is

$$R_1 = R_1^0 \left(\left(\frac{M_1}{M_1^0}\right)^2 - 1 \right) \quad (413)$$

Considering Eq. 406, for a given torque M_1 , the required tension becomes zero when the spacing be between support verifies

$$M_1 < M_1^0 \quad (414)$$

$$L < 2\pi \frac{EI}{M_1} \quad (415)$$

1.3 Infinite domain

Roots b_1 and b_2 are real iff the determinant $M_1^2 - 4R_1EI \geq 0$. As loads evolve from a stable situation, an unstable situation will first be encountered for a zero determinant, so that

$$M_1^2 = 4R_1EI \quad (416)$$

$$b_1 = b_2 = \frac{M_1}{2EI} \quad (417)$$

$$= \sqrt{\frac{R_1}{EI}} \quad (418)$$

so that

$$x = X \exp\left(i \frac{M_1}{2EI} s\right) \quad (419)$$

The corresponding pitch length is still

$$L_p = \frac{4\pi EI}{M_1} \quad (420)$$

J Multilingual glossary

Table 4 provides translation of key technical terms in selected languages.

English	Norwegian	French
Roll	Rull	Rouli
Spatial roll rate	Romlig rull rate	Taux de rouli spatial
Material roll rate	Materiell rull hastighet	Taux de rouli matériel
Link	Lenke	Liage
Twist	Tvist	Torsade
Writhe	Vridning	Vrille
Torsion	Torsjon	Torsion
Torque, torsional moment	Torsjonsmoment, dreiemoment	Moment de torsion

Table 4: Translation of some technical terms

K Literature review of failure modes

K.1 Local failure modes

K.1.1 Lateral buckling of tensile armor

Numerous research efforts have addressed tensile armor lateral buckling of flexible pipes subjected to dynamic bending during operation. This is because flexible pipes may be exposed to significant negative wall tension in empty condition in deep waters. The lateral buckling mode was first described in 1997 [38]. Since then, experimental work included laboratory mechanical tests without radial pressure, as well as costly full-scale deep immersion performance tests, and laboratory pressure chamber tests [6, 3, 58, 63]. The tests results showed that the driving mechanism is cyclic bending that reduces the friction and gives accumulation of wire transverse slip, which at a certain stage results in lateral buckling. Novitsky and Sertã [34] pointed out that the buckling process differs for dry and wet annulus conditions. The buckling process seems to be primarily elastic if the tensile armor is exposed to sea water, whereas severe plastic deformations typically occur for the dry annulus condition since friction then plays a more important role.

Vaz and Rizzo [65] created a computationally light finite element model by utilizing a single wire approach for each tensile armor layer in a flexible pipe. A pure external pressure load condition was applied for varying interlayer friction for the tensile armor. They identified two lateral and two birdcaging buckling modes dependent on the amount of friction and the strength of the anti-buckling tape. Yang et al. [69] created a similar model with an improved interlayer contact modelling and curved beam elements for the tensile armor wires. Their results confirmed the findings of Vaz and Rizzo.

Østergaard et al. [38, 40, 41, 42] conducted mechanical tests for the wet annulus condition of flexible pipes, and developed a numerical frictionless single wire model. As expected, the model predicted lower bound buckling loads due to frictionless assumption. The numerical model was extended to account for friction [39], but due to unresolved issues it was not possible to conclude that wire friction imposed a significant influence on the mode of deformation and the load carrying ability [38].

Sævik and Thorsen [53] proposed an analytical model for the lateral buckling mode accounting for wire friction. They simulated the buckling response by means of tailor-made finite elements and found that their analytical model over-predicted the capacity both for static and cyclic curvature. Sævik and Ji [51] developed a new frictionless analytical model. The model was shown to agree well with the frictionless numerical model developed by Østergaard [38], and had as expected an inherent safety margin in the range of 2 when compared against the Østergaard tests. They also performed numerical simulations using the BFLEX software and predicted the same failure and no failure cases as the Østergaard tests. The frictionless analytical model and the test comparison are also presented in work by Sævik and Thorsen [54] which in addition deals with the birdcaging failure mode. The frictionless analytical model is strongly related to the periodic buckling mode that was considered in later work by Li et

al. [26]. In fact, these models are identical if the buckling length is set equal to half the wire length in a pitch, instead of conservatively assuming infinite buckling length as proposed by Sævik and Ji [51].

Zhou et al. [70] studied the effect of the anti-buckling tape on the lateral buckling behavior. They found that the tape lay angle direction should be the same as applied for the outer tensile armor layer, and that a smaller lay angle will perform better than a larger lay angle.

Paiva and Vaz [43] formulated a frictionless numerical model based on the Østergaard model [38]. They validated the model against experiments and applied symbolic regression to derive an empirical equation for the compressive failure load.

Li et al. [23] developed a frictionless analytical model similar to the model presented by Sævik and Thorsen [54]. They extended the work by distinguishing between a global and a periodic buckling mode in Ref. [26], where the global mode was identical to the one in Ref. [23]. The periodic buckling mode was shown to be in good agreement with the Østergaard tests [38] and to reduce the conservatism compared to the global mode. The effect of cyclic bending was considered in later work [24] and was shown to result in the same critical load as for the frictionless periodic buckling mode in Ref. [23]. Li et al. [25] extended the analytical work by considering the effect of wire axial rotation constraint and presented an analytical equation for the compressive failure load of circular tensile armor wires.

It is important to note that for the torsion-induced failures studied in this handbook, the loading, lateral friction behavior and triggering mechanisms can differ from what has been addressed in previous research. Further, the loading in previous research has consisted of axial compression and external radial pressure. For such loads, the inner tensile armor layer is more susceptible to buckling since it has less radius, a lower number of wires and may have less transverse friction resistance. For torque loading, the lateral buckling mode may equally well occur for the outer tensile armor layer.

In handling operations, the product is typically exposed to only a few bending cycles, while many hundred or thousands of cycles were needed to trigger the buckling process in previous research. Application of the models formulated in previous research may thus yield overly conservative predictions. The tensile armor of power cables and umbilicals are often smeared with corrosion coating with a highly temperature-dependent viscosity, which increases the friction resistance at low temperatures and may function as a lubricant at high temperatures. These aspects motivate development of a new analytical model applicable for a limited number of bending cycles that accounts for interlayer friction. This will require validation against experiments with dry annulus condition, possible at varying temperature. However, most of the available tests for flexible pipes have been performed for wet annulus condition.

The previous research has focused on flexible pipes with anti-buckling tape and rectangular tensile armor wires. As of today, there are no experimental tests for circular tensile armor wires that can be used for validation [25]. Umbilicals and power cables do not have anti-buckling tape, and may thus display a more pronounced interaction with the external polymer layer.

K.1.2 Birdcaging

The first known incident of birdcaging failure occurred in 1977 for a flexible pipe operating at 1700m water depth [6]. In 1989, the failure mode was recognized as a potential failure for damaged external sheaths at large water depth [3]. The failure is well known by flexible pipe producers and is described in design codes [1]. Birdcaging failures for flexible pipes may be avoided by ensuring that the anti-buckling tape layer has sufficient strength.

Vaz and Rizzo [65] performed finite element simulations with pure external pressure loading. They found that birdcaging failure could take place as anti-buckling tape failure and radial buckling on an elastic foundation.

A detailed finite element model of a 2.5m flexible pipe with almost 400 000 degrees of freedom was created by de Sousa et. al [12]. They performed full-scale laboratory tests focusing on failure of the anti-buckling tape in axial compression without radial pressure. The numerical model was shown to predict birdcaging failure with good accuracy compared to the laboratory tests.

Rabelo et al. [44] investigated whether birdcaging failure could be triggered by instabilities of the external sheath. They studied previous birdcaging experimental observations and concluded that strong evidences of validity were obtained for their hypothesis.

Sævik and Thorsen [53] developed an analytical model for birdcaging of flexible pipes based on separate treatment of anti-buckling tape failure and radial buckling of a straight beam on an elastic foundation. The analytical model was shown to agree fairly well with simulations based on tailor-made finite elements. In more recent work [54], they improved the analytical model by using curved beam theory and proposed a capacity interaction formula considering anti-buckling tape failure, radial elastic buckling and wire yielding. They reported that the curved beam approach gave the best fit when compared against the de Sousa tests [12], whereas the straight beam assumption was on the conservative side.

Regarding use in this handbook, the analytical model proposed by Sævik and Thorsen [54] is applicable for flexible pipes with anti-buckling tape and an external sheath. Although they considered only pure axial compression, their analytical model should be valid also for flexible pipes subjected to torque loading which compresses the outer tensile armor layer. The main concern regarding validity is the radial stiffness contribution from the supporting layers. For instance, a power cable or an umbilical with an outer layer consisting of wound polypropylene yarns provides far less support against radial outward displacements. Using the analytical model in a different application without sufficient experimental validation may be questionable, as also indicated by Sævik and Thorsen [54] in view of the limited available test data for birdcaging failure.

K.1.3 Other local failure modes

Wu et al. [67] recently addressed tensile armor failure of flexible pipes subjected to large torsion. Based on knowledge of existing failure modes they identified wire yielding, birdcaging

and core collapse as potential failures. Regarding the critical collapse pressure of flexible pipes, an extensive literature review is available in recent work by Li et al. [22].

As of 2022, there exist presently no research in the open literature addressing the herniation buckling mode in Section 20.4 and the skew kinking failure in Section 10.2. The reason may be that these failure modes are specific to torsional loads, and thus not encountered in normal operating conditions. The failure modes may also be wrongly attributed to excessive bending or birdcaging. Nevertheless, it is clear that new criteria must be developed to cover the skew kinking and herniation buckling failure modes.

K.2 Global failure modes

K.2.1 Loop formation and kinking

A criterion for loop formation was first presented by Greenhill in 1883 [20] who studied the mechanics of ship propeller shafts. Loop formation problems of cables for oceanic applications have since then been studied by numerous authors. Liu [27] performed kinking tests of electromechanical cables with tensile armor that was compared against Greenhill's equation for infinite cable lengths. These and other test results were reviewed by Rosenthal [45, 46] who concluded that long straight cables subjected to tension and torque will become unstable according to Greenhill's equation modified by an appropriate safety factor. Ross [47] used energy considerations and found that loop formation could occur for twice the critical tension predicted by Greenhill's equation.

Yabuta [68] addressed loop formation and subsequent kinking by considering the potential energy of an assumed helical deformation pattern. He derived a criterion for maximum allowable slack for avoiding loop formation and a criterion for re-opening the loop when the cable is re-tensioned, Yabuta validated the theoretical results against experiments and concluded that the cable kinking phenomenon is governed by initial slack, initial torsion, cable diameter and the ratio of bending stiffness to torsional stiffness.

Coyne [11] used equilibrium equations to find an expression for the axial end-shortening in the loop formation problem. The end-shortening was applied to derive a criterion for the maximum allowable slack before loop formation occurs and an expression for re-opening the loop. Expressions for the required tension and the maximum curvature at re-opening was presented. Coyne concluded that the prediction of loop formation was in agreement with Ross' work [47] and existing experiments, but the loop re-opening criterion deviated when compared against a single experimental data set.

Thompson and Champneys [64] conducted experiments and mathematical analysis of the energetically preferred post-buckling mode, to gain insight about the localized loop formation in Coyne's work [11]. Champney and Thompson later applied an analytical approach based on Cosserat beam theory to show that the critical torque and tension predicted by Greenhill's equation is reasonable for small initial curvature, but becomes non-conservative for large initial curvature.

Ermolaeva et al. [16] performed loop formation experiments of wire ropes at zero tension and low tension. Their work showed that Yabuta's criterion for slack was non-conservative, and that the slack criteria proposed by Ross [47] and Coyne [11] were conservative. For low tension, they found that Greenhill's equation with a safety factor of 2 was reasonable.

Gay Neto and Martins [33] conducted parametric studies of loop formation for catenary risers using a geometrically-exact beam model including seabed frictional contact. They developed an empirical correction factor for Greenhill's equation dependent on the tension at the touchdown point before loop formation, the bending stiffness and the submerged weight. For very low values of tension, the empirical correction factor may give overly conservative predictions due to the large relative increase of tension during the loop formation process.

Sævik and Koloshkin [52] re-constructed the riser model of Gay Neto and Martins [33], and incorporated the effect of tension-torsion coupling and applied a non-linear bending moment model to account for internal friction of the tensile armor layers. In dynamic applications, they found that it was more conservative to apply the linear-elastic bending model for low utilization with respect to loop formation, and that non-linear bending models gave the most conservative predictions for high utilization. They also proposed to apply the maximum curvature predicted in quasi-static analysis at the onset of instability as a curvature criterion for avoiding kinking deformation in dynamic applications. Later, Opgård [35] reported that the maximum curvature criterion could fail to detect formation of loops with smaller curvature than those expected from the quasi-static analysis. This underlines that prediction of loop formation in dynamic applications is a complex task.

Regarding relevance to the present work, the analytical formulae proposed by Gay Neto and Martins [33] for loop formation is applicable when the tension is not too low. For low tension, it may be necessary to apply numerical simulation to avoid too conservative capacity predictions. Further, it will be challenging to account for dynamic motions, and internal friction which may result in both conservative and non-conservative predictions in time-domain simulations [52, 35].

L Example route geometry

The following provides the X, Y and Z coordinates (3 columns) of points along a loadout route (406 rows). The table starts upstream (on-shore turntable) and ends downstream (on-board basket).

-2.2213485025	-21.4683521540	0.0000000000
-2.2686090947	-21.6135858499	0.0000000000
-2.3203197209	-21.7572912550	0.0000000418
-2.3764200575	-21.8993304808	0.0000003832
-2.4368401969	-22.0395675212	0.0000019699
-2.5015016638	-22.1778689876	0.0000070528
-2.5703182333	-22.3141050374	0.0000196902
-2.6431972684	-22.4481501662	0.0000461149
-2.7200411214	-22.5798836439	0.0000949026
-2.8007488565	-22.7091899057	0.0001769108
-2.8852183576	-22.8359590511	0.0003049600
-2.9733483380	-22.9600868915	0.0004932440
-3.0650404386	-23.0814748503	0.0007564779
-3.1602013937	-23.2000298294	0.0011088314
-3.2587447715	-23.3156635922	0.0015626568
-3.3605925212	-23.4282919798	0.0021270463
-3.4656762803	-23.5378340571	0.0028063222
-3.5739379460	-23.6442108382	0.0035985536
-3.6853297418	-23.7473439009	0.0044942158
-3.7998137870	-23.8471539960	0.0054750942
-3.9173607866	-23.9435594219	0.0065135084
-4.0379481959	-24.0364744702	0.0075719634
-4.1615578893	-24.1258080392	0.0086033286
-4.2881730053	-24.2114622567	0.0095516240
-4.4177744297	-24.2933313970	0.0103534623
-4.5503370472	-24.3713011732	0.0109401399
-4.6858255654	-24.4452482928	0.0112403739
-4.8241904318	-24.5150405016	0.0111836476
-4.9653639272	-24.5805371431	0.0107040925
-5.1092562735	-24.6415901349	0.0097448058
-5.2557523534	-24.6980455048	0.0082624509
-5.4047090972	-24.7497454471	0.0062319710
-5.5559533858	-24.7965307891	0.0036512373
-5.7092809780	-24.8382438993	0.0005454565
-5.8644563560	-24.8747319358	-0.0030288525
-6.0212133577	-24.9058504628	-0.0069807448
-6.1792567864	-24.9314665812	-0.0111815619
-6.3382651244	-24.9514624567	-0.0154630737
-6.4978944457	-24.9657395726	-0.0196179318

-6.6577833947	-24.9742222292	-0.0234005979
-6.8175587632	-24.9768605629	-0.0265293938
-6.9768413763	-24.9736330270	-0.0286897712
-7.1352524556	-24.9645482356	-0.0295387516
-7.2924198782	-24.9496461307	-0.0287104320
-7.4479840374	-24.9289984097	-0.0258224176
-7.6016034533	-24.9027081576	-0.0204829911
-7.7529595327	-24.8709087584	-0.0122988173
-7.9017602984	-24.8337621108	-0.0008829471
-8.0477433202	-24.7914561474	0.0141371301
-8.1906773220	-24.7442018578	0.0331116189
-8.3303624851	-24.6922299112	0.0563609753
-8.4666298216	-24.6357869133	0.0841691124
-8.5993392312	-24.5751316249	0.1167774198
-8.7283764633	-24.5105312961	0.1543798048
-8.8536495010	-24.4422582824	0.1971188837
-8.9750840437	-24.3705871643	0.2450835518
-9.0926184042	-24.2957941395	0.2983082368
-9.2061982885	-24.2181556629	0.3567741312
-9.3157711851	-24.1379456032	0.4204124856
-9.4212809468	-24.0554337648	0.4891094014
-9.5226631757	-23.9708848521	0.5627118446
-9.6198411459	-23.8845584000	0.6410348679
-9.7127227203	-23.7967088048	0.7238694627
-9.8011987356	-23.7075851557	0.8109907639
-9.8851424611	-23.6174312816	0.9021663248
-9.9644104621	-23.5264856226	0.9971639093
-10.0388451456	-23.4349804999	1.0957585632
-10.1082784164	-23.3431412642	1.1977384890
-10.1725366015	-23.2511848965	1.3029094981
-10.2314467039	-23.1593177590	1.4110977824
-10.2848432726	-23.0677331034	1.5221508060
-10.3325758876	-22.9766079738	1.6359363060
-10.3745171455	-22.8860993690	1.7523393320
-10.4105704123	-22.7963403719	1.8712574832
-10.4406772476	-22.7074360396	1.9925944904
-10.4648243191	-22.6194590042	2.1162524437
-10.4830491700	-22.5324456103	2.2421229966
-10.4954447784	-22.4463924171	2.3700779456
-10.5021627970	-22.3612531002	2.4999596619
-10.5034150768	-22.2769365752	2.6315718064
-10.4994734602	-22.1933060904	2.7646708245
-10.4906677891	-22.1101792892	2.8989586544
-10.4773818629	-22.0273299089	3.0340770692
-10.4600478463	-21.9444908315	3.1696040036
-10.4391397140	-21.8613585002	3.3050521389

-10.4151657538	-21.7775990414	3.4398699464
-10.3886596368	-21.6928554396	3.5734452695
-10.3601701948	-21.6067554887	3.7051114399
-10.3302466411	-21.5189208013	3.8341558119
-10.2994260797	-21.4289766206	3.9598304855
-10.2682279793	-21.3365622554	4.0813649305
-10.2371471150	-21.2413415498	4.1979800902
-10.2066447854	-21.1430126179	4.3089035498
-10.1771410847	-21.0413166676	4.4133852178
-10.1490082817	-20.9360456014	4.5107130503
-10.1225653889	-20.8270481971	4.6002282607
-10.0980758375	-20.7142341937	4.6813394125
-10.0757452598	-20.5975771117	4.7535349338
-10.0557186860	-20.4771161199	4.8163934065
-10.0380809654	-20.3529556128	4.8695916077
-10.0228592742	-20.2252627220	4.9129101734
-10.0100268325	-20.0942630721	4.9462366957
-9.9995079034	-19.9602349102	4.9695662591
-9.9911838135	-19.8235019012	4.9829992788
-9.9848997517	-19.6844244214	4.9867368487
-9.9804720911	-19.5433899735	4.9810737031
-9.9776959710	-19.4008041437	4.9663892016
-9.9763529041	-19.2570812731	4.9431364465
-9.9762181294	-19.1126338750	4.9118299217
-9.9770674661	-18.9678623481	4.8730321773
-9.9786835064	-18.8231456172	4.8273399499
-9.9808609913	-18.6788325945	4.7753703423
-9.9834112810	-18.5352349848	4.7177473251
-9.9861658323	-18.3926215712	4.6550891502
-9.9889786189	-18.2512139205	4.5879969604
-9.9917275179	-18.1111835597	4.5170450423
-9.9943147281	-17.9726506841	4.4427729074
-9.9966663263	-17.8356843686	4.3656792879
-9.9987310654	-17.7003041885	4.2862182798
-10.0004785049	-17.5664830790	4.2047975249
-10.0018966269	-17.4341512922	4.1217784787
-10.0029891095	-17.3032012264	4.0374784911
-10.0037724137	-17.1734929393	3.9521745721
-10.0042728560	-17.0448601064	3.8661085324
-10.0045237505	-16.9171161813	3.7794931208
-10.0045627095	-16.7900605815	3.6925189343
-10.0044292319	-16.6634846657	3.6053616363
-10.0041626433	-16.5371773756	3.5181891979
-10.0038004375	-16.4109303807	3.4311687671
-10.0033770072	-16.2845424716	3.3444731052
-10.0029229716	-16.1578239247	3.2582851636

-10.0024646517	-16.0305996120	3.1728022104
-10.0020234713	-15.9027107159	3.0882397320
-10.0016157066	-15.7740163629	3.0048331149
-10.0012525570	-15.6443947602	2.9228378295
-10.0009404774	-15.5137437988	2.8425282531
-10.0006817191	-15.3819811555	2.7641952039
-10.0004750207	-15.2490439835	2.6881423735
-10.0003163947	-15.1148882558	2.6146818146
-10.0001999504	-14.9794878323	2.5441287227
-10.0001186968	-14.8428333365	2.4767957569
-10.0000652802	-14.7049308990	2.4129871390
-10.0000326153	-14.5658008264	2.3529927960
-10.0000143781	-14.4254762571	2.2970827862
-10.0000053418	-14.2840018297	2.2455022281
-10.0000015464	-14.1414323860	2.1984669284
-10.0000002988	-13.9978317139	2.1561598676
-10.0000000260	-13.8532712888	2.1187286197
-10.0000000000	-13.7078288877	2.0862837844
-10.0000000000	-13.5615872543	2.0588983001
-10.0000000000	-13.4146311987	2.0366074644
-10.0000000000	-13.2670463610	2.0194093733
-10.0000000000	-13.1189198590	2.0072657601
-10.0000000000	-12.9703399252	2.0001036693
-10.0000000000	-12.8213952506	1.9978179002
-10.0000000000	-12.6721739788	2.0002739390
-10.0000000000	-12.5227629038	2.0073114831
-10.0000000000	-12.3732468075	2.0187483695
-10.0000000000	-12.2237078200	2.0343846666
-10.0000000000	-12.0742248102	2.0540069487
-10.0000000000	-11.9248728717	2.0773925415
-10.0000000000	-11.7757228115	2.1043136592
-10.0000000000	-11.6268407088	2.1345413153
-10.0000000000	-11.4782874910	2.1678488448
-10.0000000000	-11.3301185437	2.2040150468
-10.0000000000	-11.1823833765	2.2428267972
-10.0000000000	-11.0351253002	2.2840811391
-10.0000000000	-10.8883811689	2.3275868610
-10.0000000000	-10.7421811364	2.3731654913
-10.0000000000	-10.5965484970	2.4206518170
-10.0000000000	-10.4514996116	2.4698938543
-10.0000000000	-10.3070438978	2.5207524225
-10.0000000000	-10.1631837670	2.5731003559
-10.0000000000	-10.0199145858	2.6268213949
-10.0000000000	-9.8772250457	2.6818089052
-10.0000000000	-9.7350978522	2.7379643826
-9.9999999954	-9.5935103051	2.7951960404

-9.9999993318	-9.4524345558	2.8534176056
-9.9999960091	-9.3118378543	2.9125472035
-9.9999863516	-9.1716830978	2.9725063835
-9.9999639668	-9.0319296601	3.0332195185
-9.9999191194	-8.8925341403	3.0946132223
-9.9998387515	-8.7534511129	3.1566157385
-9.9997064358	-8.6146340873	3.2191565019
-9.9995030555	-8.4760360992	3.2821655255
-9.9992079281	-8.3376101601	3.3455727484
-9.9988000495	-8.1993097791	3.4093073704
-9.9982599218	-8.0610890211	3.4732969600
-9.9975717047	-7.9229023525	3.5374663720
-9.9967253097	-7.7847045474	3.6017366761
-9.9957186251	-7.6464502665	3.6660239262
-9.9945597726	-7.5080933352	3.7302377137
-9.9932688989	-7.3695862218	3.7942799725
-9.9918795204	-7.2308795212	3.8580437812
-9.9904394407	-7.0919211937	3.9214121652
-9.9890108482	-6.9526561433	3.9842573185
-9.9876695091	-6.8130260657	4.0464402194
-9.9865030863	-6.6729693113	4.1078106020
-9.9856084916	-6.5324213895	4.1682074002
-9.9850882148	-6.3913159706	4.2274600461
-9.9850457118	-6.2495852598	4.2853902418
-9.9855799754	-6.1071609693	4.3418142867
-9.9867794413	-5.9639772238	4.3965463854
-9.9887154002	-5.8199738065	4.4494026492
-9.9914351084	-5.6750992276	4.5002053327
-9.9949549588	-5.5293141320	4.5487874750
-9.9992540111	-5.3825947206	4.5949980318
-10.0042680339	-5.2349359453	4.6387067877
-10.0098844523	-5.0863546154	4.6798091641
-10.0159386374	-4.9368924490	4.7182309190
-10.0222114825	-4.7866186695	4.7539322012
-10.0284285741	-4.6356320283	4.7869108909
-10.0342613933	-4.4840623316	4.8172053724
-10.0393301205	-4.3320711466	4.8448961896
-10.0432085487	-4.1798517371	4.8701064152
-10.0454310812	-4.0276282584	4.8930010320
-10.0455006632	-3.8756537874	4.9137849021
-10.0428986327	-3.7242075963	4.9327003992
-10.0370957652	-3.5735915991	4.9500242083
-10.0275631255	-3.4241257684	4.9660619992
-10.0137831763	-3.2761429061	4.9811419695
-9.9952602827	-3.1299827029	4.9956076078
-9.9715302431	-2.9859852778	5.0098099964

-9.9421693399	-2.8444844745	5.0241002053
-9.9068023417	-2.7058011325	5.0388220120
-9.8651095949	-2.5702365810	5.0543052424
-9.8168330226	-2.4380665544	5.0708597297
-9.7617808518	-2.3095357713	5.0887703163
-9.6998313792	-2.1848533539	5.1082932215
-9.6309353632	-2.0641892671	5.1296536888
-9.5551174662	-1.9476719177	5.1530452671
-9.4724765234	-1.8353869886	5.1786303909
-9.3831849115	-1.7273775646	5.2065425232
-9.2874869182	-1.6236455354	5.2368895523
-9.1856962346	-1.5241542216	5.2697582655
-9.0781932539	-1.4288321246	5.3052195628
-8.9654218158	-1.3375776444	5.3433340414
-8.8478843587	-1.2502645824	5.3841582568
-8.7261350560	-1.1667482117	5.4277508584
-8.6007739882	-1.0868716694	5.4741779455
-8.4724433146	-1.0104724287	5.5235180323
-8.3418219872	-0.9373885916	5.5758667765
-8.2096186915	-0.8674647556	5.6313406084
-8.0765641874	-0.8005572431	5.6900789566
-7.9434026702	-0.7365384819	5.7522448258
-7.8108821726	-0.6753004040	5.8180236296
-7.6797439990	-0.6167567310	5.8876201634
-7.5507112435	-0.5608440847	5.9612537322
-7.4244765233	-0.5075219191	6.0391515400
-7.3016890384	-0.4567712907	6.1215404661
-7.1829414626	-0.4085925800	6.2086375358
-7.0687560484	-0.3630022640	6.3006393170
-6.9595713326	-0.3200289304	6.3977103712
-6.8557307189	-0.2797087195	6.4999709794
-6.7574718819	-0.2420803953	6.6074849056
-6.6649177540	-0.2071803030	6.7202480221
-6.5780696445	-0.1750374098	6.8381782341
-6.4968028510	-0.1456686788	6.9611073224
-6.4208650993	-0.1190749506	7.0887750158
-6.3498780482	-0.0952375136	7.2208257062
-6.2833419900	-0.0741155076	7.3568081082
-6.2206438314	-0.0556442441	7.4961778896
-6.1610682573	-0.0397345259	7.6383034581
-6.1038118955	-0.0262729358	7.7824746889
-6.0480001982	-0.0151230632	7.9279145112
-5.9927065850	-0.0061276323	8.0737929263
-5.9369733897	0.0008884565	8.2192430434
-5.8798339914	0.0061144328	8.3633786588
-5.8203354721	0.0097497982	8.5053127410

-5.7575611234	0.0120003122	8.6441762284
-5.6906521287	0.0130735881	8.7791362819
-5.6188283901	0.0131743606	8.9094148454
-5.5414065824	0.0124999736	9.0343061557
-5.4578143209	0.0112364984	9.1531896652
-5.3676013867	0.0095555907	9.2655393804
-5.2704465072	0.0076117445	9.3709306849
-5.1661599024	0.0055402548	9.4690439456
-5.0546824334	0.0034561194	9.5596650675
-4.9360808040	0.0014533426	9.6426827535
-4.8105396020	-0.0003950300	9.7180822735
-4.6783508539	-0.0020360549	9.7859361055
-4.5399013506	-0.0034356906	9.8463921071
-4.3956584743	-0.0045771166	9.8996595798
-4.2461555743	-0.0054583748	9.9459936518
-4.0919770939	-0.0060899132	9.9856788844
-3.9337441088	-0.0064920993	10.0190127532
-3.7721012135	-0.0066923189	10.0462893706
-3.6077048382	-0.0067222003	10.0677843834
-3.4412132930	-0.0066152194	10.0837417514
-3.2732788787	-0.0064043653	10.0943625859
-3.1045420829	-0.0061200597	10.0997965727
-2.9356277445	-0.0057886090	10.1001364844
-2.7671429389	-0.0054311336	10.0954157991
-2.5996763956	-0.0050627448	10.0856092368
-2.4337990104	-0.0046922577	10.0706364087
-2.2700649784	-0.0043225331	10.0503684607
-2.1090131391	-0.0039509938	10.0246368694
-1.9511680673	-0.0035705218	9.9932442122
-1.7970405458	-0.0031708226	9.9559766813
-1.6471270007	-0.0027398931	9.9126173235
-1.5019076087	-0.0022655780	9.8629594083
-1.3618430757	-0.0017372667	9.8068197077
-1.2273699148	-0.0011475939	9.7440509024
-1.0988941636	-0.0004939214	9.6745523154
-0.9767840326	0.0002203038	9.5982790053
-0.8613616336	0.0009843430	9.5152487258
-0.7528939075	0.0017793929	9.4255461523
-0.6515837303	0.0025780118	9.3293247963
-0.5575611360	0.0033439256	9.2268064418
-0.4708752343	0.0040322953	9.1182779874
-0.3914882641	0.0045900221	9.0040861511
-0.3192709015	0.0049565525	8.8846293804
-0.2539998826	0.0050649319	8.7603481586
-0.1953590282	0.0048428844	8.6317151933
-0.1429429096	0.0042141686	8.4992250223

-0.0962636781	0.0030999319	8.3633832158
-0.0547607732	0.0014200986	8.2246956144
-0.0178125352	-0.0009051987	8.0836577355
0.0152502420	-0.0039541632	7.9407448707
0.0451295801	-0.0078019101	7.7964032683
0.0725446724	-0.0125191365	7.6510429093
0.0982158650	-0.0181708845	7.5050318911
0.1228488853	-0.0248155109	7.3586924600
0.1471195626	-0.0325038183	7.2122989469
0.1716598034	-0.0412784016	7.0660773734
0.1970448298	-0.0511732544	6.9202069954
0.2237826250	-0.0622134837	6.7748231904
0.2523054431	-0.0744151961	6.6300217824
0.2829637045	-0.0877854847	6.4858645614
0.3160233564	-0.1023224156	6.3423855411
0.3516663220	-0.1180150613	6.1995974130
0.3899925430	-0.1348437293	6.0574974998
0.4310237846	-0.1527803656	5.9160730254
0.4747124474	-0.1717887722	5.7753058284
0.5209544446	-0.1918252274	5.6351753719
0.5696010869	-0.2128398851	5.4956595460
0.6204704440	-0.2347785559	5.3567342605
0.6733594016	-0.2575846976	5.2183717976
0.7280548628	-0.2812015021	5.0805383737
0.7843440558	-0.3055744558	4.9431912009
0.8420234372	-0.3306538295	4.8062753841
0.9009056710	-0.3563973343	4.6697210085
0.9608244372	-0.3827731494	4.5334407763
1.0216367298	-0.4097627164	4.3973285315
1.0832229272	-0.4373637211	4.2612589684
1.1454837345	-0.4655926167	4.1250887732
1.2083353407	-0.4944868330	3.9886596385
1.2717035892	-0.5241067605	3.8518032762
1.3355160153	-0.5545369241	3.7143480094
1.3996925130	-0.5858867409	3.5761265778
1.4641353702	-0.6182902389	3.4369849548
1.5287190730	-0.6519049223	3.2967918843
1.5932804402	-0.6869098859	3.1554488308
1.6576096878	-0.7235027482	3.0128999503
1.7214427384	-0.7618958779	2.8691416249
1.7844555008	-0.8023114706	2.7242311797
1.8462602883	-0.8449758103	2.5782943017
1.9064046666	-0.8901129340	2.4315307533
1.9643730734	-0.9379375257	2.2842180263
2.0195909634	-0.9886476221	2.1367125922
2.0714318384	-1.0424169213	1.9894485611

2.1192267144	-1.0993871456	1.8429335905
2.1622757766	-1.1596607505	1.6977420068
2.1998620397	-1.2232939862	1.5545052964
2.2312662423	-1.2902908596	1.4139001299
2.2557829565	-1.3605978981	1.2766328414
2.2727365390	-1.4341000622	1.1434220944
2.2814962917	-1.5106179992	1.0149827607
2.2814909464	-1.5899066444	0.8920094172
2.2722215996	-1.6716554084	0.7751590972
2.2532735036	-1.7554898708	0.6650343252
2.2243259819	-1.8409750597	0.5621666791
2.1851602386	-1.9276202729	0.4670020679
2.1356649526	-2.0148852171	0.3798883777
2.0758390385	-2.1021874003	0.3010657690
2.0057921696	-2.1889105435	0.2306599638
1.9257425226	-2.2744137251	0.1686787725
1.8360121413	-2.3580411070	0.1150120285
1.7370200980	-2.4391318585	0.0694348957
1.6292733629	-2.5170300426	0.0316144419
1.5133563039	-2.5910942744	0.0011192382
1.3899186651	-2.6607067529	-0.0225684014
1.2596627490	-2.7252816066	-0.0400379623
1.1233301970	-2.7842722547	-0.0519346151
0.9816884469	-2.8371775740	-0.0589420104
0.8355178566	-2.8835469889	-0.0617645773
0.6855993656	-2.9229841389	-0.0611099700
0.5327033224	-2.9551493469	-0.0576722319
0.3775797595	-2.9797608413	-0.0521162300
0.2209499600	-2.9965946089	-0.0450638432
0.0634999640	-3.0054833532	-0.0370822818
-0.0941243326	-3.0063142964	-0.0286748535
-0.2513202490	-2.9990263023	-0.0202743546
-0.4075296182	-2.9836064492	-0.0122391587
-0.5622387619	-2.9600859030	-0.0048519831
-0.7149769359	-2.9285357650	0.0016788100
-0.8653137521	-2.8890626031	0.0072156043
-1.0128556583	-2.8418041996	0.0116859169
-1.1572417534	-2.7869255932	0.0150751525
-1.2981393975	-2.7246151302	0.0174181375
-1.4352396319	-2.6550811851	0.0187898618
-1.5682528103	-2.5785491028	0.0192958669
-1.6969045444	-2.4952588196	0.0190626973
-1.8209321568	-2.4054630682	0.0182287910
-1.9400818370	-2.3094257181	0.0169361503
-2.0541064991	-2.2074208478	0.0153230533

References

- [1] API recommended practice 17B, fifth edition, Recommended practice for flexible pipe. Technical report, American Petroleum Institute, March 2014.
- [2] Z. P. Bažant and L. Cedolin. Spatial buckling of beams under torque and axial force. In *Stability of structures: elastic, inelastic, fracture, and damage theories*, pages 46–49. Oxford University Press, Inc., 1991.
- [3] F. Bectarte and A. Coutarel. Instability of Tensile Armour Layers of Flexible Pipes Under External Pressure. In *Proceedings of OMAE04 23rd International Conference on Ocean, Offshore and Arctic Engineering*, June 2004.
- [4] S. Benecke and J. H. van Vuuren. Modelling torsion in an elastic cable in space. *Applied mathematical modelling*, 29:pp. 117 – 136, 2005.
- [5] M. A. Berger and C. Prior. The writhe of open and closed curves. *Journal of physics A: Mathematical and general*, 39:pp. 8321–8348, 2006.
- [6] M. P. Braga and P. Kaleff. Flexible Pipe Sensitivity to Birdcaging and Armor Wire Lateral Buckling. In *Proceedings of OMAE04 23rd International Conference on Ocean, Offshore and Arctic Engineering*, June 2004.
- [7] G. Calugareanu. L integrale de gauss et l analyse des noeuds tridimensionnels. (4):pp. 5–20, 1959.
- [8] G. Calugareanu. Sur les classes d isotopie des noeuds tridimensionels et leurs invariants. (11):pp. 588–625, 1961.
- [9] H.-C. Chang and B.-F. Chen. Mechanical behavior of submarine cable under coupled tension, torsion and compressive loads. *Ocean Engineering*, 189:106272, 2019.
- [10] S. Chen and S. Billings. Neural networks for nonlinear system modeling and identification. *International Journal of Control*, 56(2):319 –346, 1992.
- [11] J. Coyne. Analysis of the Formation and Elimination of Loops in Twisted Cable. *IEEE Journal of Oceanic Engineering*, 15(2):72–83, April 1990.
- [12] J. R. M. de Sousa, P. F. Viero, C. Magluta, and N. Roitman. An Experimental and Numerical Study on the Axial Compression Response of Flexible Pipes. *Journal of Offshore Mechanics and Arctic Engineering*, 134, 2012.
- [13] M. R. Dennis and J. H. Hannay. Geometry of calugareanu’s theorem. *arXiv*, 0503012v2:–, 2005.
- [14] G. Endal, O. B. Ness, R. Verley, K. Holthe, and S. Remseth. Behaviour of offshore pipelines subjected to residual curvature during laying. In *OMAE 1995*, OMAE.
- [15] G. Endal and R. Verley. Cyclic roll of large diameter pipeline during laying. In *OMAE 2000*, 2000.

- [16] N. S. Ermolaeva, J. Regelink, and M. P. M. Krutzen. Hockling behaviour of single- and multiple-rope systems. *Engineering Failure Analysis*, 15:142–153, 2008.
- [17] D. Fergestad and S. A. L  tveit. Handbook on design and operation of flexible pipelines. Technical report, MARINTEK, 2014.
- [18] F. Frenet. Sur les courbes a double courbure. (17):437–447, 1852.
- [19] I. Fylling and A. Bech. Effects of internal friction and torque on the global behavior of flexible risers and umbilicals. In *International Conference of Offshore Mechanics and Arctic Engineering*, 1991.
- [20] A. G. Greenhill. On the Strength of Shafting when Exposed to Torsion and to End Thrust. In *Proceedings of the Institution of Mechanical Engineers*, volume 34 of Issue 1, pages 182–225, June 1883.
- [21] E. Koloshkin. Torsion buckling of dynamic flexible risers. Master’s thesis, Norwegian University of Science and Technology, Trondheim, Norway, 2016. Available at <http://hdl.handle.net/11250/2402196>.
- [22] X. Li, X. Jiang, and H. Hopman. Prediction of the Critical Collapse Pressure of Ultra-Deep Water Flexible Risers - a Literature Review. *FME Transactions*, 46:306–312, 2018.
- [23] X. Li, M. A. Vaz, and A. B. Cust  dio. Analytical prediction for lateral buckling of tensile wires in flexible pipes. *Marine Structures*, 61:268–281, 2018.
- [24] X. Li, M. A. Vaz, and A. B. Cust  dio. Analytical and experimental studies on flexible pipes tensile armors lateral instability in cyclic bending. *Marine Structures*, 67, 2019.
- [25] X. Li, M. A. Vaz, and A. B. Cust  dio. Analytical model for lateral instability of quasi-rectangular or circular armor wires in flexible pipes and umbilicals. *Ocean Engineering*, 190, 2019.
- [26] X. Li, M. A. Vaz, and A. B. Cust  dio. Analytical model for tensile armors lateral deflections and buckling in flexible pipes. *Marine Structures*, 64:211–228, 2019.
- [27] F. C. Liu. Kink Formation and Rotational Response of Single and Multistrand Electromechanical Cables. Technical Note N-1403, Civil Engineering Laboratory, Naval Construction Battalion Center, Port Hueneme, California 93043, October 1975.
- [28] V. Longva. *Formulation and application of finite element techniques for slender marine structures subjected to contact interactions*. PhD thesis, Norwegian University of Science and Technology, Trondheim, Norway, 2015. Available at <http://hdl.handle.net/11250/2358726>.
- [29] V. Longva and S. S  vik. A Lagrangian–Eulerian formulation for reeling analysis of history-dependent multilayered beams. *Comput Struct*, 146:44–58, 2015.
- [30] V. Longva and S. S  vik. On prediction of torque in flexible pipe load-out operations using a Lagrangian–Eulerian fe framework. *Mar Struct*, 46:229–254, 2016.

- [31] P. Mainçon. Torsion in flexible pipes, umbilicals and cables under loadout to installation vessels. In *OMAE*, page 62716, 2017.
- [32] A. G. Neto and C. de Arruda Martins. Structural stability of flexible lines in catenary configuration under torsion. *Marine structures*, 34:16–40, 2013.
- [33] A. G. Neto and C. A. Martins. Structural stability of flexible lines in catenary configuration under torsion. *Marine Structures*, 34:16–40, December 2013.
- [34] A. Novitsky and S. Sertã. Flexible Pipe in Brazilian Ultra-Deep Water Fields - A Proven Solution. In *Proceedings of Deep Offshore Technology 2002*, 2002.
- [35] M. F. Opgård. Torsion instability of dynamic cables during installation. Master's thesis, Norwegian University of Science and Technology, Trondheim, Norway, 2017. Available at <http://hdl.handle.net/11250/2452268>.
- [36] N. Østergaard, A. Lyckegaard, and J. H. Andreasen. Imperfection analysis of flexible pipe armor wires in compression and bending. *Applied Ocean Research*, 38:pp. 40–47, 2012.
- [37] N. Østergaard, A. Lyckegaard, and J. H. Andreasen. On modelling of lateral buckling failure in flexible pipe tensile armour layers. *Marine Structures*, 27:pp. 64–81, 2012.
- [38] N. H. Østergaard. *On lateral buckling of armouring wires in flexible pipes*. PhD Thesis, Aalborg University, Department of Mechanical and Manufacturing Engineering, Fibigerstræde 16, DK-9220 Aalborg East, Denmark, February 2012.
- [39] N. H. Østergaard, A. Lyckegaard, and J. H. Andreasen. Simulation of frictional effects in models for calculation of the equilibrium state of Flexible pipe armouring wires in compression and bending. *Journal of Structural Mechanics*, 44:243–259, 2011.
- [40] N. H. Østergaard, A. Lyckegaard, and J. H. Andreasen. A method for prediction of the equilibrium state of a long and slender wire on a frictionless toroid applied for analysis of flexible pipe structures. *Engineering Structures*, 34:391–399, 2012.
- [41] N. H. Østergaard, A. Lyckegaard, and J. H. Andreasen. Imperfection analysis of flexible pipe armor wires in compression and bending. *Applied Ocean Research*, 38:40–47, 2012.
- [42] N. H. Østergaard, A. Lyckegaard, and J. H. Andreasen. On modelling of lateral buckling failure in flexible pipe tensile armour layers. *Marine Structures*, 27:64–81, 2012.
- [43] L. F. Paiva and M. A. Vaz. An empirical model for flexible pipe armor wire lateral buckling failure load. *Applied Ocean Research*, 66:46–54, 2017.
- [44] M. A. Rabelo, C. P. Pesce, C. C. P. Santos, R. R. Junior, G. R. Franzini, and A. G. Neto. An Investigation on flexible pipes birdcaging triggering. *Marine Structures*, 40:159–182, 2015.
- [45] F. Rosenthal. Greenhill's Formula and the Mechanics of Cable Hocking. Technical report 7940, Ocean Technology Division, Naval Research Laboratory, Applied Mechanics Branch, Washington, D.C. 20375, November 1975.
- [46] F. Rosenthal. The Application of Greenhill's Formula to Cable Hocking. *Journal of Applied Mechanics*, 43(4):681–683, December 1976.

- [47] A. L. Ross. Cable Kinking Analysis and Prevention. *Journal of Engineering for Industry*, 99(1):112–115, February 1977.
- [48] S. Sævik. Theoretical and experimental studies of stresses in flexible pipes. *Computers and structures*, 89:2273–2291, 2011.
- [49] S. Sævik and K. I. Ekeberg. Non-linear stress analysis of complex umbilical cross-section. In *OMAE 2002*, 2002.
- [50] S. Sævik, J. K. Gjoesteen, and A. Figenschou. Comparison between predicted and measured umbilical bending stresses during manufacturing. In *OMAE 2006*, 2006.
- [51] S. Sævik and G. Ji. Differential Equation for Evaluating Transverse Buckling Behavior of Tensile Armour Wires. In *Proceedings of the ASME 2014 33rd International Conference on Ocean, Offshore and Arctic Engineering*, July 2014.
- [52] S. Sævik and E. Koloshkin. Torsion Instability of Offshore Cables During Installation. In *Proceedings of the ASME 2017 36th International Conference on Ocean, Offshore and Arctic Engineering*, June 2017.
- [53] S. Sævik and M. J. Thorsen. Techniques for Predicting Tensile Armour Buckling and Fatigue in Deep Water Flexible Risers. In *Proceedings of the ASME 2012 31st International Conference on Ocean, Offshore and Arctic Engineering*, July 2012.
- [54] S. Sævik and M. J. Thorsen. An Analytical Treatment of Buckling and Instability of Tensile Armors in Flexible Pipes. *Journal of Offshore Mechanics and Arctic Engineering*, 139, August 2017.
- [55] S. Sævik and N. Ye. *Aspects of Design and Analysis of Offshore Pipelines and Flexibles*. Deep Ocean Space Technology Publication Project, 2016.
- [56] D. Sarchi, B. Knuepfer, G. Coletta, A.-G. Carl, C. Kemnitz, R. gaspari, T. Kittel, and R. Ewald. Monitoring method and system for detecting the torsion along a cable provided with identification tags, Dec. 2014. U.S. Patent 8,912,889 B2.
- [57] D. Sarchi and L. Palmieri. Method for detecting torsion in a cable, electric cable with torsion sensor and method for manufacturing said cable, Jul. 2016. U.S. Patent 9,400,221 B2.
- [58] P. Secher, F. bectarte, and A. Felix-henry. Lateral buckling of armor wires in flexible pipes: reaching 3000m water depth. In *Proceedings of the 30th International Conference on Ocean, Offshore and Arctic Engineering*, 2011.
- [59] J. A. Serret. Sur quelques formules relatives a la theorie des courbes a double courbure. (16), 1851.
- [60] C. P. Sparks. The influence of tension, pressure and weight on pipe and riser deformations and stresses. *Journal of engineering resources technology*, 1984.
- [61] E. L. Starostin. On the writhe of non-closed curves. *arXiv:physics*, page 0212095v1, 2002.

- [62] D. M. Stump. The hocking of cables: a problem in shearable and extensible rods. (37):pp. 515 – 533, 2000.
- [63] Z. Tan. Monte carlo integration with acceptance-rejection. *Journal of computational and graphical statistics*, 15(3):735 – 752, 2006.
- [64] J. M. T. Thompson and A. R. Champneys. From Helix to Localized Writhing in the Torsional Post-Buckling of Elastic Rods. *Proceedings of the Royal Society A: Mathematical, Physical and Engineering Sciences*, 452(1944):117–138, January 1996.
- [65] M. A. Vaz and N. A. S. Rizzo. A finite element model for flexible pipe armor wire instability. *Marine Structures*, 24:275–291, 2011.
- [66] T. Worzyk. *Submarine Power Cables: Design, Installation, Repair, Environmental Aspects*. Springer, 2009.
- [67] S. Wu, Z. Yang, J. Chen, Q. Lu, Q. Yue, J. Yan, and B. Gao. Study on the Failure Mechanism of Flexible Pipes under Large Torsion Considering the Layer Interaction. In *Proceedings of the ASME 2018 37th International Conference on Ocean, Offshore and Arctic Engineering*, June 2018.
- [68] T. Yabuta. Submarine Cable Kink Analysis. *Bulleting of JSME*, 27(231):1821–1828, September 1984.
- [69] X. Yang, S. Sævik, and L. Sun. Numerical analysis of buckling failure in flexible pipe armor wires. *Ocean Engineering*, 108:594–605, 2015.
- [70] C. Zhou, S. Sævik, N. Ye, and G. Ji. Effect of Lay Angle of Anti-Buckling Tape on Lateral Buckling Behavior of Tensile Armors. In *Proceedings of the ASME 2015 34th International Conference on Ocean, Offshore and Arctic Engineering*, May-June 2015.